DREDGE SPOIL DISPERSION FROM AN INNER SHELF DUMP-MOUND

A thesis

submitted in fulfilment

of the requirements for the degree

of

Master of Philosophy in Earth Science

at the

University of Waikato

by

CARSTEN HARMS

University of Waikato

1989

ABSTRACT

A study was undertaken on the dispersion of dredge spoil from a dump-mound on the inner shelf in 11 - 17 m water depth, 3 km offshore from Tauranga Harbour, New Zealand.

Graphic and volumetric analysis of bathymetric changes over the dump-mound and its near vicinity, based on echo-sounding surveys between 1978 and 1988, showed that a high reduction in dump-mound volume occurs in the first two to three years after the dumping. These changes can be explained by high compaction and erosion of the unconsolidated dredge spoil. Between 1980 and 1985 about two thirds of the eroded material accumulate in a semi-circle up to 400 m south of the dump-mound. From 1985 onwards, after about seven years, the dump-mound appears to be stable.

A sea-floor survey was undertaken, including side-scan sonar, sub-bottom seismic profiling, visual observations by underwater-video and SCUBA diving, and remote sediment sampling. It showed the existence of a natural coarse sand facies with wave-generated megaripples (coarse-grained ripples) which is overlain by a lightly rippled to flat fine sand facies. Repeated surveys indicate that the bedforms react to storms. It is suggested that the fine sand blanket is stripped off the coarse sand at places causing a patchy coarse sand distribution. The natural sediment facies distribution at the dump-sites is masked by dumped medium sands from Tauranga Harbour and its ebb tidal delta. Sorting and skewness parameters and pumice content indicate that a lag surface has formed over the dump-site. Natural sediments in the onshore vicinity of the dump-sites have been altered by the deposition of fine sand and pumice after their erosion from the dredge spoil suggesting a general net onshore movement of sediment. The mineralogical similarity of the dredge spoil and the natural inner shelf sediments prevents any larger scale tracing of dredge spoil.

Wave data collected outside of this study indicate that the threshold velocity for fine sand (2 ϕ) over the dump-mound is exceeded 30 - 50 % of the time. Current meter records over a period of 18 days in June 1988 show a weak southerly directed current associated with light onshore and strong offshore winds, and a

strong northwest directed alongshore flow during an easterly storm. Threshold velocities of unidirectional and combined flow (unidirectional flow modified by waves) are rarely exceeded over a rippled bed of fine sand during peak flow. Total boundary shear stresses indicate that stresses induced by waves are increased by the additional effect of currents. The current also provides a directional component to the stress.

It is suggested that low threshold velocities on a gentle slope increase erosion of coarse material from the dump-mound. This material is only transported over a small distance and deposited in a small zone south of the mound. Fine sand and pumice are temporary deposited in the coarse sand facies but eventually mix with the fine sand blanket entering the exchange zone between the inner shelf and beach systems.

No serious environmental impacts can be assessed from the dumping of dredge spoil so far. Dumping of dredge spoil on the inner shelf are not very effective for beach nourishment as fine sand and pumice do not remain at the beach permanently because of their hydraulic difference to the medium sized beach sand.

ACKNOWLEDGEMENTS

This study was initiated by Dr. Healy and financed by the Bay of Plenty Harbour Board. Therefore, they are thanked.

I am thankful to my three supervisors, Drs. Healy, Nelson and De Lange, for advice during my study.

I had the pleasure to enjoy the company of the hydrographers, John Stephenson and Owen Maynard, the boatsdriver Nobbie and helpful deckhands of the Bay of Plenty Harbour Board, and the technician Mike Dravitzki during my field work in Tauranga.

The mysteries of computers, in particular the SAS program, were revealed to me by Toni Fenton. Helpful comments on thesis and life were given by Thomas Clemm, Richard Stevenson, Mark Tippett, Wayne McLennan, Roger Grace, Barry Bradshaw and Frank Bailey, only to give the names of a few. Thank you all.

Last not least, I thank Brigitte for spending a very enjoyable time with me in New Zealand. Without her, I may already have completely turned into a boring scientist.

TABLE OF CONTENTS

ABBREVIATIONS

BOPHB: Bay of Plenty Harbour Board

THS: Tauranga Harbour Study

RSA: Rapid Sediment Analyser

CHAPTER 1

INTRODUCTION AND AIMS

1.1 Introduction

With the increasing importance of international trading at the end of the last century, deep water ports came into existence to accommodate large ocean vessels. In many cases dredging was, and still is, necessary to make the ports accessible for the vessels. The dredged material was mainly disposed on the inner shelf adjacent to the harbours. With the industrial growth in the 20th century, the dumping of contaminated material affected the marine ecosystem at areas with high population and industrial activity such as the New York Bight in the USA (KETCHUM *et al.*, 1981; KESTER *et al.*, 1983) causing research on the environmental consequences of dredge spoil disposal.

Studies which connect the dispersion of dredge spoil with sediment transport models on the inner shelf are relatively rare. This may be partly due to the lack of scientific evidence of how the hydrodynamic processes which act on the inner shelf influence the magnitude and direction of sediment transport processes. WRIGHT (1987) notes in his review of the current state of knowledge on cross-shore sediment transport that the transport phenomena are diverse and complex and that future field studies are needed to test the numerous partly contradictory hypotheses for sediment transport.

In the case of the dumping of dredge spoil, the input of a different material to a natural shelf sediment environment ideally provides the opportunity to use it as a tracer. The monitoring of its dispersion pattern over time, combined with the measurement of the hydrodynamic components, can contribute to a better understanding of the general sediment transport processes on the inner shelf.

1.2 Study background

Tauranga Harbour is a tidal inlet located in the northern part of the Bay of Plenty (Fig. 1.1). Near the eastern entrance to the Harbour (Tauranga Entrance), the port of Tauranga (Fig.1.2) has been developed as a reloading point for timber, steel and the local kiwifruit industry.

To make the Harbour accessible for the increasing tonnage of ships, dredging has been necessary to open and maintain shipping channels. About 4.5 million m^3 of dredge spoil have been dredged over the last 20 years to deepen and maintain the Entrance Channel, Cutter Channel and Maunganui Channel to a water depth of about 10.5 m (DAHM and HEALY, 1980; BLACK, 1984; Fig.1.2). The dredge spoil has been disposed of in four different ways. Dredged material from the Entrance and Cutter Channel was dumped over small areas on the inner shelf off Mount Maunganui (Fig.1.2). A small part of the

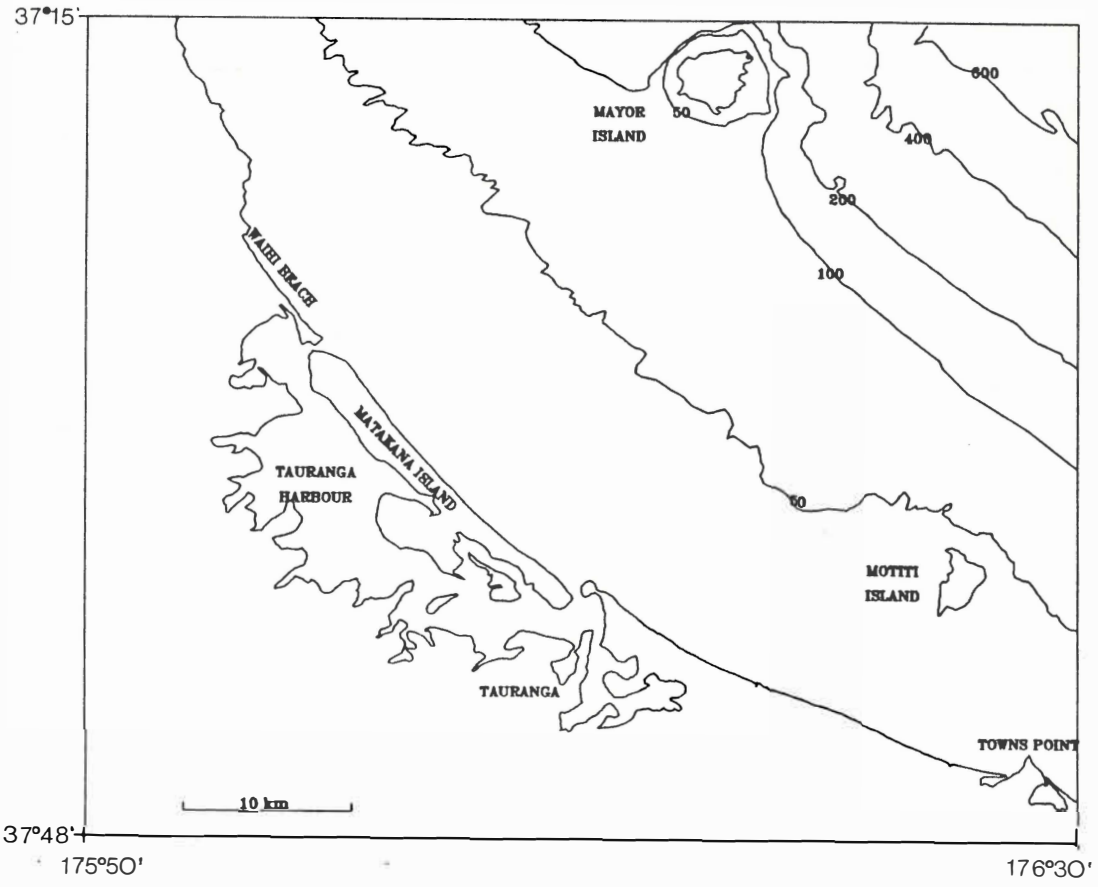

Fig.1.1 - Location map of Tauranga Harbour and its vicinity

dredge spoil was used to renourish the Pilot Bay beach in 1983, which was in a critical state of erosion (DE LANGE, 1988). Dredge spoil from the Maunganui Channel was partly pumped onshore to create the Sulphur Point reclamation, an artificial peninsula forfuture port development. Furthermore, dredging of small quantities of sand have been undertaken for commercial purposes.

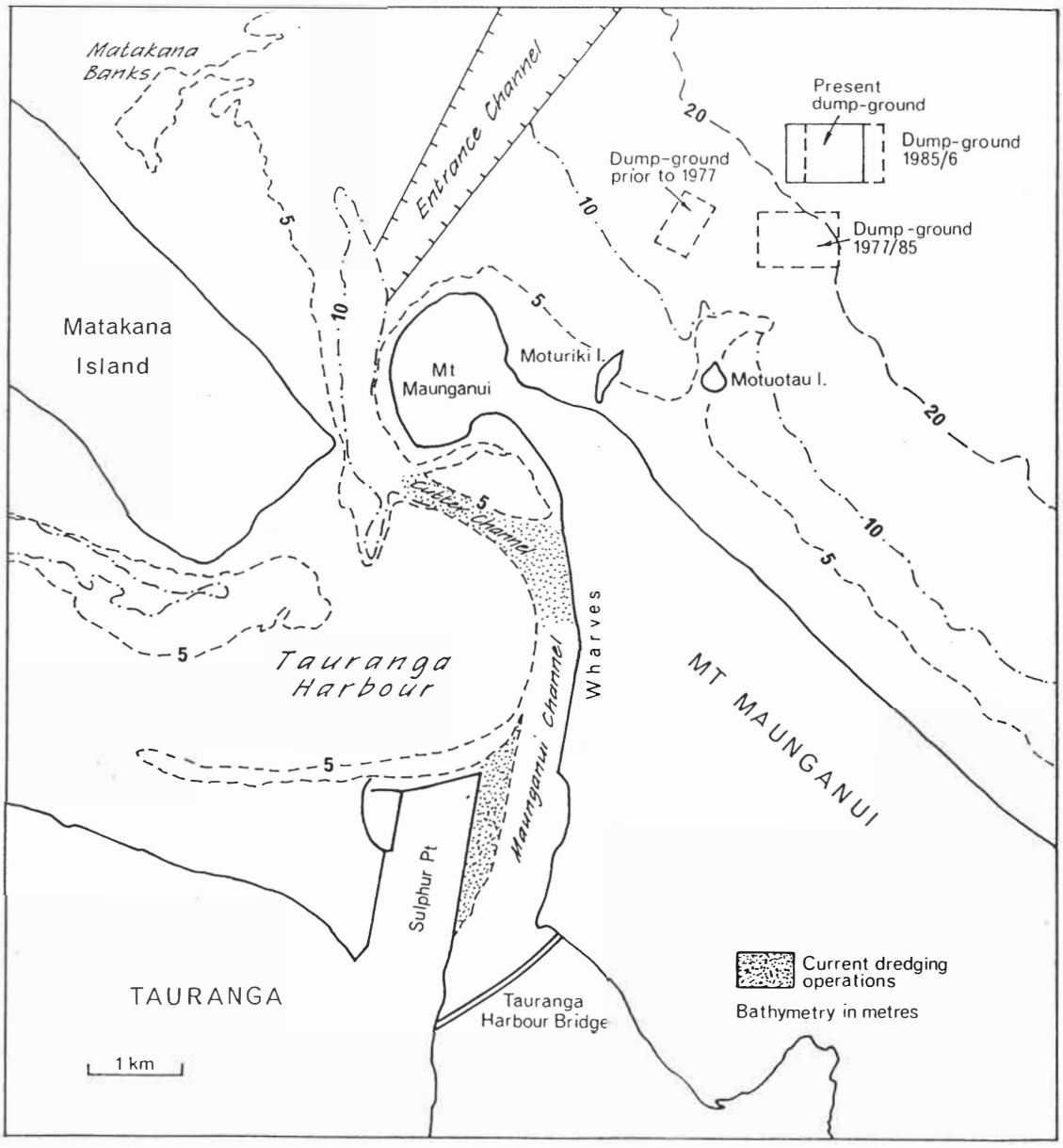

Fig.1.2 - Location map of the Mount Maunganui port with sites of dredging operations in 1988 and dump-sites.

The legislative procedure to apply for a dredging permit has been tightened since the uncontrolled dumping of dredge spoil from the Waitemata Harbour, Auckland, on snapper spawning grounds near Browns Island in the Hauraki Gulf in October 1987. This resulted in a significant reduction in the abundance and variety of marine life in the dump area (GRACE, 1988).

The dredging permit must now be accompanied by an environmental assessment based upon the criteria listed in Section 24 of the Marine Pollution Act 1974. Permission to dredge is issued by the Ministry of Transport, but the Ministry of Agriculture and Fisheries/Fish (MAFFish) and the Department of Conservation can also enter the decision-making process. Additionally, a Water Right under the Water & Soil Conservation Act, 1967, which has to be renewed yearly and is controlled by the Regional Water Boards is required for dumping. The legislation background of dredge spoil disposal in New Zealand is described in more detail in HEALY *et al.* (in press).

The stricter supervision of dredge spoil disposal required greater cognizance of environmental impact assessments to evaluate the effects of the dumping to the marine environment. This particularly concerns Harbour Boards, now Port Operating Companies, because they are the major organisations undertaking dredging.

In the case of the port of Tauranga, maintenance dredging in the channels and capital dredging on the east side of Sulphur Point became necessary in 1988. In order to gain a dredging permit for 1989, an environmental study was initiated by the Bay of Plenty Harbour Board and the University of Waikato, Earth Science Department, which included biological, chemical and dredge spoil dispersal investigations. The biological and chemical investigations were undertaken by consultants. The environmental study is the basis of this thesis on dredge spoil dispersion on the inner shelf off Tauranga.

1.3 Aims of the study

The research project was set up to investigate the following points:

1. To what extent, at what rates and in which directions does the dredge spoil disperse?

2. How does the dredge spoil change the natural sediment facies distribution on the inner shelf?

3. How do the hydrodynamic processes which act on the inner shelf relate to the dredge spoil dispersion and inner shelf sediment transport?

4. What effects are caused by the dumping with respect to the marine ecosystem and to beach nourishment?

1.4 Structure of the study

The following structure was chosen to achieve the aims mentioned above:

The physical setting of the Tauranga area is presented in Chapter 2. It includes the geomorpological and geological charactersation of the Tauranga area and the current data available on the hydrodynamics acting on the inner shelf off Tauranga.

Chapter 3 reviews the current international scientific literature about the hydrodynamic processes acting the shoreface-inner shelf environment and their role in respect to sediment transport. Research undertaken in areas similar to the inner shelf off Tauranga, such as the east coast of the United States, the New South Wales coast in Australia and the east coast of New Zealand, and previous work at Tauranga is reviewed. The dispersion history of dredge spoil from one dump-mound is presented in Chapter 4 by comparing depth sounding charts from 1978 onwards. Graphic displays and volumetric sediment budget calculations are used to characterize the dispersion pattern.

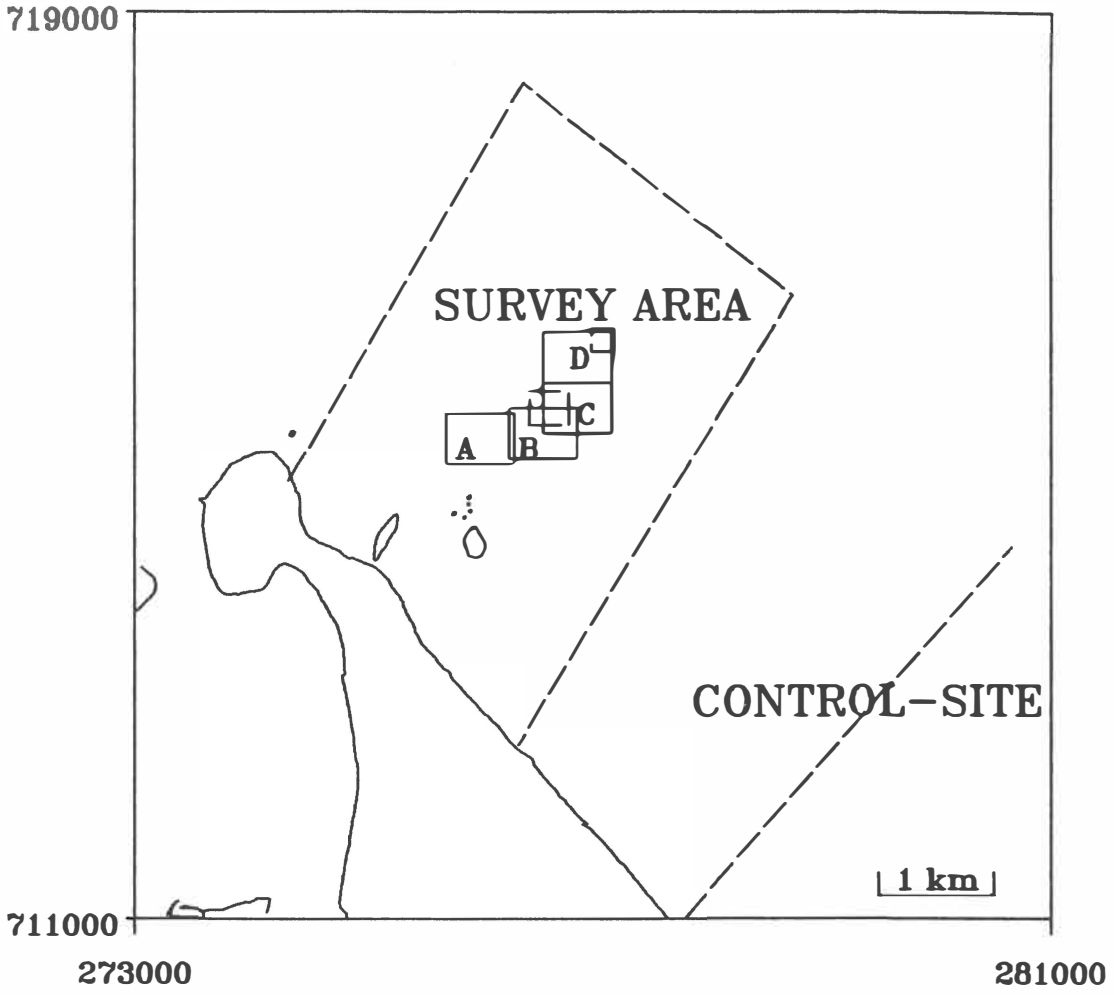

Fig.1.3 - Location of the survey area and the control-site. The dump-sites (solid lines) are indicated with letters. Dump-mounds are shown by dashed lines.

Chapter 5 consists of the sediment facies investigation of the sea-floor in the survey area and a control-site prior to dumping operations in 1988 (Fig.1.3). Side-scan sonar, remote sediment sampling, subbottom seismic profiling and visual observations by a remote operated video (ROV) and SCUBA diving are used for the pre-dump survey. Implications on the formation of sediment facies and sediment transport are drawn from the survey.

In Chapter 6, the hydrodynamic processes acting on the inner shelf are characterised from current measurements undertaken during this study and wave and wind data collected in former studies. Waves and currents are related to sediment transport for conditions assumed to be typical for the survey area.

Chapter 7 integrates the field observations from chapters 4 to 6 in order to develop a conceptual model for the dredge spoil dispersion. It discusses the hydrodynamic processes which are responsible for the sediment facies distribution in the survey area. The effects of dumping to the marine ecosystem, particularly near Motuotau Island, which has been gazetted as a Marine Reserve, and the possibility of beach nourishment of Mount Maunganui Beach are outlined.

CHAPTER 2

PHYSICAL SETTING

2.1 Coastal geomorphology and geology

The survey area is located north of the Mount Maunganui coast extending c. 5 km offshore (Fig.1.3). In order to characterise the bathymetry of the area, a bathymetry map of the inner shelf was produced from data obtained by an echo sounding survey in 1988 along 9 beach-offshore profile-lines. (profile-lines in HEALY *et al.*, 1988).

The 30 m depth contour line on the shelf off Tauranga is located c. 4.5 to 5 km offshore which results in an inner shelf slope gradient of about 1:130. The shape of the inner shelf slope changes from the west to the east of the survey area. In the west the extension of the ebb tidal delta of the harbour entrance causes a more gradual dipping with 1:120 to the 22 m depth contour line than in the east where the slope is more concave with a gradient of 1:80. Further east at the control-site the gradient steepens further to 1:70 to 21 m water depth flattening offshore from there to 1:1000. This abrupt change in gradient may represent the shoreface/inner shelf boundary although additional criteria are used to define this boundary (Chapter 3).

The survey area is the inner part of the Bay of Plenty continental shelf which extends as far as 30 km offshore to the 200 m depth contour line with a steep shelf gradient of 1:150 (Fig.1.1; HARRIS, 1985).

Tauranga Harbour, is a meso-tidal estuarine lagoon impounded by a barrier island (Matakana Island) and two barrier tombolos (Fig.1.1; Mount Maunganui and Bowentown tombolo; HEALY and KIRK, 1981). Tauranga Harbour displays the typical range of coastal morphological features of a tidal inlet as illustrated in Fig.2.2 (from HEALY, 1985).

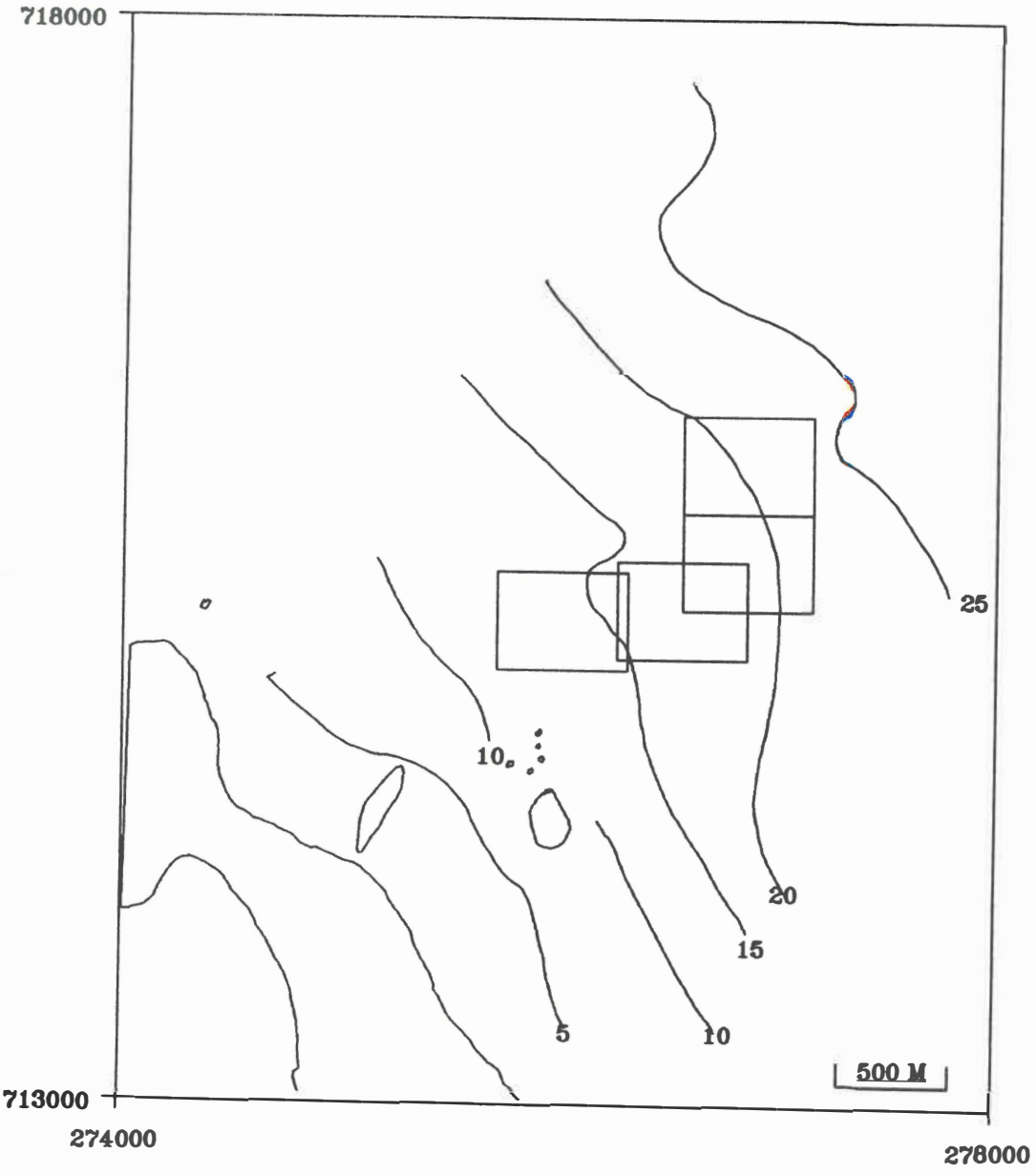

Fig.2.1: Bathymetry map of the survey area from the echo-sounding survey 1988. Note the differences of the depth contour lines in relation to Fig.1.2 (from NZ chart 5412 and DAHM and HEALY, 1980).

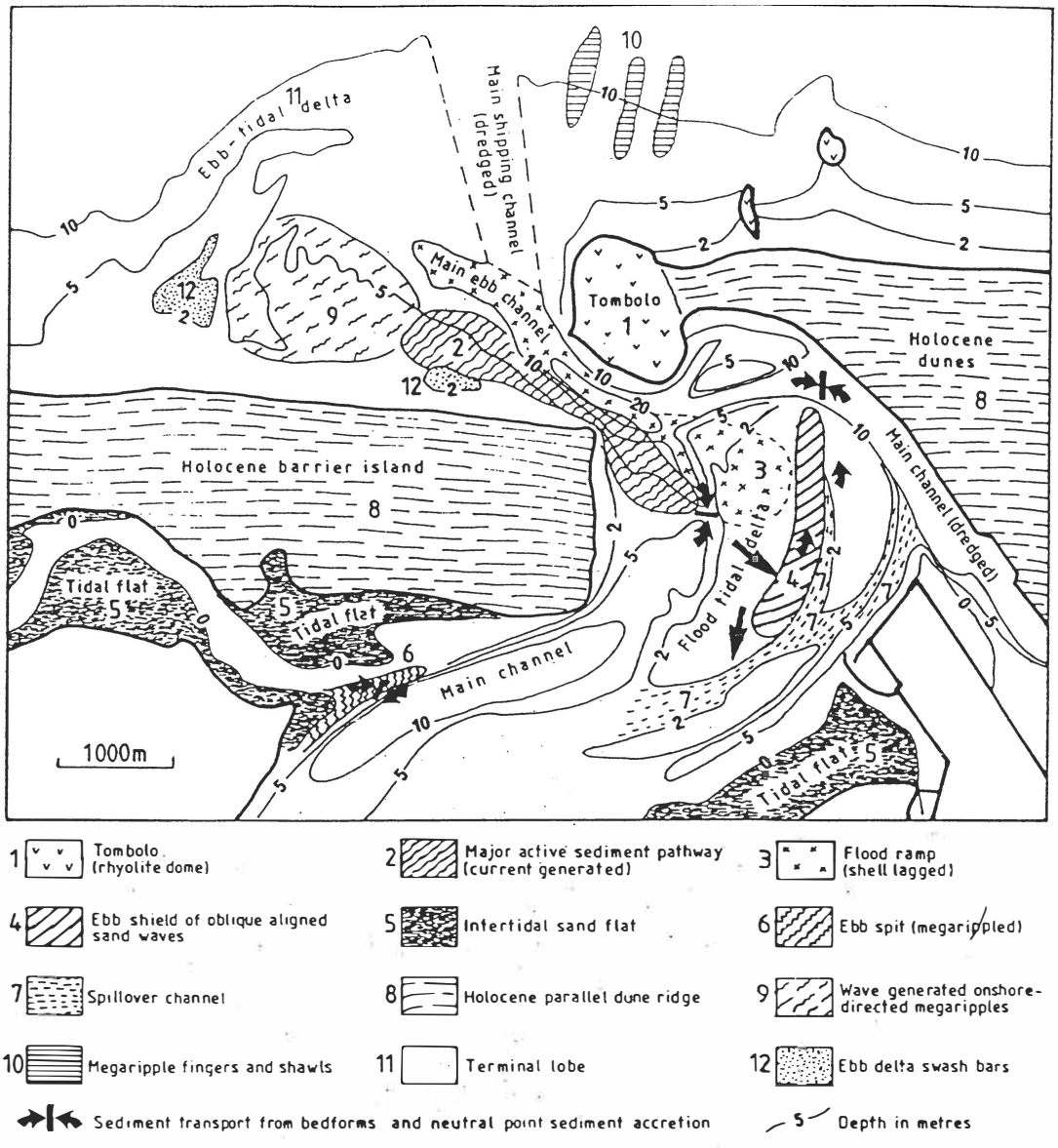

Fig.2.2: Major morphological features of Tauranga Harbour (from HEALY, 1985). Note that the Mount Maunganui rhyolite dome is not a tombolo. A tombolo is defined as the spit which links the mainland with an offshore island (KOMAR, 1976). Therefore the land southeast of the Mount Maunganui is a tombolo. The small rhyolite outcrop of Mount Drury, inland from Moturiki Island, is not mentioned in the map.

The ocean beach of the Mount Maunganui tombolo is a long sandy ocean beach characterised by a dune, berm and an offshore bar (HEALY *et al.*, 1977). Erosion of the beach occurred between 1943 and 1974, resulting in a dune retreat of about 20 m. Most of the erosion was limited to the period between 1943 and 1959 (HEALY *et al.*, 1977). Since the late 1970's Mount Maunganui Beach is building up (HEALY, 1989, pers.comm.). HEALY *et al.* (1977) explain the weaker erosion at Mount Maunganui Beach, compared to Waihi Beach (HARRAY, 1977), with the interruption of the strong northwest-southeast directed littoral drift system through the Tauranga Entrance. Long-term observations of erosion at Mount Maunganui and accretion further east, however, still suggest that there is a small net littoral drift from the northwest to the southeast. More recently onshore movement of dredge spoil may have contributed to the build-up of the beach.

Geologically, the survey area is located in the Tauranga Basin, a marginal basin developed along a tensional graben structure, called the Taupo Volcanic Zone, 2-3 million years ago in response to major adjustments of the Indian-Pacific plate margin (COLE, 1979). On a basement of Pliocene Minden Rhyolite, the basin has been infilled by a sequence of volcanic, fluvial and estuarine deposits with a maximum thickness of 500 m of Pleistocene (Matua Subgroup) and Holocene age (HARMSWORTH, 1983; DAHM, 1983).

The present harbour basin is a former fluvial course, incised into semi-consolidated Pleistocene sediment and volcanic material, drowned by the most recent post-glacial rise in sea-level (DAHM, 1983). The formation of the barrier system in the Tauranga Basin has been attributed to an abundant sediment supply on the continental shelf by DAVIES-COLLEY (1976). The sediments were originally derived from the erosion of tephra deposits of the volcanic hinterland, which is reflected by their acid-volcanic composition. These were reworked on the continental shelf and transported onshore during the Holocene transgression forming the present barrier system (DAVIES-COLLEY, 1976; DAHM, 1983).

DAVIES-COLLEY's observations indicate that shelf and barrier sediments and the material presently deposited in the harbour are of same origin and therefore mineralogically similar. The sediment

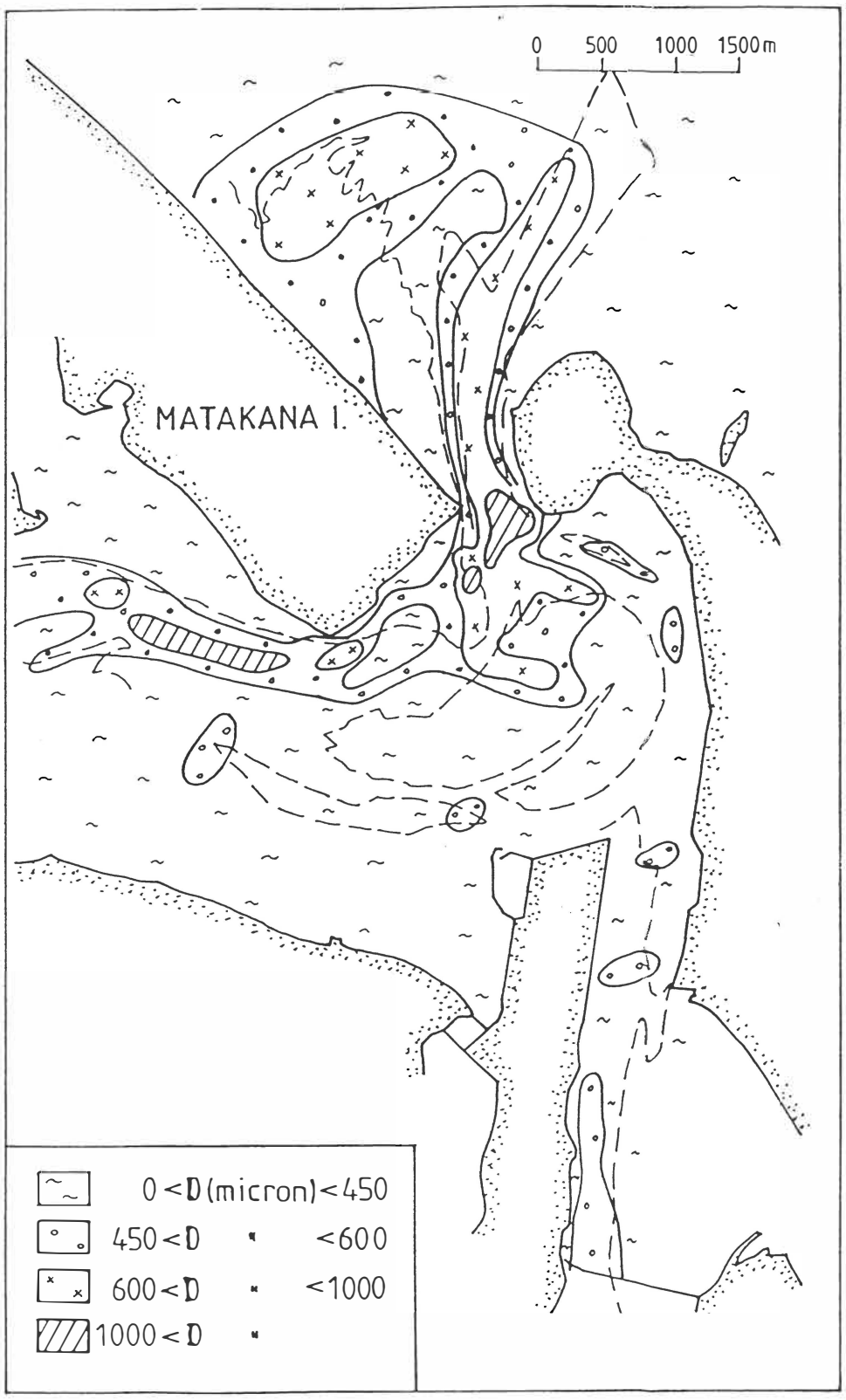

Fig.2.3: Contours of the median grain-size at Tauranga Harbour. Sizes were obtained from 296 bed sediment samples taken by divers and analysed in the University of Waikato Rapid Sediment Analyser (from BLACK, 1984).

do not show large textural changes either consisting predominantly of sand. The surficial sediment distribution (DAHM, 1983; BLACK, 1984, Fig.2.3) shows coarse sands in the channels near the entrance, in the entrance itself and on the ebb tidal delta, where tidal current speeds and waves are highest. The banks and channels further inside the harbour consist of medium and fine sands.

The sediment distribution on the inner shelf is characterized by an inshore fine sand facies and an offshore coarse sand facies (DAHM and HEALY, 1980). The bedforms reflects the grain-size distribution with large wave-generated ripples in the coarse sand facies. Thus, HEALY's (1985) side-scan sonar observations of megaripple 'fingers' on the inner shelf can be associated with the coarse sand facies of DAHM and HEALY (1980).

2.2 Hydrodynamic processes

2.2.1 Wave climate

The Bay of Plenty wave climate is determined by its exposure to the prevailing winds from the east and the sheltering effect of the North Island in the west (QUAYLE, 1984). Thus wind-forced waves develop under westerly winds, whereas swell waves are dominant from the east to the northeast because of the longer fetches (Fig.2.4).

Due to the presence of land in the south and west, the wave distribution changes on the inner shelf off Tauranga Harbour. Wave observations by Bay of Plenty Harbour Board pilots in 1974-75, taken near the Tauranga Entrance, show the highest (up to 5 m) and most frequent (33%) wave approach from the northeast (DAVIES-COLLEY and HEALY, 1978; Fig.2.5). Visual wave height observations from the Mount Maunganui beach, mentioned in DAHM and HEALY (1980), show an average wave height around 1 m. Wave periods are comparable to those observed by HARRAY (1977) at Waihi Beach between 5 and 15 s with a mean period of 11 s. HARRIS *et al.* (1983) came to similar results when measuring wave characteristics off Hicks Bay at the East Cape during a nine months period in 1979. They measured an average significant wave height of 1.25 m with a peak period of 9.4 s.

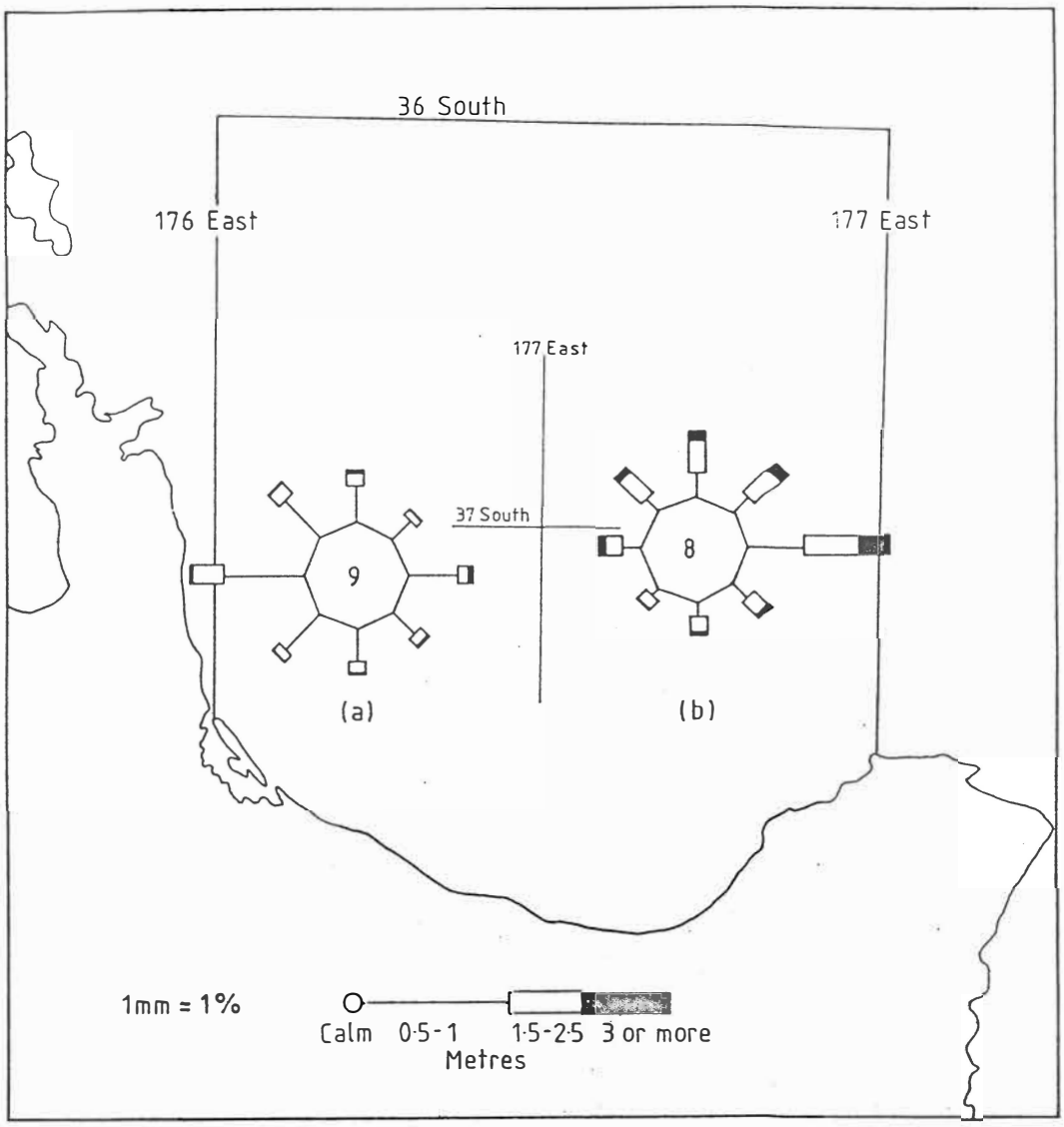

Fig.2.4: Wind wave (a) and swell (b) roses based on ship reports (1200 observations between 1975 and 1980) in a 2-degree square centred on 37°S 177°E (from QUAYLE, 1984).

The wave observations, mentioned in DAVIES-COLLEY (1976) and QUAYLE (1984), have to be treated cautiously because of the accidental and estimated form of observation they are based on they show a trend of the main wave approach changing from the east to the northeast when approaching the coast. This observation can be explained by wave refraction which turns waves approaching the coast in an oblique angle into a more shore-normal direction (NE) and by the wave-blocking effect of Motiti Island in the east.

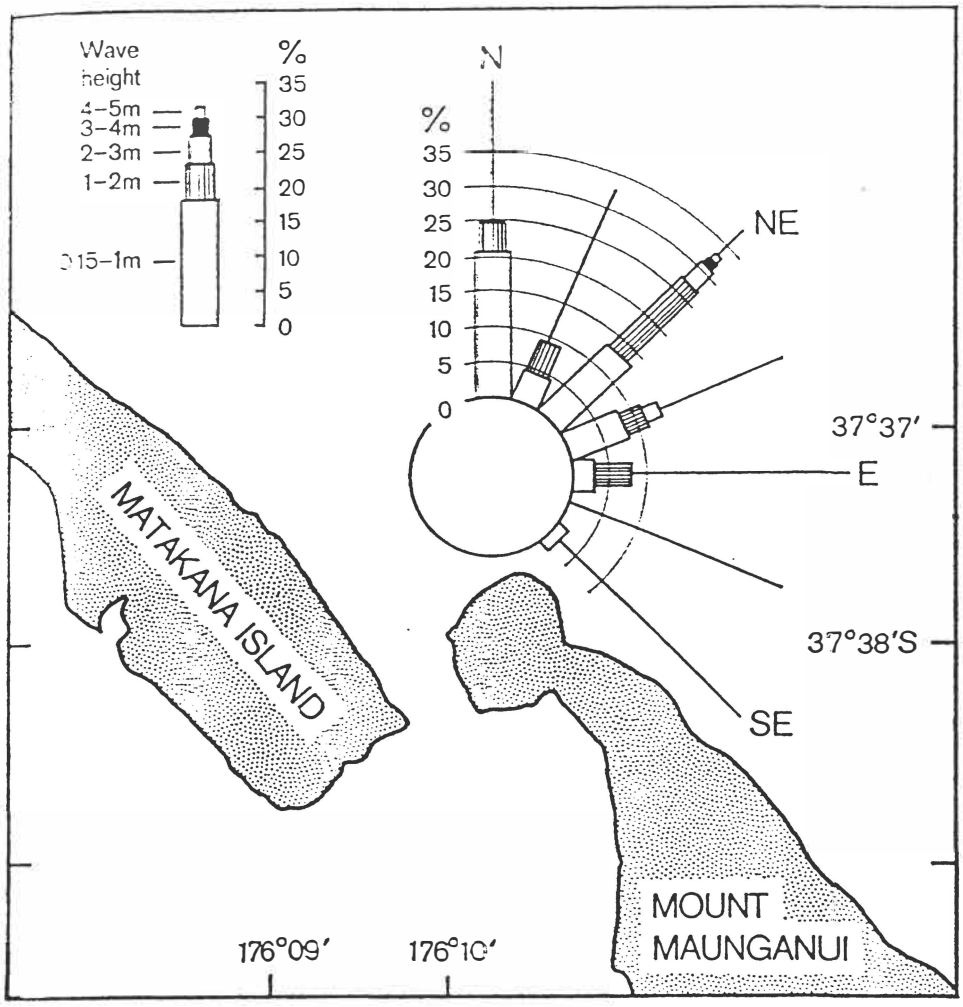

Fig.2.5: Wave rose based on Tauranga Harbour pilot observations for the period 1974-75 off the Tauranga Harbour Entrance. (from DAVIES-COLLEY and HEALY, 1978).

2.2.2. Tides and currents

Tidal height values (MHWS - MLWS) for Tauranga Harbour range between 1.5 and 1.6 m (NZ Chart 541, DAVIES-COLLEY, 1976), and according to the hydrographer of the Bay of Plenty Harbour Board (MAYNARD, pers. comm., 1988) between 1.5 and 2.1 m with an a mean tidal height of 1.75 m. Tides at the east coast of New Zealand are dominated by semidiurnal tides but contain a small diurnal component (HARRIS, 1985).

Using DAVIS and HAYES (1984) classification for wave and tide dominated coast, the survey area with an average wave height of about 1 m and a tidal height of 1.7 m belongs to the mixed energy (wave dominated) category. The reported non-existence of tidal

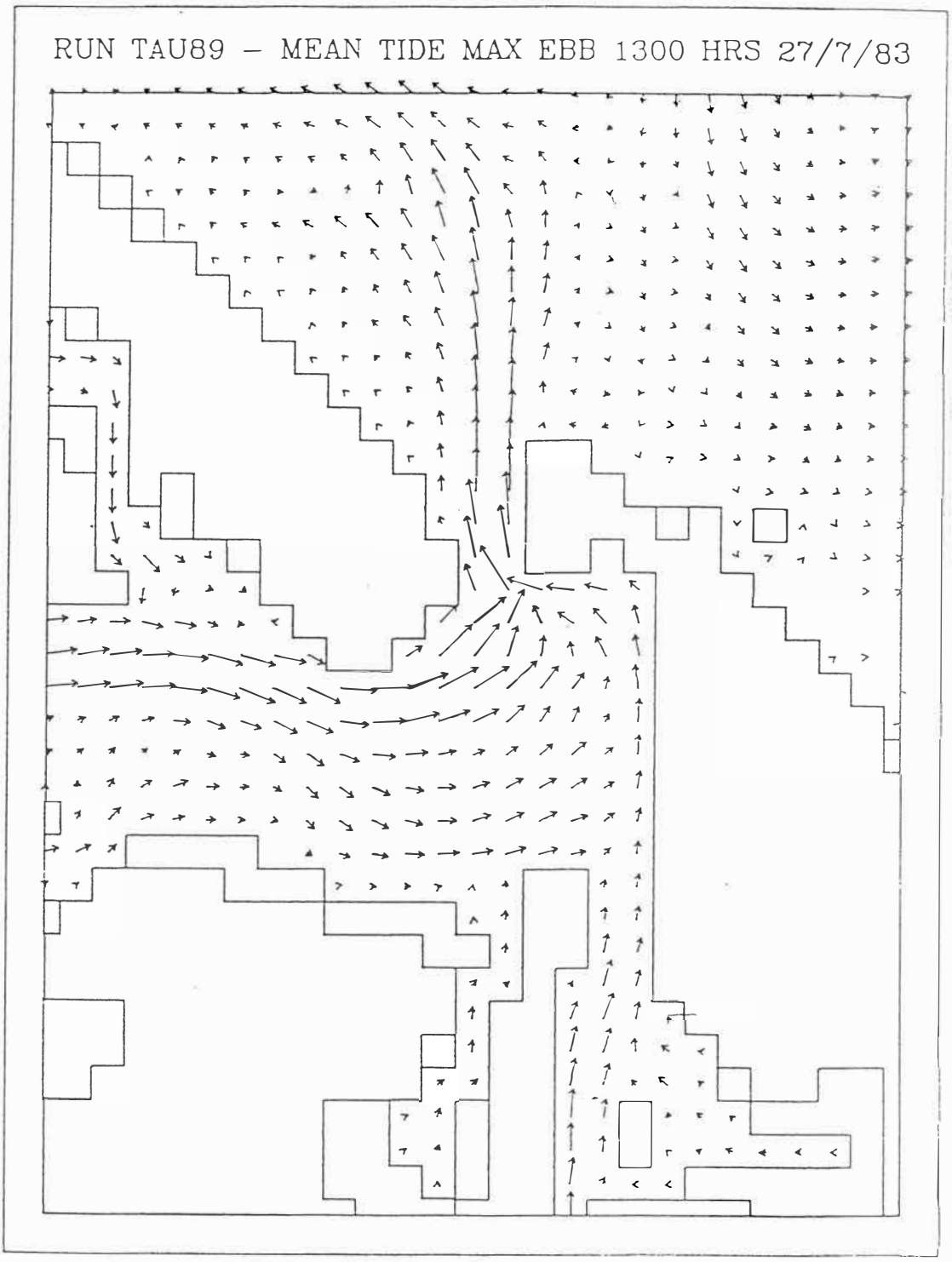

2.6 Tidal current streamlines for Tauranga Harbour showing the ebb jet in the entrance and a south to southeast flow towards the inner shelf off Mount Maunganui (from BARNETT, 1985).

features in the east of the survey area assumed to be not influenced by tidal currents in the harbour entrance supports this classification. CARTER and HEATH (1975) note that most of New Zealand's shelf is not tide-dominated.

Tidal currents determine the flow pattern inside the harbour and in the entrance. DAVIES-COLLEY (1976) observed a strongly ebb dominated tidal flow in the entrance flow with eddy systems breaking off the main ebb jet. He suggests that these recirculatory currents enter the survey area but are too weak to be significant in bedload transport. A strong ebb jet in the entrance was modelled by BLACK (1984) and BARNETT (1985; Fig.2.6). Because of the sediment budget BLACK suggests the return of the sand carried out by the ebb jet occurs by wave stirring and weaker flood currents from the Matakana banks.

Current data in the survey area have been restricted to that collected during the THS. The measurements were undertaken for two months in June/July 1984 with an Aanderaa current meter at the 20 m depth contour line on the shelf east off the Entrance (HEALY, 1985). BARNETT (1985) interprets the data and concludes from modelling of a short period of the current data (5 days), that the currents on the inner shelf are not consistent in their direction and therefore do not depend primarily on local tidal forcing. From numerical modelling and Braystoke measurements BARNETT (1985) suggests the existence of a weak shore-parallel tidal current in a southeast direction. It is not known whether oceanographic currents, as in the case of the east coast of New Zealand the predominantly southeasterly directed East Auckland Current (HARRIS, 1985), enter the survey area.

2.2.3. Wind climate

Because of the limited field measurements of waves and currents on the inner shelf off Tauranga, a characterisation of the wind climate of the Bay of Plenty provides additional information on the direction and magnitude of waves and wind-driven currents.

According to QUAYLE (1984), the wind climate in the Bay of Plenty is influenced by:

a) north to northeast airstreams;
b) disturbed west to southwest airflows;
c) south to southeast airstreams;
d) west to northwest flows;
e) tropical cyclones from the northeast.

Most wind affecting the Bay of Plenty result from the first two groups (Fig. 2.7). With respect to the generation of significant waves north to northeast airstreams and tropical cyclones from the northeast are of major importance (HARRAY, 1977).

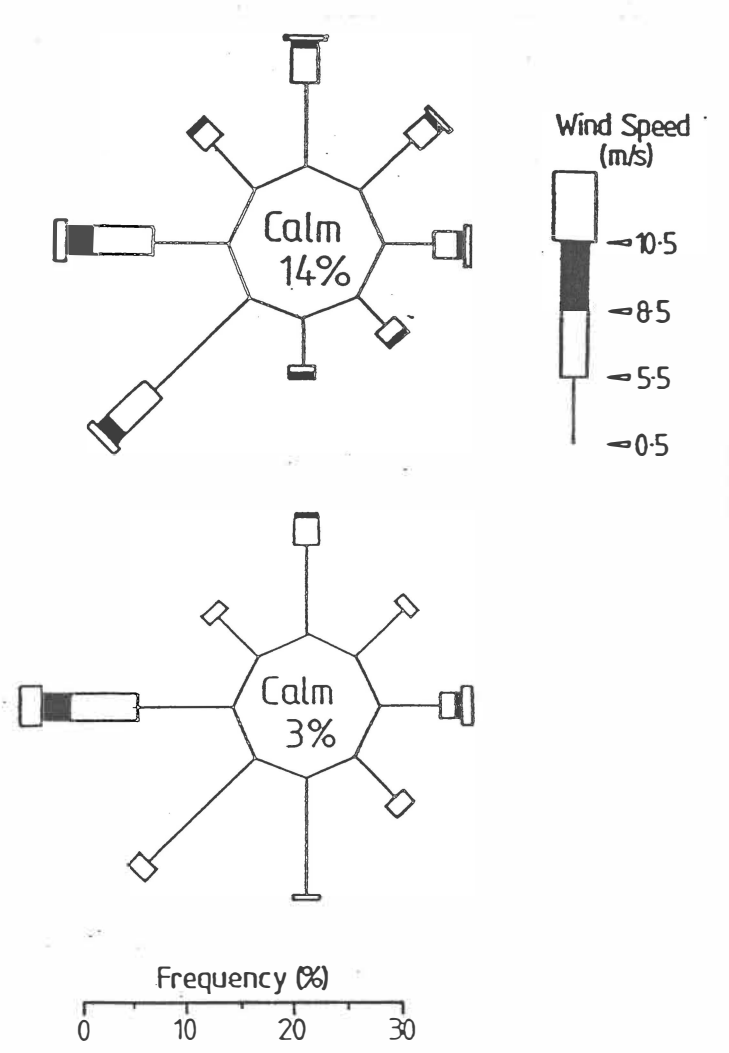

Fig.2.7: Mean annual frequency of of wind speed and direction for Tauranga Airport 1970-1979 (A) (from QUAYLE, 1984); for Mt. Drury (B) 1984-1985 (from DE LANGE, 1988). Southwest to west are dominant, followed by north to east winds.

CHAPTER 3

INNER SHELF PROCESSES AND SEDIMENTATION: A LITERATURE REVIEW

3.1 Introduction

The movement of sediment on the shoreface/inner shelf is a function of the acting hydrodynamic processes (waves and currents). The effects of the hydrodynamics on magnitude and direction of sediment transport seaward of the surfzone can still be considered as unsolved (WRIGHT, 1987) as it is technically difficult to measure sediment transport directly in the field. However, various theoretical approaches and laboratory experiments have been undertaken to relate the hydrodynamics to sediment transport in the shoreface/inner shelf zone.

This chapter summarises the current knowledge of inner shelf sediment transport processes in theory and practice highlighting the existing problems and open questions in the field. In addition, three inner shelf environments similar to the Tauranga inner shelf are briefly described with respect to their sediment facies distribution, bedforms and hydrodynamic processes. Finally previous work on the Tauranga inner shelf is reviewed.

3.2 Definition of the inner shelf/shoreface zone

The shoreface and inner shelf are the inner parts of the continental shelf in which COWELL and NIELSEN (1984) distinguish four zones in relation to boundary layer processes associated with distinctive hydraulic regimes (Fig.3.1). The outer-shelf zone is characterised by near-bottom flows dominated by frontal processes between shelf and ocean water masses. The mid-shelf zone is dominated by geostrophic flow because of weak boundary layer effects. The inner-shelf zone is characterised by storm generated flows in which friction effects are dominant and where boundary layers are thick. The shoreface zone occurs where the thin boundary layer of wind-generated waves dominates the flow pattern.

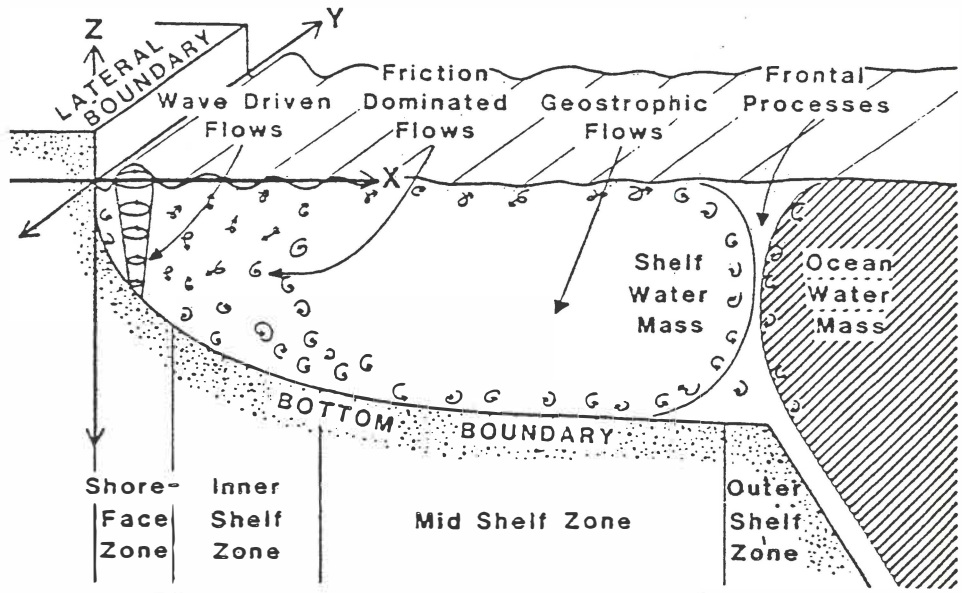

Fig.3.1: Process zones on the continental shelf in which boundary layer processes are associated with distinctive hydraulic regimes and morphological provinces (from COWELL and NIELSEN, 1984).

Hydraulic criteria for the boundary between the mid-shelf zone and the inner-shelf zone is the vertical Ekman number; for the shoreface/inner shelf boundary the Froude number (COWELL and NIELSEN, 1984). However, these criteria are not widely used. The shoreface/inner shelf boundary is more generally referred to as the beginning of seaward fining and significant flattening of the slope gradient (e.g. RILEY *et al.*, 1985). As this can change from case to case, the precise position of the shoreface/inner shelf boundary is subject to different interpretations of reseachers on varying shelves.

3.3 Hydrodynamics of sediment transport

3.3.1 Sediment transport modes

Sediment transport can occur as bedload (grain to grain interaction understood as rolling and saltating near the bed) and suspended-load transport (fluid to grain interaction maintained above the bottom by the turbulence of the water). Up to present it is not known which of the two processes is more significant for sediment

transport as it is technically difficult to measure bedload transport precisely with bedload traps (KOMAR, 1976; VINCENT *et al.*, 1982; HANES, 1988). Measurements of near-bottom sediment concentrations profiles showed that bedload and suspended-load are related through the bedload concentration and can be calculated on the basis of wave and current data (VINCENT *et al.*, 1982). HANES (1988) concludes from sediment tracer experiments that the two separate processes do not explain the sediment transport process precisely. In his opinion the term 'intermittent suspension', which can be imagined as a short-time suspension, is more appropriate to describe the sediment transport process under waves in many cases.

3.3.2 The role of waves

Surface gravity waves initiate grain motion when the wave orbital velocity exceeds the threshold velocity. The threshold velocity of sediment movement depends on the water depth, wave height, wave period and the grain-size diameter.

Under linear Airy wave theory, sediment is only stirred up by waves but not transported with a net translation. In shallow water the onshore movement of sediment under waves is considered to be an important process (e.g. NIEDORODA *et al.*, 1985). The concept of onshore sediment bedload transport is based on the observation that waves approaching shallow water change from linear Airy waves to more sharp-crested waves represented by 2nd or higher order Stokes' theory. Waves behaving according to Stokes' theory develop not closed asymmetric wave orbitals which cause an onshore wave-driven current in the thin wave boundary layer. NIEDORODA *et al.* (1985) state that the critical water depth for the development of wave orbital asymmetries is between 5 and 15 m depending on the wave period.

However, this onshore net current which is thought to transport sediment onshore has never been proven in the field (KOMAR, 1976; NIEDORODA *et al.*, 1985). In addition, TROWBRIDGE and MADSEN (1984) show from theoretical calculations and flume experiments that a reversal mass transport also exists produced by long waves and that

variations in bed roughness strongly influence the direction of mass transport under wave-induced turbulent flow, so that the sediment transport can be in either direction.

A recent concept, developed by SHI and LARSEN (1984), supports TROWBRIDGE and MADSEN's (1984) results postulating that alternating sets of high and low waves produce a forced long wave between wave troughs and crests inducing bedload and suspended-load transport of sediment in the reverse direction of the wave propagation. Although SHI and LARSEN note that this weak drift, controlled by the wave orbital bottom velocity, is able to transport fine and silty sediment, it can be easily overwhelmed by moderate unidirectional currents.

Concepts of net sediment flux under waves are restricted to theoretical and laboratory investigations as it is practically impossible to measure net sediment transport in the field. The proposed models suggested to be responsible for sediment transport under waves do not only favor transport in an onshore direction which was the common concept for a long time. More recent research shows that the possibility of offshore transport under waves has also to be taken into account.

3.3.3 The role of currents

Currents on the shelf can be distinguished as tidal, wind-driven and oceanographic currents (e.g. WALKER, 1984). Generally, the main component of an inner shelf current is in a longshore direction but the weaker shore-normal transport is more important for beach-inner shelf sediment interaction (NIEDORODA *et al.*, 1985).

Tidal currents on the shelf vary over a tidal cycle in a rotary elliptic pattern (WRIGHT, 1981; NIEDORODA *et al.*, 1985). Shoreward of about 20 m water depth, the tidal currents tend to diminish rapidly as a result of enhanced frictional effects (NIEDORODA *et al.*, 1985). On microtidal open coasts tidal currents are important for keeping sediment in suspension but are because of their symmetry of limited importance in net sediment flow (NIEDORODA *et al.*, 1985).

Wind-driven currents are probably of highest importance in a shoreface/inner shelf environment (WRIGHT, 1987). Wind-driven currents in the ocean are influenced by the Coriolis effect, which generates a varying flow pattern thoughout the water column, termed the 'Ekman boundary layer flow'. In the southern hemisphere, the Coriolis effect causes the flow in the middle geostrophic layer to diver to the left. Near the coast in shallow water frictional effects dominate the flow pattern so that no Coriolis effects occur. The pressure gradient induced by the wind-driven surface currents leads to a "set-up" or "set-down" of water at the shore. This causes downwelling in an offshore direction connected with onshore winds and upwelling with offshore winds (Fig.3.2).

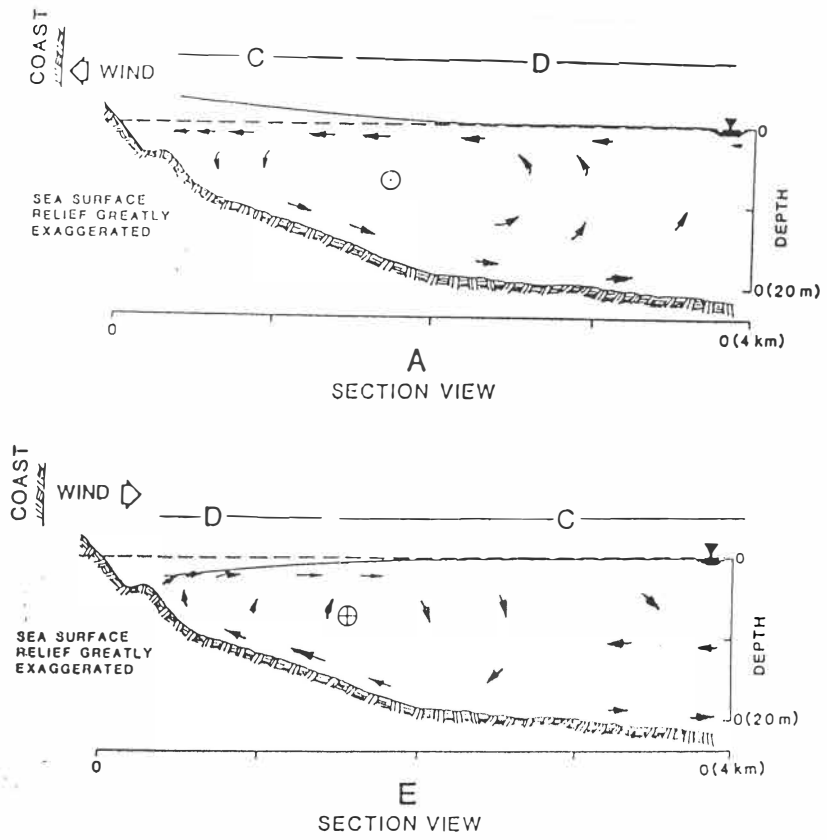

Fig.3.2: Schematics of shoreface transport under onshore (3.2a) and offshore wind (3.2b) in the northern hemisphere producing downwelling and upwelling in the shoreface and more complicated flow pattern offshore. Circles describe longshore flow.

NIEDORODA *et al.* (1985) divide the flow pattern in the coastal boundary layer into a zone of geostrophic flow, a transition zone and a friction-dominated zone, which offshore limits depend on the strength of a storm. In the friction-dominated zone, comparable with the upper and mid shoreface, downwelling is an important process for offshore sediment transport. Upwelling currents are considered to be weaker and of less importance for sediment transport (NIEDORODA *et al.*, 1984). On the lower shoreface and inner shelf in the transition zone the downwelling effect becomes weaker and more complex with the longshore flow being more important (Fig.3.2). These observations do not agree completely with COWELL and NIELSEN's (1984) definition of the shoreface as wave-dominated and inner shelf as friction-dominated. NIEDORODA *et al.* (1985) investigated the wind-driven flow circulation for a model shoreface in the northern hemisphere for 8 different wind direction showing that an oblique wind approach to the shore produces more complicated flow pattern with changing longshore flows.

3.3.4 Wave-current interaction

In reality, waves and currents occur together on the shelf. The interaction of oscillatory and non-oscillatory flow and the resulting net sediment flow is therefore the key to determine direction and magnitude of sediment transport processes on the shoreface and inner shelf (GRANT *et al.*, 1984).

The simplest way to imagine wave current interaction is that waves stir up the sediment and currents transport it. COWELL and NIELSEN's (1984) "rule of thumb" is that waves define when and the superimposed currents where the sediment moves.

However, there are however more complicated non-linear wave-current interactions. According to HAMMOND and COLLINS (1979), the threshold velocity for sediment movement under combined flow increases with decreasing wave period. The interaction of waves and currents results in the complication of the boundary layer where the thin wave boundary layer is nested in the larger mean flow boundary layer (GRANT and MADSEN, 1979). GRANT and MADSEN's (1979)

theoretical investigations that the mean shear stress increases, the current speed is reduced and the "apparent" bed roughness increases was later verified by laboratory experiments by KEMP and SIMONS (1982, 1983) and COFFEY and NIELSEN (1987). KEMP and SIMONS (1982, 1983) investigated wave-current interaction with and against the current. They conclude an increase in sediment concentration in the near bed region from their observed reduction of the current boundary layer by waves with higher transport with a current over a smooth bed and lower transport over a rough bed. Depending on the angle between waves and current sediment transport can also be with or opposite to the mean current which was already observed by BOWEN and INMAN (1963, in WRIGHT, 1987). Thus, the bed roughness and the angle between wave incidence and current are the two most important factors with respect to the magnitude and direction of sediment transport under combined waves and currents (WRIGHT, 1987).

WRIGHT (1987) concludes that the "conventional wisdom" of weak fair weather onshore transport by waves and strong offshore transport by downwelling or rip currents during storms which had been developed for beaches and the upper shoreface, is not automatically applicable for the lower shoreface and consequently the inner shelf, particularly if waves and currents interact on a rippled bed.

3.4 Sediment facies distribution

For the continental shelf KENNETT (1982) distinguishes three depositional zones:

a) a modern nearshore sand prism (a seaward thining and fining wedge of nearshore sand);

b) a modern shelf mud blanket;

c) a shelf relict sand blanket.

The term 'relict' was created by SHEPHARD (1932) and re-stated by EMERY (1968) naming shelf sediments which were deposited in the past during lower sea levels (in WALKER, 1984). As SWIFT *et al.* (1971) found that relict sediments can still be modified by present sediment transport processes they called them "palimpsest" sediments.

Sediment facies distribution and their possible generation by hydrodynamic processes have been described for many shelves on the world. Reflected by the sediment facies distribution shelves can be distinguished in tide dominated, storm dominated shelves and shelves dominated by intruding ocean currents (WALKER, 1984).

Three examples of shelf environments will be shortly described, particularly with respect to facies distribution, suggested mode of formation and the sediment transport processes. As the Tauranga shelf can be considered as a storm dominated shelf because of its low tidal range (Chapter 2) the examples chosen are the storm dominated shelves of the Middle Atlantic Bight of the United States, off New South Wales coast, Australia, and off the east coast of New Zealand.

Middle Atlantic Bight

The Middle Atlantic Bight is a shallow north-south trending shelf between 35° N and 42° N off the east coast of the United States. It is a storm dominated shelf with a microtidal range (LAVELLE *et al.*, 1978).

The east coast of the U.S.A. has a retreating coast-line (NIEDORODA *et al.*, 1985). On the shoreface a seaward-fining and thinning blanket of sand covers coarse sand. This blanket is stripped off the underlying coarse sand during storm events (SWIFT and FREELAND, 1978; NIEDORODA *et al.*, 1985). The coarse sand lag thickens in a seaward direction on the lower shoreface and inner shelf. It is interpreted as a back barrier or older coastal deposit on the upper shoreface and as the basal gravel of the Holocene transgression on the lower shoreface and inner shelf (SWIFT *et al.*, 1983, NIEDORODA *et al.*, 1985).

Bedforms of various sizes have been observed in the Middle Atlantic Bight which WALKER (1984) summarizes:
a) Shoal retreat massifs: shore perpendicular sand bodies of 10-15 km x 30-40 km size and 2-20 m high;

b) Linear sand ridges: 10-45° angle to the coast, 2-3 km wide, up to 10 m high and with spacings of 2-7 km. They produce the so called ridge and swale topography;
c) Transverse bedforms as sandwaves, megaripples and ripples have been described by SWIFT *et al.* (1979).

The observed megaripples were divided into sharp-crested (coarse sand) and hummocky megaripples (fine sand, SWIFT *et al.*, 1983). SWIFT *et al.* (1979) observe that megaripples develop during winter storms and erase in the summer in calmer periods. SWIFT *et al.* (1983) explain the generation of both megaripples in storm events when a high-frequency wave orbital is superimposed on a mean flow. Erosional windows in the surficial fine sand which expose the coarse sand deposit with megaripples are explained by downwelling and offshore sediment transport (SWIFT and FREELAND, 1978).

The flow pattern and its effect on sediment transport processes has been investigated intensively on the inner shelf of the Atlantic Bight. LAVELLE *et al.* (1978) show with current measurements and tracer experiments that wind-driven currents during winter storms are the major mechanisms for transport of sediment in a westward shore-parallel direction on a yearly scale on the inner shelf at 20-22 m water depth. On the shoreface, NIEDORODA *et al.* (1985) postulate a landward moving of sediment under waves most of the time. During storms the jet-like alongshore flows on the inner shelf cause downwelling with net offshore transport on the shoreface down to 10 m water depth (NIEDORODA *et al.*, 1985; WRIGHT *et al.*, 1986).

New South Wales Coast

The shelf off the cliff-lined, embayed Sydney coast is very steep with a gradient of 1:50 to 1:100 (GORDON and HOFFMAN, 1984). COWELL and NIELSEN (1984) note that the steep gradient results in the absence of the shoreface zone. The New South Wales coast is a high energy coast where local wind-stress Ekman currents are likely to be more important than the tidal currents in a microtidal

environment (COWELL and NIELSEN, 1984). In addition, there is a southerly oceanographic current, the East Australia Current, which intrudes into the inner shelf but seldom induces sufficient seabed shear to entrain sediment (GORDON and HOFFMAN, 1984).

FIELD and ROY (1984) describe large sand bodies of Holocene age running discontinously along the coast extending down to 70 m water depth. They interpret the existence of surface channels, filled with coarse sand, in the sand bodies as evidence for seaward down-channel transport from the surfzone and upper shoreface to the lower shoreface. The accumulation of material at the southern side of a trans-shelf volcanic dyke outcrop reported by FIELD and ROY (1984) and the current observations of GORDON and HOFFMAN (1984) indicate a net northward sediment transport caused by short duration downwelling events. Based on facies distribution and hydrodynamic modelling BOYD (1982) states that bidirectional sediment exchange between the surfzone, shoreface and inner shelf at the New South Wales coast can reach as far out as to 20 - 30 m water depth.

A contrasting situation with a strong shoreward current and deduced onshore transport during a onshore storm and weak offshore flow during calm weather was measured by WRIGHT *et al.*, 1986 (in WRIGHT, 1987) at a depth of 10 m over the shoreface fronting the Gippsland coast of Eastern Bass Strait.

COWELL and NIELSEN (1984) conclude from their observations on the inner shelf south of Sydney that the sand movement is not as intense as might be expected for an inner-continental shelf subjected to a high energy wave climate as that characteristic of the south Sydney coast. In contrast to GORDON and HOFFMAN (1984), they note that predicted concentrations of mobile sediments induced by waves are more significant to long-term sedimentation processes than those acting on a short time scale during storms.

New Zealand east coast

Local investigations at the east coast of the North Island, New Zealand, have been undertaken in the past.

On the ebb tidal delta of Whangarei Harbour, BLACK and HEALY (1983, 1988) found distinct shore-normal aligned bands of ripples surrounded by flat sands. From wave refraction modelling they found that regional wave height reinforcement and the associated shoreward current are likely to be responsible for the zonal nature of the bands.

At Omaha Bay north of Auckland, RILEY *et al.* (1985) observed that short-term changes in sea-level within one year can cause erosion and accretion at the beach as well as in the upper part of the offshore coarse sand belt (20-30 m water depth) suggesting that the coarse sands are not relict deposits. From these observations and Carbon14 measurements of shallow cores they suggest that long-term changes in sea-level caused erosion on the lower portion of the shoreface during the Holocene.

A similar coarse sand belt with symmetrical megaripples from 20 to 40 m was observed by DELL *et al.* (1985) on the eastern Coromandel inner shelf. They postulate that the coarse sand moves shorewards during onshore storm swells to the depths of 20 m and possibly to the beach. BRADSHAW (1989, pers. comm.) suggests from analysis of sea-bed drifter experiments and Aanderaa current meter measurements that a downwelling current develops during easterly storms. The current turns to the north further offshore on the inner shelf. Thus, offshore and alongshore sediment transport during storms may be of higher importance than suggested by former research (DELL *et al.*, 1985).

3.5 Previous work on the inner shelf off Tauranga

Previous work on the inner shelf off Tauranga Harbour was undertaken by DAHM and HEALY (1980) and during the THS. DAHM and HEALY (1980) undertook a survey along two transects adjacent to an offshore dumping ground prior, during and subsequent to two periods of dumping. In addition, two transects east and west of the dump-ground, assumed not to be influenced by the dumping, were examined. The examinations were based on textural, mineralogical and visual observations by SCUBA diving. The authors concluded:

i) The sediment facies on the inner shelf near Tauranga Harbour is characterised by two distinct facies - an offshore coarse sand facies and a further inshore fine sand facies. The size of the wave generated bedforms correlates with the grain-size (coarse sand facies - symmetrical ripples with λ = 40-80 cm and η = 10-30 cm; fine sand - ripples with λ = 2-15 cm, η = 2-10 cm). The fine sand contains more pumice than the coarse sand.

ii) The dredge spoil on the inner shelf is only moved by wave action with a $H_{1/3}$ > 1 m, which occurs 30 % of the time.

iii) Pumice and sand < 1.5 phi is preferentially suspended and dispersed from the spoil site by mean flows accompanying wave action in an onshore direction, which leads to a reformation of the "natural" coarse sand facies at the spoil site. The authors associate the onshore movement with Stokesian-type mass transport beneath shoaling waves.

iv) Dispersal of the dredge spoil is unlikely to increase sedimentation rates in the entrance shipping channel, but is evidently promoting beach nourishment at Mount Maunganui.

During the THS a side-scan sonar survey and sediment sampling was undertaken in the entrance and on the inner shelf (Fig.3.3). For the survey area, HEALY (1985) distinguishes a clean sands facies (4a) and a megaripple and sandwave facies (3a+b). HEALY's facies 4a corresponds with DAHM and HEALY's fine sand facies and facies 3 with their coarse sand facies. HEALY also notes that the megaripples are wave-formed and occur in megaripple 'fingers' similar to the observations made on the ebb tidal delta off Whangarei Harbour by BLACK and HEALY (1983).

The sediment samples taken during the Tauranga Harbour Study suggests that fine sand dominates in the survey area (Fig.2.3). To the west an abrupt coarsening in grain-size occurs in the entrance and on the ebb tidal delta indicating strong tidal currents which is consistent with the shell lag and megaripple/sandwave facies described by HEALY (1985) for the area.

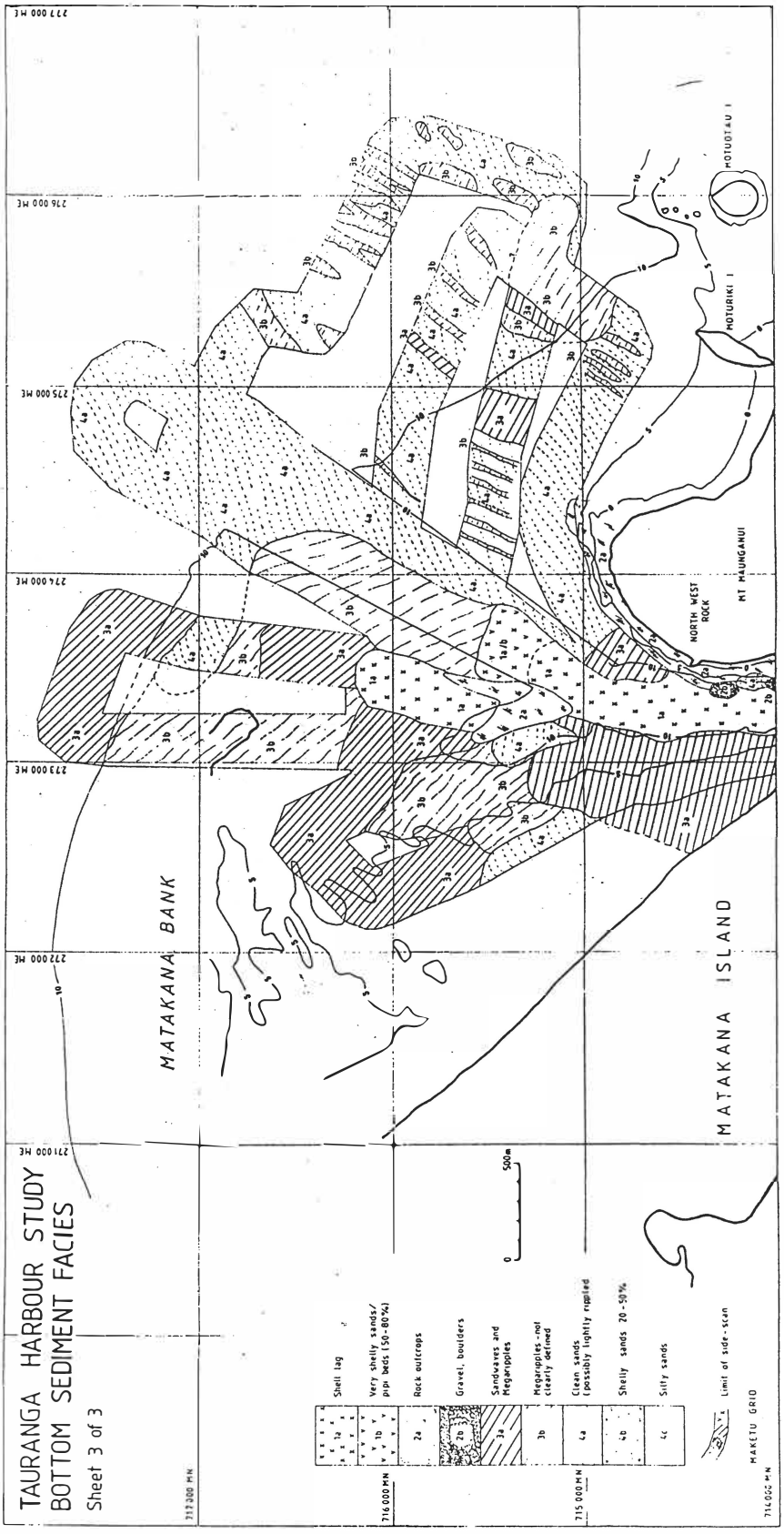

Fig.3.3: THS bottom sediment facies map based on side-scan sonar observations (from HEALY, 1985). Megaripples and clean sands occur in the survey area.

3.6 Conclusions

In the literature, onshore sediment transport over the shoreface has been mostly associated with wave orbital asymmetries under fair weather conditions whereas offshore sediment transport occurs during downwelling events in storms. On the inner shelf, the onshore movement by waves decreases and currents are mostly oriented in a shore-parallel direction.

More recently, laboratory experiments have shown that waves may also cause an offshore movement of sediment. The interaction of waves and currents changes the flow in a non-linear relationship Wave-current interaction influences the magnitude and direction of sediment transport depending on the bed roughness and angle between wave and currents. These new concepts should be taken into consideration when interpreting field studies.

Field studies suggest that the individual shelf morphology, sediment facies distribution and the wave/current regime of a shelf results in a different net sediment flow pattern from one shelf to another.

For the inner shelf off Tauranga an onshore movement of pumice has been postulated by former research undertaken by DAHM and HEALY (1980).

CHAPTER 4

BATHYMETRIC CHANGES OVER A DUMP-MOUND

4.1 Introduction

Sediment dredged from inside Tauranga Harbour and the ebb tidal delta has been dumped at selected dump-sites on the inner shelf off Mount Maunganui (Fig.1.2; 1.3). In order to limit the effects of the dumping it was restricted to dump-sites of relatively small size (600 m x 450 m), which created the build-up of dump-mounds.

High-resolution bathymetric surveys have been used in some areas in the U.S.A. to monitor the stability of dump-mounds over time (BOKUNIEWICZ and GORDON, 1980; MORTON, 1983; HANDS and DeLOACH, 1984; DEMARS *et al.*, 1984). After the end of dumping operations in 1977/78 the Hydrographer's Office of the Bay of Plenty Harbour Board undertook seven echo-sounding surveys over dump-site C until 1987. In this chapter the depth-sounding charts of these surveys were used to qualify and quantify the dispersion of material from the dump-mound at dump-site C over the 10-year period.

4.2 Data

4.2.1 Dumping operations

Dates and volumes of the dredging and dumping operations are necessary to relate bathymetric changes at the dump-sites to dumping of dredge spoil.

Dredging in the Tauranga Harbour has been undertaken for about 40 years. Records of the dredging operations are kept since 1968 (DAHM and HEALY; 1980; BLACK 1984). The dumping occurred on four dump-sites (Fig.1.3). Dump-sites A and B were used for dumping prior to 1977. There is only a small topographic high of 0.5 - 1 m noticeable on the echo-sounding chart of the 1988 survey 100 m west of the western dump-site A margin. During dumping in 1988 the dredged material was, in contrast to former dumping operation,

spread over a large area thus preventing the formation of a dump-mound.

Date	Dredged Channels	Quantity [m3]	Dump-site
prior 1975	all	3,500,000	A,B,C?
1977/78	Entrance	1,200,000	C
	Cutter	600,000	C
	Maunganui	210,000	C (pump?)
1980	Cutter	17,000	C?
1985/86	all	352,000	D
1988	Entrance	31,500	D
	Cutter	62,600	D
	Maunganui	41,700	D

Table 4.1: Dredging operations in Tauranga Harbour from 1968 to 1988. The volumes until 1984 are from DAHM and HEALY (1980) and BLACK (1984); after 1984 from the Hydrographer's Office (BOPHB). Information about the dump-sites before 1977 and the volumes of onshore pumping are rare.

As mentioned in Chapter 1, parts of the dredge spoil were used to build up Sulphur Point as an artificial island. The onshore pumping of material was mainly restricted to the upper Maunganui Channel or Maunganui Roads.

I. Dredging and disposal method
- Dredging technique
- Quantity of spoil released
- Insertion speed
- Mechanical properties of the spoil
- Speed of the discharging vessel

II. Disposal site
- Water depth
- Current in receiving water
- Density gradient in the water column
- Bottom hardness
- Critical erosion velocity of the bottom sediment
- Bottom slope
- Bottom roughness.

Table 4.2: Factors controlling the placement of dredge spoil on open water disposal sites (from BOKUNIEWICZ and GORDON, 1980).

According to BOKUNIEWICZ and GORDON (1980) the placement of dredge spoil on an open water disposal site is controlled by the factors given in Table 4.2.

JOHNSON *et al.* (1988) note that the accuracy of a dumping operation is mainly a function of the water depth, the current motions, especially during dumping operations in deep water (> 100 m) and the discharge rate of the dredge. They note that down to a water depth of 100 m one dredge load of 3000 m^3 spoil can be dumped precisely within a radius of 150 m accumulating to a thickness between 5 and 18 cm. Given a relatively low water depth (15-25 m) at the dump-sites on the inner shelf off Tauranga and dredges with high discharge rates (dredges W.D. Orbell and Geopotes V; MAYNARD, 1988, pers. comm.) the dumping can be expected to be reasonably accurate inside the permitted dump-sites.

The loss of material during dumping due to suspension is according to TRUITT (1988) between 1 and 5%. JOHNSON *et al.*'s (1988) observation that up to 95% of a sand/silt mixture is deposited within 1 hour down to a water depth of 200 m indicates a similar trend. Turbidity measurements over dump-site D off Tauranga within 30 minutes after the dumping of medium sand in 1988 showed no abnormally increased turbidity values suggesting the quick deposition of the material and only a small loss of material due to suspension.

4.2.2 Sounding charts

The hydrographers of the BOPHB undertook seven echo-sounding surveys over dump-site C and its vicinity between 1978 and 1987 (survey dates: 27/7/78; 7/1/80; 30/3/81; 23/12/83; 30/10/85; 15/10/86; 21/9/87). The surveys were extended from 1986 onwards further offshore due to dumping operations in 1985/86 at dump-site D. The surveys were undertaken along parallel lines (distances between lines 50-100 m), varying in direction and area covered between each survey. An Atlas Deso 20-33kHz echo-sounder was used to measure the water depth and the position was fixed with sextants. The measured water depths were reduced to Moturiki datum, the regional datum relating to the Mean Sea Level (MSL), and drawn

up in a 1:4000 chart.

4.3 Methods

The SAS system, available on the University of Waikato's VAX computer system, was used to examine bathymetric changes by producing two- and three-dimensional plots and map plots.

Four transects crossing the dump-mound at different angles were produced by digitising the water depth every 50 m off the sounding charts along a line and loading it to a data file (Fig.4.1). For the three-dimensional plots and map plots the same system was used by subdividing a 600 x 600 m grid oriented parallel with the dump-site in a N-S direction in 50 x 50 m cells (Fig.4.1).

The GPLOT procedure of the SAS system was applied to plot the transects as distance versus water depth. The line was smoothed with the SMxx statement (SM5; SAS/GRAPH User's Guide, 1985: p.70). The transects were first plotted to include all seven surveys, and then reduced to five surveys for better clarity.

The SAS system G3D procedure was applied to plot a 3D picture of the 1978, 1980, 1983 and 1986 bathymetry surveys with the x-axis oriented to the east and the y-axis to the north. The GRID/SPLINE statement of the SAS system was used to smooth the contours of the 3D plot. The option results in an order N^3 algorithm being used, where N is the number of input data points (SAS/Graph User's Guide, p.65). In this case the number of points was increased from 144 to 900 by reducing the interval between points from 50 to 20 m.

With the GCONTOUR procedure of the SAS system the bathymetry and bathymetric changes between two surveys were transformed into a two-dimensional map.

To quantify the volume changes of the grid between surveys, a PASCAL program was written. The program calculated the differences in water depth of a 50 m square, transformed it to a volume and added up the volumes of the squares, to obtain the net change in volume of the whole grid. Additionally, accretion and degradation

within the grid were calculated.

The programs used for the graphic display and volume calculations are presented in App.4.

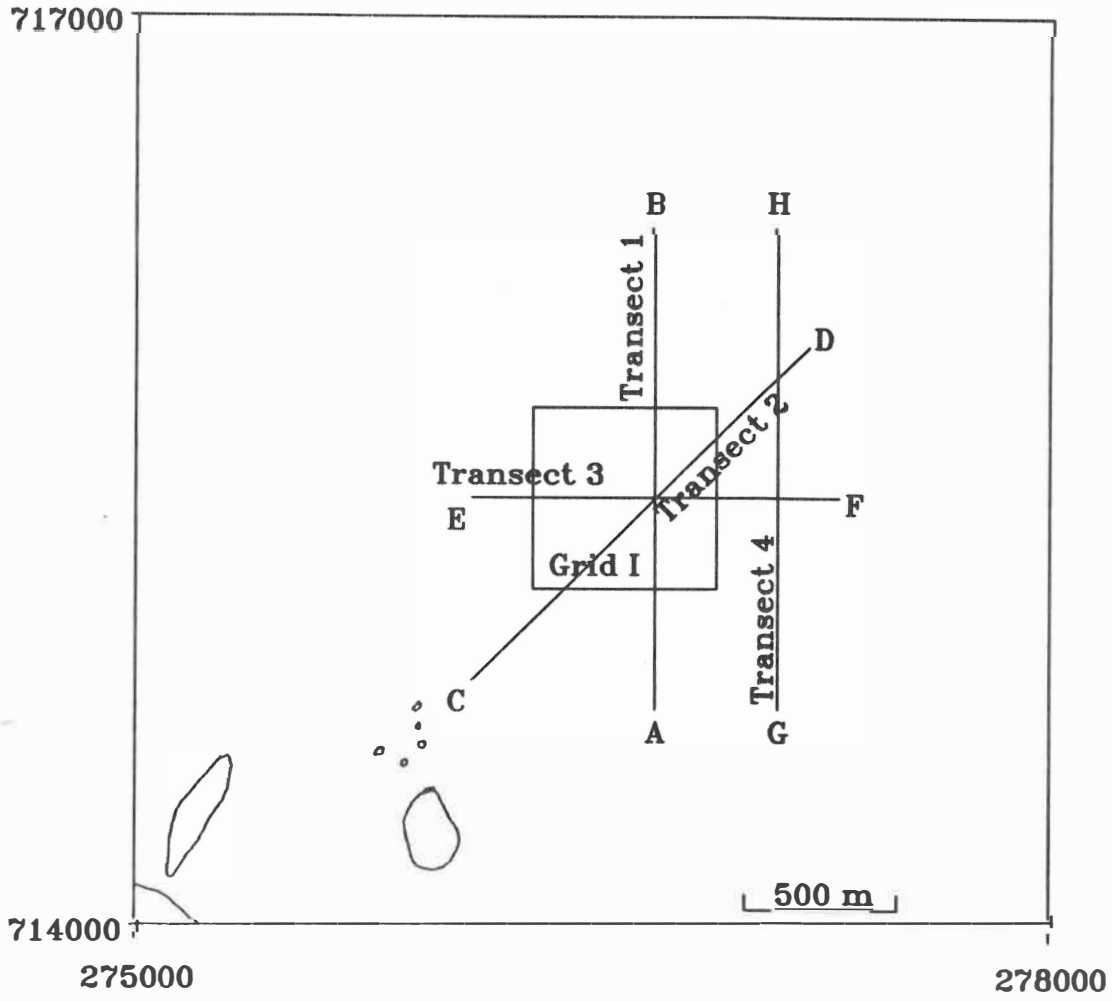

Fig.4.1: Location of transects and grid

4.4 Limitations of data and method

According to the hydrographer (STEPHENSON, 1988, pers. comm.) the accuracy of the echo-sounding surveys lies within ± 0.05 m for the water depth and within 10-20 m for the position fixing with sextants under calm conditions. With an increase in wave height the accuracy of the records decreases. A value of ± 0.1 m has to be added for instrument and operation error and for the reduction of the measured water depth to the tidal datum.

The accuracy of the data input for the transects and the grid plots is limited by the density of the sounding data over the survey area. The distance between sounding lines is up to 200 m so that some values had to be estimated especially when a transect or a grid line crossed a sounding line. The accuracy of the digitising should be within ± 0.05 - 0.1 m. Especially at the relatively steep slopes of the dump-mounds the inaccuracy of the position fixing can cause a wrong digitised water depth.

The inaccuracy of the data used for producing the plots should not exceed ± 0.2 - 0.3 m. NIEDORODA *et al.* (1982) and MORTON (1983) give a similar value for the accuracy of their sounding measurements.

A statistical analysis, outlined by MORTON (1983), was used to evaluate the standard error for the grid. The standard error is given by

$$\epsilon = A\,\sigma / M(n-1) \qquad (4.1)$$

where A is the area of the survey region (3.6×10^5 m), σ is the standard deviation (± 0.2 m), M is the number of cells (144) and n is the number of measurements per cell (c.1.5). Because the number of measurements per cell is relatively small, the standard error is high with 8500 m^3 compared with the error in MORTON's survey (1200 m^3). Since two surveys are required to accomplish a volume difference calculation, the total error could be as much as 17,000 m^3.

In order to avoid large volume errors in the future, the distance between echo-sounding lines should be reduced to 20 - 30 m.

4.5 Observations

The three transects (Fig.4.2, 4.3, 4.4) crossing the dump-mound at dump-site C show that a dump-mound of about 800 m diameter and up to 9 m high was built by dumping prior to 1978. The steepness of the dump-mound ranges between 1:40 and 1:60. The slope is steeper and longer in the east than in the west of the dump-mound (Fig.4.5). The regular shaped dump-mound and the lack of unconformaties around the mound indicate that the dumping was reasonably precise.

The transects and the three-dimensional pictures of the bathymetry of the dump-mound (Fig.4.6a-d) demonstrate a flattening between 1978 and 1986. The rate of reduction of the mound height decreases with time being greatest between 1978 and 1980 (Fig.4.2, 4.4a; 1.2 m from the top of the mound) and tending to zero from 1985 onwards (Fig.4.4b; Fig.4.7) which is also indicated by the 1988 survey. Furthermore it appears that the summit of the dump-mound seems to migrate between surveys, in particular between the 1980, 1981 and 1983 surveys (Fig.4.2, 4.4a). This could be either the result of inaccurate position-fixing or a real change.

Contour plots were undertaken to identify bathymetric changes within the grid. As the bathymetric changes between the 1978 and 86 surveys are the greatest, this plot was used for the observation to avoid misinterpretations caused by the limited accuracy of data and method. The contour plot (Fig.4.8) shows erosion of material in the north of the grid and accumulation in the south. The loss of material is greatest (> 3 m) at the top of the dump-mound. The accumulation has its maximum in a short distance south of the dump-mound with over 1.5 m. The same trend is observed when comparing both the 1978 and 1983 and the 1980 and 1986 surveys (Fig.4.9, 4.10).

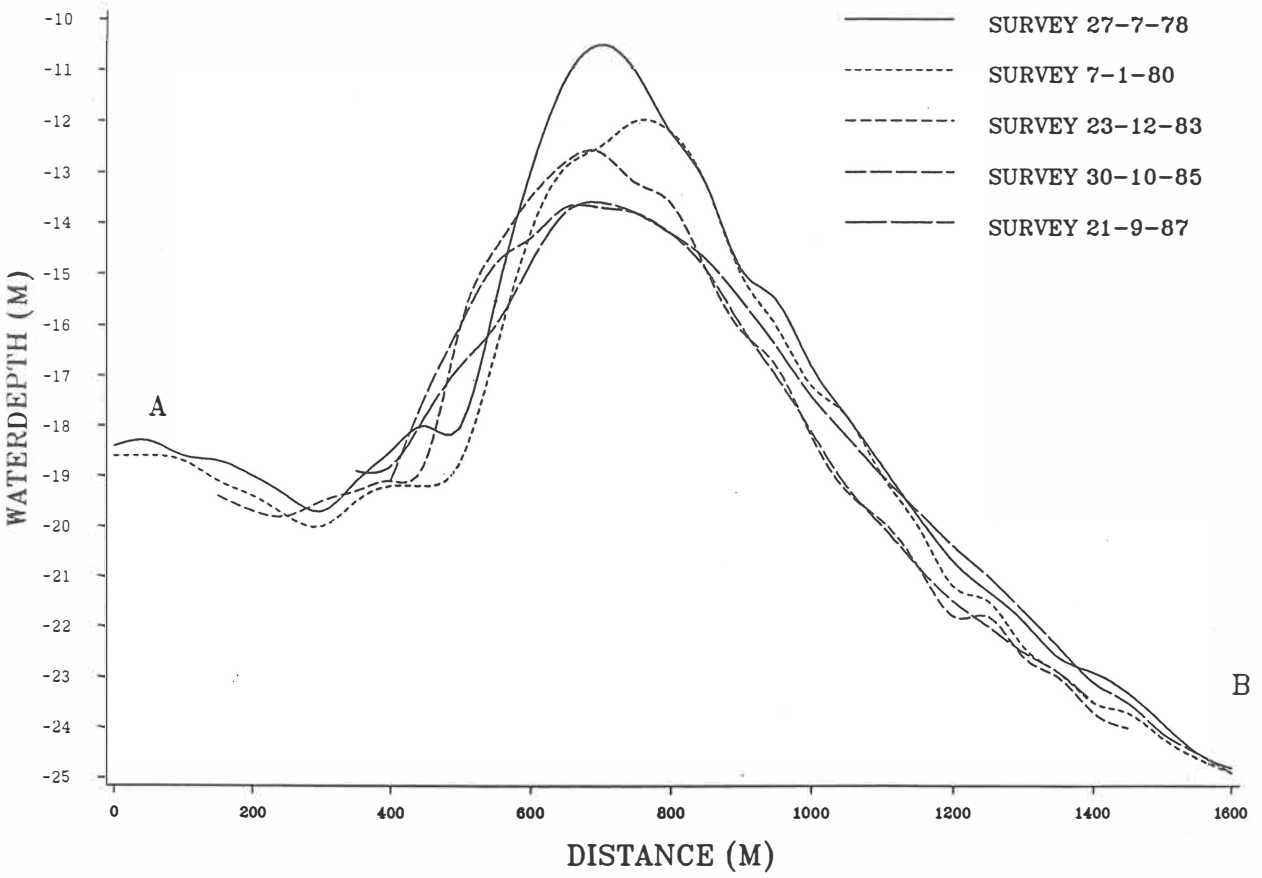

Fig.4.2: Transect 1

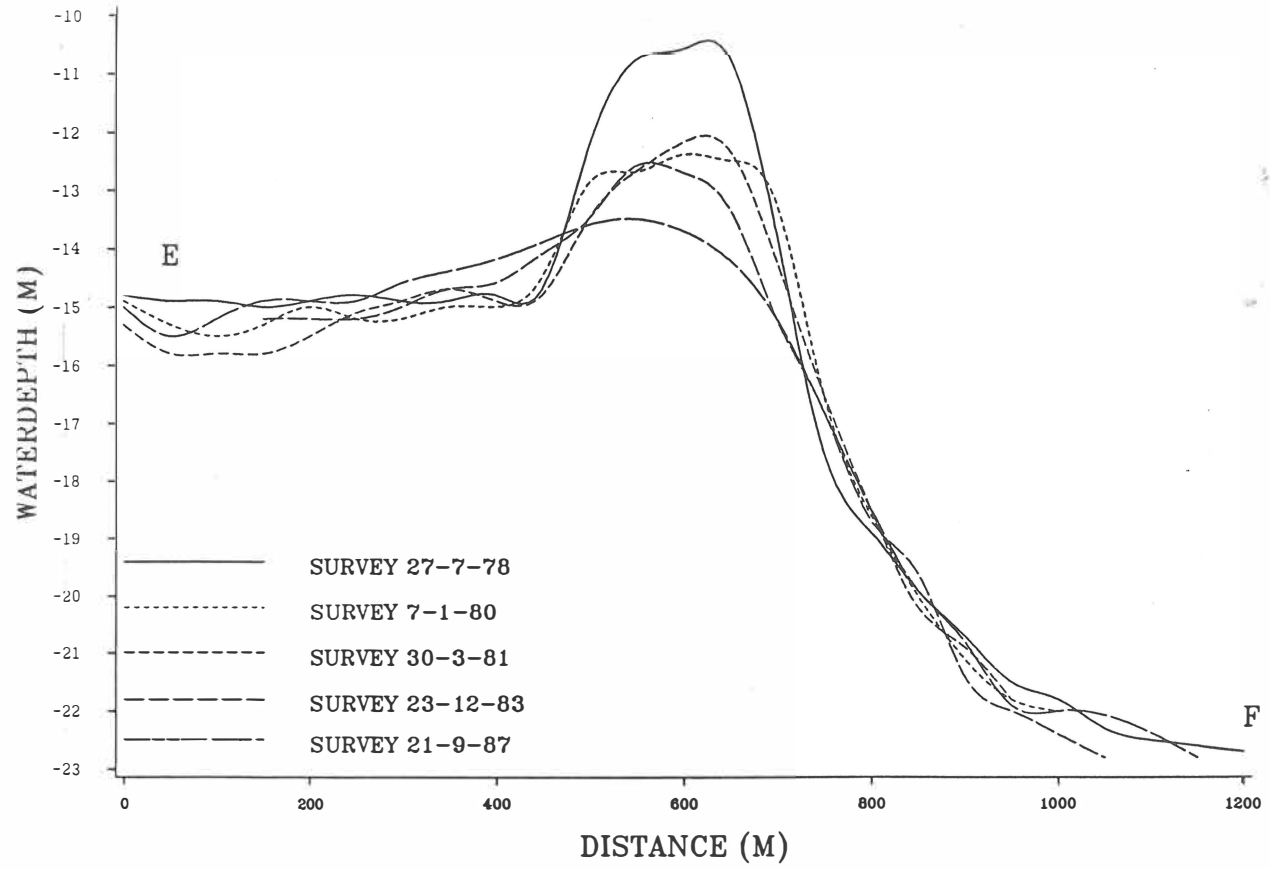

Fig.4.3: Transect 3

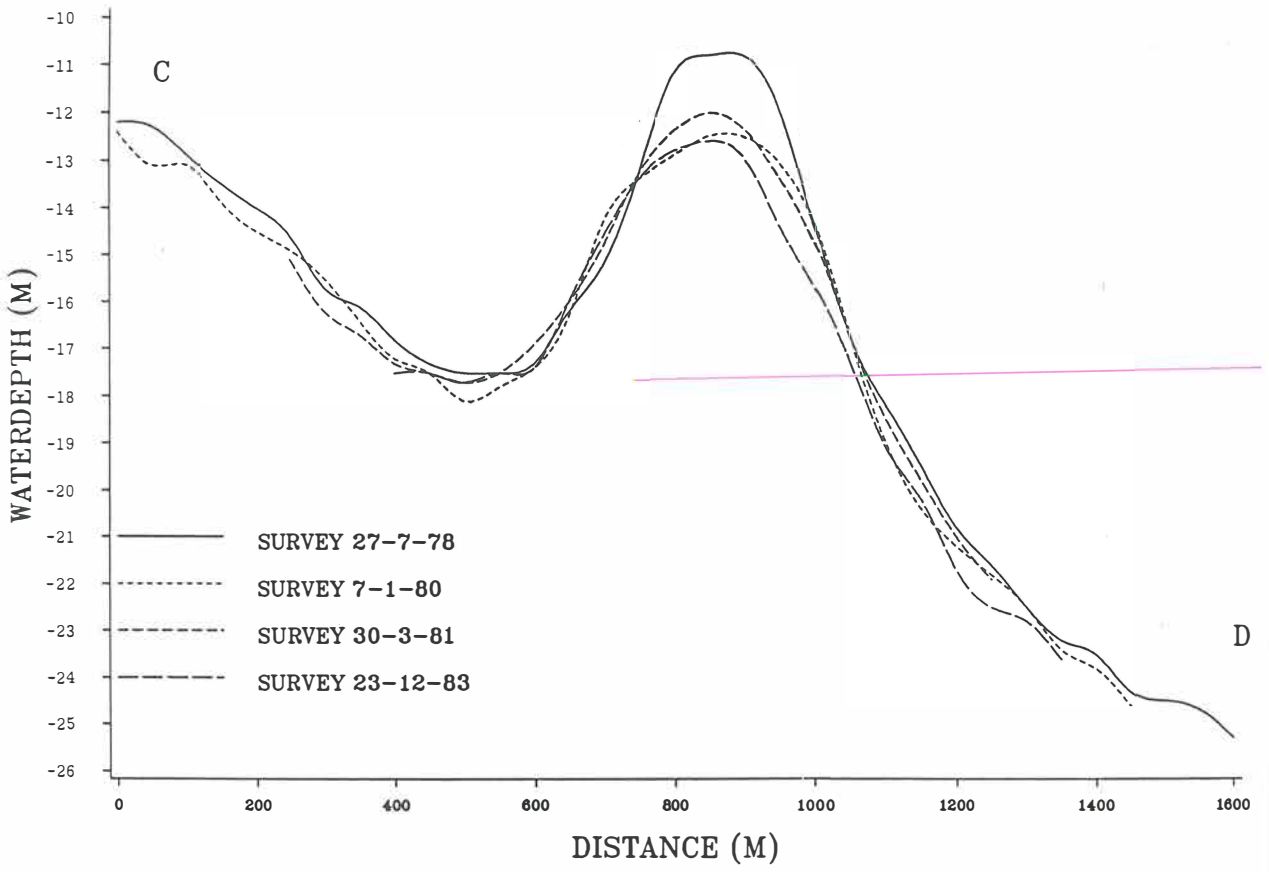

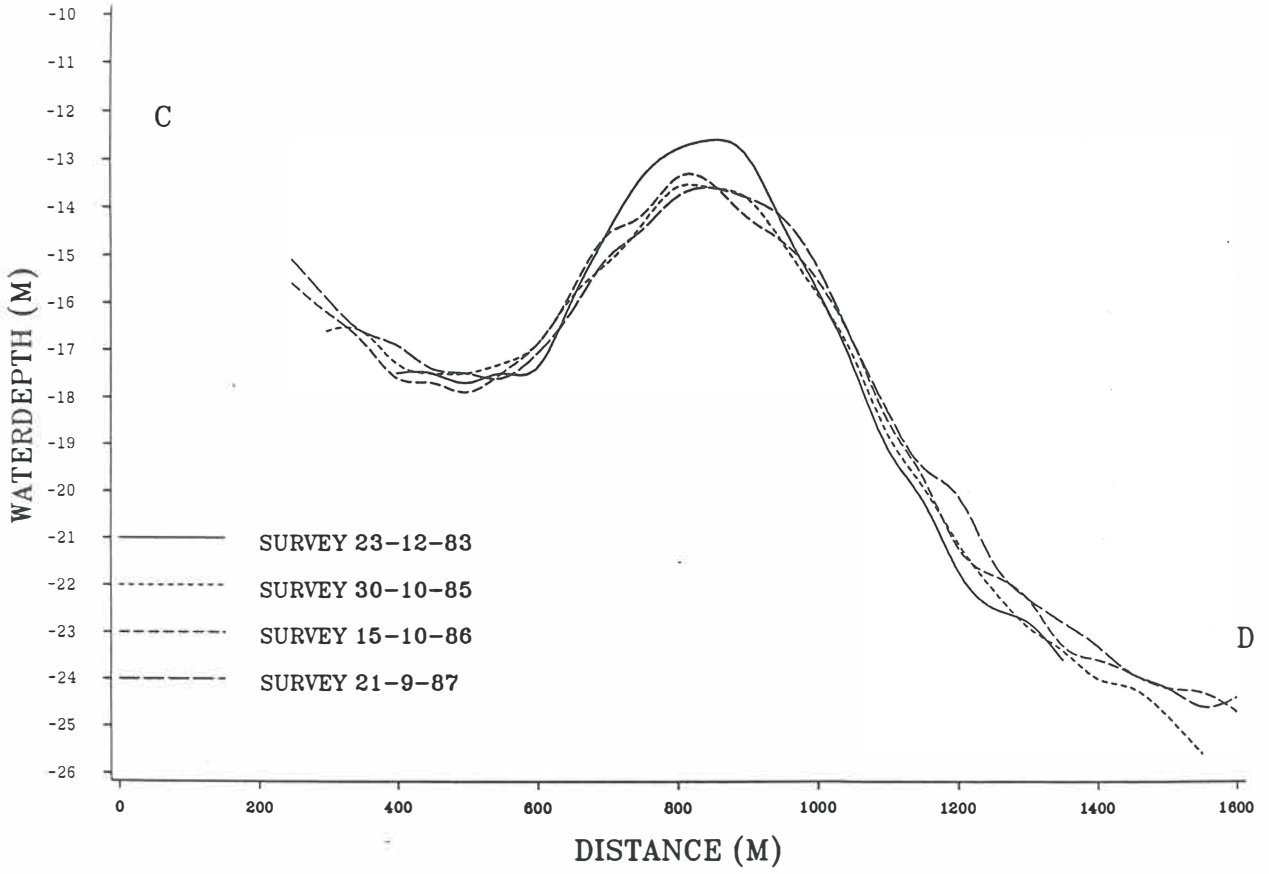

Fig.4.4: Transect 2; upper plot (a) shows the high volume reduction between 1978 and 1980 compared with after 1983 (b).

BATHYMETRY 1978

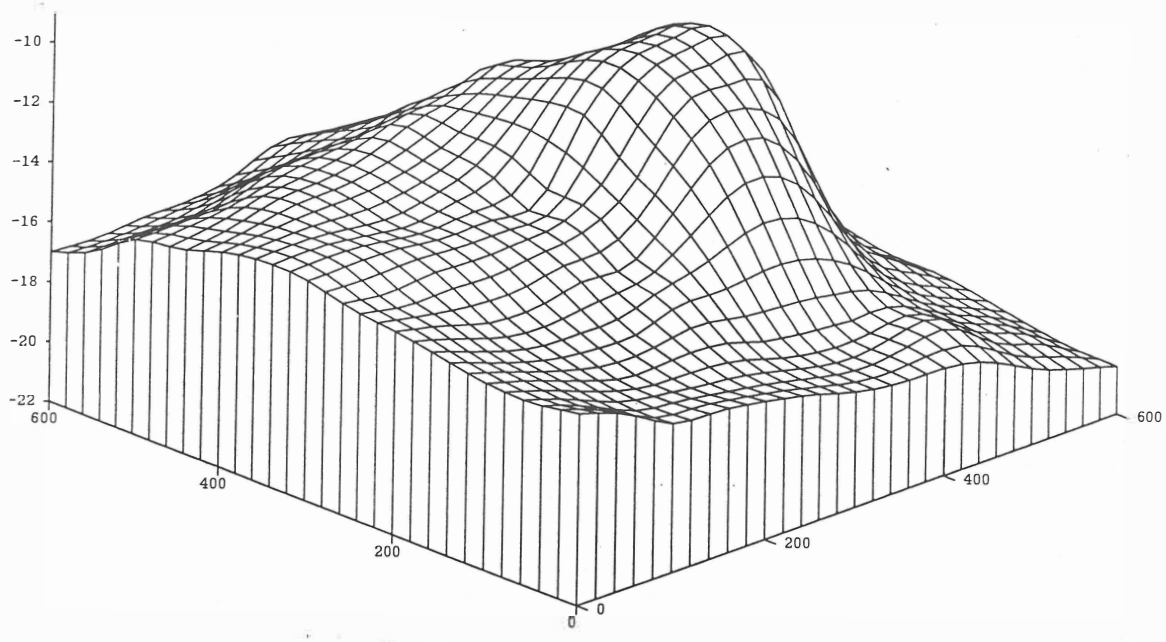

BATHYMETRY 1980

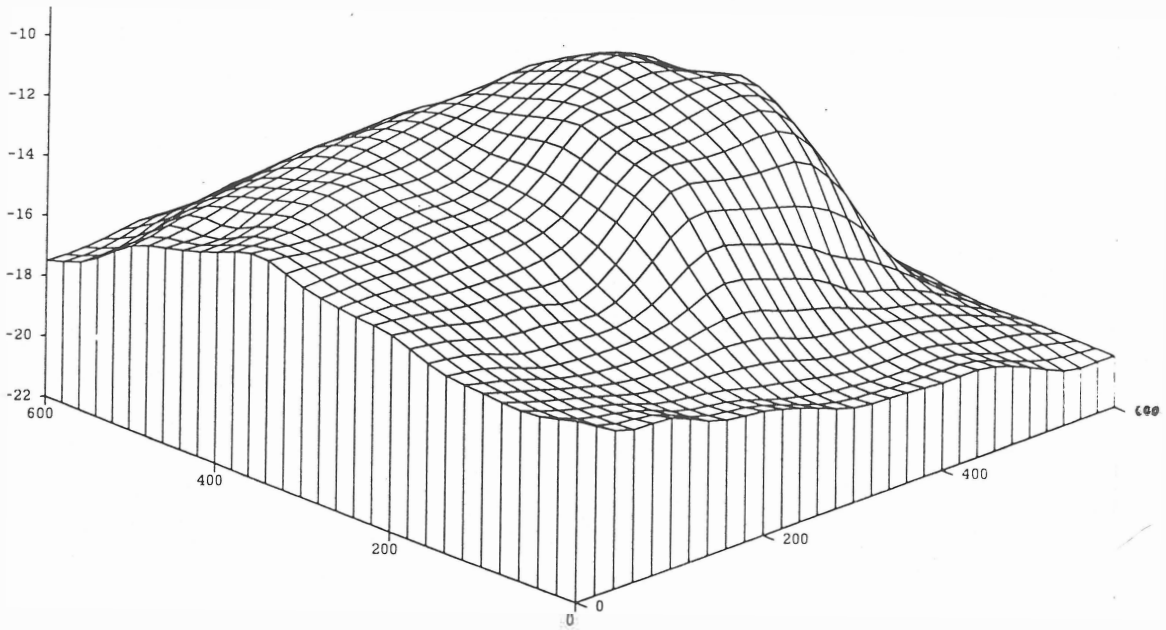

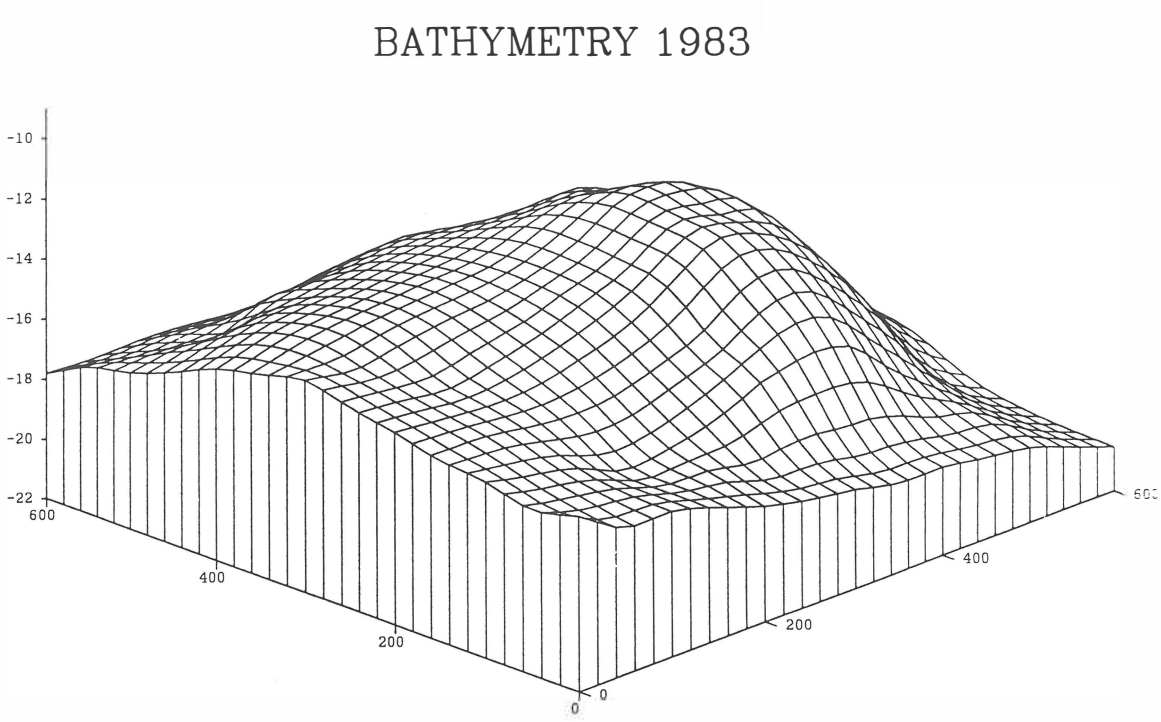

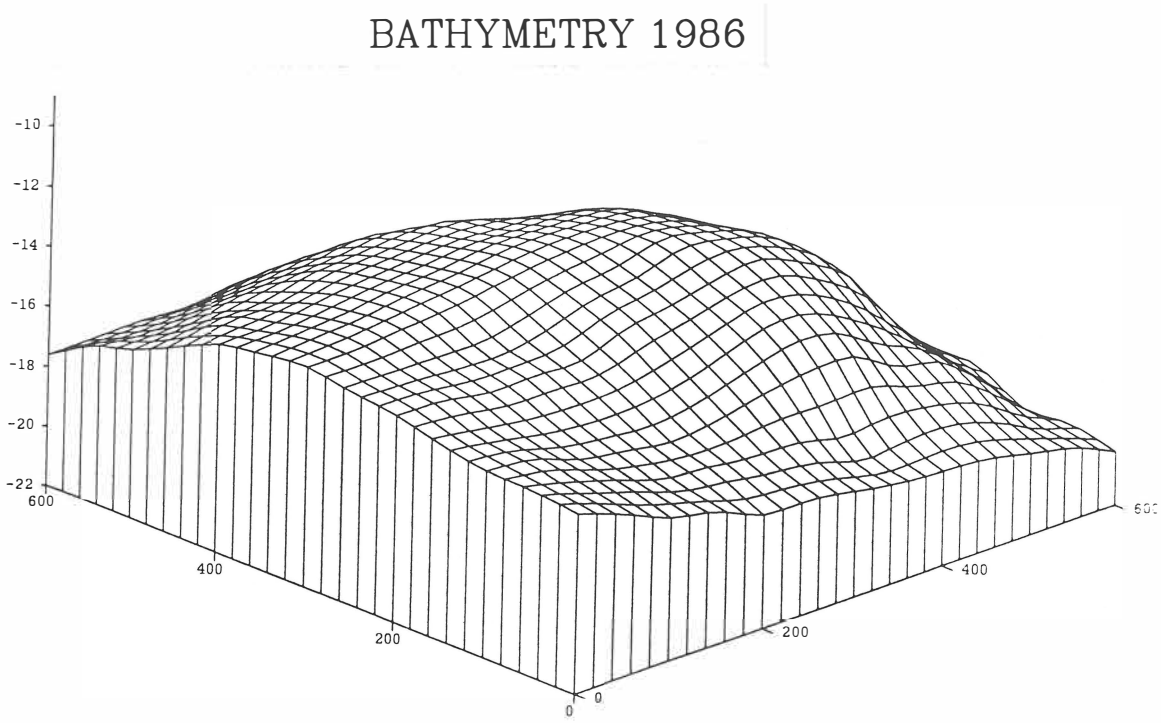

Fig.4.6a-d: 3D plots of dump-mound C between 1978 (a) and 1986 (d). View from the southwest. A flattening of the dump-mound is clearly noticeable.

BATHYMETRY 1978

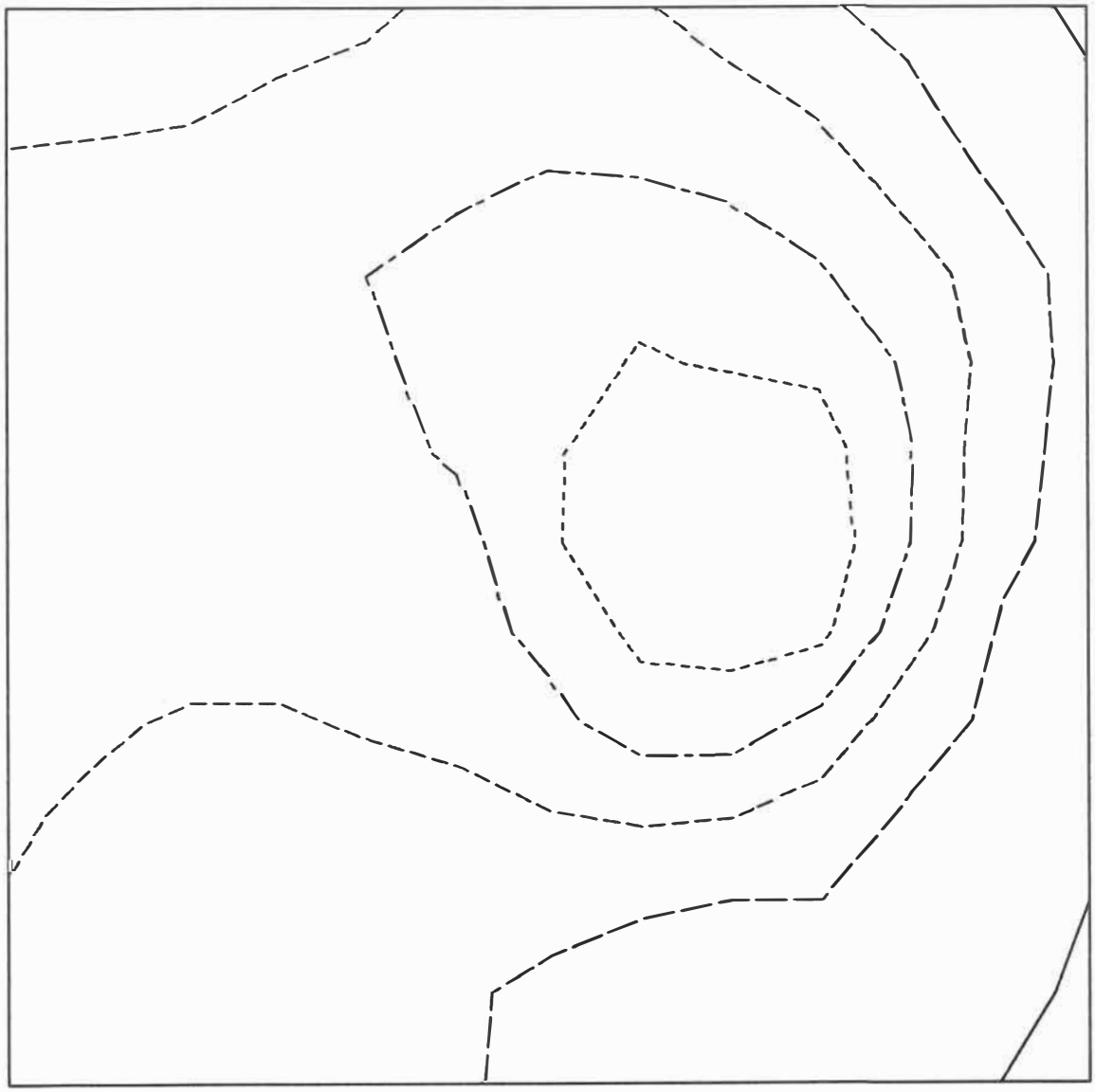

Z78 ----- 12 -—-- 14 ---- 16 —— 18 ——— 20

Fig.4.5: Contour plot of the bathymetry subsequent to the dumping in 1978. Note the steeper gradient on the eastern side compared with the western side.

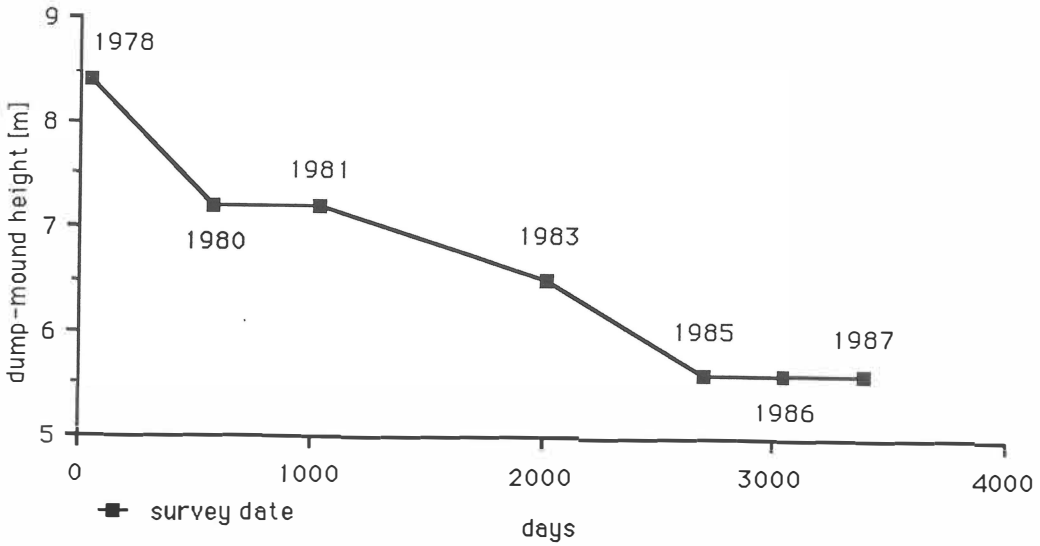

Fig.4.7: Reduction in dump-mound height between 1978 and 1987. The reduction rate is highest between 1978 and 1980 and varies from 1980 onwards, possibly reflecting storm events.

Transects 1 and 2 (Fig.4.2, 4.4) show similar trends with accumulation of material in an onshore direction and erosion offshore. The area of significant accumulation is restricted to the region directly shoreward of the dump-mound. No accumulation is detectable further than 300 m away from the dump-mound. Accretion is higher at transect 1 in the south than at transect 2 in the southwest. Loss of material offshore occurs up to 1985 and then accumulation starts (Fig.4.2). Transect 3 (Fig.4.3) indicates that no significant bathymetric changes occur east of the dump-mound whereas accumulation occurs from 1983 onwards in the west. At transect 4 (Fig.4.11) east of the dump-mound a decrease in water depth is noted subsequent to dumping in 1978 until 1983 with the sea-floor elevation increasing again after the dumping in 1985. The dump-mound at dump-site D shows the same significant reduction in height in the first year which was observed at the dump-mound at dump-site C.

The volume calculations (Table 4.3) are consistent with the graphic observations. The loss of volume is highest in the first two years and decreases with time. Volume changes between 1980 and 1983 show that the net loss of material out of the grid is relatively small with about 40,000 m^3 compared to the movement of material within the grid. Between 1983 and 1986 accumulation of material inside the grid exceeds the loss of volume.

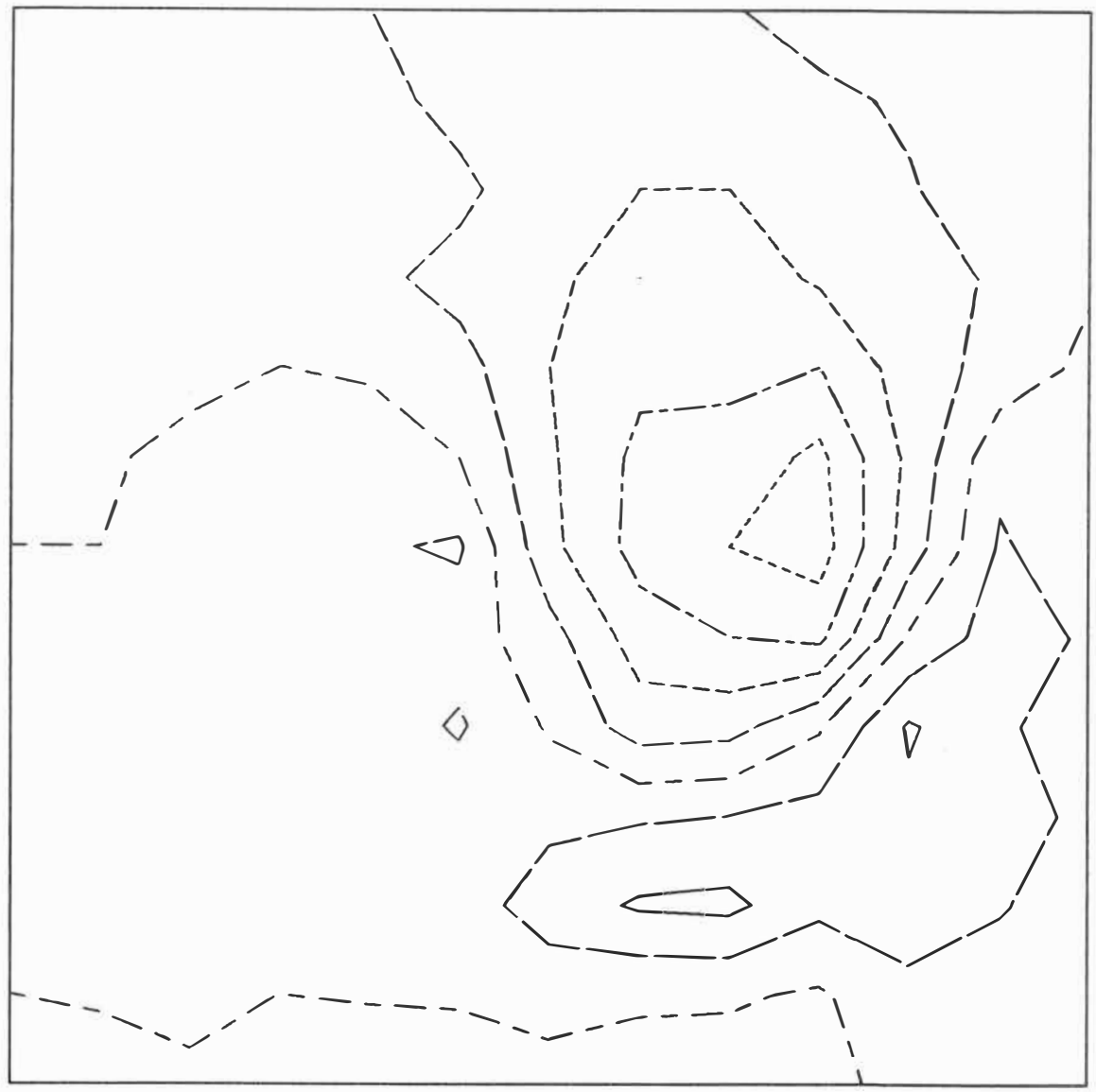

----- -3.2 -—-- -2.4 ---- -1.6 —— -0.8 — — · -0.0

——— 0.8 ——— 1.6

Fig.4.8: Contour plot of bathymetric changes over dump-site C between 1978 and 1986. The plot indicates the loss of volume from the dump-mound and accumulation in its southern vicinity.

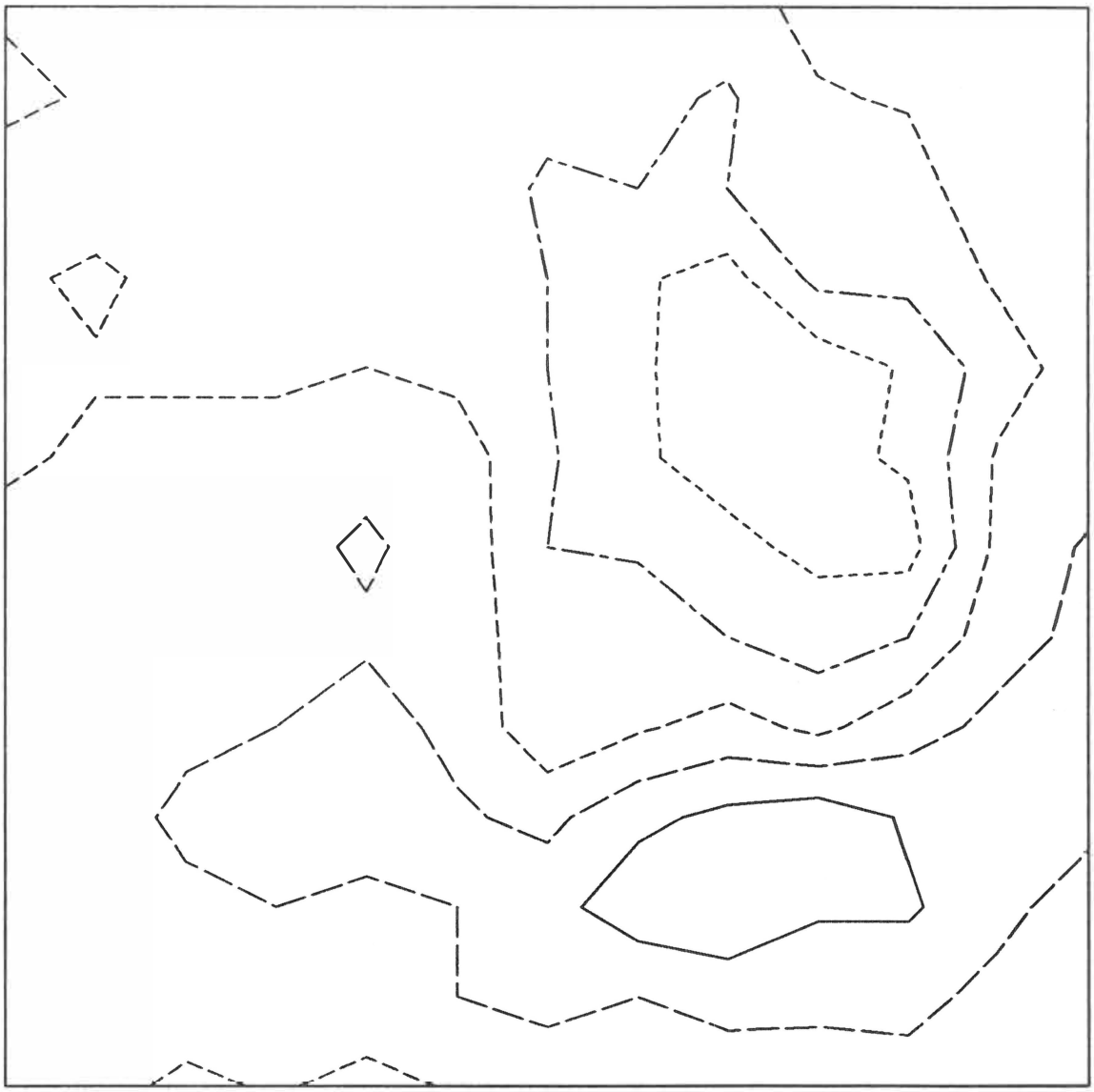

----- -1.6 -—-- -0.8 – – – – 0.0 — — 0.8 —— 1.6

Fig.4.9: Bathymetric changes between 1980 and 1986.

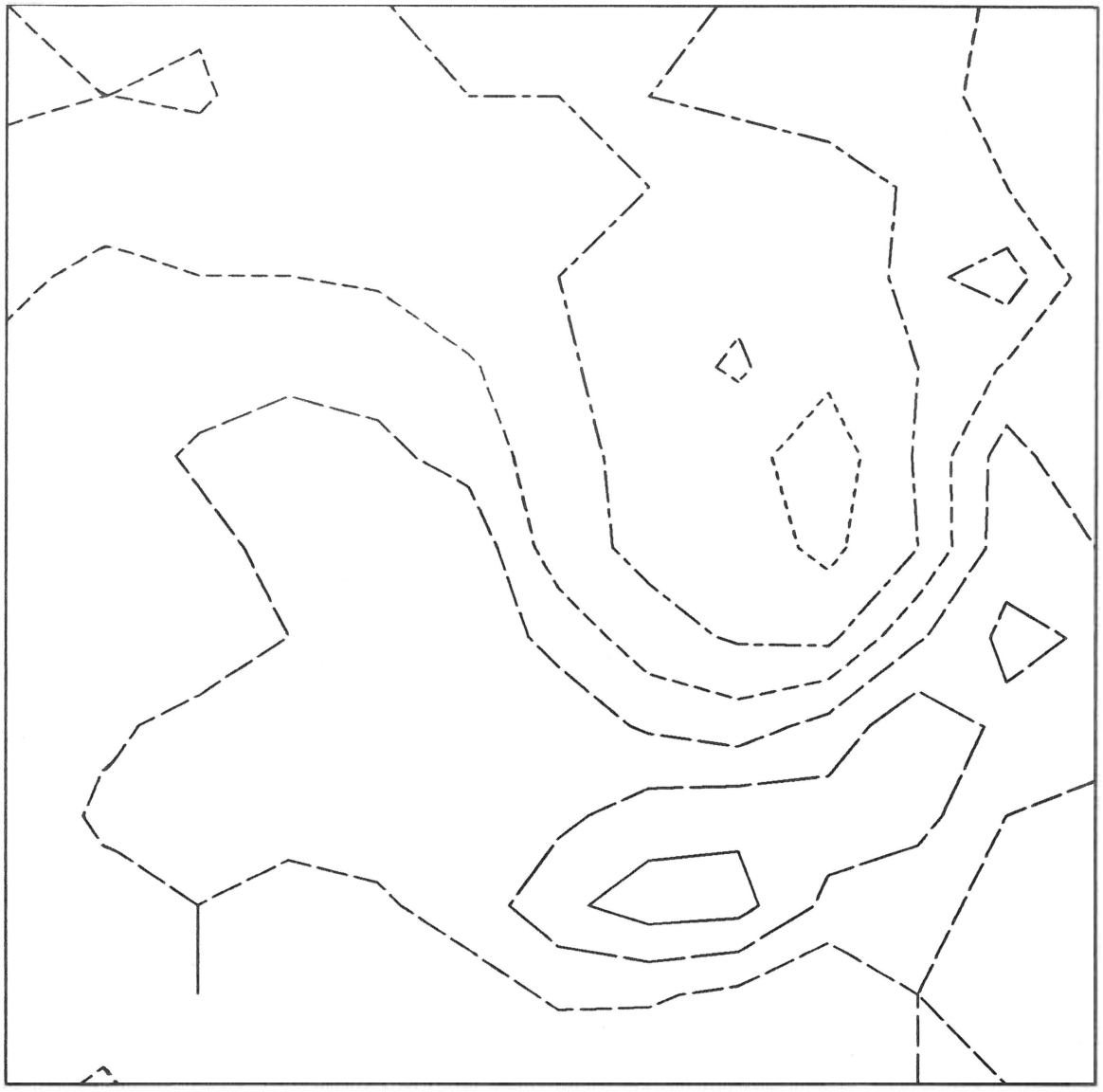

----- -2.4 -—-- -1.6 - - - - -0.8 —— —· -0.0 ——- 0.8

—— 1.6

Fig.4.10: Bathymetric changes between 1978 and 1983. A similar trend as observed in Fig.4.8 indicates that the changes are real.

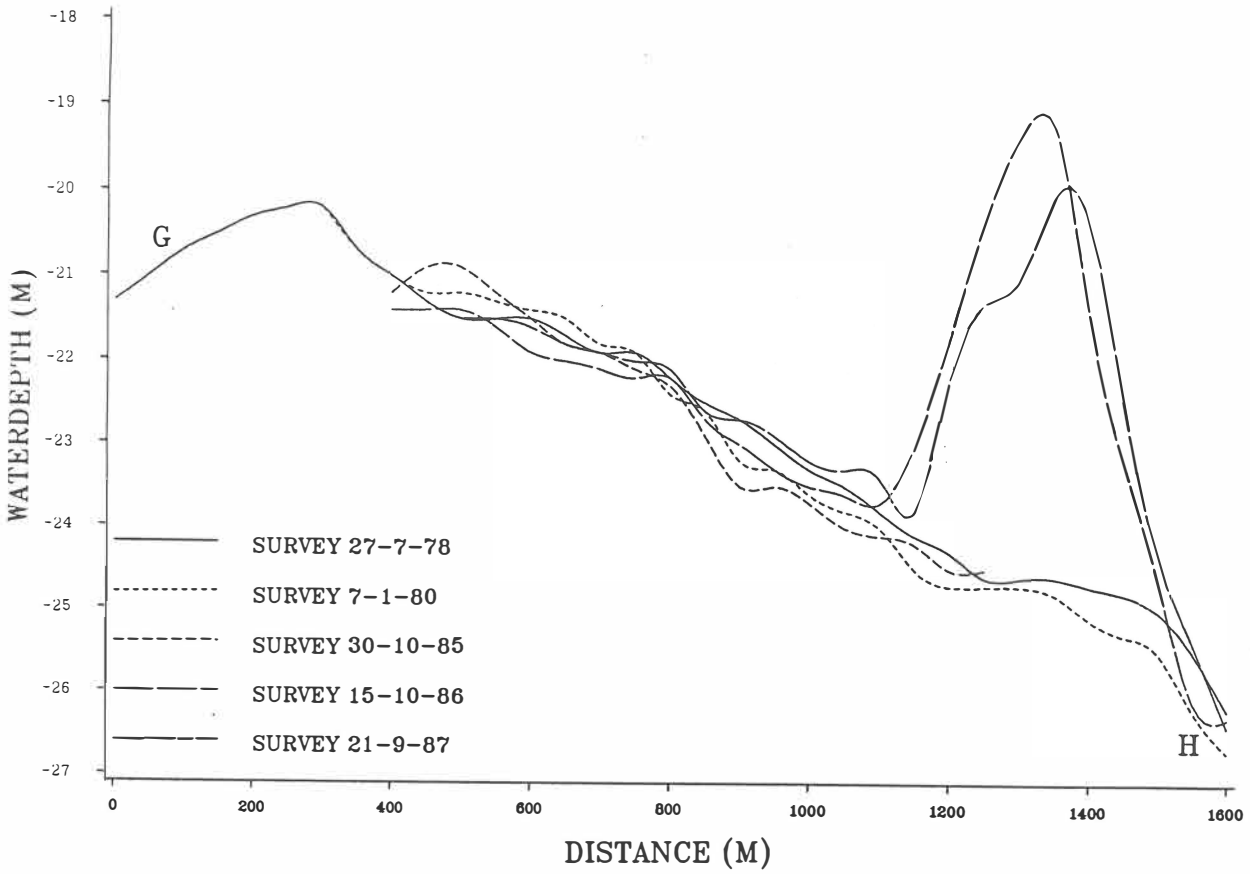

Fig.4.11: Transect 4 in the eastern vicinity of dump-mound C. A volume reduction is also observed at the dump-mound at dump-site D.

	Survey periods			
[m^3]	78-80	80-83	83-86	78-86
Volume change	-192,700	-40,750	+68,000	-124,750
Reduction	-238,000	-130,875	-30,125	-200,500
Accumulation	+45,300	+90,100	+98,100	+75,750

Table 4.3: Volume changes in the grid between 1978 and 1986.

4.6 Interpretation

The flattening of the investigated dump-mound between 1978 and 1985 is caused by two processes:

1) Self-consolidation through mechanical compaction within the mound;

2) Loss of material caused by erosional processes.

4.6.1 Self-consolidation process

Because of the high water content of the dredge spoil (KESTER *et al.*, 1983), self-consolidation of dump-mounds is an important process (BOKUNIEWICZ and GORDON, 1980; DEMARS *et al.*, 1984). DEMARS *et al.* (1984) undertook echo-sounding surveys of dump-mounds and compaction tests of the dump-mound material in the Long Island Sound at the east coast of the U.S.A. to assess the settlement and stability of dump-mounds. They concluded from the echo-sounding data that a contaminated mud mound capped with sand (about 1/2 mud, 1/2 sand) is consolidated to 90% after 3.4 years. The field settlement of the mound was about 1.5 times faster than the laboratory tests suggested. The difference is probably due to erosional processes acting on the mound as MORTON (1983), monitoring the same mounds, reports a significant loss of volume subsequently to a hurricane with large waves.

Compaction tests of dump-mound material were not undertaken in this study so that it is not possible to prove that compaction of the Tauranga dump-mounds really occurs and how significant it is in relation to erosion. Although the results from DEMARS *et al.* (1984) are not transferrable to the Tauranga conditions because of different dump-mound material and hydrodynamic conditions, they strongly suggest that compaction occurs and give an indication which time periods are involved in the consolidation of a dump-mound.

The large reduction in dump-mound volume between 1978 and 1980 together with the small accumulation near the dump-mound (compared with later periods) is supportive that compaction was a significant process in the first two years after the dumping (Table 4.4). The July 1978 storms which may have also explained the reduction of volume by a large erosion event occurred one week before the echo-sounding survey. The dump-mound reduction decreases significantly after the 1980 survey which may be caused by the dumping of a small (compared to former dump amounts) quantity of dredge spoil (17,000 m^3) in 1980 (Table 4.1) but also suggests that compaction processes are of minor importance.

4.6.1 Dispersion from the dump-mound

Reduction of dump-mound volume and accumulation of material south of the dump-mound between 1978 and 1985 suggest that erosion of dredge spoil, subsequent short-distance transport in a southerly onshore direction and deposition occur (Fig.4.8 - 4.10). The increasing accumulation of material inside the grid from 1980 onwards is suggestive that dispersion processes dominate over compaction. The constant height of the dump-mound from 1985 to 1988 suggests that the mound is stable. The positive volume balance of the grid since 1986 can be explained by dumping operations in 1985 at dump-site D. Possible random dumping and onshore sediment movement from the new dump-mound are likely to cause accumulation of material in the grid. The rate of reduction in dump-mound height cannot be expressed by either a linear or exponential function (Fig.4.7) which suggests that the frequency of erosional events (storms) is an important factor for the settling and dispersion of dredge spoil.

The period between 1980 and 1983 can be considered as not strongly influenced by compaction and dumping in the vicinity of the dump-mound. Therefore it should characterise the dispersion pattern of dredge spoil best. The volume calculations and the contour plot (Fig.4.12) indicate that 70 % of the material eroded from the north of the grid accumulated in the south of the mound inside the grid and that only 30 % were dispersed over a larger area. The transects support the trend that most of the eroded material from the dump-mound is deposited within a semi-circle of 300 m south of the dump-mound. To trace the dispersion of the dredge spoil over larger distances others methods based on the sediment characteristics of the dredge spoil are more appropriate (Chapter 5).

The subsequent deposition of eroded material in the south of the dump-mound is indicative of onshore movement of dredge spoil from the dump-site.

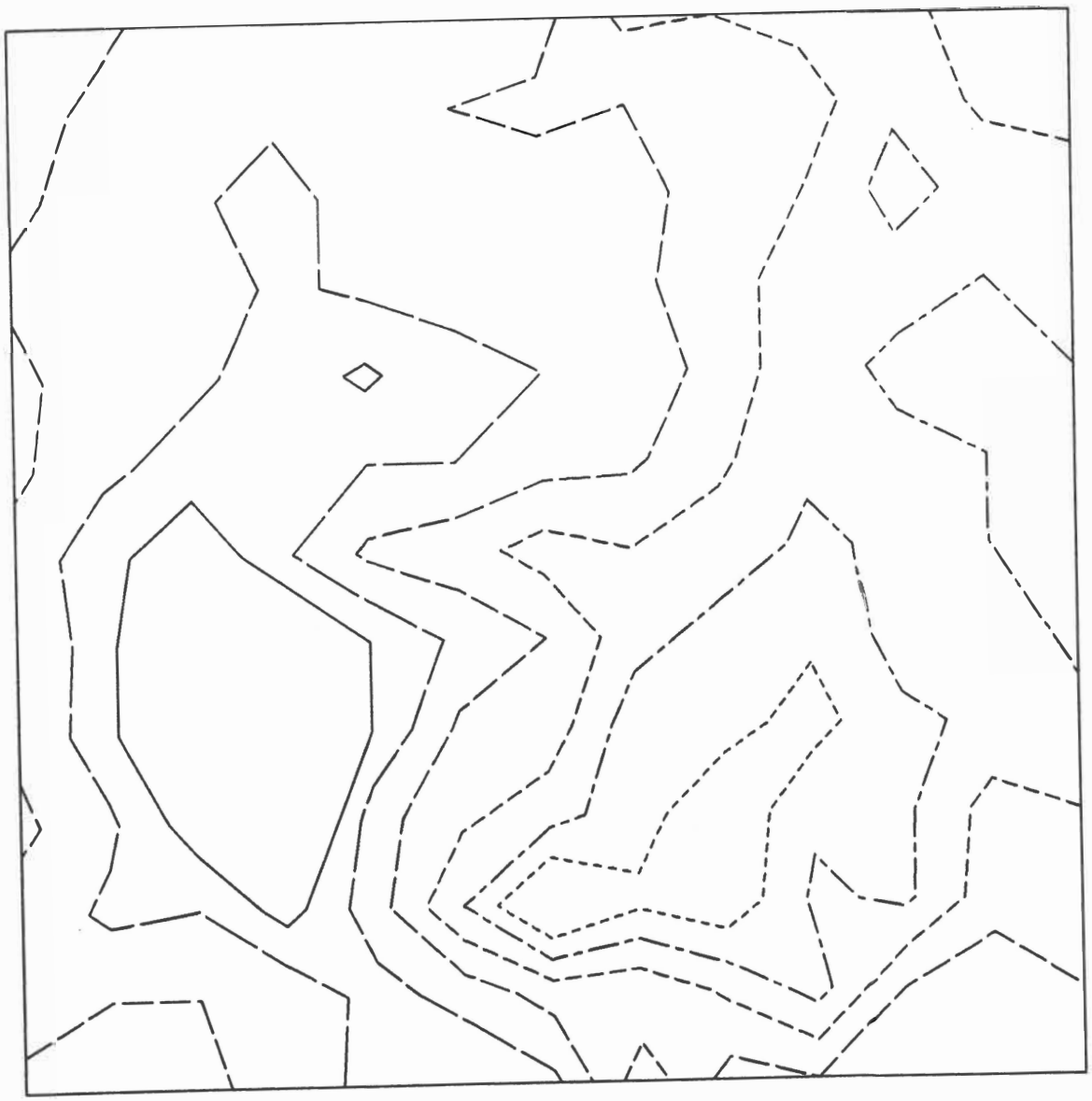

----- -1.5 -—-- -1.0 – – – - -0.5 —— 0.0 ——- 0.5

——— 1.0

Fig.4.12: Bathymetric changes between 1980 and 1983.

4.8 Conclusions

1) The investigated dump-mound flattens over time. The reduction of the dump-mound height is largest in the first two years (1.2 m or c. 240,000 m^3 volume loss) and decreases after 1980. After seven years the mound appears to be stable.

2) Although no compaction tests were undertaken in this study, overseas investigations (DEMARS *et al.*, 1984) strongly suggest that, apart from erosion, self-consolidation through compaction is a significant process in dump-mound reduction. Accumulation rates inside the grid are supportive of the DEMARS *et al.* (1984) data that compaction rates are highest in the first three years after the dumping and of minor importance afterwards.

3) Volume calculations and graphic display suggest that the dredge spoil eroded from the dump-mound accumulates to about two thirds in a small semi-circle 300 m south of the dump-mound. The rest is transported over a large area not monitored during the depth sounding surveys.

4) The irregular settling rate of the dump-mound suggests its reaction to the frequency of erosional events during storms.

5) The major accumulation of dredge spoil south of the dump-mound suggests an onshore movement of material in a southward direction on the inner shelf.

CHAPTER 5

SEA-FLOOR SURVEY

5.1. Introduction

A sea-floor study of the survey area and of the control-site was undertaken in order to identify the natural sediment distribution on the inner shelf off Tauranga and changes caused by dumping of dredge spoil and its dispersion. The study included a side-scan sonar survey, visual sea-floor observations by underwater-video and SCUBA diving, sub-bottom seismic profiling and sediment sampling. Parts of the sea-floor survey data have already been reported by HEALY *et al.* (1988). In this chapter the sediment properties of the material from the dredge-sites are described first. Then the results of the sea-floor survey on the inner shelf are presented. Based on these observations, the sediment facies distribution and its implications for sediment transport are interpreted.

5.2 Characterisation of sediment from the dredge-sites

In order to determine the textural and mineralogical differences between natural shelf sediments and the dumped material, it was necessary to obtain information about the sediment from the dredged channels inside and outside the harbour. As mentioned in Chapter 2, textural data collected during the THS were available for the characterisation. In addition, DAHM and HEALY (1980) took seven samples from the dredge hopper operating in 1977/78. During this study six samples were taken from the site of the 1988 capital dredging adjacent to Sulphur Point.

5.2.1 Textural properties of dredged sediments

Sediment samples taken from the lower Maunganui Channel and Cutter Channel during the THS are consistently moderately to moderately well sorted medium sands (Fig.5.1; M_z = 1 - 2 ϕ). The sorting decreases in the upper Maunganui Channel or Maunganui Roads further

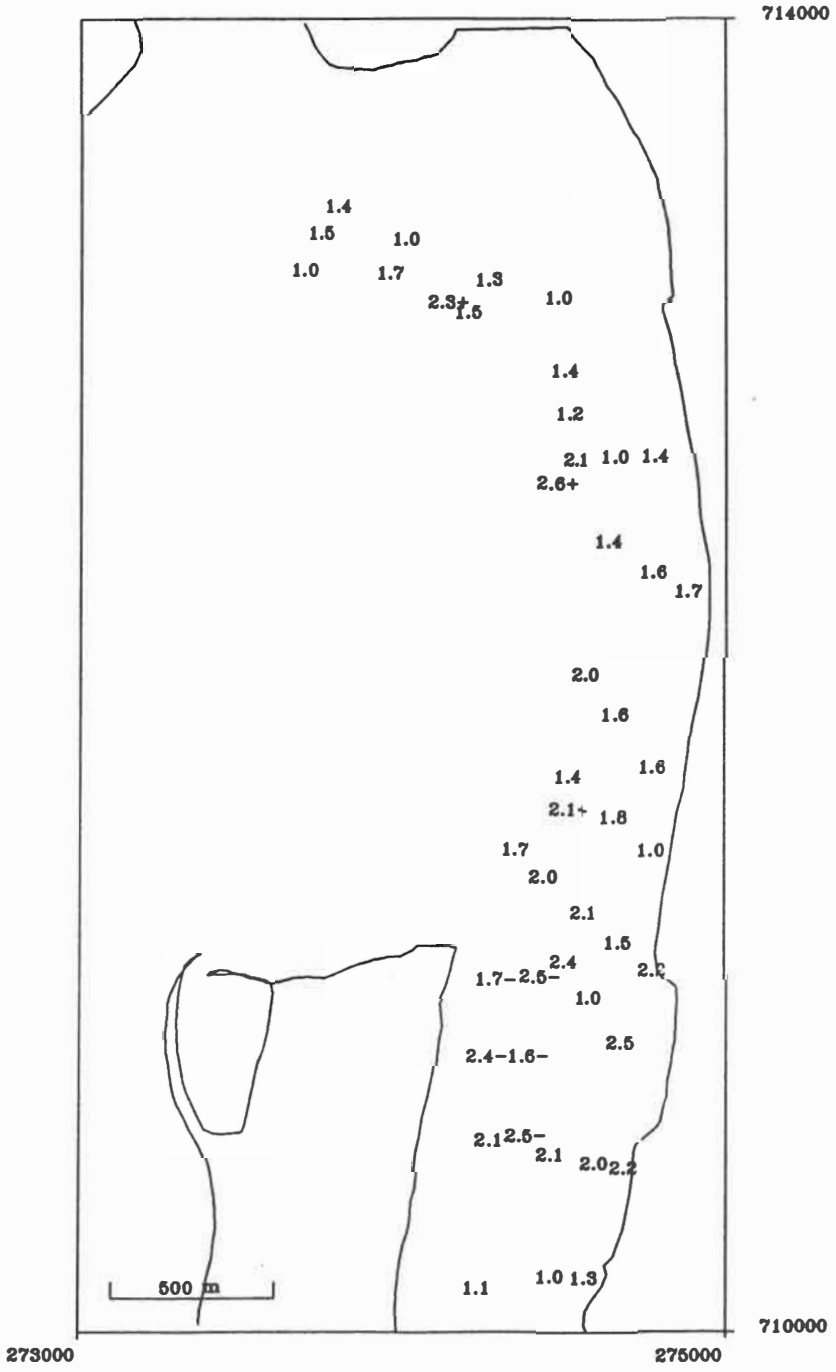

Fig.5.1: Mean grain-size of sediments from dredge-sites inside Tauranga Harbour. The majority of the data are from the THS indicating medium sand. The DAHM and HEALY (1980) grain-sizes from sieving analysis are marked with +, grain-sizes from this study with -.

inside the harbour to moderately to poorly sorted fine to medium sands. Samples collected during this study on the banks adjacent to the east side of Sulphur Point are moderately well sorted medium and fine sands. Surficial samples from the bottom of the upper Maunganui Channel can contain up to 30% of black anaerobic mud, an observation which was also made by BLACK (1984). In contrast to the THS, three samples taken from the dredge hopper inside the harbour by DAHM and HEALY (1980) indicate well sorted fine sands.

For the Entrance Channel DAHM and HEALY's (1980) samples show a progressive fining of the sediment in an offshore direction. The same observations with moderately well to well sorted coarse sand near the harbour entrance were also found during the THS (Fig.5.2). Large amounts of material have been dredged in the Entrance Channel and dumped at the dump-sites (Table 4.1) so that parts of the dredge spoil consist of coarse sand (0.5 - 1 ϕ).

5.2.2 Mineralogical composition of dredged sediments

A pilot project, consisting of optical microscope analysis of 15 thin sections from the dredged sediment, the dredge spoil and the natural shelf sediment, was undertaken during this study with the purpose to find minerals in the dredge spoil which do not occur in the natural sediment. This would provide the possibility to trace the dredge spoil over large distances in the survey area. As it was not the purpose to undertake a quantitative petrological analysis of harbour and inner shelf sediments, the mineralogical composition of the sample was estimated rather than applying the time-consuming point-counting procedure.

The three samples, selected from the dredge-site near Sulphur Point, have a very similar mineralogical composition. Plagioclase is the dominant mineral making up to 60% of the whole mineral assembly of the samples. Rock fragments, pumice, shell fragments and iron oxides form most of the rest of the harbour sand. Quartz, hornblende, hypersthene and augite-aegirine are less than 5% of the minerals.

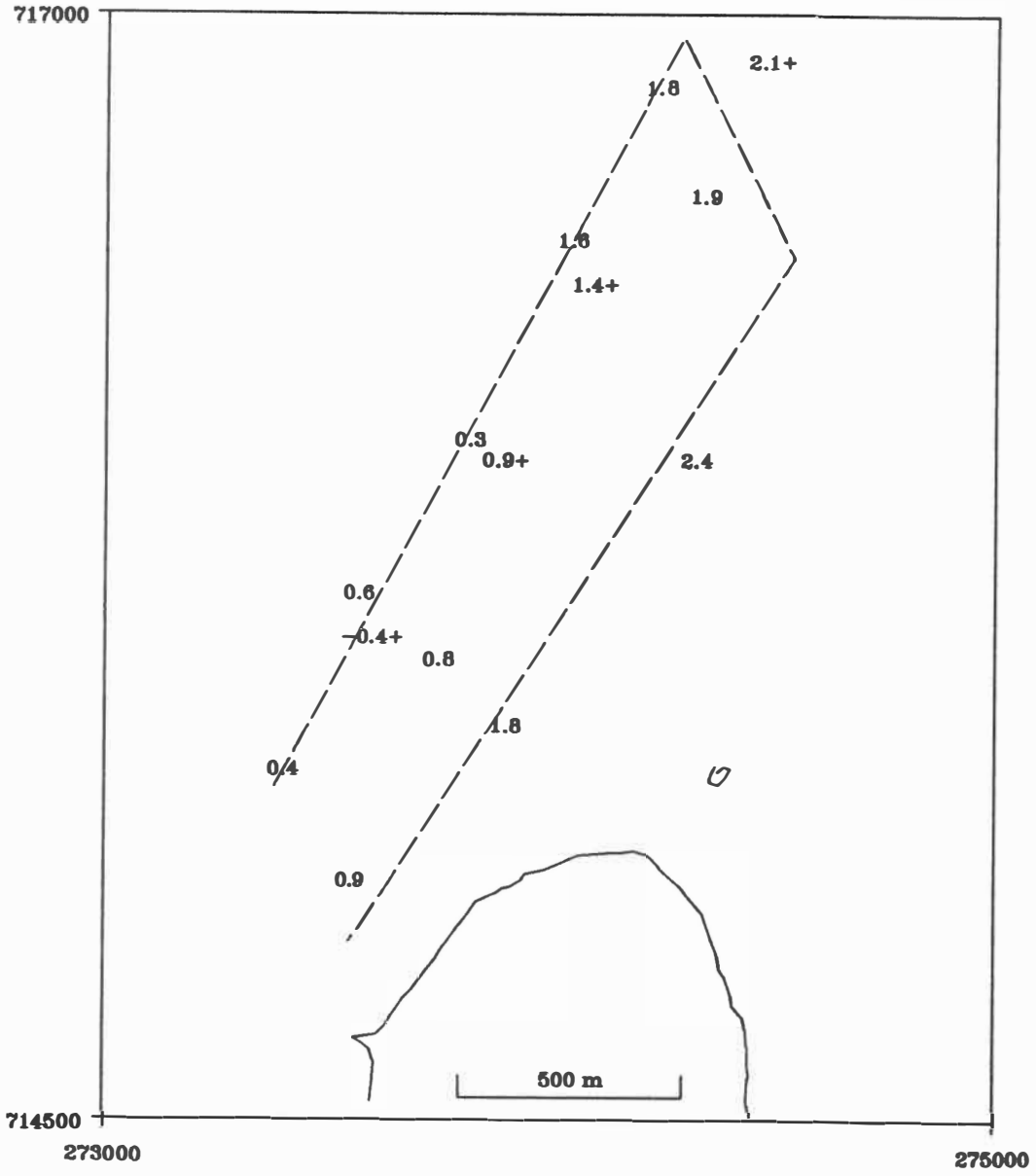

Fig.5.2: Mean grain-size map of sediments in the Entrance Channel on the ebb tidal delta of Tauranga Harbour. Data are from THS and DAHM and HEALY (1980, +). An offshore fining of sediment from coarse to fine sand is evident.

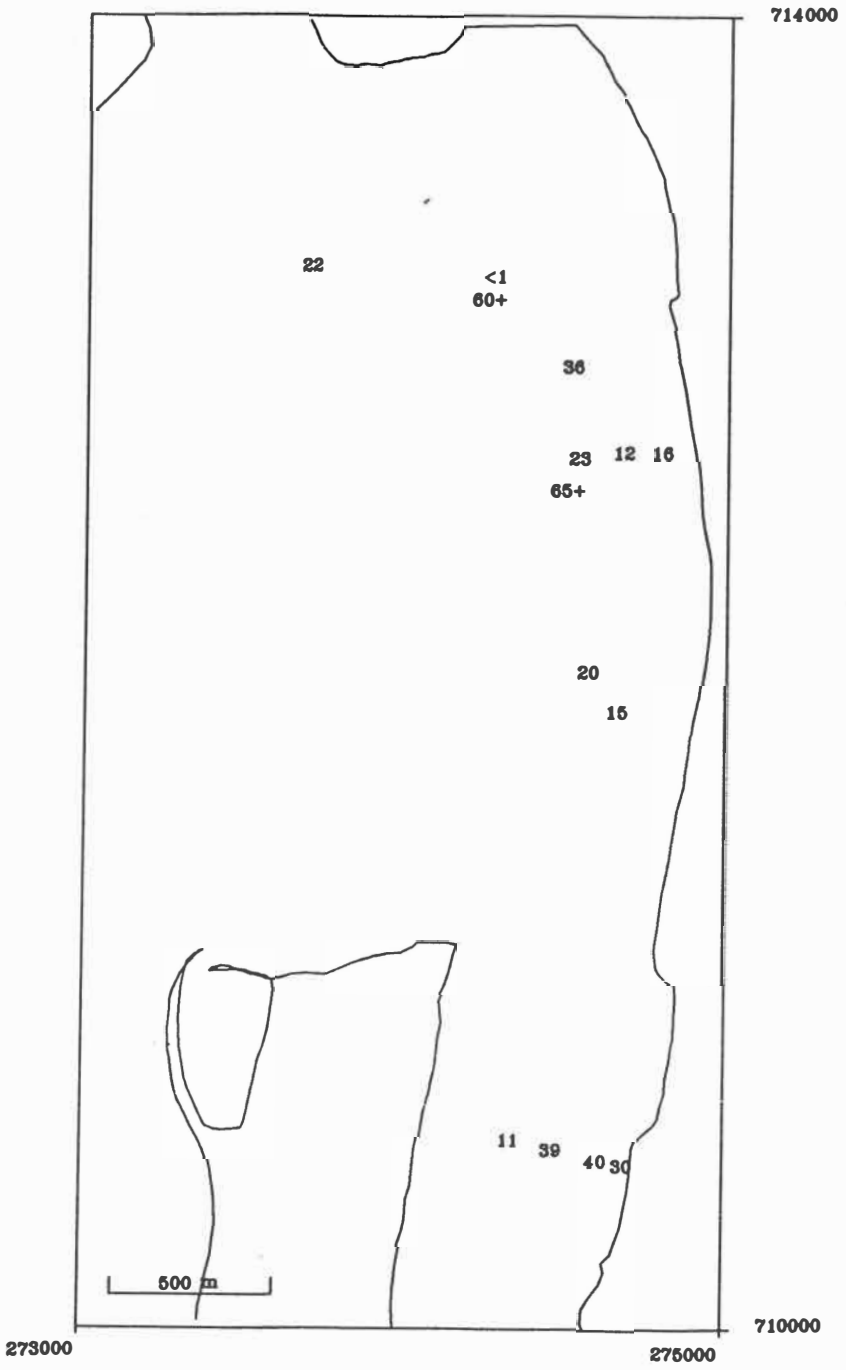

Fig.5.3: Pumice contents of harbour sediments from the THS and DAHM and HEALY (1980, +). The DAHM and HEALY data seem to overestimate the pumice content. Contents between 10 and 25% appear to be more likely for sediment from dredge-sites inside the harbour.

5.2.3 Pumice content in dredged sediments

DAHM and HEALY (1980) used the high content of pumice in shelf sediments shoreward of a former dump-site to postulate an onshore movement of sediment from the dump-sites.

Since the analysis of the pumice content of four dredged samples by DAHM and HEALY (1980), measurements of the pumice content were undertaken during the THS (BLACK, 1984). In contrast to DAHM and HEALY's (1980) measured pumice contents between 60 and 70% inside the harbour, BLACK (1984) reports significantly smaller pumice percentages ranging between 1 and 40% (Fig.5.3). Less than 10% pumice were also found in the three samples from the banks near Sulphur Point analysed during this study.

For the Entrance Channel DAHM and HEALY (1980) found that the pumice content was less than 10%. This is probably due to the higher energy regime generated by strong tidal currents and wave activity, which is also reflected by the larger grain-sizes of the sediments.

5.2.4 Discussion

Investigations during the THS (BLACK, 1984) indicate that the surface sediments of the dredge-sites from inside the harbour and from the ebb tidal delta consist of coarse sand and medium sand, are moderately to well sorted and contain between 0 and 40% pumice. Thus, the material dumped on the inner shelf does not have a typical signature; grain-size and pumice content change due to the location of the dredge-site, in particular with respect to inside and outside the harbour. As occurred during dredging operations in 1988, the dredge-sites may change on a daily basis so that a mixture of material from different locations can be expected to form a "mixed" dump-mound.

It should be noted that a surface sample from a dredge-site does not exactly represent the dredge spoil. As TRUETT (1988) notes, loss of fine material due to suspension during dredging and dumping may be important for a coarsening process in grain-size during the

dredging operations, in particular when fine sediments are moved. However, turbidity measurements in the dredged Cutter Channel and over the dump-site subsequent to dredging and dumping operations in September 1988 indicate that loss due to suspension is of minor importance. In addition, a surface sample does not necessarily give the grain-size of the material dredged under the sea-floor surface which may be finer when a lag surface has formed (Entrance Channel) or coarser when mud has deposited on the sediment surface (upper Maunganui Channel). The differences of the DAHM and HEALY data with the THS data may either be caused from the fact that their sediments are from the dredge hopper and thus may originate from a deeper sediment layer with different sediment properties or from inaccurate analysis methods.

5.3. Sea-floor characterisation of the survey area

5.3.1. Side-scan sonar observations

Side-scan sonography offers a means to assess the continuity of a sediment type in contrast to spot observations by SCUBA diving and/or sediment sampling (HOBBS, 1986). The method is commonly used to observe larger-scale elements of bed roughness such as megaripples and sandwaves but it can also be used to map smaller elements of roughness. Different grey tones on the side-scan chart which result from the strength of the reflected signal are a function of the bottom roughness which is due to the texture and the grain-size of the bottom sediment (HOBBS, 1986).

5.3.1.1. Field-data collection

A side-scan sonar survey of the survey area was undertaken on 15-16 August 1988 in calm conditions. A KLEIN Digital Sonar 590 was operated from the Harbour Board vessel "Kairuri IV". The fish was towed at approximately 4 km/h behind the vessel at a constant height of about 5-10 m above the sea-floor. To maintain the elevation with changing water depth, manual readjustments of the towing cable were required. It was found that the 150 m scan range on both sides of the fish gave an optimum resolution in relation to

the size of the area and time available for the survey. To obtain overlapping coverage, parallel runs every 200 m were undertaken. Because the bedforms were expected to be orientated more or less shore-parallel, this direction was chosen for the runs (Fig.5.4).

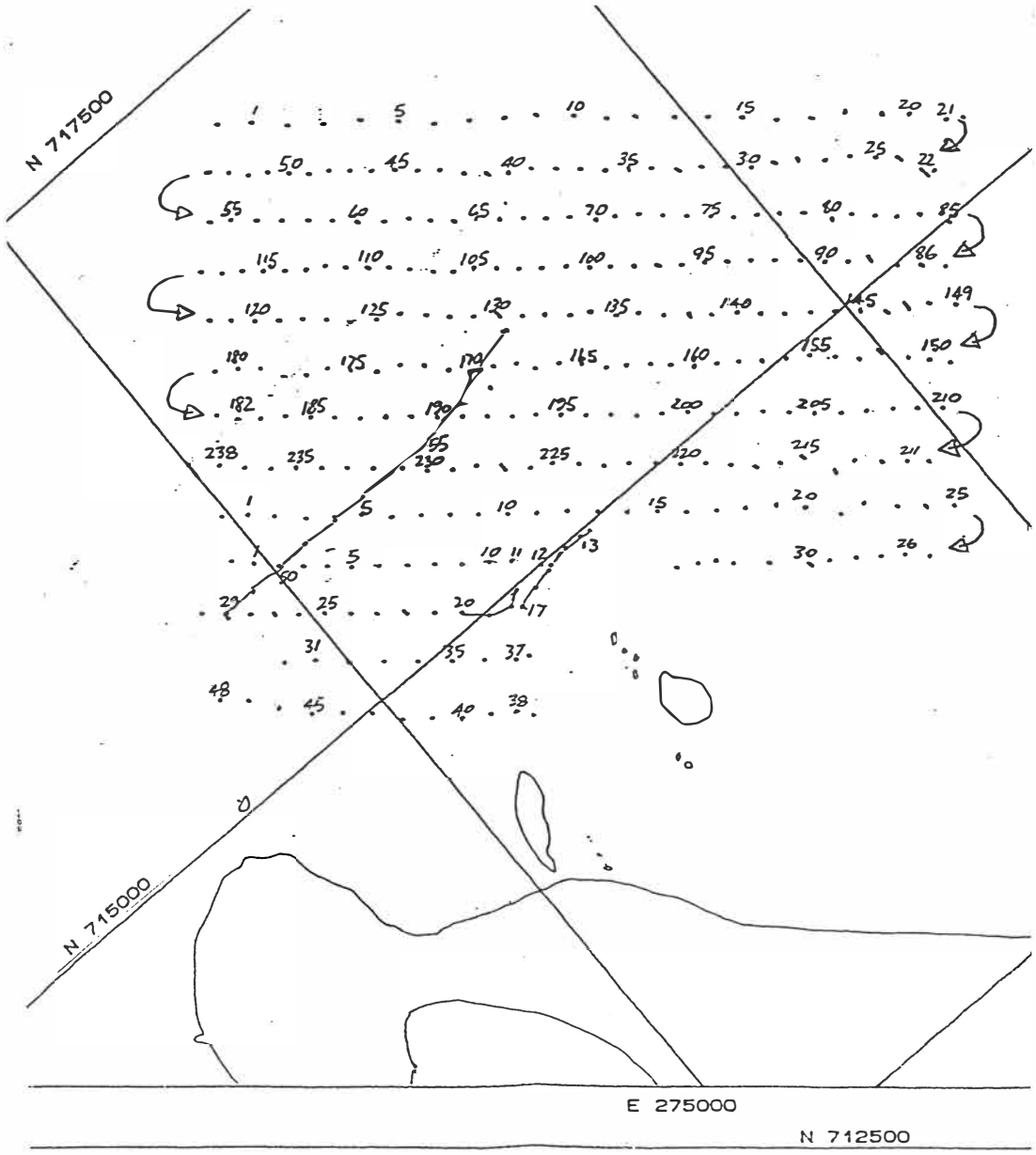

Fig.5.4: Side-scan sonar track (map from BOPHB). Fix-points 1-238 from 15/8/88; fix-points further inshore 1-35 and 1-48 from 16/8/88.

The boat position was fixed with a Racal Microfix electronic position fixing system and plotted directly on a chart. Because of the towing of the fish with varying distances between 10 and 50 m behind the boat the fixed position is not equal to the position on the side-scan chart which had to be taken into account when interpreting the chart. The water depth was recorded simultaneously with an Atlas Deso-20 33 kHz echo sounder.

5.3.1.2 Identification and classification of sonograph bottom types

Side-scan sonograph facies were created to identify and classify the bottom types in the survey area. Six main sonograph facies were distinguished:

(1) Featureless facies (Fig.5.5)
The featureless facies is defined as no identifiable features distinguished on the chart.

Bedforms were classified according to their wavelength (λ) following the scheme of HARMS *et al.* (1975), modified by BOOTHROYD (1978; Table 5.1). For this classification, the boundary between ripples and megaripples is arbitrarily set at 0.6 m, which corresponds on the side-scan sonar chart with 16 to 17 ripple crests per 10 m.

	Ripples	Megaripples	Sandwaves
Spacing	60 cm	60 cm – 6 m	6 m
Height/spacing ratio	variable	relatively large	relatively small
Geometry	highly variable	sinuous to highly three-dimensional, prominent scour pits in troughs	straight to sinuous, uniform scour in troughs
Characteristic flow velocity	low (>25–30 cm/sec, < 40–50 cm/sec)	high (>70–80 cm/sec, < 100–150 cm/sec)	moderate (>30–40 cm/sec, < 70–80 cm/sec)
Velocity asymmetry	negligible to substantial	negligible to substantial	usually substantial

Table 5.1: Classification of bedforms according to BOOTHROYD (1978).

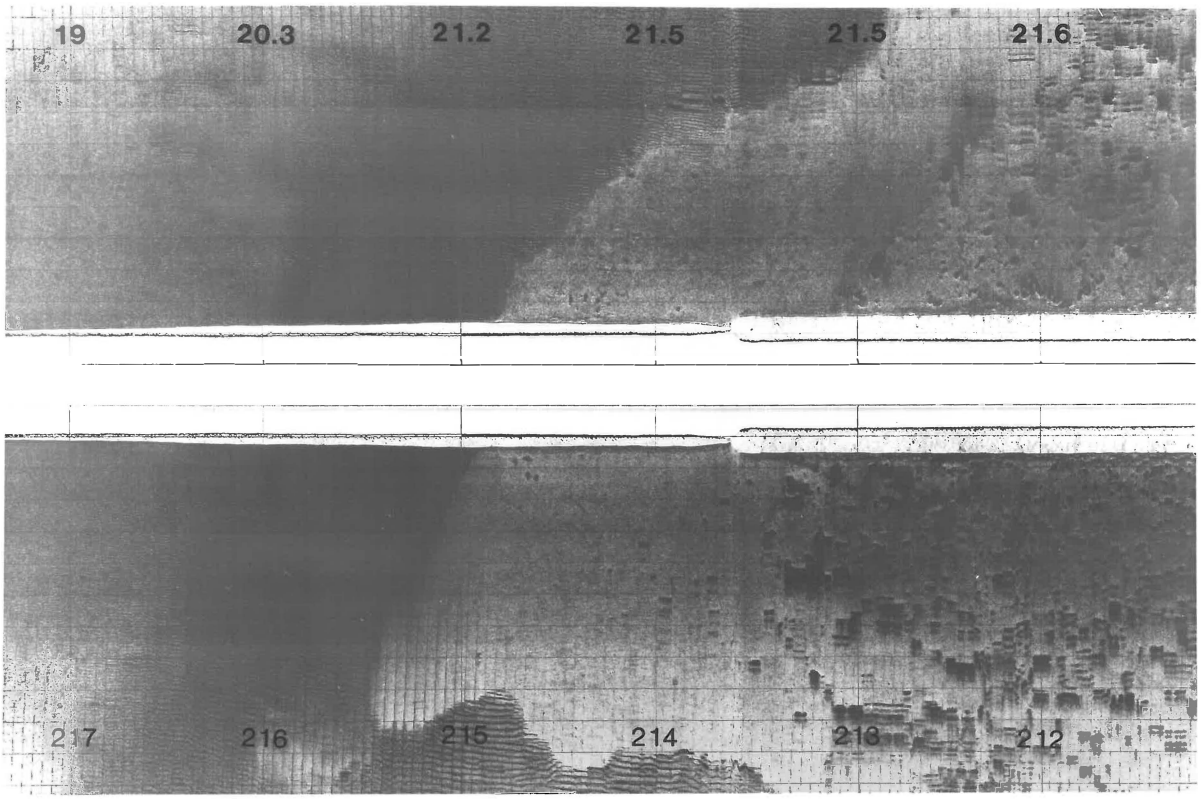

Fig.5.5: Side-scan sonograph record from fix-point 217 to 212 (bottom of photograph) at water depths (reduced to MSL) between 19 and 21.6 m (top of the photograph), oriented in an offshore direction. The scale on the record is 10 m distance between horizontal scale-lines and about 100 m between fix-points, which means that the length/width ratio is 17:27 or nearly 2:3. This distortion of the side-scan chart had to be taken into account when interpreting the spatial distribution and the shape of features. The sonograph shows:
featureless sea-floor (facies 1) between fix 214 and 215;
megaripples (facies 3) between 215 and 217;
blebby facies (4) between 211 and 213.

(2) Ripple facies ($\lambda \leqslant 0.6$ m; Fig.5.6)
Because the limited resolution of the side-scan sonar it is difficult to identify bedforms under 0.5 m wave length so that they are not clearly distinguishable from a featureless sea-floor. However, a directional pattern on the chart suggests the occurrence of bedforms under 0.6 m wave length. This pattern is interpreted as a ripple sonograph facies. The directional pattern of the ripple facies can vary slightly in its orientation within one ripple-field. Ripples occasionally change to the featureless sea-floor facies without a clear boundary.

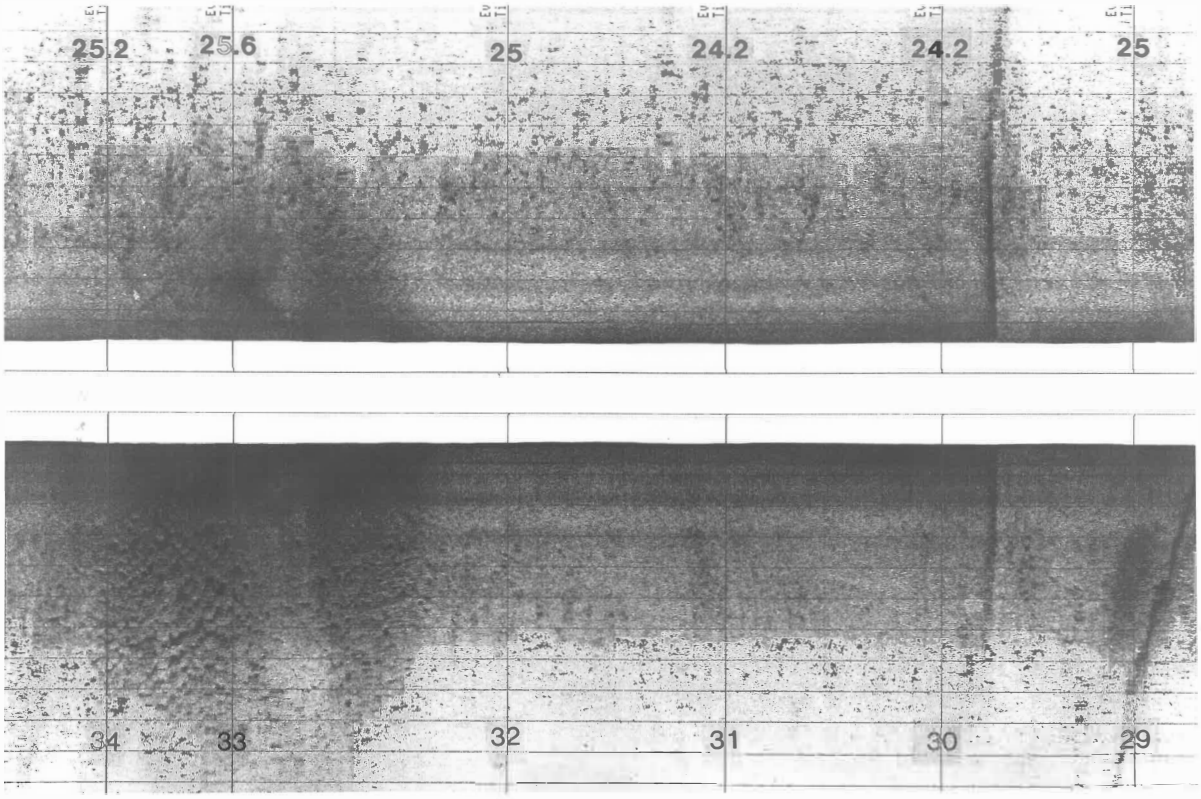

Fig.5.6: Ripples (facies 2) from 29 to 32 (not clearly visible on the photograph); sandwaves-like features (facies 6) from 32 to 34; shore-normal ridges in the left of the record.

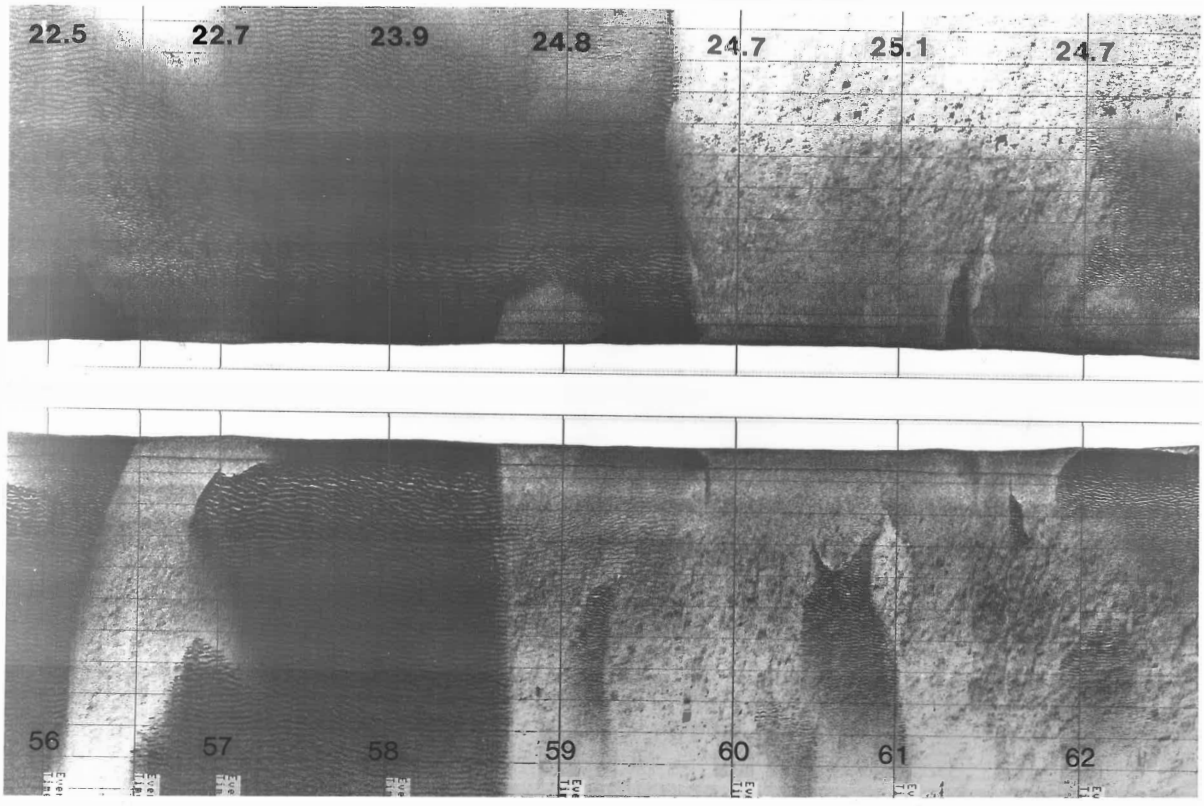

Fig.5.7: Large megaripple field (3) between 56 and 59, megaripple patches between 59 and 62. Dark tone of megaripples indicates coarser material than the surrounding featureless sea-floor.

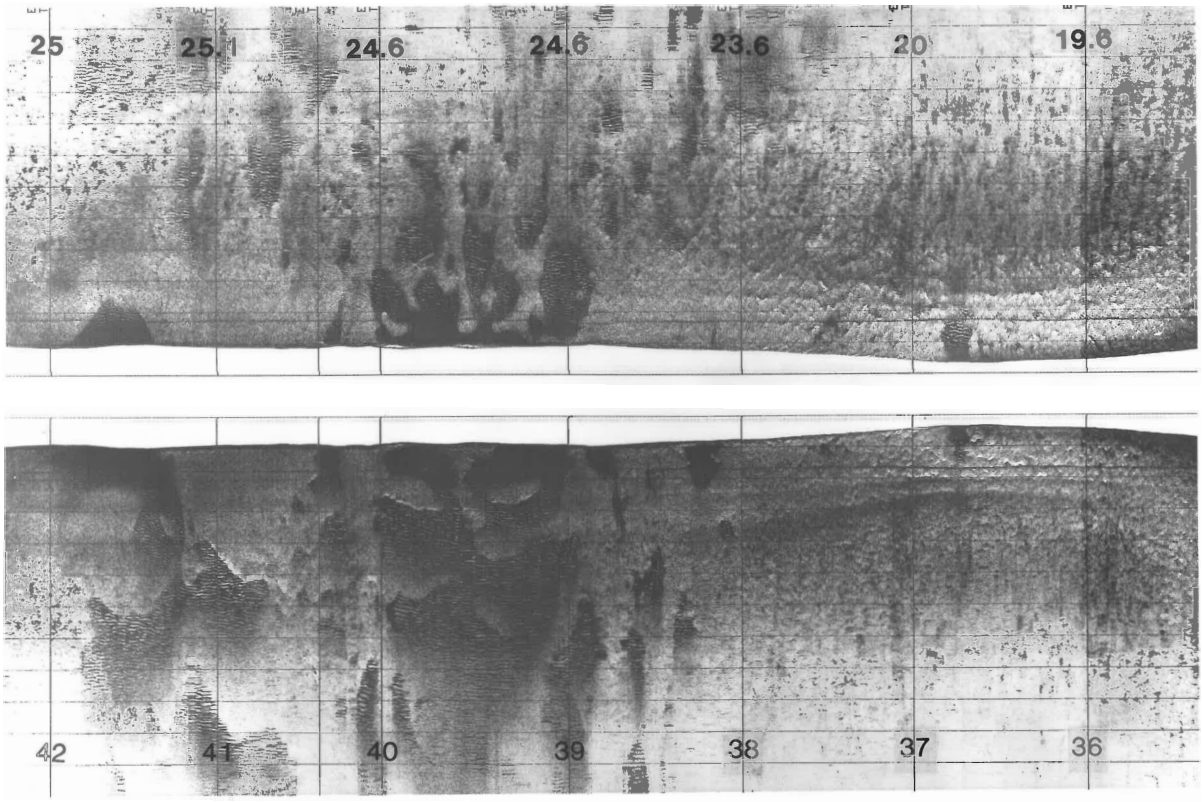

Fig.5.8: Patchy distribution of megaripples (3) in featureless sea-floor (1). Bright lines at the offshore edge of the patches indicate their occurrence in topographic lows. Diffuse dump-facies (5) at dump-site D between 38 and 36.

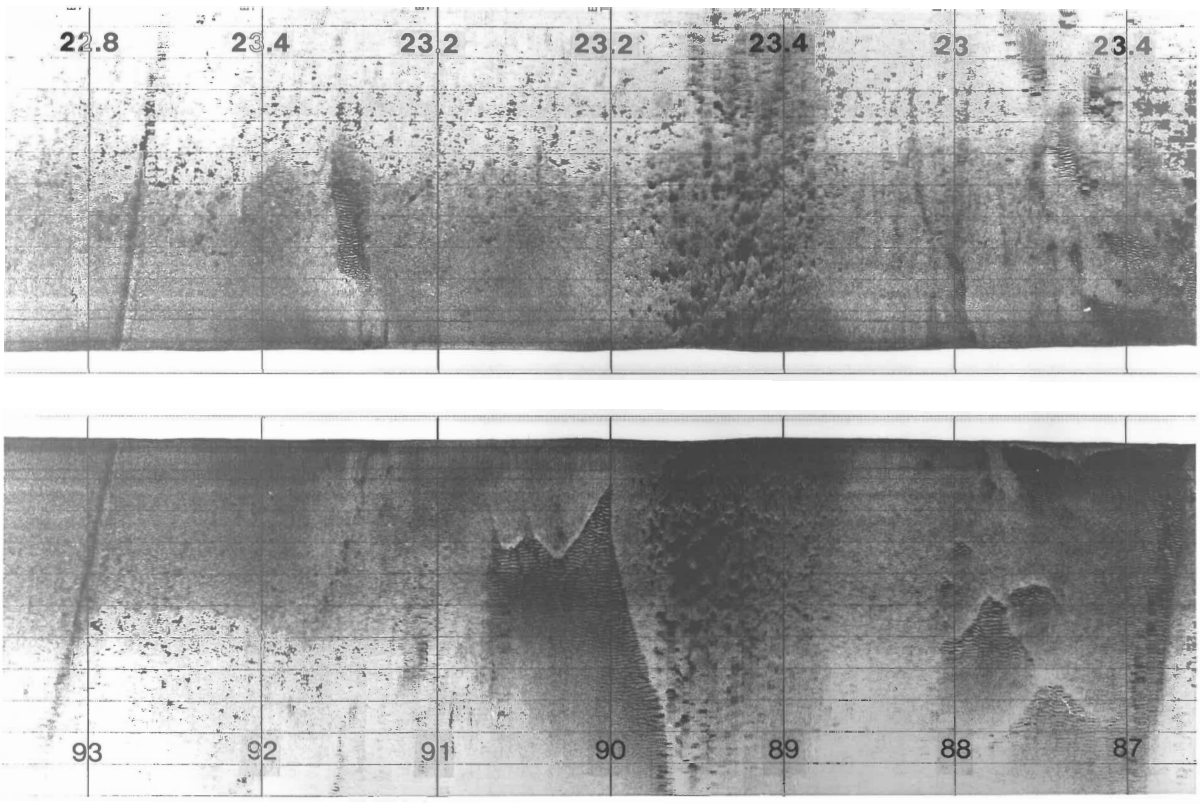

Fig.5.9: Shore-normal ridge, featureless facies (1), megaripples (3) and sandwave-like features (6).

(3) Megaripple facies (0.6 m < λ < 6 m; Fig.5.7, 5.5, 5.8, 5.9)
Bedforms with wave lengths from 0.6 m to 2 m are observed on the side-scan chart. The megaripples are aligned NW-SE parallel to the coast and typically associated with darker grey tones suggesting their occurrence in coarser material than the surrounding featureless or rippled sea-floor. In some parts of the survey area the boundary between big ripples and small megaripples is difficult to draw. There are also transitions from megaripples to ripples.

(4) Blebby facies (Fig.5.5)
It is not evident from the sonograph picture how the blebs occurring on featureless bottom can be explained. Subsequent SCUBA diving showed that the black spots are upstanding bunches of the horse mussel, Atrina zelandica, on an otherwise flat sea-floor.

(5) Dump-ground facies (Fig.5.8)
A patchy diffuse sonograph record characterises the recent input of material to the sea-floor, typical for the dump-sites in the survey area.

(6) Sandwave-like facies (λ > 6m; Fig.5.6, 5.9)
Large irregular features with wavelengths around 6 m forming an angle of 20° to the shoreline occur in a small area. It is not clear if the sonograph feature can be compared to sand waves frequently observed on shelves (e.g. Middle Atlantic Bight; SWIFT *et al.*, 1979, 1983) but they are distinctly different form those described in tidal inlets (e.g. Whangarei Harbour; BLACK and HEALY, 1983).

Shore-normal oriented ridges of varying length up to 1 km and 10-20 m width are indicated on the side-scan chart by a darker signal. From the echo-sounding survey it appears that the so called "ridges" reflect a locally steeper drop in the sea-floor to the east (Fig.5.10). On top of the "ridges" megaripples are observed which change gradually to ripples and to a featureless sea-floor in a western shore-parallel direction. Because of their singularity, the megaripple ridges were not included in one of the facies described above.

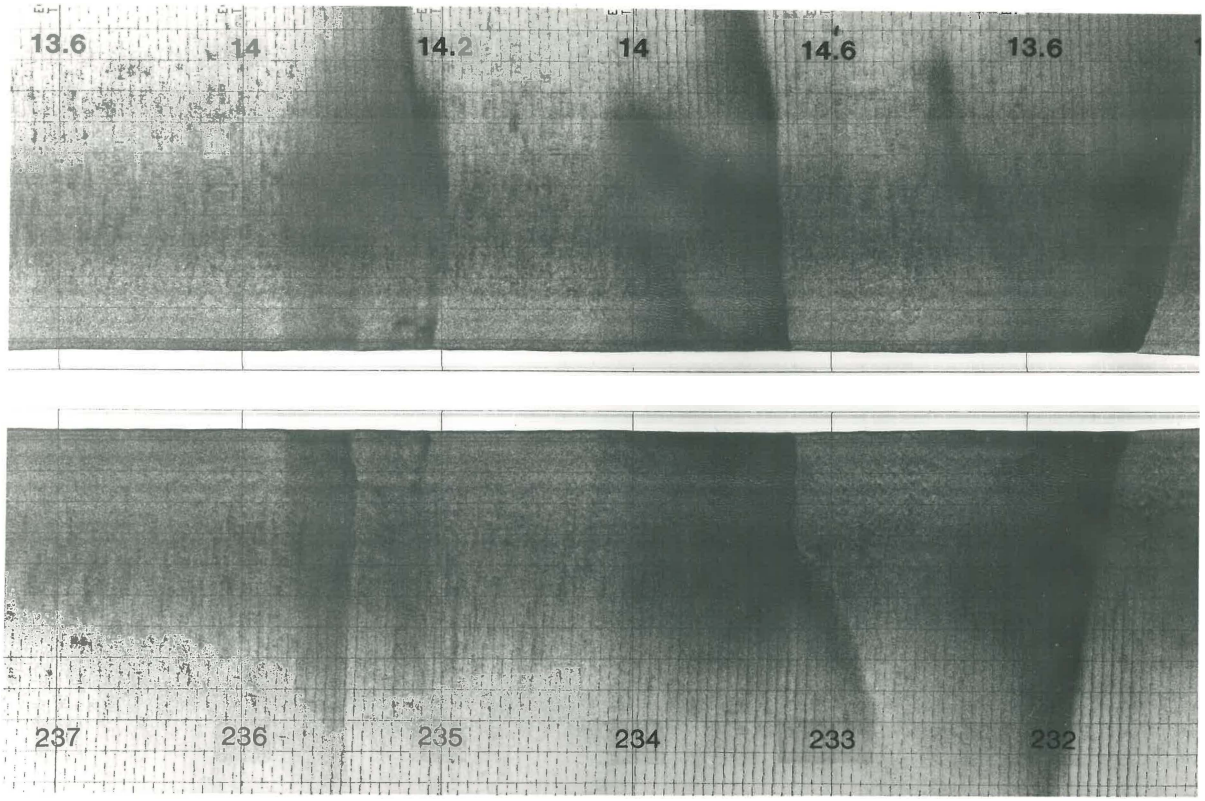

Fig.5.10: Shore-normal oriented megaripple ridges with the transition from megaripples to ripples to featureless sea-floor.

A side-scan sonograph facies map was drawn based on the classification of the facies types outlined above (Fig.5.11). The sonograph facies 1 to 3 can change frequently on a small scale; small irregularly distributed patches of megaripples of 20 m x 20 m size are typical for the northwestern part of the survey area. To avoid a confusing map mixed facies were created with the first facies number being the predominant facies. In addition, solid and dashed lines were used to show abrupt and gradual changes between sonograph facies.

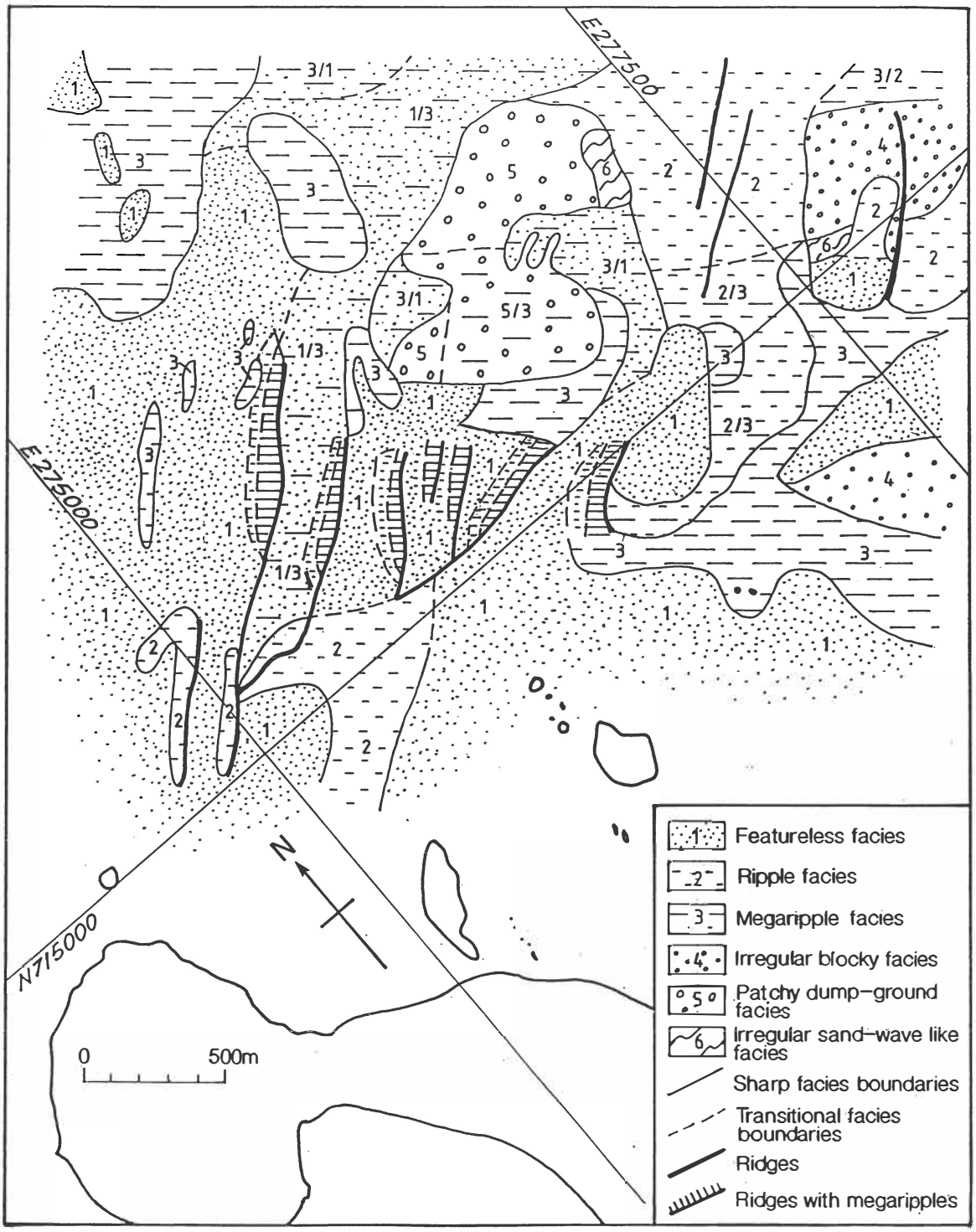

Fig.5.11: Side-scan sonograph facies map; solid lines indicate abrupt changes between facies, dashed lines gradual transitions.

5.3.1.3 Sea-floor types

Four clearly distinguishable sea-floor types were observed in the survey area:

1) Rippled and featureless sea-floor occurs throughout the survey area. Parts of the survey area in the east are covered with horse mussels (side-scan facies 1,2 and 4; Fig.5.5, 5.6, 5.8).

2) Megaripple patches and fields: Numerous megaripple patches of varying size surrounded by featureless and rippled sea-floor are observed in the survey area (Facies 3, 3/1, 3/2, 1/3, 2/3; Fig.5.5, 5.7, 5.8, 5.9). The patches are irregularly shaped but mostly elongated in a shore-normal direction. Bright lines of the megaripple patches towards the side-scan track on the seaward side of the patch indicate a shadow zone of the side-scan signal suggesting that the patches are often bound to topographical depressions (Fig.5.8, 5.9). The wavelength of the bedforms is generally between 0.8 m and 1.2 m. Two irregular shaped megaripple fields of 1000 m x 600 m and 400 m x 1000 m occur in the northwest and southeast of the survey area (Fig.5.5, 5.7). The wavelength of the megaripples in the bigger fields is up to 2 m. The darker grey tone of the megaripples also indicates that they consist of coarser sediment than the surrounding featureless and rippled sea-floor. The megaripple patches mainly occur in the further offshore part of the survey area in water depth beyond 20 m.

3) Megaripples and ripples on ridges: Megaripples ripples were observed on the shore-normal oriented ridges striking perpendicular to the ridges (Fig.5.10). Their wavelength being at the eastern edge of the ridge around 0.8 m decreases to the west to ripple size and finally to a featureless sea-floor. The megaripple ridges are limited to the southwest of the area in water depth lower than 20 m. Further inshore the bedforms do not exceed ripple size.

4) Dump-grounds with and without bedforms (facies 5, 5/3; Fig.5.8): This sea-floor type occurs on and around the dump-grounds. On dump-site C, where dumping occured in 1977/78 patches of megaripples (λ = 0.8 m) were found in the dump-site facies in contrast to the more recent dump-site D.

5.3.2 Visual sea-floor observations

Visual sea-floor observations by underwater-video and SCUBA diving were undertaken to verify the side-scan sonograph facies map and to obtain more accurate information on the bedforms. Three different sets of observations were undertaken. The positions of the dive-sites are shown in Fig.5.12.

5.3.2.1 Underwater-video

An underwater-video survey of the sea-floor was undertaken with the Remote Operated Vehicle Phantom 300 (ROV). The ROV consists of an underwater-vehicle with the photographic-recording equipment and a control panel with a screen from which the vehicle is driven. Both units are connected with a cable (Fig.5.13).

The ROV survey was undertaken around Motuotau Island on the 17-18 August 1988, subsequent to the side-scan sonar survey. Originally it was planned to drive the ROV parallel to the BOPHB vessel "Kairuri IV" along a beach-offshore transect to obtain a constant record of the sea-floor. However, it was discovered that the vehicle is insufficiently powered to drive at a continuous speed next to a boat. Accordingly, the operation of the ROV was restricted to spot-diving. As well as the underwater-video record, an underwater camera was used. Unfortunately, problems with the film transport occurred and thus the photos are of limited quality. Because of a missing scale, the size of features could only be estimated.

A second ROV survey in the middle of November 1988 was stopped because of limited water visibility and failure of equipment.

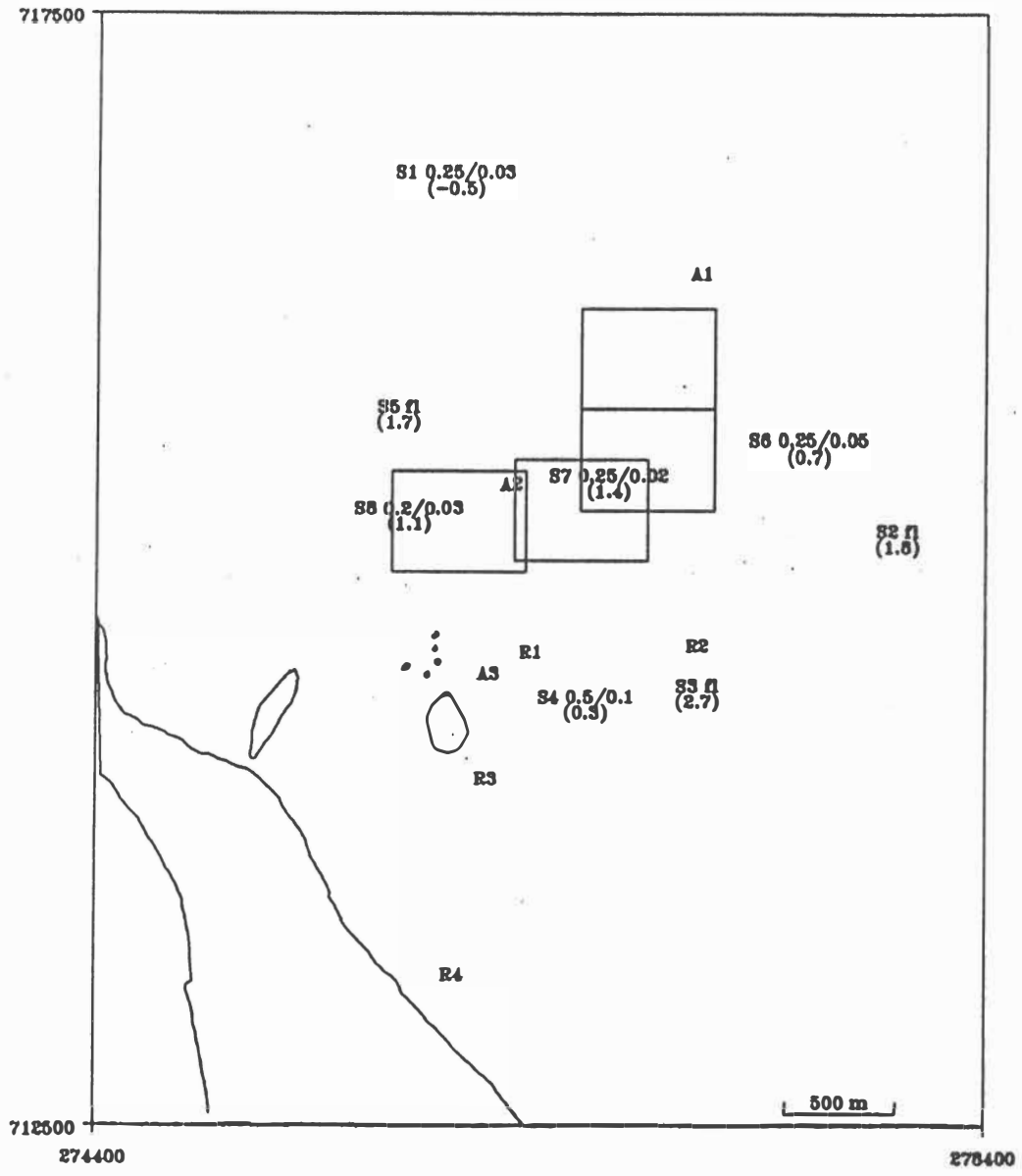

Fig.5.12: Positions of visual sea-floor observations. ROV locations (17-18/8/88) are marked with R; Aanderaa-sites (July 88) with A; SCUBA-sites (16/11/88) with S. The λ/η are in meter. Note that the bedforms do not occur in sand finer than 1.5 ϕ.

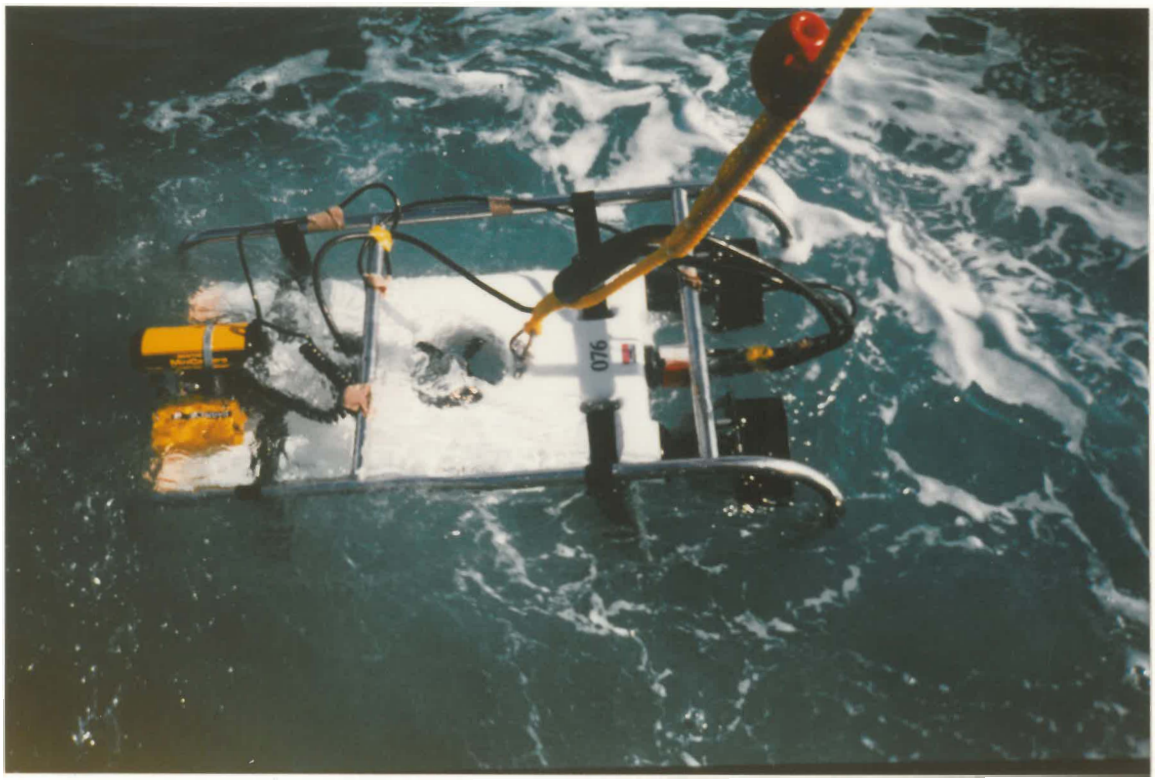

Fig.5.13: The Remote Operated Vehicle (ROV) with the yellow stillwater camera at the front and the connecting cable to the boat.

The ROV was used at four spots around Motuotau Island (Fig.5.12):

1) Irregular small ripple-features (λ = 0.1 - 0.3 m) with small holes and mounds were observed at R1 (water depth h=16 m) which is located near a rock outcrop (Fig.5.14). Bioturbation seems to be responsible for the irregular feature; for instance some of the bigger holes are probably fish nursery and resting places also indicated by the observed abundance of fish. Shells are not very common except two gastropods Struthiolaria papulosa and Zeotrophus ambiguus. The volcanic rock outcrops are grown over by colorful sponges and algae. The abundance and variability of marine life around the rocks of Motuotau Island is also reported in HEALY *et al.* (1988).

2) Symmetrical ripples and megaripples were found at R2 (h=21.5 m; Fig.5.15), located in the southeast megaripple field observed in the side-scan survey. Within one ripple-field the bedforms show different heights (η = 0.1 - 0.3 m) and wavelengths (λ = 0.5 - 1.2 m) which is smaller than indicated on the side-scan chart (up to 2

Fig.5.14: Irregular small ripple features with small holes and mounds indicating bioturbation (R1)

Fig.5.15: Symmetrical ripples (R2)

m). The size difference is probably due to the fact that smaller bedforms in the shadow of larger bedforms are missed by the side-scan beam. From the visual observations, the megaripples are associated with coarser sediment compared with R1 and have shell lag in the troughs, whereas the crests are nearly shell-free.

3) At site R3 (h=10-12 m) an abrupt change from the rippled and megarippled sea-floor to the irregularly small rippled sea-floor was observed. These abrupt changes, also noted on the side-scan sonar chart, were first described by STEVEN and FITZMAURICE (1971; in DAHM and HEALY, 1980) on the inner shelf off Tauranga.

4) Southeast of Motuotau Island, 200 m off the beach (R4), the bottom consists of small ripples (λ = 0.1 - 0.2 m). Shells are rare.

5.3.2.2 SCUBA observations

SCUBA observations were carried out by Mike Dravitzki in connection with the deployment and checking of Aanderaa current meters and during an extra survey (Fig.5.12).

The SCUBA survey of the Aanderaa sites (A1 to A3) in July 1988 offered the opportunity to monitor the short-term changes of the sea-floor, particularly the response of the bedforms to an easterly storm which had occurred between the two diving operations (15-17/7/88; Table 5.2).

	d	$M_z[\phi]$	sea-bed 8/7/88	sea-bed 21/7/88
A1	28 m	2.2	flat	ripples λ=0.1-0.2 m
A2	18 m	0.6	megaripples NW-SE	megaripples NNE-SSW
			λ=0.6 m; η=0.2 m	λ=0.8-1 m; η=0.3-0.4m
A3	16 m	2.2	flat	ripples λ=0.1-0.25 m,
				η=0.05 m

Table 5.2: Sea-floor changes observed from SCUBA diving within two weeks after an easterly storm (15-17/7/88).

The association of coarse sand with symmetrical megaripples and fine sand with flat or rippled sea-floor is consistent with the observations of the side-scan sonar survey. The development of ripples on flat sea-floor and the increase in megaripple size and between the surveys shows the active response of the sea-floor to a storm. The different alignment of the megaripples at A2 before and after the storm indicates that the ripples not only change in size and but also in direction due to the wave approach during a storm. Active sediment transport processes are also suggested by the fact that four sediment traps set up next to the Aanderaas could not be located again, probably because they were buried under sediment.

During a SCUBA survey covering eight sites (16/11/88; Fig.5.12) it was observed that the bedforms were again of considerably smaller wavelength and height than would be expected from the side-scan sonar records. S1, for instance, showed solitary ripples with flat troughs separating isolated crests (named after INMAN's, 1957, classification of oscillatory ripples, in KOMAR, 1976) of 0.25 m wave length and 0.03 m height. In contrast, megaripples with wavelengths of up to 2 m were measured on the side-scan chart about four months before the SCUBA survey. The same decrease in ripple size was observed at S4, S6, S7 and S8. From the SCUBA observations ripples seem to occur permanently in sediment coarser than 1.5 ϕ. Storm ripples in fine sand appear not to persist for a long time period (weeks).

The ROV observation that gravel and shell occur in the troughs but sand in the crests of ripples was confirmed by diving. However, the sand is only a thin layer at the top of a crest; underneath the gravel and the shells from the troughs occur. Differences in grain-sizes within megaripples (λ = 1 m) were also described at the ebb tidal delta off Whangarei Harbour (BLACK and HEALY, 1983) and elsewhere (LECKIE, 1988).

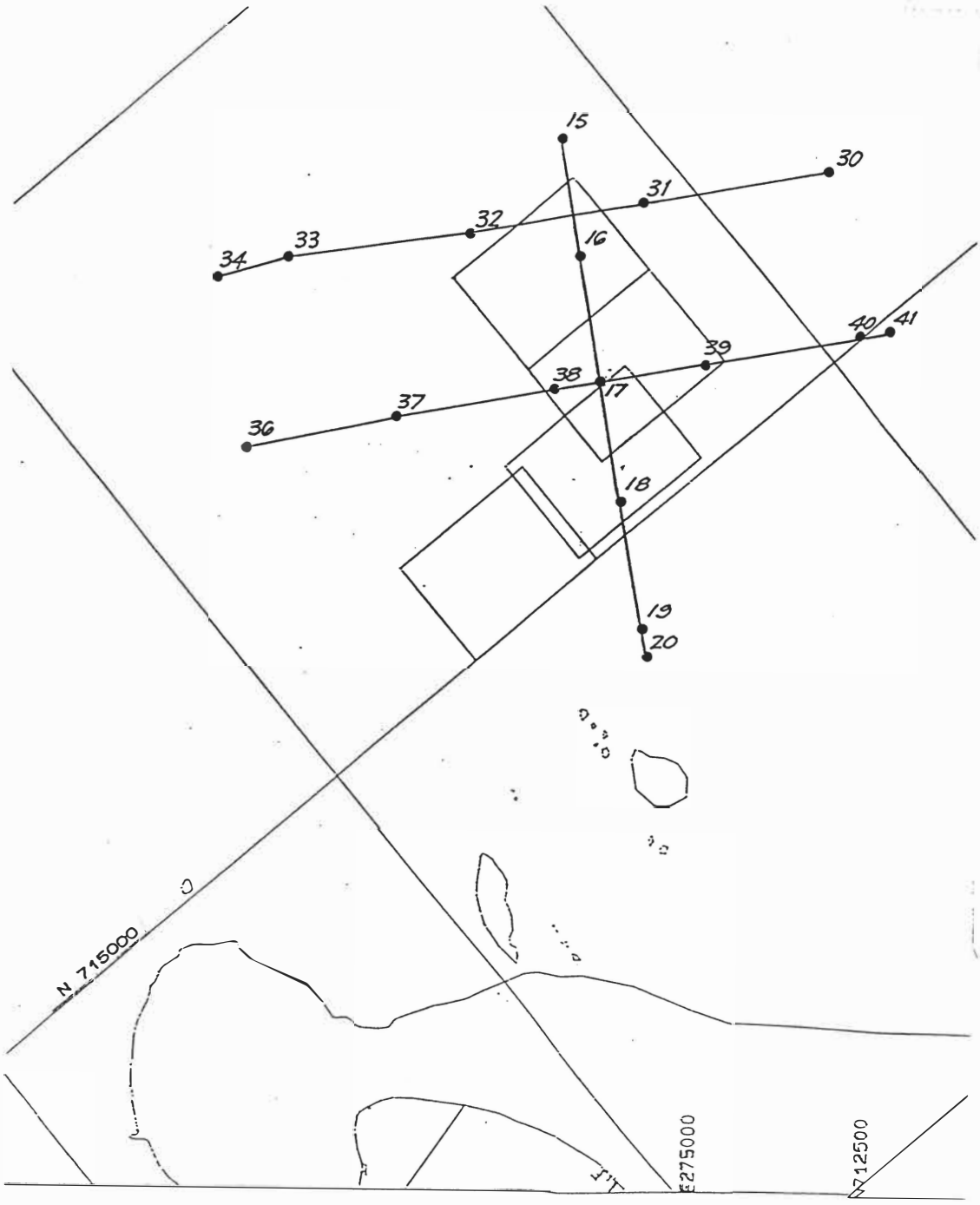

Fig.5.16: Sub-bottom seismic profiling track, provided by the BOPHB.

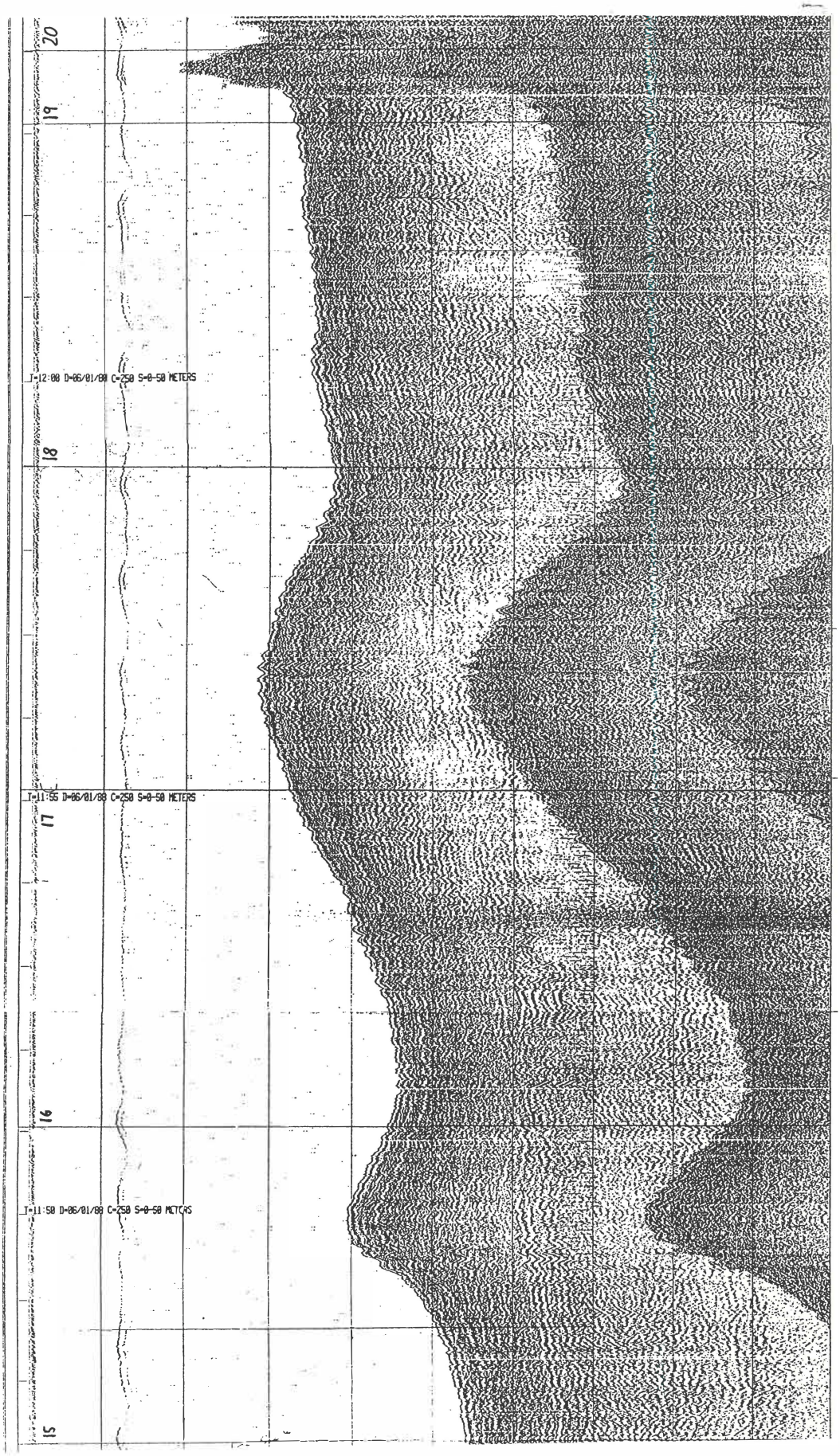
20
19
18
17
16
15
T=12:00 D=06/01/88 C=250 S=0-50 METERS
T=11:55 D=06/01/88 C=250 S=0-50 METERS
T=11:50 D=06/01/88 C=250 S=0-50 METERS

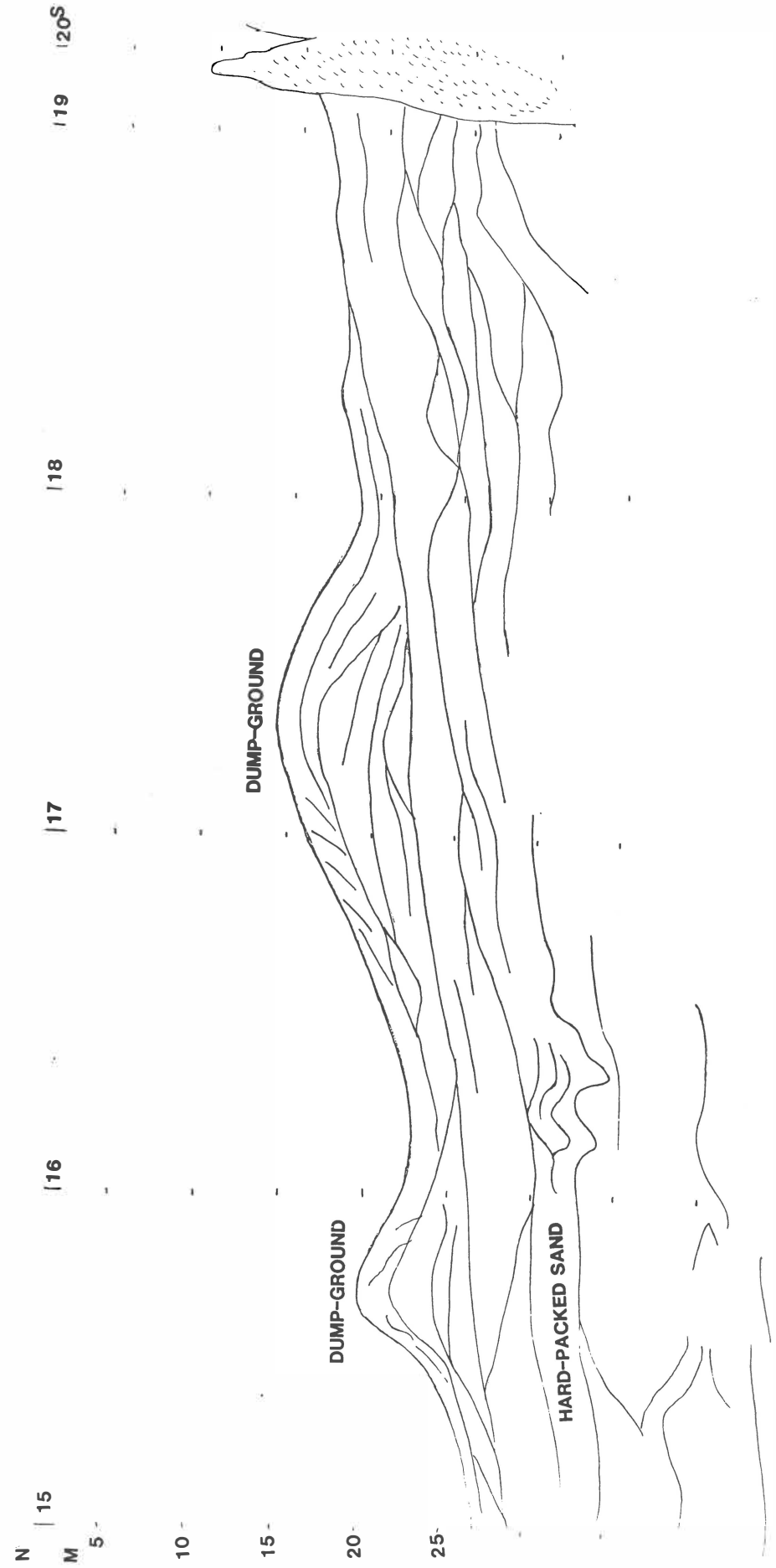

Fig.5.17: Original (a) and interpretation (b) of the shore-normal transect.

5.3.3 Sub-bottom seismic profiling

A sub-bottom seismic survey was undertaken on 1 June 1988 under calm wave conditions. An ORE Farranti Geopulse system with an EPC 4800 graphic recorder was operated from the BOPHB vessel "Mahi". Every five minutes the position was fixed and the water depth recorded simultaneously by echo-sounder. Four profiles along beach-offshore transects and three shore-parallel profiles were undertaken.

The sub-bottom picture was interpreted along three profile-lines which crossed dump-sites C and D (Fig.5.16). Significant reflectors were traced from the original recording and photographically reduced to A4 format (5.17a,b).

The shore-normal profile shows up the dump-mounds at dump-sites C and D (Fig.5.17). A strong reflector underneath the mounds slightly dipping in an offshore direction and wedging inshore probably represents the original sea-floor before any dumping occurred. Since then, either irregular dumping not always inside the permitted dump-grounds and/or the dispersal of dredge spoil from the dump-mounds has resulted in a continuous cover of the pre-dump sea-floor between the two dump-mounds and the deposition of a noticeable amount of material in a small zone up to 300 m shoreward of the dump-mound at dump-site C. This accumulation zone was also noted from echo-sounding surveys investigated in Chapter 4.

A second strong reflector at 25 to 30 m water depth may represent the sea-floor during a lower sea-level in the late Holocene. The reflector may be consistent with observations from a high resolution seismic survey undertaken by CARTER *et al.* (1984, in GIBBS, 1986) who reports a sediment wedge at 28 +/- 2 m from the Otago continental shelf and associates it with a sea-level stillstand between 9.2 and 8.4 ka.

U-shaped structures and wedging strata, also observed at the two shore-parallel sub-bottom records, indicate channel fillings and/or sand-bodies (Fig.5.18; 5.19). These features are most common in the inner shore-parallel profile.

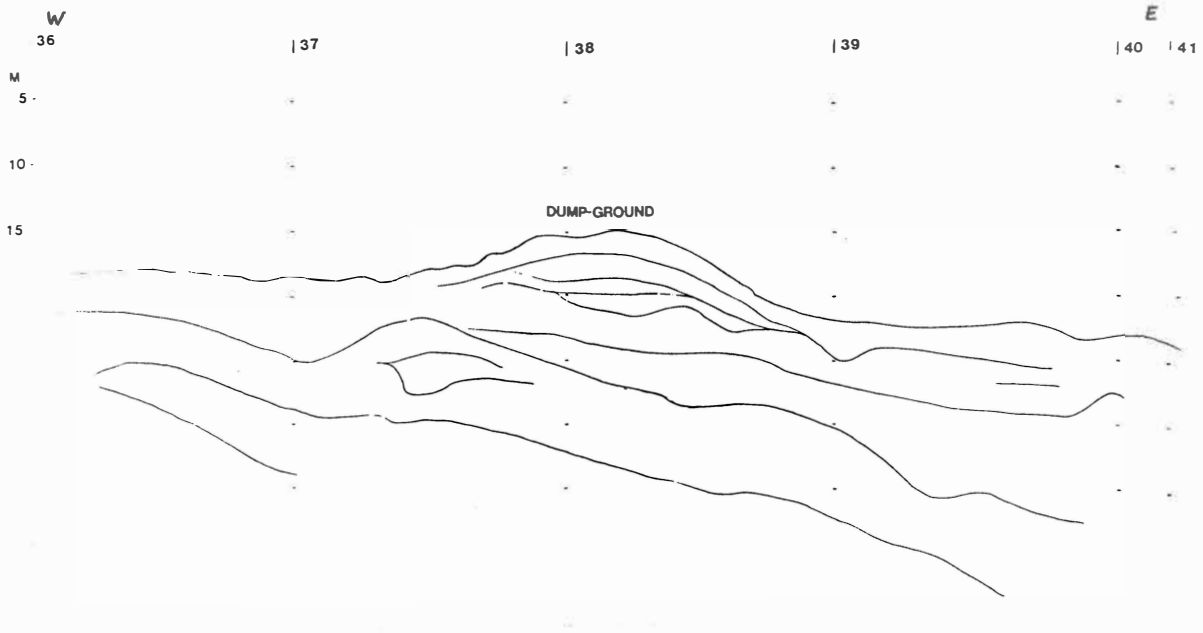

Fig.5.18: Shore-parallel line over dump-site C

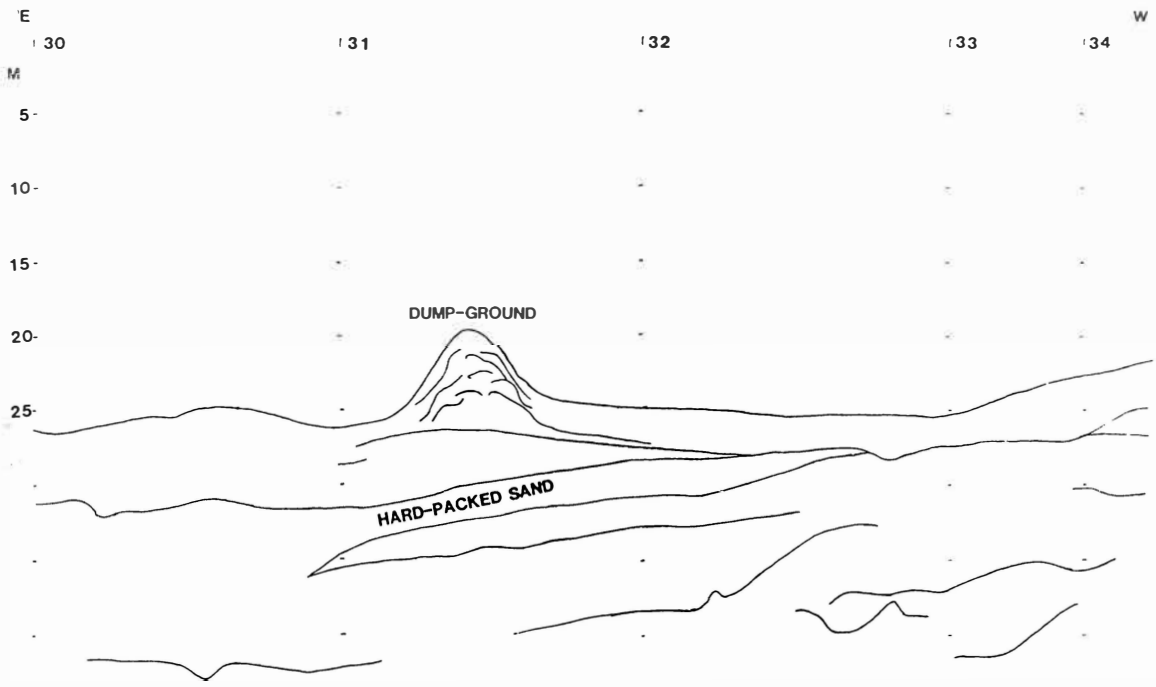

Fig.5.19: Shore-parallel line over dump-site D further offshore.

A stronger reflected signal underneath dump-site D is interpreted as "hard-packed" sand. The restriction of the hard-packed sand to the dump-site can be explained by the overlying weight of the mound causing a higher compaction rate compared with the natural sea-floor stratification.

5.3.4. Textural analysis of inner shelf and nearshore sediments

5.3.4.1 Sediment sampling program

The initial sampling program, consisting of 97 sediment samples, was undertaken in the first two weeks of May 1988 (Fig.5.20). Besides 6 samples taken inside the harbour from the dredge-site adjacent to Sulphur Point, 91 samples were collected along 8 beach-offshore profiles in the survey area and along 1 beach-offshore line at a control-site to the east of the survey area (Fig.1.3).

The first 40 samples were taken with a Smith-McIntyre grab sampler consisting of a 0.33 x 0.33 m half cylinder which enabled an undisturbed surface sample of the sea-floor to be obtained. To avoid the heavy handling of the Smith-McIntyre grab a smaller grab (200 g per sample) with a messenger triggering mechanism was used for the rest of the samples. The small grab failed to work on shelly bottom, because shells blocked the jaws preventing it from complete closure. For that reason some samples had to be repeated with the Smith-McIntyre grab. During further investigations (Aanderaas, underwater-photography) additional samples were taken by SCUBA diver (Fig.5.12).

Beach samples were taken at four locations along the Mount Maunganui Beach. One sample each from the berm and the bottom of the beach exposed at low tide were collected. In addition, one sample from the dune near Moturiki Island was taken (B1).

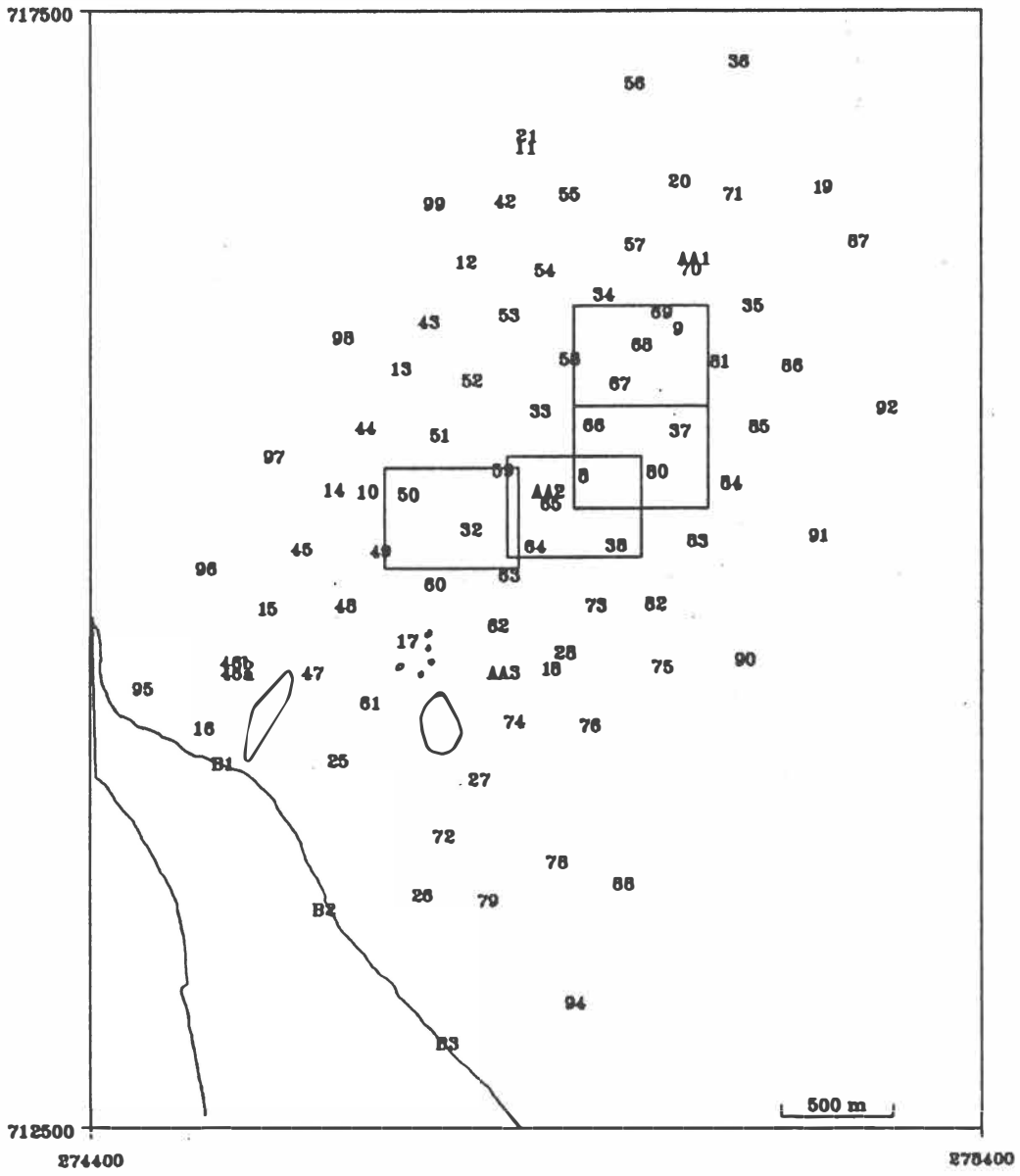

Fig.5.20: Locations of the sediment samples in the survey area. Samples from the Aanderaa-sites indicated by Aa and from the beach by B.

5.3.4.2 Sediment analysing method

The textural parameters of the sediment samples were determined by using the Rapid Sediment Analyser (RSA) at the Earth Sciences Department of the University of Waikato.

The Rapid Sediment Analyser consists of a settling tube and a linked McIntosh Computer with a printer. After removal of the silt and clay fraction by washing the sample through a 4 Φ sieve 20-50 g of the sample are analysed in the settling tube. The loss of the material finer than 4 ϕ does not affect the accuracy of the analysis considerably as most of the inner shelf samples contain less than 1% mud.

The settling velocity of the grains in the tube is measured and converted to grain-size weight-percent. The computer analysis of the textural data includes size distribution curves, the arithmetic cumulative and cumulative probability curves, and the parameters of mean and median grain-size, sorting, skewness and kurtosis of FOLK and WARD's (1957) graphic method and the momentum method.

The grain-size analysing procedure is based on Stokes' Law (i.e., the grain-size is a function of the settling velocity). The settling velocity of a grain depends on its size, density and shape (BABA and KOMAR, 1981). Natural sediments commonly do not consist of grains of a material with one typical density and shape but are mixtures of grains with different properties. Therefore the RSA has its limitations for determining the accurate grain-size. For the samples analysed in this study, the generally applied density of 2650 kg/m^3 for quartz was used although some samples contain high amounts of light or heavy minerals such as pumice or titanomagnetite (Section 5.3.5). Consequently, for samples with a considerable amount of pumice in the medium and fine sand fraction the mean grain-size values used are probably too high. Coarse sand samples contain up to 10% of titanomagnetite which makes their mean grain-size too low. Some samples also have a high shell content. The planar shape and lower density of the shells causes a higher mean grain-size. In addition to the inaccuracy implied by the system, operational errors can occur. The triggering of the sediment release mechanism on top of the tube and walking up and

down the stairs to the top of the tube can introduce balance errors.

The RSA method for textural analysis was chosen instead of sieving because the main aim of the survey was to determine the hydraulic textural parameters of the sediments, which then can be better related to calculations of threshold velocities.

Typically the Tauranga inner shelf sediment samples possess a unimodal grain-size distribution which means that the mean, median and modal grain-size values are reasonably similar. In most samples the mean and median grain-size parameters do not differ by more than 0.1 ϕ. Textural parameters are defined in App.5.1.

5.3.4.3 Natural shelf sediments at the control-site

One aim of the study was to assess, if and in which way, the dumping of dredge spoil changes the natural sediment distribution on the inner shelf. To obtain a comparison with the survey area a control-site in the east of the survey area along a beach - offshore line from Omanu Beach was sampled.

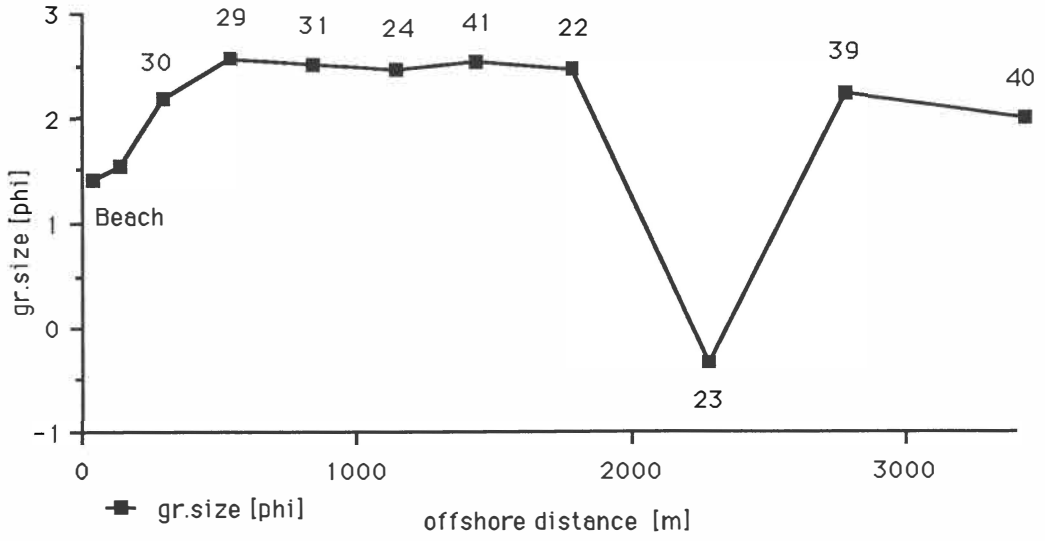

Fig.5.21a: Beach - offshore mean grain-size profile along the control-site. Fine sand (M_z=2.5ϕ) is interrupted by very coarse sand at 2200 m offshore.

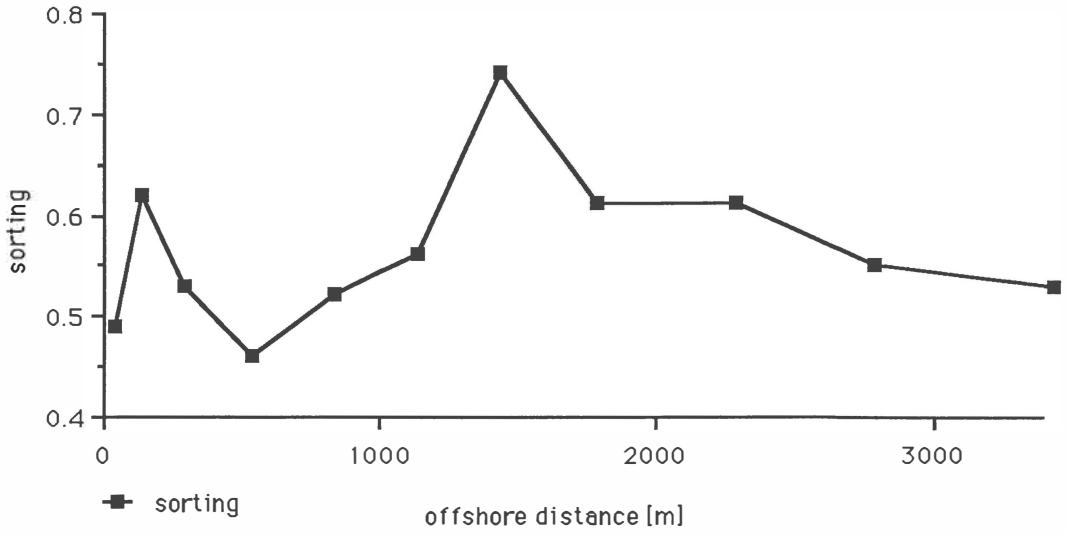

Fig.5.21b: Beach - offshore sorting profile. Natural shelf sediments are generally moderately well sorted.

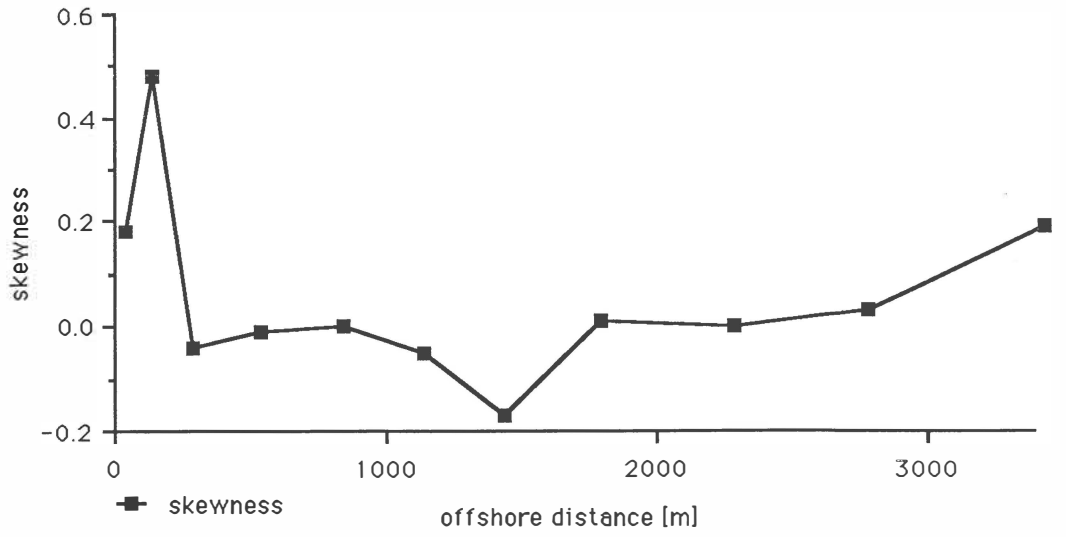

Fig.5.21c: Beach - offshore skewness profile. Apart from the beach sand, the sediments are symmetrically skewed.

The beach-offshore line shows a constant distribution of fine sand up to about 2200 m offshore (Fig.5.21a). At about 22 m water depth, an abrupt change to very coarse sand occurs. The very coarse sand appears not to be widely distributed as fine to medium sand occurs again 2600 m offshore.

DAHM and HEALY (1980) sampled two beach-offshore profile-lines for their survey of inner shelf sediments; one of them near the control-site of this survey. They noticed the same reduction in grain-size at about 3 km offshore in a similar water depth but did not observe a return to fine sand further offshore. From their observations of the absence of medium sand, also noted at their other beach-offshore transect off Matakana Island, they named the fine sand as "fine sand facies" and the coarse sand as the "coarse sand facies". A similar cross-shelf grain-size distribution was observed on the inner shelf off the east Coromandel coast by DELL *et al.* (1985). They mention very fine and fine sand occurring down to 20-30 m water depth followed by coarse and medium sand down to 40-50 m. Their observation of patches of fine sand within the offshore coarse sand was also noticed over the Tauranga control-site during a recent second side-scan sonar survey. Fine sand inshore and offshore medium to coarse sand belts have also been reported for Omaha Bay north of Auckland by RILEY *et al.* (1985).

The natural shelf sediments are generally moderately well sorted (0.6 +/- 0.15) and near-symmetrically skewed (Fig.5.21b+c).

5.3.4.4 Survey area

To characterise the sediment distribution in the survey area, maps showing the mean grain-size, sorting and skewness were produced (FOLK and WARD graphical method). In addition, beach-offshore profiles plotting textural parameters versus offshore distance and versus each other were undertaken. Beach-offshore plots of all profile-lines containing mean grain-size and sorting are presented in HEALY *et al.* (1988). Differences to the texture maps of HEALY *et al.* (1988) are caused by additional data available in this study.

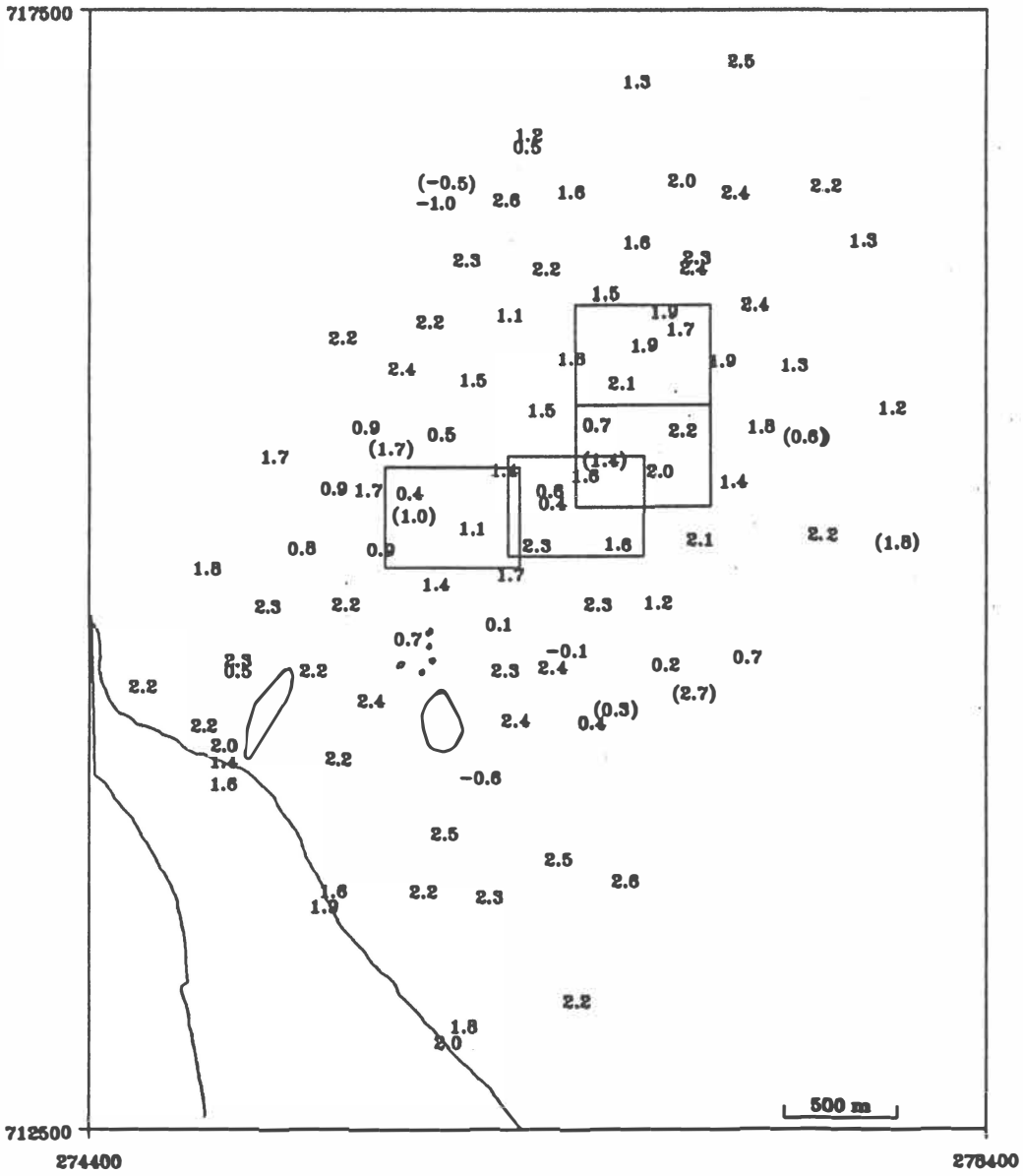
717500
712500
274400
276400
500 m

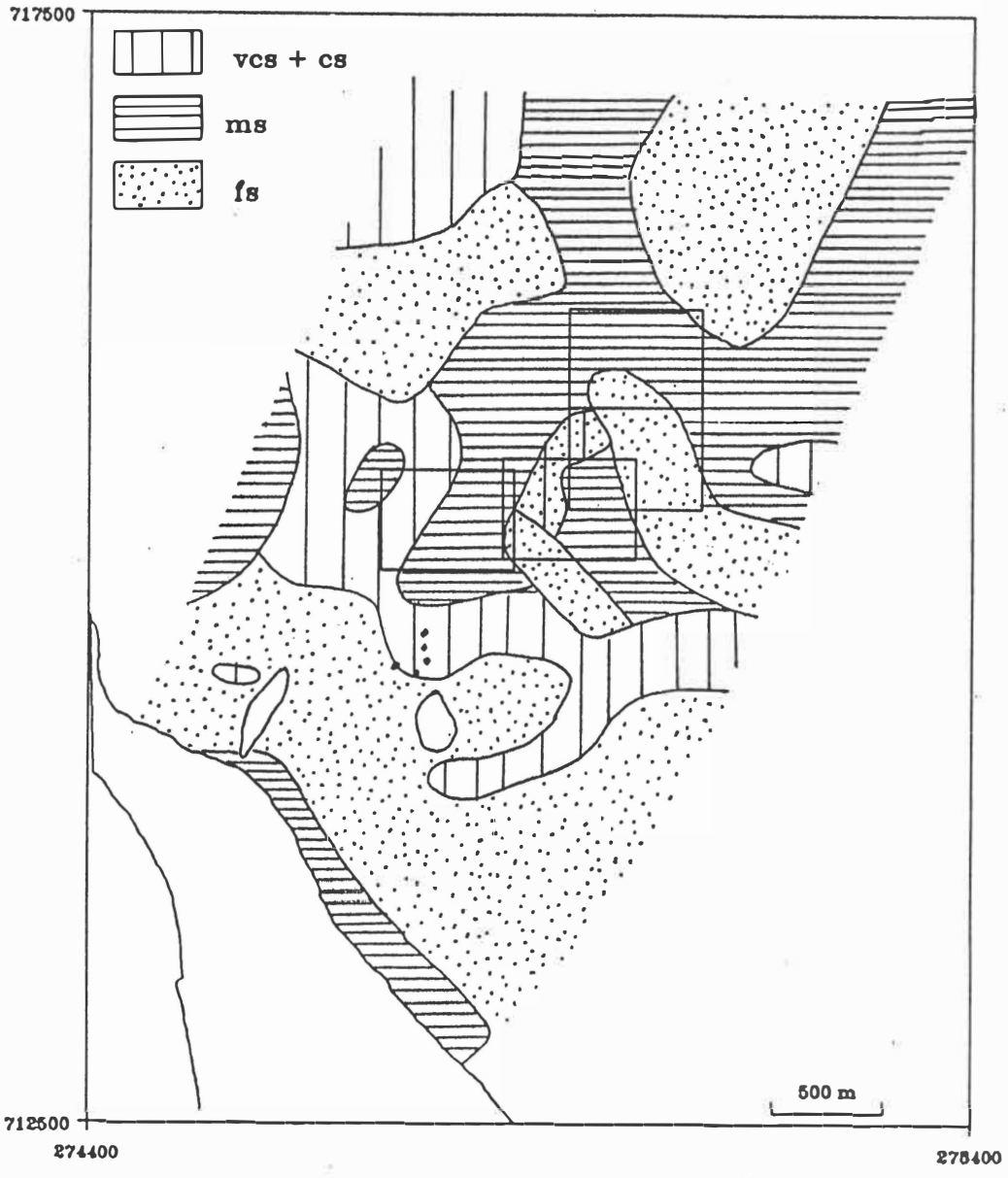

Fig.5.22: Grain-size distribution in the survey area; mean grain-size values (a) and interpretation (b). Grain-size values in brackets from samples collected during the SCUBA survey.

Mean grain-size distribution (M_z)

The following trends of the grain-size distribution of the survey area were interpreted from the mean grain-size map (Fig.5.22a+b) and a beach-offshore plot containing all samples in the survey area (Fig.5.23).

A shore-parallel zone of fine sand (2.2 - 2.6 ϕ), comparable to DAHM and HEALY's (1980) fine sand facies and observed at the control-site, is also evident in the survey area. In contrast to the control-site it only extends up to 1000 m offshore from the beach down to 10 m water depth. Two patches of coarse sand occur within the fine sand zone (east of Motuotau and northwest of Motiti).

Offshore of the fine sand belt, an irregular distribution of coarse, medium and fine sand occurs over and adjacent to the dump-sites up to 2500 m offshore. The coarse sand which contains up to 10% gravel and shell hash, equivalent to DAHM and HEALY's (1980) coarse sand facies, roughly forms a shore-parallel belt which is interrupted by medium and fine sand near and over the dump-sites. The fine sand occurring in this zone can be compared with the fine sand facies observed further inshore. Samples taken close together (18+28; 46a+b; 75a+b) show that the grain-size changes abruptly from coarse to fine sand rather than gradually, a feature also observed on the side-scan sonograph.

Further offshore the coarse sand disappears and medium and fine sand dominate. Some fine sand samples contain a noticeable amount of mud (c.5%; 19, 70). The coarse sand in the northwest of the survey area may be the result of higher current velocities at the margin of the ebb tidal delta.

The grain-size distributions obtained from the THS sampling program in the Cutter Channel and partly in the Entrance is consistent with the medium sand found over the dump-sites. Coarse sand over dump-site C also originates from the harbour which is demonstrated by the occurrence of pipi shells in the samples (HEALY *et al.*, 1988).

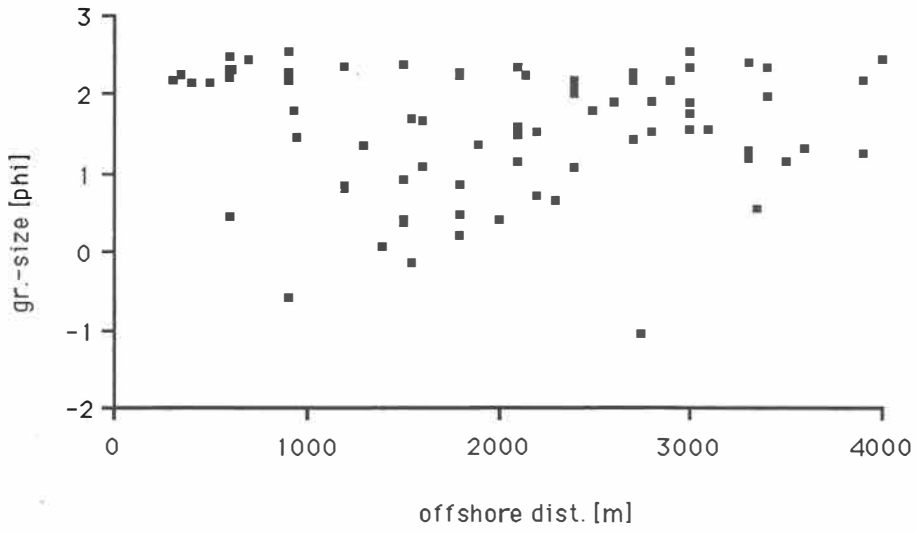

Fig.5.23: Mean grain-size versus offshore distance. Fine sand is typical for the nearshore zone up to 1000 m. The whole range of grain-sizes occur between 1000 and 2500 m. Medium and fine sand dominate from 2500 m offshore.

Sorting and skewness

Zones of well sorted sediment occur at the dump mounds over the dump-sites A, C and D, east of the dump-sites and in the southeast of the survey area (Fig.5.24a+b). An area of moderately sorted material is located southeast of the dump-sites. The sorting parameter does not change with offshore distance and water depth (Fig.5.25)

A west-east aligned band of coarse or negatively skewed material shoreward of the dump-sites could be observed in the skewness map (Fig.5.26a+b). The sediment at the dump-mounds is generally fine or positively skewed. There is a general trend of a west-east oriented fine skewed offshore zone and a coarse skewed onshore zone.

Coarse sands are statistically poorer sorted and finer skewed than the fine sand (Fig.5.27; 5.28). Poor sorting and coarse skewness in some fine sand samples is caused by the abundant occurrence of juvenile whole Tawera spissa (samples 19, 57, 79, 83; Fig.5.29).

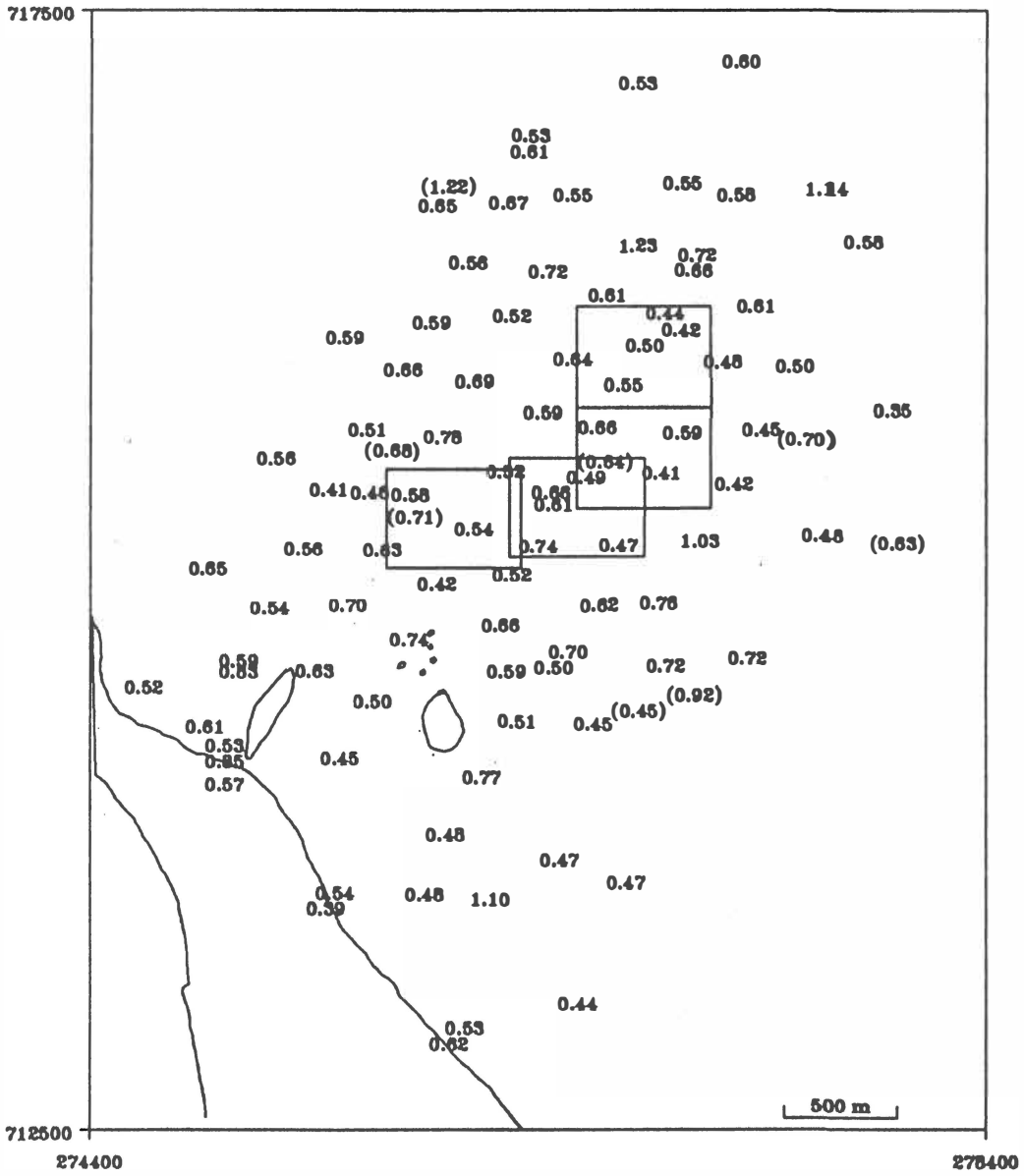
717500
712500
274400
278400
500 m
0.60
0.53
0.53
0.61
(1.22)
0.65
0.67
0.55
0.55
0.58
1.14
1.23
0.72
0.66
0.58
0.56
0.72
0.61
0.44
0.61
0.59
0.52
0.42
0.59
0.50
0.64
0.48
0.50
0.66
0.69
0.55
0.59
0.35
0.51
0.78
0.66
0.59
0.45
(0.70)
(0.68)
0.56
(0.64)
0.49
0.41
0.42
0.41
0.46
0.58
(0.71)
0.54
0.61
0.56
0.63
0.74
0.47
1.03
0.48
(0.63)
0.65
0.42
0.52
0.54
0.70
0.62
0.76
0.66
0.74
0.70
0.59
0.63
0.59
0.50
0.72
0.72
0.52
0.50
(0.92)
(0.45)
0.61
0.51
0.45
0.53
0.45
0.57
0.77
0.48
0.47
0.47
0.54
0.48
1.10
0.59
0.44
0.53
0.62

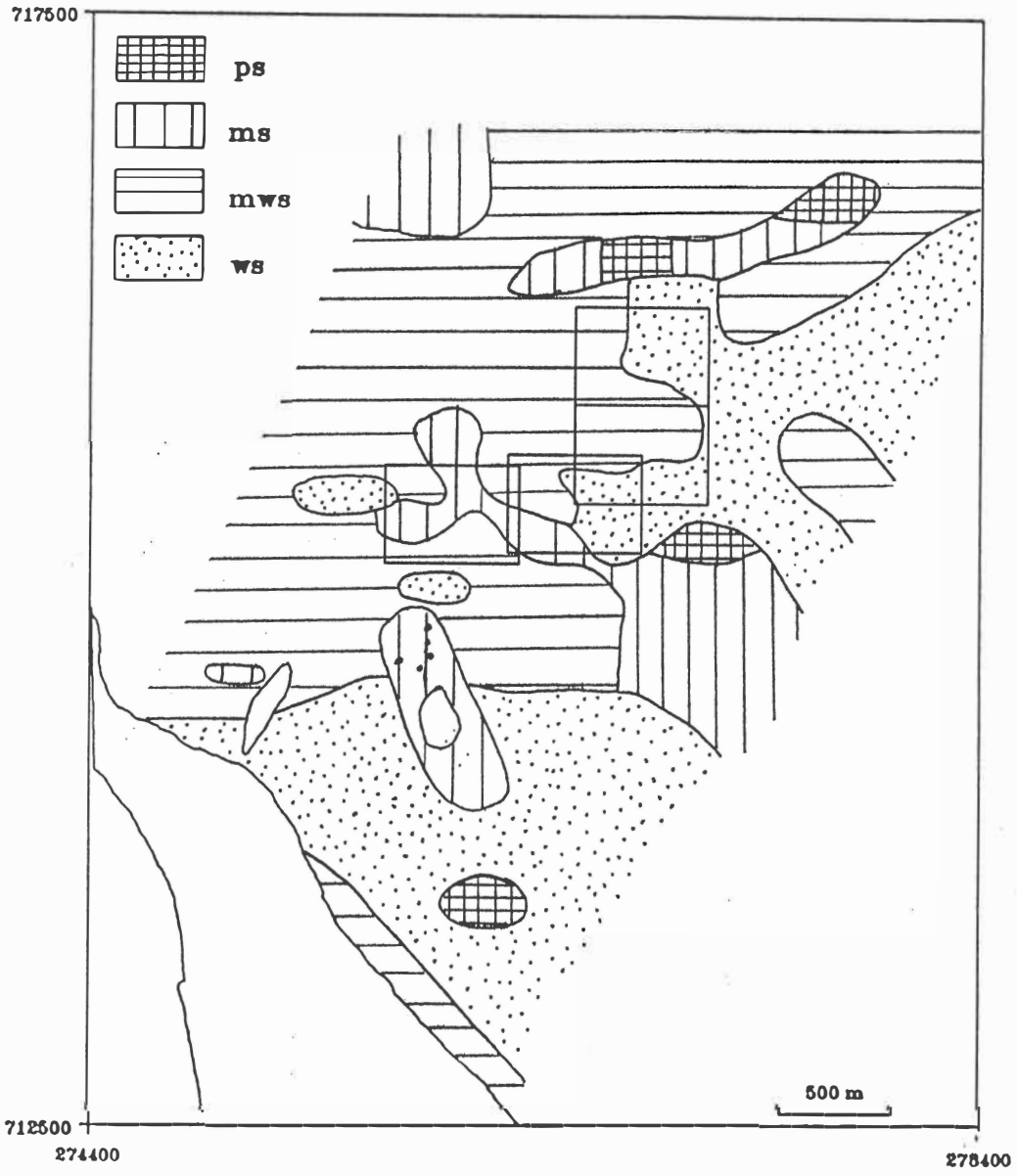

Fig.5.24a,b: Sorting map of the survey area; well sorted sediment over the dump-mounds and moderately sorted sediment south of it indicate movement of fine material in a southward direction.

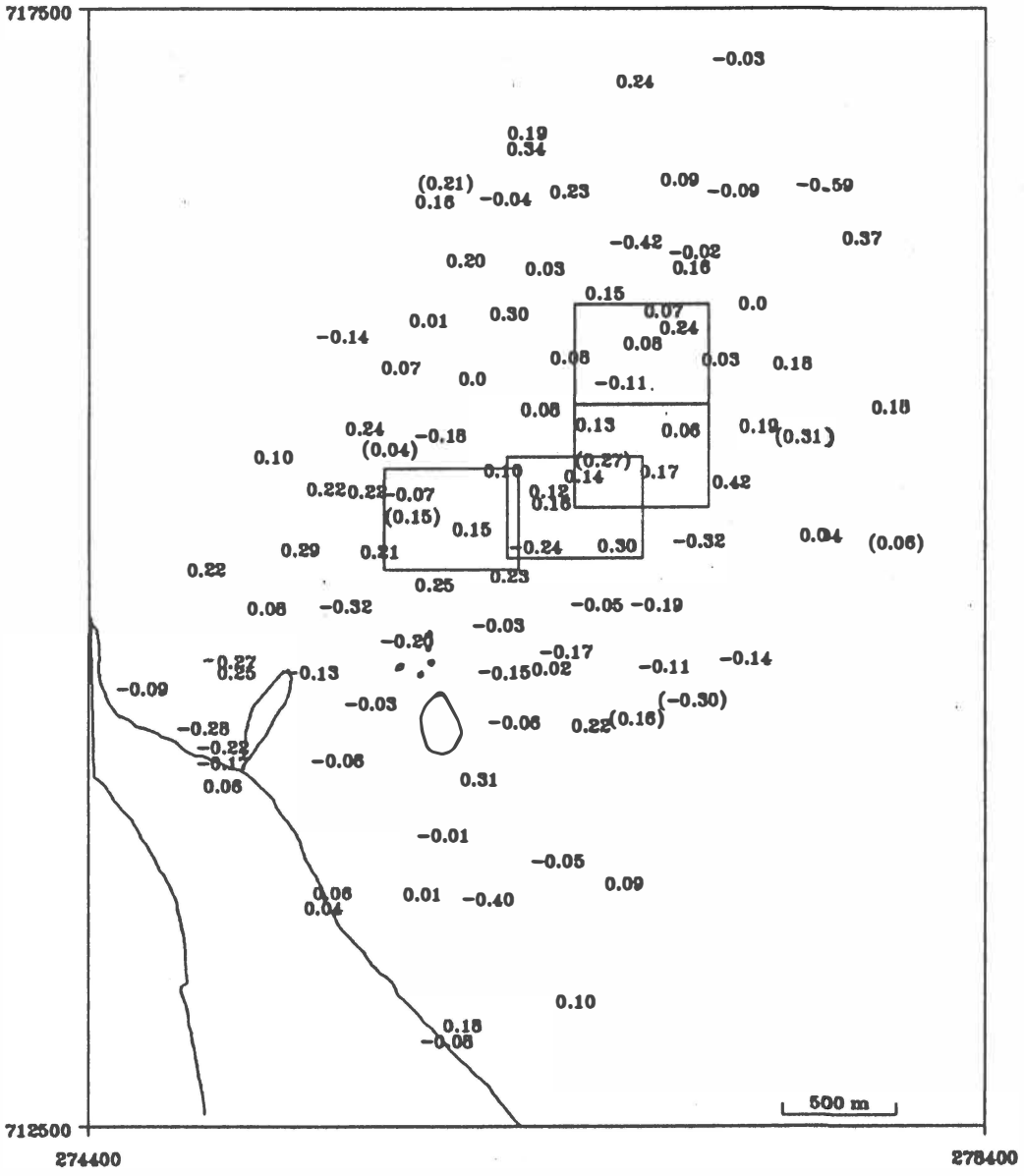
717500
712500
274400
278400
500 m
-0.03
0.24
0.19
0.34
(0.21)
0.16
-0.04
0.23
0.09
-0.09
-0.59
-0.42
-0.02
0.37
0.20
0.03
0.16
0.15
0.0
0.01
0.30
0.07
0.24
-0.14
0.08
0.08
0.03
0.18
0.07
0.0
-0.11
0.18
0.24
-0.18
0.13
0.06
0.19
(0.31)
0.10
(0.04)
(0.27)
0.14
0.17
0.42
0.22
0.22
-0.07
0.12
(0.15)
0.15
0.29
0.21
-0.24
0.30
-0.32
0.04
(0.06)
0.22
0.25
0.23
0.08
-0.32
-0.05
-0.19
-0.03
-0.20
-0.17
-0.27
0.25
-0.13
-0.15
0.02
-0.11
-0.14
-0.09
-0.03
(-0.30)
-0.28
-0.06
0.22
(0.16)
-0.22
-0.17
-0.06
0.06
0.31
-0.01
-0.05
0.09
0.06
0.01
-0.40
0.04
0.10
0.15
-0.06

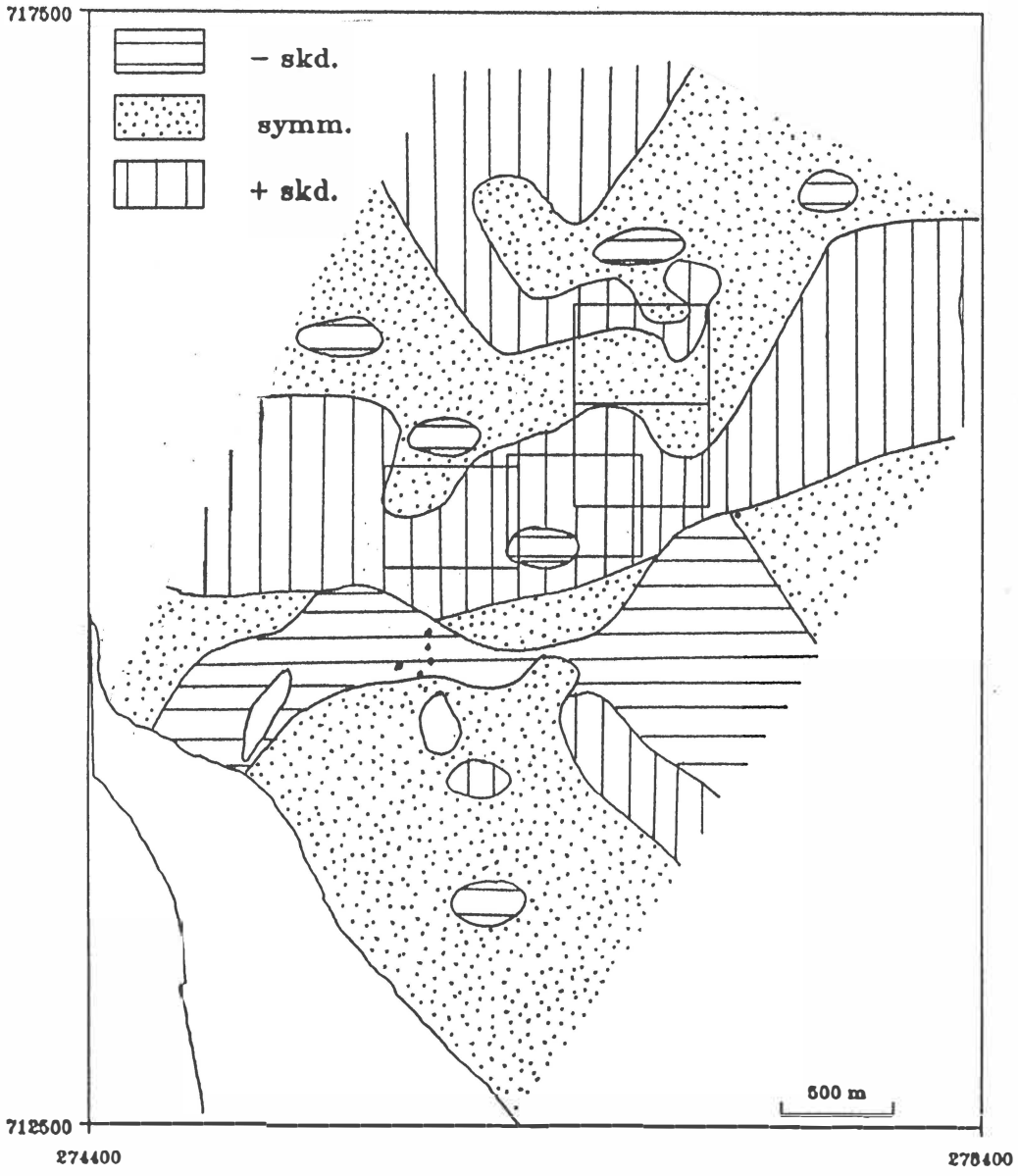

Fig.5.26a,b: Skewness map of the survey area; positive skewness in the north and negative skewness in the south suggest an north-south onshore movement of fine material.

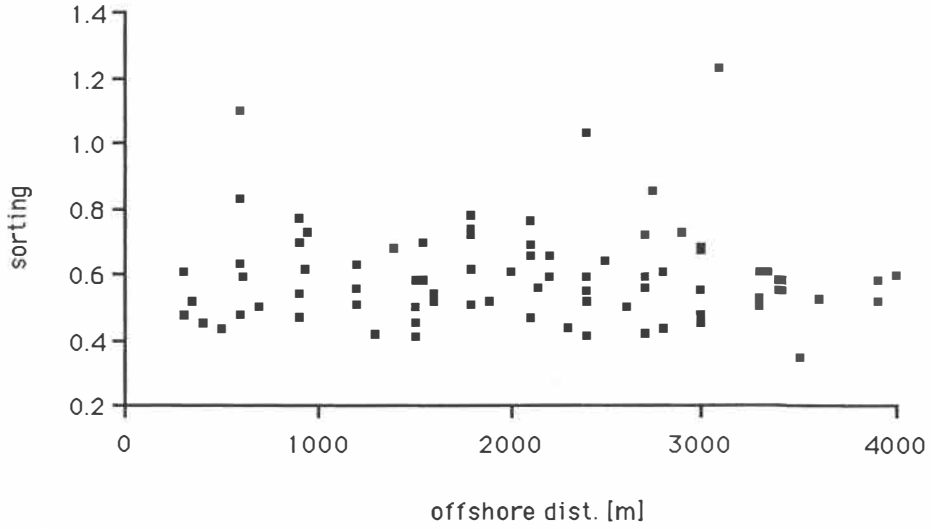

Fig.5.25: Sorting versus offshore distance; no significant changes in sorting occur with offshore distance.

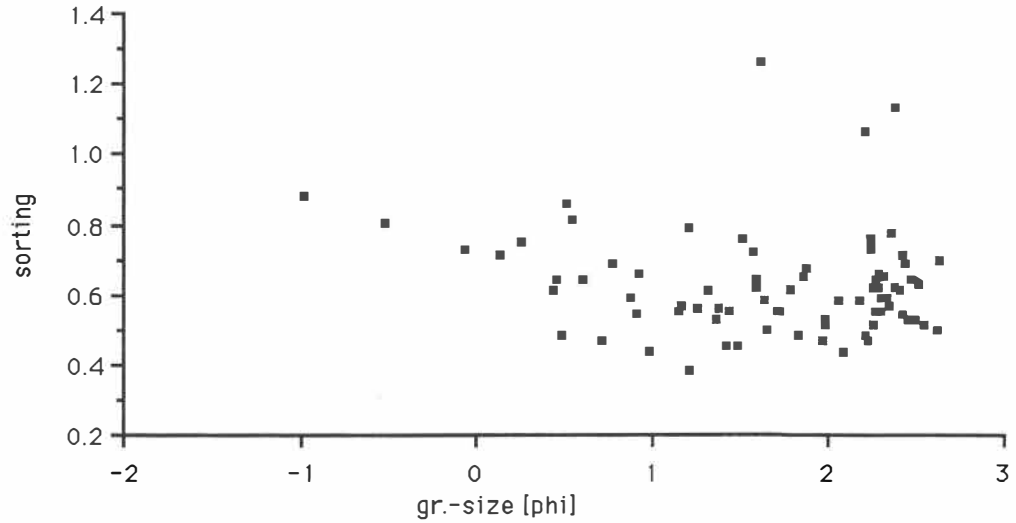

Fig.5.27: Grain-size versus sorting; coarse sand is generally poorer sorted than fine sand.

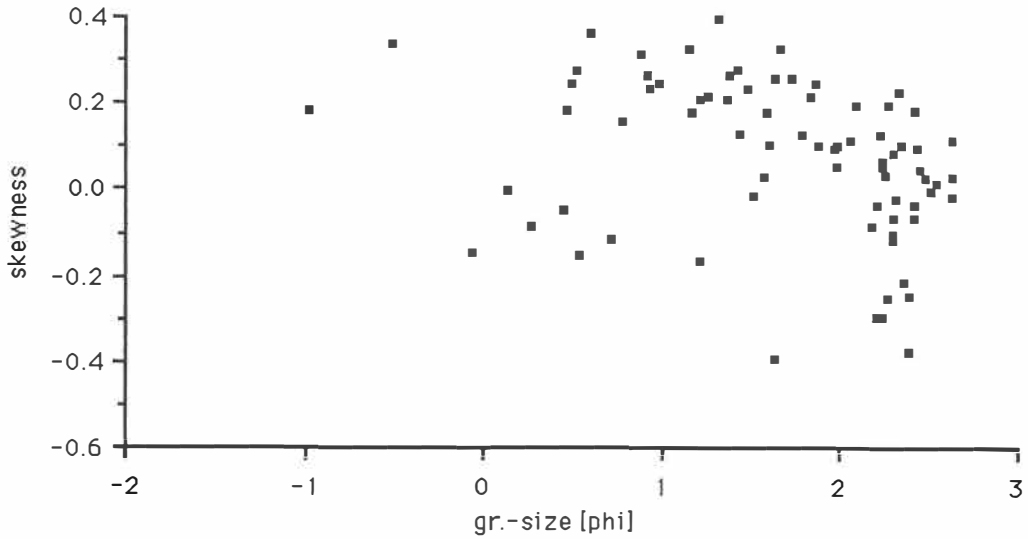

Fig.5.28: Grain-size versus skewness; coarse sands are generally more negatively skewed than fine sand.

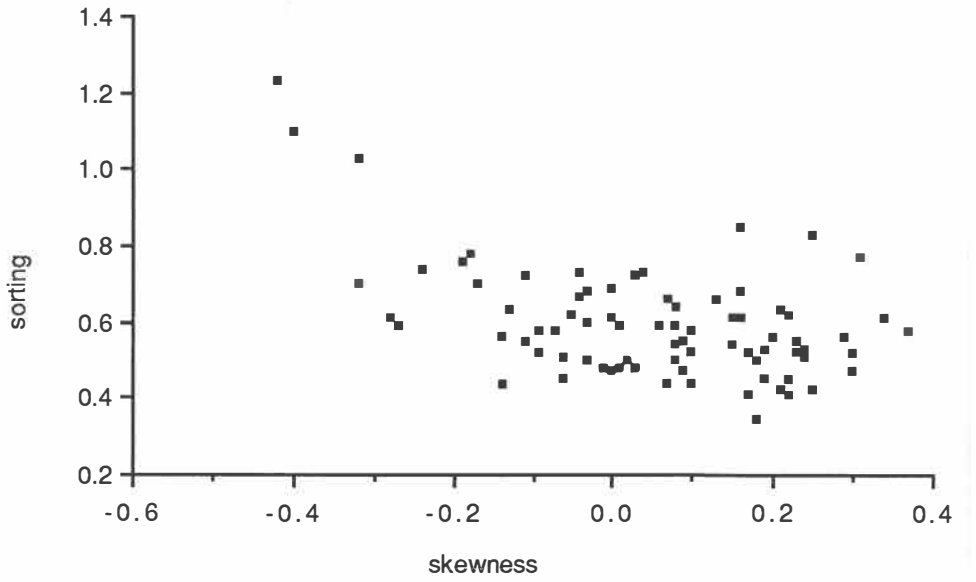

Fig.5.29: Sorting versus skewness; poorer sorted sediments are generally negatively skewed.

Beach samples

Mount Maunganui Beach consists of medium to fine sand with mean grain-sizes between 1.4 and 2 ϕ. From the collected limited number of samples it appears that the position of the samples at the beach cross-section (berm or bottom) does not show a typical grain-size distribution. The grain-sizes of this study are consistent with those reported by HEALY *et al.* (1977) from Mount Maunganui Beach and are similar to the control-site. The beach sands are moderately well sorted.

5.3.5 Mineralogical composition

Eight samples of inner shelf samples were selected from the three dump-mounds (8, 9, 10) and along one beach-offshore transect (26, 28, 37, 38 and 19) and have been petrologically analysed.

The three dump-mound samples from the dump-sites A, C and D are very similar. The only significant variation occurs in the pumice content. Sample 9 as the latest dumped material at dump-site D contains more pumice (c. 10%) than sample 8 and 10 from dump-sites A and C (c. 5%). The dredge spoil has a similar mineral assemblage to the samples from the capital dredge-site.

The samples along the shore-normal profile-line 7 (c. 100 m east of the dump-mound at dump-site C; HEALY *et al.*, 1988; samples numbers in Fig.5.20) also have a similar mineral content to the harbour samples and the dredge spoil. There appears to be a change in the mineral content with the grain-size. The coarse sand sample (28) contains c. 10% titanomagnetite and less than 10% pumice whereas medium and fine sand samples have pumice contents between 40 and 95% and low titanomagnetite contents under 2%. In fine and medium sand pumice and plagioclase as the major minerals substitute each other. The pumice content of the analysed samples is given in Table 5.3 and plotted together with grain-size versus beach-offshore distance (Fig.5.30).

No.	gr.si	sort.	pum.cont.
26	2.2	0.48	80%
28	-0.1	0.70	<10%
38	1.6	0.47	95%
37	2.2	0.59	40%
19	2.2	1.14	40%

Table 5.3: Pumice contents of sediment samples collected along profile-line 7.

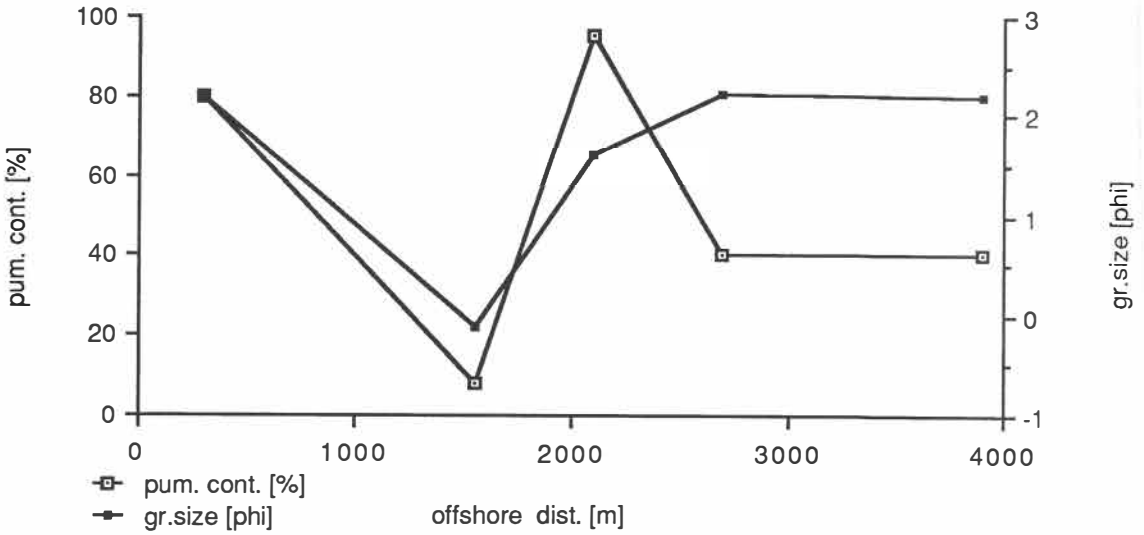

Fig.5.30: Pumice content and mean grain-size versus offshore distance along a beach - offshore line 100 m east of dump-site C.

From the limited number of analysed samples it appears that the pumice content of the fine and medium sand decreases in an offshore direction, an observation which DAHM and HEALY (1980) also made when they analysed samples from transects off Omanu beach and Matakana Island. Their investigations indicate that natural sediments have pumice contents between 30 and 100%.

It is acknowledged by the author that the textural data from the RSA gives a far too small grain-size compared to sieving when pumice contents are as high as in some of the samples in the survey area. Microscope observations show that samples 26 and 38 with high pumice contents consist of large, angular shaped pumice grains with the rest of the minerals being much smaller. The size of the pumice grains is between 0 and 1 ϕ. Therefore, the good sorting, given by the RSA data for the samples, is a hydraulically good sorting but not so size wise.

5.4 Implications for sediment transport

The input of a material from a different area and its subsequent dispersion is likely to change the natural inner shelf sediment distribution. Thus, differences in texture and mineralogy over and in the vicinities of dump-sites may give evidence about transport directions on a larger scale than the undertaken bathymetric surveys did.

Textural and petrological analysis show that the grain-size distribution and mineralogical composition of the dredged sediments does not differ considerably from the natural shelf sediments (Table 5.4). This is in agreement with DAVIES-COLLEY's (1976) proposal that the harbour sediments are reworked shelf sediments moved onshore during the Holocene transgression. The similarity and also the accidental mixture of material from different dredge-sites makes it difficult to trace a dredge spoil. The occurrence of medium sand over the dump-sites, not found at the control-site and not reported by DAHM and HEALY (1980), is the result of the dumping of predominantly medium sand in the past.

Parameters	Dredged sediment		Natural sediment	
	Harbour	Entrance	coarse sand	fine sand facies
Mz [phi]	1-2	0.5-1.5	-0.5-1	2-2.5
sorting	0.6-1.3	0.3-0.7	0.6-0.8	0.4-0.7
pumice [%]	0-40	0-10	<10	40-80

Table 5.4: Comparison of grain-size, sorting and pumice content between dredged sediment and natural sediment.

Medium sand in the vicinity of the dump-sites can be either due to random dumping outside the designated dump-sites or to the deposition of fine material subsequent to its erosion from the dredge spoil in the coarse sand facies, thus creating a "medium sand facies" (e.g. sample 82; Fig.5.31). The medium sand found further offshore represents the natural sediment. Medium sand occurring with coarse sand has also also reported for the east Coromandel shelf offshore from 20-30 m by DELL *et al.* (1985).

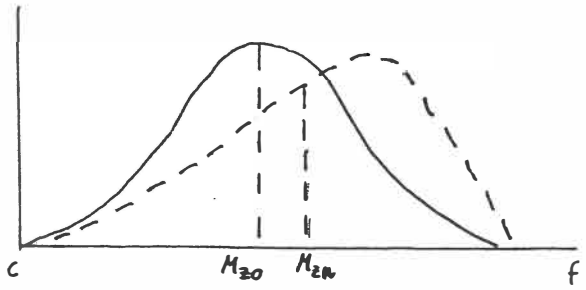

Fig.5.31: Schematic sketch of the change in textural parameters by the deposition of fine material in coarse sand.

Textural parameters have been used to indicate sediment transport directions. McLAREN (1981) and McLAREN and BOWLES (1985) found that the lag is always coarser, better sorted and more positively skewed than its source. Sediments undergoing transport become progressively finer and more negatively skewed.

As the dredge spoil over the dump mounds is generally better sorted and more positively skewed than the sediments southward it can be considered as a lag deposit according to McLAREN and BOWLES (1985). The coarser grain-sizes over older dump-sites (A,C) in comparison to dump-site D may also indicate a coarsening process over time. A zone of poorer sorting and negative skewness south of the dump-site C can be explained by the deposition of fine material in coarse sediment after erosion from the dredge spoil (Fig.5.31). This suggests an onshore movement of material from the dump-site. The two skewness zones (Fig.5.26b) with offshore positive and inshore negative skewness values may also indicate a general N-S directed onshore sediment transport trend.

The better sorting in the nearshore zone is probably due to the higher effect of wave-induced transport processes.

With the exception of the northern Mount Maunganui Beach sample (B1), the medium sand from the beach is moderately well sorted and symmetrically skewed. This indicates that not much fine material from possible onshore movement has been deposited permanently on the beach.

The low pumice content of the dredge spoil at dump-site C (c. 5%) compared with dredge spoil at dump-site D and generally higher pumice contents from the harbour (Fig.5.3; Table 5.3) suggests that pumice has been winnowed out of the dredge spoil. Although natural sediments can contain high amounts of pumice (up to 100%: DAHM and HEALY, 1980) the high pumice content in sample 38 (95%) south of the dump mound may indicate the deposition of pumice south of the dump-site subsequent to its erosion from the dredge spoil.

Interpretation of textural parameters and pumice contents in the survey area favors a net southward transport of fine sand and pumice from the dredge spoil. It has to be noted, though, that more recent dumping at dump-site D makes it difficult to recognize sediment transport trends in an offshore direction from the dredge spoil dumped at dump-site C in 1977/78.

5.5 Facies interpretation

5.5.1 Bedform/grain-size distribution

When comparing bedform and grain-size distribution in the survey area the megaripple patches and fields are generally associated with coarse sand. This is demonstrated in particular by the two megaripple fields in the NW and SE of the survey area which coincide with coarse to very coarse sand (Fig.5.11, 5.22). Flat, lightly rippled and bioturbated sea-floor (sonograph facies 1) is associated with fine sand with a high pumice content and ripples (sonograph facies 2) are often found in medium sand. This is in agreement with the observation that the bedform size increases with the grain-size, noted for the inner shelf off Tauranga before by DAHM and HEALY (1980). SCUBA observations indicate that medium sand (c. 1.5 ϕ) appears to be a critical value for the long-term persistence of ripples (Fig.5.12).

The megaripple ridges occur in coarse and medium sand towards the western side of the survey area. Compared with the megaripple fields and patches the coarse sand in the ridges is finer with the largest mean grain-size at 0.5 ϕ.

5.5.2 Generation of bedforms

The bedforms in the survey area possess a symmetrical shape and change their wavelength and height due to high wave events during storms (Table 5.2). This strongly suggests that they are wave-generated although CLIFTON and DINGLER (1984) note that it is not yet known how to recognise bedforms which have a unidirectional flow superimposed on an oscillatory flow.

The observed changes in bedform size over time can be considered as a response of the sea-bed to different wave conditions. Swell waves with high wave heights and periods following onshore storms are capable to generate large ripples and megaripples. Under fair weather conditions smaller wave orbital velocities occur which results in the degradation of storm generated large megaripples and the generation of smaller bedforms. The changing of ripples over

time has been reported by SWIFT *et al.* (1979) on the Long Island inner shelf noting the disappearance of megaripples in the summer and their generation in the winter when storms are more frequent. The occurrence of larger megaripples in August 1988 after winter storms in July (Section 6.3.5) and their smaller size in November 1988 suggests a similar process for the inner shelf off Tauranga. Especially the observed response of the sea-bed to the easterly storm between the two Aanderaa surveys supports these changes. The active response of the inner shelf off Tauranga to present-day activity is also shown by the development of megaripples at dump-site C.

Ripple sizes generally increase further onshore because the wave orbital diameter increases with decreasing water depth (e.g. MILLER and KOMAR, 1980b). As the ripple size is also a function of the grain-size (MILLER and KOMAR, 1980a), the fine sand, which occurs in the nearshore zone of the survey area, causes the formation of smaller ripples towards the shore.

5.5.3 Megaripple fields and patches

The patchy distribution of megaripples or coarse-grained ripples on the inner shelf has been reported from various other shelves (summarised in LECKIE, 1988). The water depth in which the megaripple patches have been observed varies widely from 4 m at Rhode Island, east coast of the U.S.A., to around 150 m in the Celtic Sea (LECKIE, 1988, table 1). Megaripple patches have also been reported elsewhere along the east coast of New Zealand from side-scan sonar surveys on the ebb-tidal delta off Whangarei Harbour (BLACK and HEALY, 1983) and on the inner shelf off the Coromandel coast (DELL *et al.*, 1985) and in Poverty Bay (KENSINGTON, 1989, pers.comm.). They are probably a common feature along the New Zealand east coast as coarse sand bands typically associated with the megaripple patches have been reported frequently (e.g. McCABE, 1985; RILEY *et al.*, 1985).

The megaripple patches have been characterised by COOK (1982), interpreting a side-scan sonar survey undertaken by McMASTERS and MORANG (1980) near Rhode Island off the east coast of the U.S.A., as: 1) they are elongate in a shore-normal direction and occur parallel to each other in fields; 2) they consist of coarser sediments than the surrounding fine to medium sand; and 3) they exist in topographic lows. These criteria match those observed for the megaripple patches in the survey area.

The occurrence of the megaripple patches in topographical depressions suggests that the fine sand is underlain by the coarse sand (Fig.5.32). Thus coarse and fine sand probably represent two different layers; a coarse sand layer with a relatively low pumice and high heavy mineral content overlain by a fine sand layer with a high pumice content. It was not ascertained during this study whether the coarse sand forms one thick layer throughout the survey area which is stripped off the fine sand locally or whether there are fine - coarse sand alternations. Shallow coring would provide more information on this point. Shallow cores were taken from similar deposits off the Californian coast by HUNTER *et al.* (1988). They found that the coarse sands do not simply form a thick deposit but that thin layers of coarse sand are underlain by, and interbedded, with fine sand.

Fig.5.32: Schematic sketch of the coarse-grained ripples overlain by a fine sand blanket, indicated by their occurrence in topographic depressions.

The coarser grain-size of the underlying deposit can be of two origins. Similar inner shelf deposits on the east coast of the U.S.A. have been interpreted as the basal gravel of the Holocene transgression (NIEDORODA *et al.*, 1985). According to this interpretation, the active coarse sand facies on the Tauranga inner shelf could be termed a "palimpsest" deposit (SWIFT *et al.*, 1971). On the other hand, the coarse sand could be a lag deposit generated

by the removal of the fine material and pumice through a winnowing out process. This process still occurs (lag surface on dredge spoil) but was probably initiated during a lower sea-level when wave orbital velocities were higher due to the lower water depth, and fed and formed the now overlying fine sand layer. A similar process was suggested by RILEY *et al.* (1985) for the formation of the offshore coarse sand belt at Omaha Bay. It is not possible from the collected data of this study to conclude on the age of the deposit and its original grain-size and thus decide whether it is a transgressive or lag deposit.

Large changes in size and distribution of megaripple fields surrounded by featureless sands were observed for similar deposits off the Californian coast by HUNTER *et al.* (1988) who undertook four side-scan sonar surveys over three years. They explained these changes by the migration of fine sand over coarse sand was, a process which has also been suggested by COOK and GORSLINE (1972) and CACCHIONE *et al.* (1984). Although no repeated side-scan sonar surveys have been undertaken on the Tauranga inner shelf so far, it is very likely that this process also occurs in the survey area.

The very rare exposure of the coarse sand facies further inshore is probably due to the greater thickness of the fine sand in the nearshore zone.

Although no evidence is provided by the sea-floor survey, the author suggests that the eroded fine sand and pumice from the dredge spoil eventually mixes with the fine sand facies.

5.6 Effects of the 1988 dumping

Sediment recollections from former sample points were made in early December 1988 one week after the end of dumping, to evaluate any chang s in textural parameters consequent upon the dumping. About 130,000 m^3 of dredge spoil was spread over a wide area at dump-site D. The grain-size distribution of the post-dump samples reflects the widespread dumping. Not only did the size of the material inside the dump-site change (one sample from 1.7 to 0.4 ϕ), but

significant changes were also noted outside the dump-ground (Fig.5.32). The sediment samples also show that the grain-size of the new dumped dredge spoil varies between 0.4 and 2 ϕ due to the location of the dredge-sites. The poorer sorting parameters occurring in the recently dumped dredge spoil supports the observation that the dredge spoil becomes progressively better sorted over time (Fig.5.33).

The spreading of dredged material over a large area will make it more difficult to monitor dredge spoil dispersion.

5.7. Conclusions

1) Dredged material dumped on the inner shelf varies significantly in grain-size, sorting and pumice content due to the location of the dredge-site (M_z = 0.5 - 2 ϕ, sorting = poorly to well sorted, pumice content = 0 - 40%).

2) The natural inner shelf sediment distribution in the survey area, obtained from side-scan sonar and visual records as well as textural analysis, consists of an inshore fine sand facies (up to 1000 m offshore) and irregularly distributed patches of coarse sand (coarse sand facies) surrounded by fine to medium sand up to at least 4 km offshore. Fine sands contain between 40 and 80% pumice and less than 2 % titanomagnetite. The coarse sand has a significantly lower pumice content (<10%) and a higher plagioclase and titanomagnetite (up to 10%) content.

3) The natural sediment distribution is altered by the dumping of dredged material over the dump-sites and by the dispersion of the dredge spoil in their vicinities. The mineralogical similarity dredged and natural inner shelf sediments makes it difficult to trace the dredge spoil. Sorting and skewness parameters as well as pumice contents suggest that fine sand and pumice are winnowed out of the dredge spoil and deposited southward of the dump-sites.

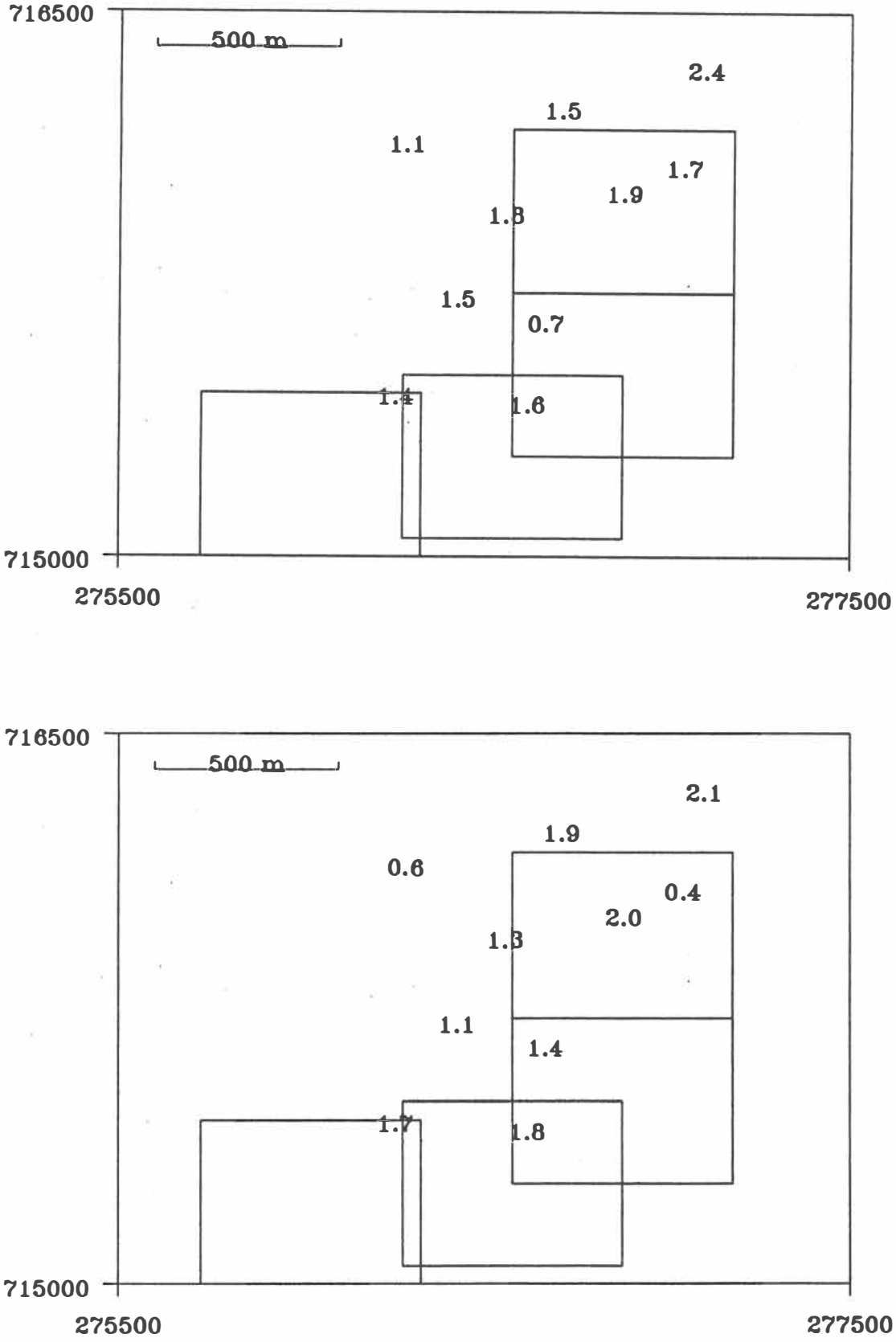

Fig.5.33: Mean grain-size of sediment at dump-site D before (a) and after dumping in 1988.

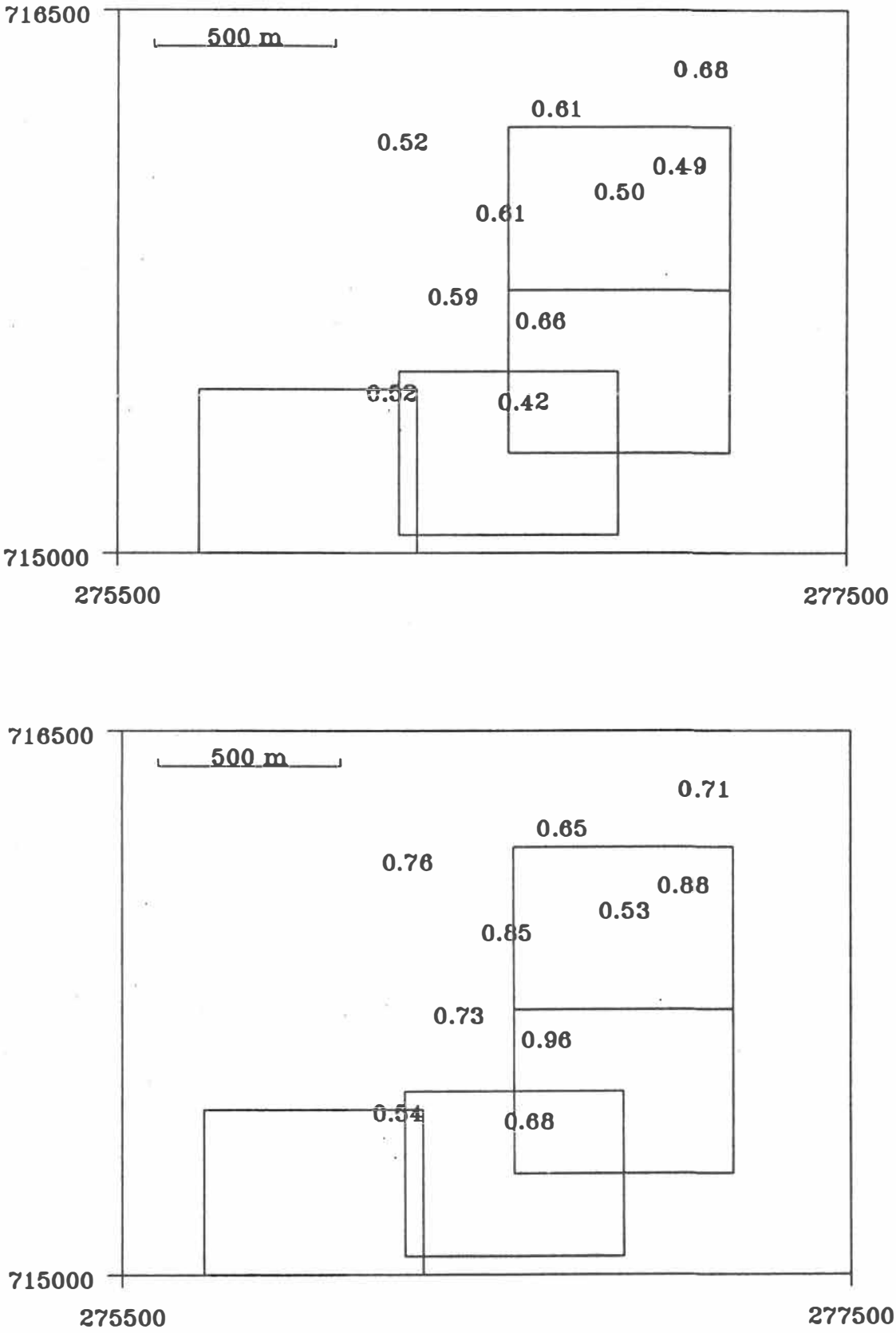

Fig.5.34: Sorting of sediment at dump-site D before (a) and after dumping in 1988 (b).

4) Symmetrical ripples and megaripples, which changed size and direction over time, were observed in the coarse sand. Fine sand is either flat, lightly rippled or bioturbated. Ripples appear to be persistent in medium sand < 1.5 ϕ. The observed sea-floor changes indicate the activity of the bottom sediments to storm events. The symmetry of the bedforms suggests their formation by waves.

5) The occurrence of the megaripple or wave-formed coarse-grained ripple patches in topographical depressions, surrounded by fine to medium sand, suggests that the coarse sand is overlain by fine sand. The coarse sand may either represent a transgressional deposit from the late Holocene or a lag deposit which produced the overlying fine sand sheet. The fine sand blanket is likely to migrate as a whole over the coarse sand. The megaripple patches occur beyond 20 m water depth. Further inshore they are replaced by shore-normal oriented megaripple ridges. The non-exposure of coarse sand patches further inshore indicates the increasing thickness of the fine sand deposit.

6) It is suggested that the fine sand and pumice eroded from the dump-sites eventually mixes with the fine sand facies.

CHAPTER 6

THE HYDRODYNAMICS IN THE SURVEY AREA AND THEIR ROLE IN SEDIMENT TRANSPORT

6.1. Introduction

As discussed in Chapter 3, waves and currents are responsible for the movement of sediment in the nearshore and the inner shelf zones. This chapter investigates the hydrodynamics acting in the survey area using data collected during previous studies (Chapter 2) as well as during this study. The data are used to interpret the direction and frequency of sediment movement, in particular over the dump-sites, at first for waves and currents separately, and then for the wave-current interacting case.

6.2 Waves and their effects on sediment transport

6.2.1 Threshold conditions

The threshold velocity is the critical velocity at which the first sediment particles start to move. It was first defined for uni-directional flow and later also applied to oscillatory flow (see KOMAR, 1976). During experiments on threshold velocities in flume experiments, the definition of the threshold criterion may have been different due to the experimental procedure leading to slightly different results (e.g. GRANT and MADSEN, 1976; BLACK and HEALY, 1982). The threshold velocity does not specify a sediment transport rate; grains may only move for a limited period during any given time interval (KOMAR, 1976).

In order to characterise the wave conditions under which sediment transport is initiated two nomograms were produced for dump-site C (h=13 m) and D (h=20 m) determining the critical wave height for three typical grain-sizes of the survey area and varying wave periods reported to be representative for the New Zealand east coast (HARRAY, 1977; HARRIS *et al.*, 1983; Fig.6.1).

To calculate the threshold velocity for grains smaller than 0.5 mm the dimensionless equation of KOMAR and MILLER (1973) was used

$$\frac{\rho u_{cr}^2}{(\rho_s - \rho)gD} = 0.21 \left(\frac{d_o}{D}\right)^{1/2} \qquad (6.1)$$

where u_{cr} is the threshold velocity, ρ_s is sediment density, ρ is density of sea-water (1025 kg/m^3 = 1.025 g/cm^3), g is the gravitational constant and D is grain-size diameter in cm. KOMAR and MILLER's empirical equation from 1973, developed for a rippled bed, is still widely used (e.g. CLIFTON and DINGLER, 1984; DRAKE *et al.*, 1985). More recent investigations (RIGLER and COLLINS, 1984) only corrected the proportion factor of the equation slightly. The equation was rearranged for an average sediment density of quartz (2.65 g/cm^3) to give

$$u_{cr} = 32.4\ (TD)^{1/3} \qquad (6.2)$$

for units in centimeters and seconds.

For grain-sizes coarser than 0.5 mm the equation

$$\frac{\rho u_{cr}^2}{(\rho_s - \rho)gD} = 0.46\pi \left(\frac{d_o}{D}\right)^{1/2} \qquad (6.3)$$

suggested by KOMAR and MILLER (1973) assuming quartz density gives

$$u_{cr} = 69.9\ (TD^3)^{1/7} \qquad (6.4)$$

As pumice is a major component of the fine sand facies in the survey area and since it has a significantly lower density than quartz, the threshold velocities for pumice were also calculated by rearranging equations 6.1 and 6.3 for a density of 1.25 g/cm^3. For grains smaller than 0.5 mm equation 6.1 was reformed to

$$u_{cr} = 8.7\ (TD)^{1/3} \qquad (6.5)$$

and for grain coarser than 0.5 mm

$$u_{cr} = 22.5\ (TD^3)^{1/7} \qquad (6.6)$$

was obtained. The threshold velocities for pumice grains are very

small compared to quartz grains (D = 1 mm: pumice 10 cm/s; quartz 30 - 35 cm/s).

To calculate the critical wave heights which appear in Fig.6.1 the equation

$$H = u_{cr} \, T \sinh (kh)/\pi \qquad (6.7)$$

was applied where k is the wave number defined as $2\pi/L$ with L being the wavelength. Because the wavelength decreases when a deep water wave approaches shallow water, three equations were used to calculate L for different water depth/wavelength ratios (KOMAR, 1976).

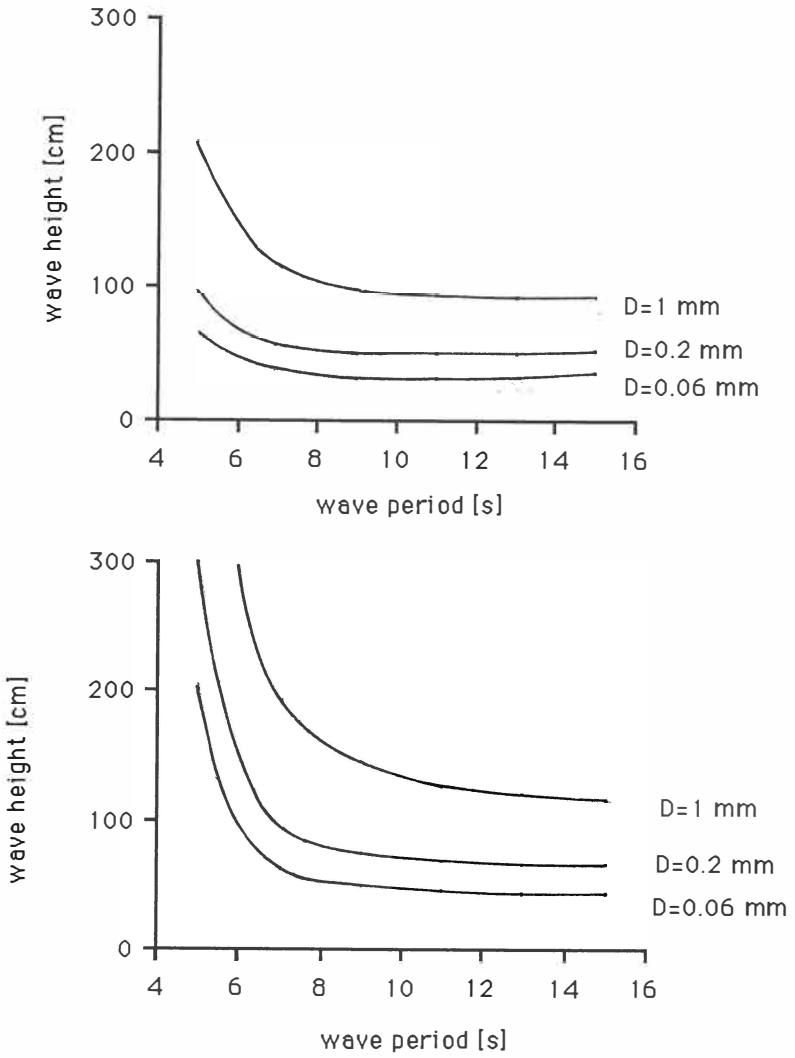

Fig.6.1: Critical wave height for exceeding of the threshold velocity at dump-site C (a; h = 13 m) and at dump-site D (b; h = 20 m).

Deep water (h/L > 1/4): $L = L_d = (g/2\pi)\ T^2$

Intermediate water: $L = L_d\ [\tanh\ (2\pi h/L_d)]^{1/2}$ (6.8)

Shallow water (h/L < 1/20): $L = T\sqrt{gh}$

where L_d is the deep water wavelength.

The nomograms show a significant difference in the critical wave height with water depth for wave periods from 5 to 8 s (Fig.6.1). The critical wave height does not change significantly when wave periods exceed 8 s. At the top of dump-site C (h=13 m) material finer than fine sand (D < 0.2 mm) starts to move when H > 0.6 m; at dump-site D when H > 0.9 m for swell waves with periods exceeding 7 s. Short-period wind waves initiate fine sand transport at dump-site C when H < 1 m whereas at dump-site D fine sand is only moved under storm conditions with H > 1.5 m.

It should be noted that the equations used above have been developed for a horizontal bottom. However, the dump-mounds possess gentle slopes (1:40 to 1:60) on which, according to KOBAYASHI (1982), the threshold velocity is exceeded under smaller wave orbital velocities in a downward directed slope. This suggests a higher frequency of sediment initiation at the shoreward side of the dump-mounds.

6.2.2 Frequency of initiation of sediment movement

To relate the calculated critical wave heights to the wave conditions in the survey area DAVIES-COLLEY's (1976) wave data shown in Chapter 2 (Fig.2.5) were expressed in a bar diagram (Fig.6.2). However, the non-existence of data on the frequency of typical wave periods or the ratio of swell to wind waves makes it difficult to characterise the frequency of initial grain motion. The preceding analysis suggests that all waves with H > 0.7 m exceed the threshold velocity for fine sand over dump-site C. These conditions occur at least 40%, probably up to 50-60% of the time. At dump-site D, the frequency of fine sand motion is less than 40%.

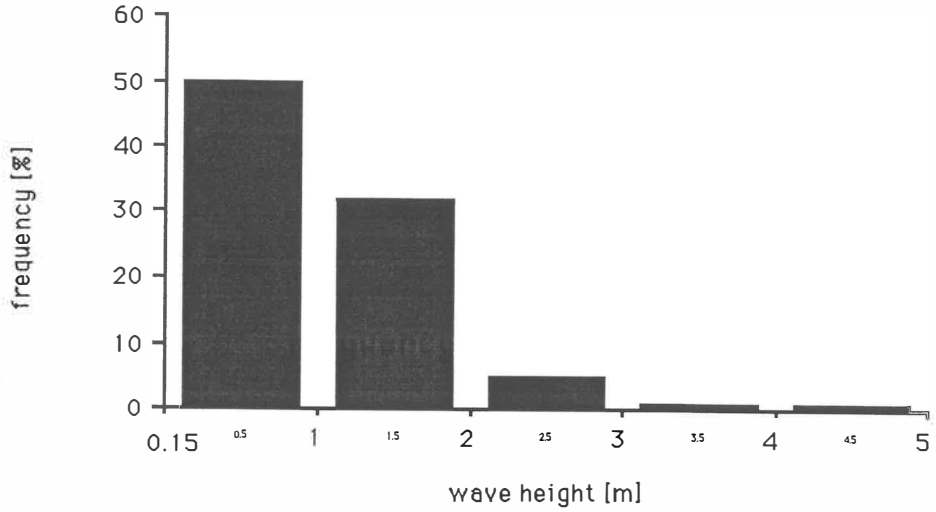

Fig.6.2: Frequency of wave heights, based on Tauranga Harbour pilot observations for the period 1974-75 off the Tauranga Entrance of Tauranga Harbour (from DAVIES-COLLEY and HEALY, 1978; Fig.2.5).

The exceeding of the threshold velocity under fair conditions is not necessarily connected with large sediment transport rates. Large sediment transport events occur during storms when large volumes of sediment are stirred up by high wave orbital velocities and transported by the additional effect of currents (e.g. NIEDORODA *et al.*, 1985). In the case of the survey area storms with H > 2 m occur 7 % of the time (Fig.6.2).

The wind data reported by QUAYLE (1984) and DE LANGE (1988; Fig.2.7) were used to characterise storm conditions by applying them to the JONSWAP 1976 program developed by BLACK and HEALY (1981) which is available on the VAX computer system of University of Waikato. The JONSWAP wave spectrum was obtained empirically during an experiment in the North Sea measuring wave growth (BLACK and HEALY, 1981).

Winds with velocities above 8.5 m/s were considered to be sufficient to create a storm. Assuming a fetch-limited (fetch = 700 km) and duration-limited (48 h) storm JONSWAP 1976 gives deep water waves of 3.5 m wave height and with a wave period of 9.5 s. Onshore winds with velocities above 8.5 m/s occur between 4 % (QUAYLE, 1984) and 2 % (DE LANGE, 1988) of the time. Ignoring the change of wave height when waves approach the shore, the frequency of strong storm events predicted from the wind data and JONSWAP is consistent

with the frequency of waves above 3 m (2%) reported by DAVIES-COLLEY (1976).

In summary, waves are capable of stirring up sand over the dump-sites during fair weather conditions between 30 and 60 % of the time depending on the water depth and grain-size. However, large sediment transport events are more likely restricted to storm events occurring between 2 and 4 % of the time. It is acknowledged by the author that the results presented in this chapter are based on a small number of data of dubious quality. They have to be considered as a basis for further data collected by a wave recorder planned to be set up by the BOPHB in the second half of 1989.

6.2.3 Net sediment transport by waves

Airy waves approaching shallow water display increasingly non-linear behavior which may be approximated by 2nd or higher order Stokesian wave theory. It was discussed in Chapter 3 that "Stokes' waves" have been associated with onshore movement because their asymmetric particle orbits are not closed thus permitting a weak net shoreward mass transport.

In order to ascertain whether this onshore movement occurs over the dump-sites two nomograms given by KOMAR (1976) and NIEDORODA *et al.* (1985) were tested for a minimum water depth of 13 m typical for dump-site C in 1983 (Fig.6.3a+b). In this depth KOMAR's (1976) nomogram needs wave heights around 4 m for a wave period of 7 s to apply Stokes' wave theory (Fig.6.3a). The NIEDORODA *et al.* (1985) nomogram shows that waves with H=4m and T>10 s lie in the transition zone indicating the beginning of small wave orbital asymmetries (Fig.6.3b). Both nomograms indicate that wave orbital asymmetries are of minor importance for an onshore movement during strong storms from the dump-site C but are insignificant for average conditions. These results are in contrast to DAHM and HEALY's (1980) suggestion that onshore movement from the dump-sites to the beach is caused by Stokesian-type mass transport. A net sediment transport by waves in an onshore direction is likely to be more important in the nearshore zone where water depths are below 7 m.

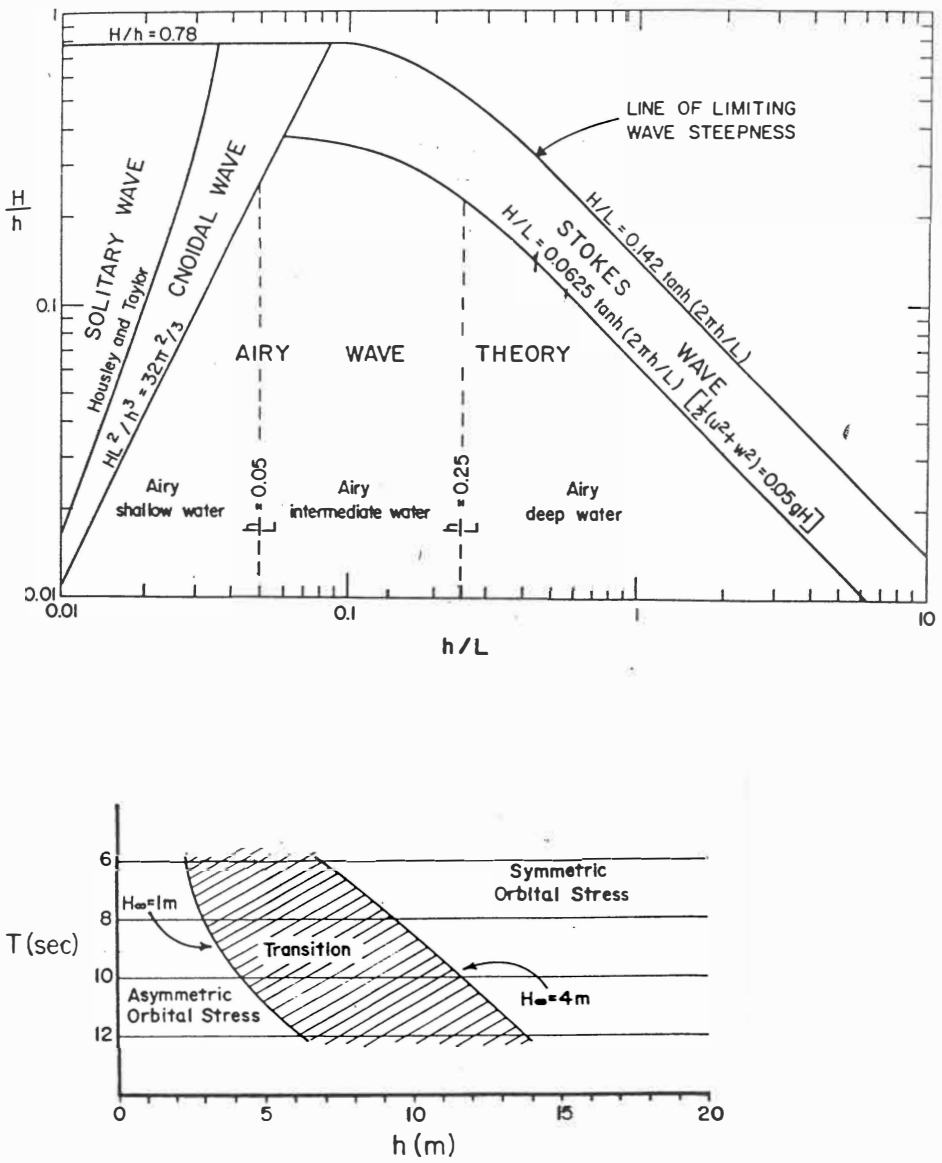

Fig.6.3: Nomograms to evaluate the application of Stokesian wave theory. Both diagrams (a; KOMAR, 1976 and b; NIEDORODA *et al.*, 1985) indicate that Stokesian mass transport over dump-site C may only be important during strong storms with wave heights above 4 m. At shallower water depth asymmetric orbital stresses are of larger importance.

6.2.4 Bedforms and related wave conditions

It is possible to calculate the wave conditions responsible for the generation of bedforms by applying a method introduced by CLIFTON and DINGLER (1984). The basic assumption of the method is that a relationship between ripple spacing (λ) and orbital diameter (d_0)

exists for a given grain-size until a critical maximum orbital diameter is reached when bedforms disappear again (e.g. LOSADA *et al.*, 1987). The method ignores that, apart from the particle-size, parameters like sorting, particle shape and particle density influence the ripple spacing (CLIFTON, 1976), but it is uncertain how these parameters relate to the generation of bedforms (CLIFTON and DINGLER, 1984). As the following relationships have been developed for quartz grains, the method was only applied to the pumice-poor sands of the coarse sand facies of the sediments in the survey area.

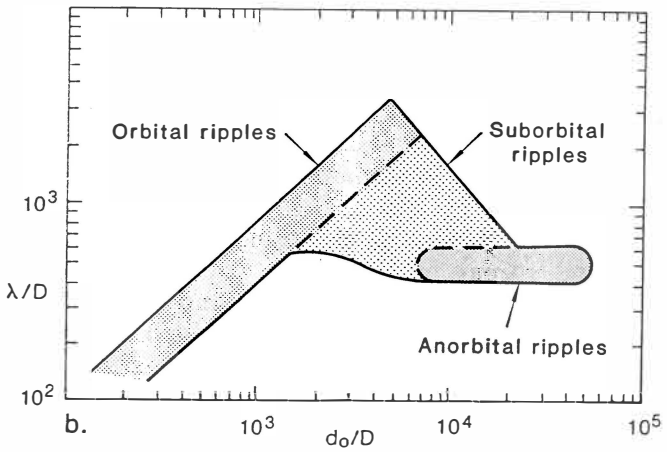

Fig.6.4: Plot of ratio of ripple spacing to grain-size against ratio of orbital diameter to grain-size. The classification of the ripples was undertaken by CLIFTON (1976) using field and experimental data from various studies (from CLIFTON and DINGLER, 1984).

Depending on their λ/D and d_0/D ratios CLIFTON (1976) subdivided symmetric ripples into three types shown in Fig.6.4. Orbital ripple spacings are proportional to the orbital diameter in an approximate relationship introduced by MILLER and KOMAR (1980a) as

$$\lambda = 0.65\ d_0 \qquad (6.9)$$

Ripples become suborbital when d_0/D exceeds 1500 for λ/D = 1000-2000. Suborbital ripple spacings appear to depend both on orbital diameter and grain size in some undefined relationship (CLIFTON and DINGLER 1984).

As SCUBA bedform observations were undertaken at Aanderaa site 2, this site was chosen to apply the method. In order to find out whether eq. 6.9 can be applied the d_0/D ratio was roughly estimated by applying

$$d_0 = u_o \, T/\pi \qquad (6.10)$$

for λ = 60 cm and λ = 100 cm and D = 0.1 cm in Fig.6.4. Orbital ripples form until d_0 = 200 cm is exceeded. Thus, eq. 6.9 cannot applied for very strong storms with high wave periods. Assuming that the critical d_0 was not exceeded during the formation of the bedforms at A2, eq. 6.9 gives for λ=60 cm; d_0=90 cm and for λ=100 cm; d_0=150 cm.

From d_0 the maximum wave height can be obtained by

$$H = d_0 \sinh (kh) \qquad (6.11)$$

For the calculated wave orbital diameter at aanderaa site 2 (h=18 m) the wave height was calculated for different wave periods (Table 6.1).

T [s]	H [cm] d_0=150	H [cm] d_0=90 cm
7	315	189
9	190	114
11	137	82
14	100	60

Table 6.1: Wave heights for varying wave periods and the wave orbital diameters calculated from observed ripple spacing before and after a storm.

According to CLIFTON and DINGLER (1984) it is also possible to obtain the maximum wave period by applying an equation either by KOMAR and MILLER (1975)

$$T = 0.065 \, (d_0^7/D^3)^{1/8} \qquad (6.12a)$$

or by DINGLER (1979)

$$T = 0.17\ (d_0^3/D)^{1/4} \qquad (6.12b)$$

For a mean grain-size of 0.75 mm at Aanderaa-site 2, KOMAR and MILLER's equation gives a wave period of 13.8 s, DINGLER's equation a period of 11.3 s.

For the easterly storm responsible for the generation of the bedforms, wind waves with T = 7 s and H > 3 m were necessary to produce the bedforms, whereas for swell waves (T = 11-14 s) H = 1 - 1.5 m is sufficient. During the 15-18 July storm wave heights exceeding 3 m were reported by BOPHB pilots (STEPHENSON, 1988, pers. comm.) which is consistent with the calculated wind wave heights. However, swell waves above the calculated wave height in Table 6.1 would have formed larger ripples than the observed size, although the ripple size does not increase unlimitedly. There is a relationship between maximum ripple size for a given grain-size which, according to MILLER and KOMAR (1980b), can be expressed by

$$\lambda_{max} = (1.47 \times 10^4)\ D^{1.68} \qquad (6.13)$$

Applying eq. 6.13 for D = 0.75 mm gives λ = 190 cm which means that the reported ripple size from SCUBA observations is about half the maximum ripple size. However, this does not imply that the maximum ripple size was not reached during the storm. The reported ripple size may reflect a late phase of the storm when orbital velocities produced by swell waves of H = 1 m and T = 14 s occurred and generated the bedforms.

6.3 Currents and their effects on sediment transport

Current measurements were undertaken during this study over a time period of eight weeks using Aanderaa recording current meters (RCM4). The functioning and accuracy of Aanderaa RCM4 is described in BARNETT (1985) and HAN and MEYER (1980).

6.3.1 Field data collection

Three RCM4 were deployed in a Motiti Island - offshore line at the 8/7/1988 at a depth of 28 m on flat sea-floor (A1), at 18 m on rippled sea-floor (A2) and at 16 m on flat sea-floor surrounded by rocks (Fig.5.12, Section 5.3.2.2). The purpose of the selection of these positions was to ascertain whether currents change across the survey area.

The Aanderaa RCM were anchored to the sea-floor by attachment of 80 kg chains. Their position was fixed with the Racal Microfix electronic position fixing system with an accuracy +/- 5 m, and, in addition, they were marked with a buoy at the water surface. Their recording interval was set at 15 minutes.

Checking by diver on 21/7/88 showed that A2 and A3 had stopped recording. A2 was repaired and A3 retrieved. A2 was later separated from its surface buoy and in spite of searches by divers could not be located again. A1 was retrieved on 29/8/88 and appeared to have run continuously.

The magnetic tapes were processed by the NZOI (New Zealand Oceanographic Institute). Unfortunately, the A1 current data after 18 days were lost.

Measurements of wind speed and direction, used in this study, were collected by employees of the Mount Drury Signal station.

6.3.2 Presentation of data

The GPLOT procedure of the SAS package, already used to produce the bathymetric plots in Chapter 4, was also used to plot both current speed and direction and wind speed and direction versus time for A1 and A3. The SPLINE statement (Chapter 4) was applied to smooth the data, as single current direction observations scattered considerably, in particular during a storm.

6.3.3 Observations

The A1 data being the longest record were plotted with wind and current direction versus time (Fig.6.5), wind and current velocity versus time (Fig.6.6), and the current direction and velocity versus time (Fig.6.7). The plots show that no significant changes in the current direction during one tidal circle occurred at 1 m above the sea-floor which was also noted by BARNETT (1985). The reaction of the current speed to high wind speed during storms indicates that the currents are wind-driven.

During the recording period the following events could be distinguished:

i) High wind speeds over a period of at least 48 hours during a storm are associated with high current velocities directed in the wind direction. These situations occurred from 15/7 - 18/7 with the wind speed up to 15 m/s from the SE and current speed U_{100} up to 40 cm/s to the NW; and from 23/7 onwards with the wind from the N up to 15 m/s and the current to the S with speeds up to 30 cm/s.

ii) Weak currents moving in a southerly onshore direction with U_{100} below 10 cm/s were associated with either light winds from varying directions or strong winds from onshore. These conditions occurred between 10/7 and 15/7 and after the storm from 18/7 to 23/7. A short period of northerly winds with velocities around 10 m/s at 12/7 increased U_{100} to 15 cm/s.

iii) A NW current with velocities up to 20 cm/s and light offshore winds from the S. This situation occurred from 8/7 to 11/7.

A comparison of the same recording period of A1 and A3 showed that the current direction at A3 changed more than at A1 (Fig.6.8). Current velocities were on average c. 5 cm/s lower and did not react to strong winds as much as at A1 (Fig.6.9). More scattered directions and the lower velocities are probably due to the position of the current meter between rocks causing a more complicated flow pattern and a reduction of the current velocity caused by the surrounding rocks and higher bottom friction due to a lower water depth.

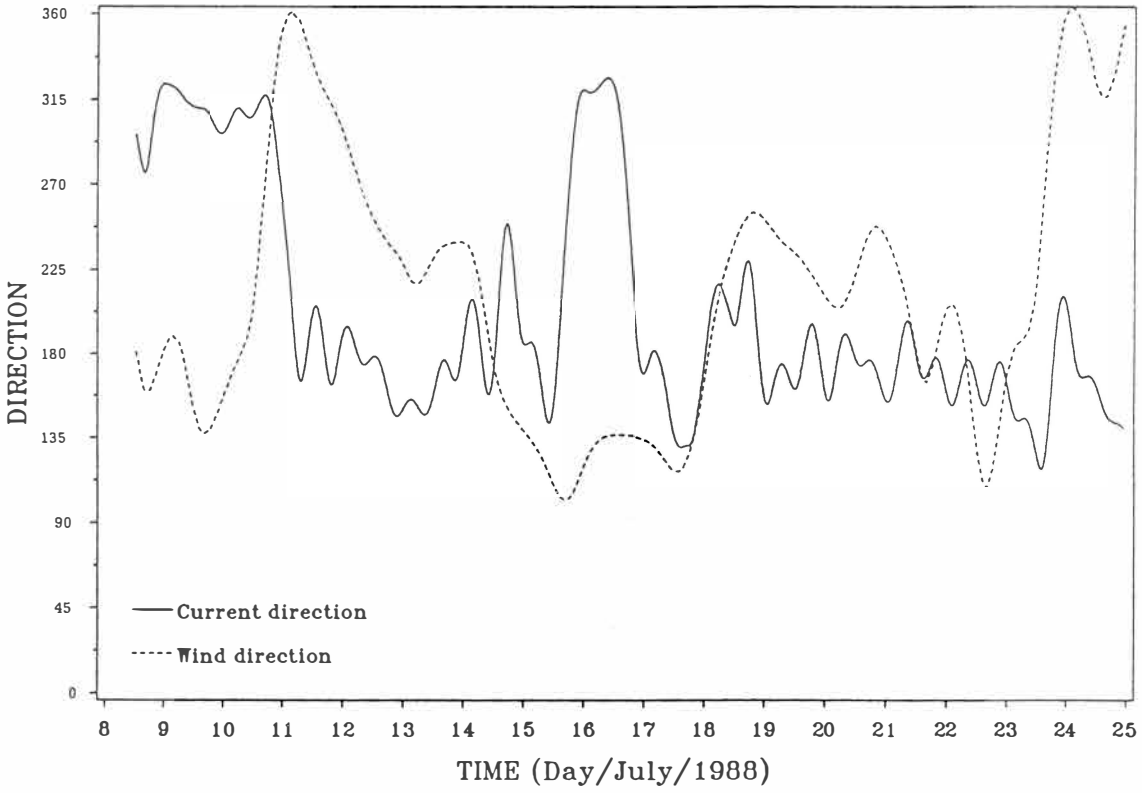

Fig.6.5: Current (A1) and wind direction versus time

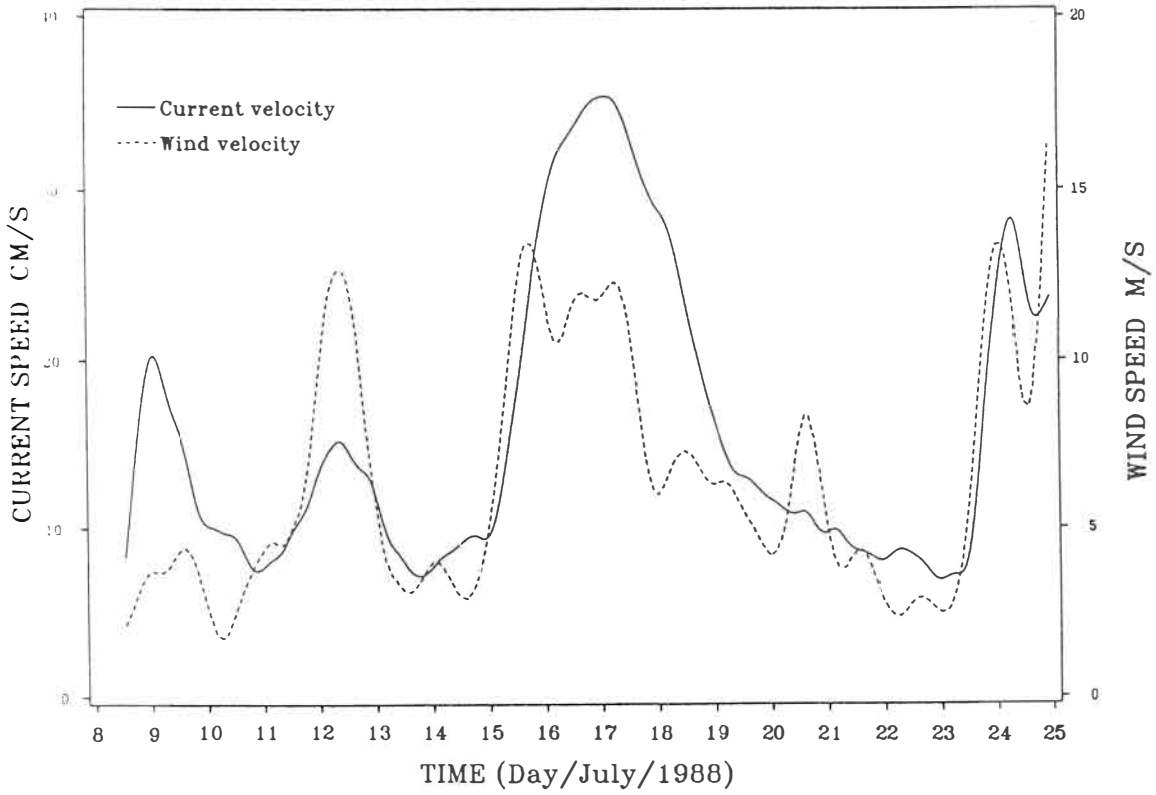

Fig.6.6: Current (A1) and wind velocity versus time

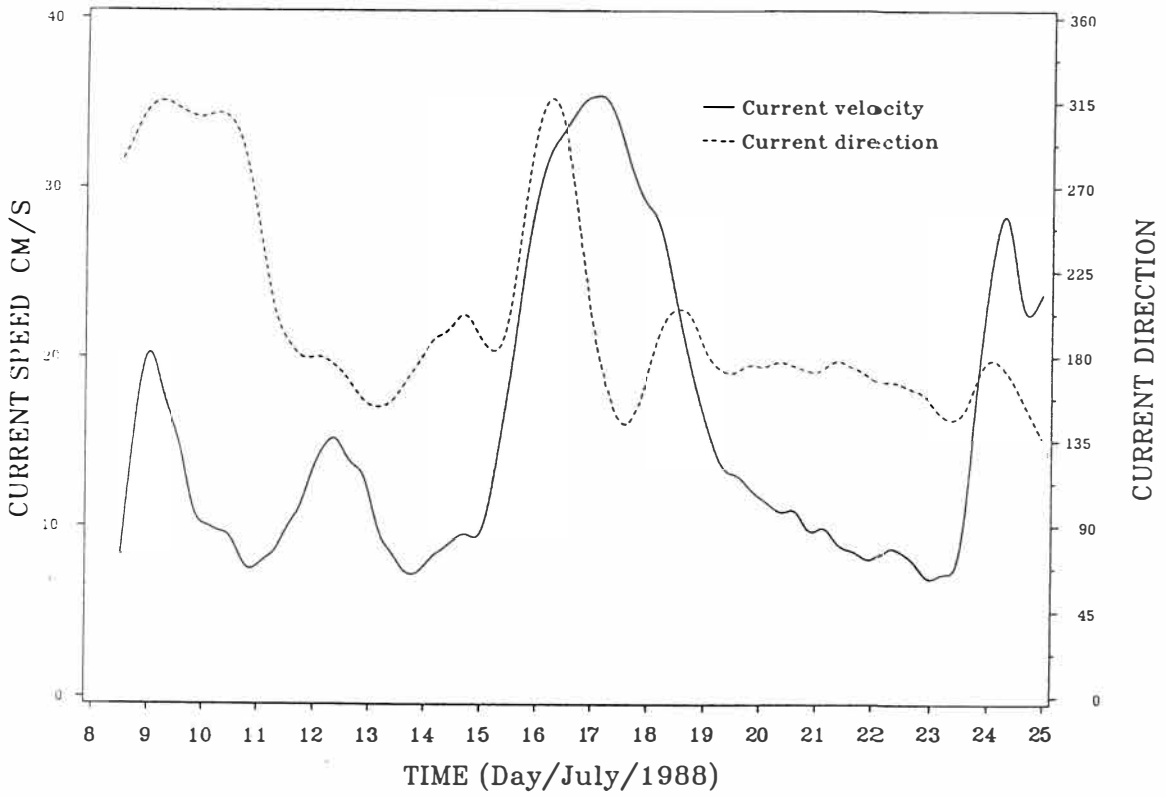

Fig.6.7: Current direction and velocity (A1) versus time. The direction is more smoothed than in Fig.6.5.

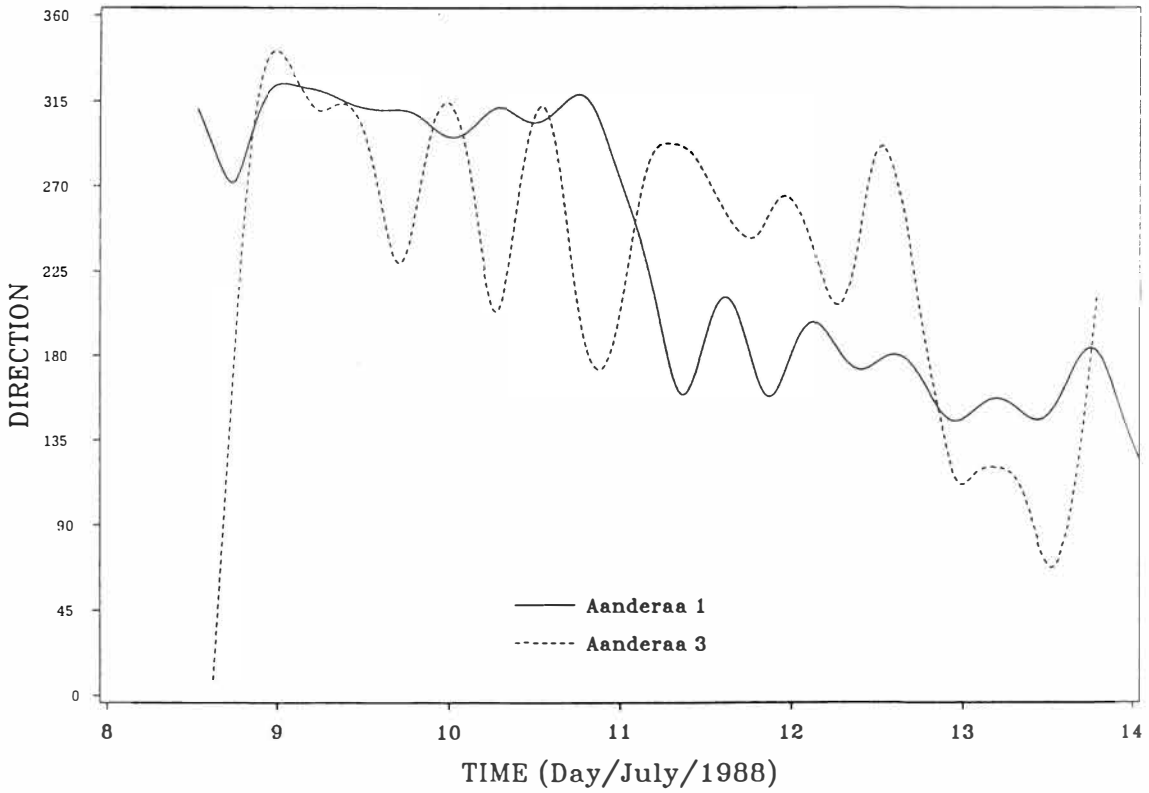

Fig.6.8: Current direction of A1 and A3 versus time

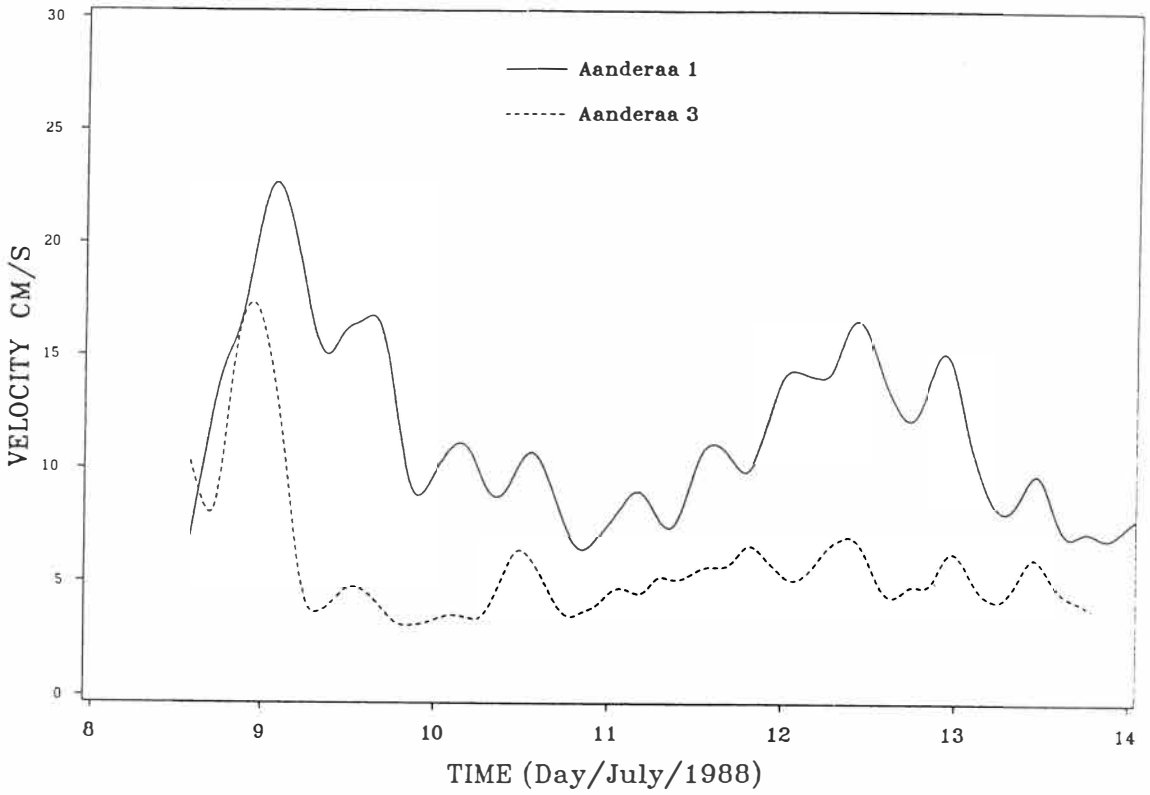

Fig.6.9: Current velocity of A1 and A3 versus time. The velocity is lower at the inshore current meter than further offshore.

6.3.6 General flow pattern

Because the current data are too short and limited to one device, only some generalisations can be made about the flow pattern on the inner shelf off Tauranga.

From the measured current data during a storm, it appears that the currents at 1 m above the sea-floor have the same direction as the wind. As long as no additional measurements further inshore and along the water column are available, the flow pattern can be explained by:

i) No Coriolis effect occurs in the Coastal Boundary Layer because of the shallow water depth. The surface current is simply transmitted throughout the entire water column.

ii) Long-term current measurements across the shoreface and inner shelf show that coastal downwelling associated with Ekman boundary layer flow occurs (e.g. NIEDORODA *et al.*, 1985; SNEDDON *et al.*, 1988). Applying this concept to the shore-parallel easterly to southeasterly storm (15/7 - 18/7), the surface current is diverted to the left by the Coriolis effect and piles up against the shoreline. This causes a downwelling current in the bottom boundary layer which diverts to the left further offshore thus producing a shore-parallel northwesterly current.

Weak currents appear to occur preferentially in a southerly onshore direction. No real wind pattern combined with these current could be observed. Their association with strong offshore winds (12/7) may suggest coastal upwelling as a possible process for their generation (NIEDORODA *et al.*, 1985). Another explanation may be the southerly directed East Auckland Current which occurs along the New Zealand east coast especially during the winter (BRODIE, 1960; HARRIS, 1985). A weak southerly current on the east Coromandel shelf, observed during long-term current measurements, has been interpreted as caused by the East Auckland Current by BRADSHAW (1989, pers.comm.). Current measurements off East Australia (GORDON and HOFFMAN, 1984) indicate that oceanographic currents can well intrude the inner shelf.

6.3.5 Threshold conditions of current flow

As currents were measured 1 m above the sea-floor, the measured current velocity (U_{100}) and direction can only be related to sediment transport in suspension which is approximately 10 times less concentrated than 10 cm above the bed (after GLEN and GRANT, 1987). To characterise the conditions for bedload transport it is necessary to reduce U_{100} to the bottom friction velocity u_* by applying the von Karman-Prandtl equation

$$U = u_*/\kappa \ln (z/z_0) \qquad (6.14)$$

where κ is the von Karman's constant (0.4), z is the height above the bed and z_0 is the bed roughness length. Before solving eq.6.14 for different U_{100} the bed roughness has to be determined. The bed

roughness is a function of the grain-size and the bedforms. For a plane bed z_0 is expressed according to NIKURADSE (1933, in BLACK and HEALY, 1982) by

$$z_0 = D/30 \qquad (6.15)$$

For a rough bed z_0 is defined according to GRANT and MADSEN (1982) by

$$z_0 = \eta^2/\lambda \qquad (6.16)$$

It is difficult to define the bed roughness for the changing sea-floor conditions observed during this study, in particular during a storm when bedform sizes change due to varying orbital velocities and diameters. It is of large importance whether a bed can be considered as flat or whether small bedforms or bioturbated structures as at R1 cause a rough bottom, which changes z_0 significantly. GRANT and MADSEN (1979) note that the bed roughness can hardly be determined with a higher accuracy than 2-3 times.

bottom type	H/L or D	zo	u* (35)	u* (15)	u* (8)
megaripple A2	30/100	4.5	4.5	1.9	1.0
megaripple A2	20/60	3.3	4.1	1.8	0.9
ripple	3/20	0.22	2.3	1.0	0.5
plane bed	0.018	0.0006	1.2	0.5	0.3
DRAKE et al. (1984);	bedforms D=0.03	1.0	3.0	1.3	0.7
		2.0	3.5	1.5	0.8

Table 6.2: Bottom types characterised by ripple height (H) and ripple spacing (L) and grain-size (D) and associated z_0 and u_* for three different U_{100} (units in cm).

The friction velocities were calculated for different bed roughness and U_{100} velocities (Table 6.2). For comparison bed roughness values determined by DRAKE *et al.* (1985) for comparable sediments on the inner shelf off California were included.

Table 6.2 shows that small changes in bottom roughness do not change u_* significantly but it is of major importance whether a bed is plane or rippled and how steep the bedforms are.

For a plane bed MILLER *et al.* (1977) give a u_* threshold value of 1.0 to 1.2 cm/s which is reached during the peak flow on the initially plane bed observed at A1 before the 15-18 July storm.

From their observations MILLER *et al.* (1977) developed an empirical threshold equation for unidirectional flow which allows calculation of a critical threshold grain-size directly from U_{100}. The relationship obtained under flume conditions with a plane bed and no wave-current interaction is given by

$$U_{100} = 122.6\ D^{0.29} \qquad (6.17)$$

for quartz grains with D < 2 mm. The application of eq.6.17 shows a similar trend with the exceeding of the threshold velocity for grain-sizes of 0.125 mm (3 phi) during peak flow (U_{100} = 35 cm/s).

Over a rippled bed the skin friction becomes higher which increases the total drag. The total drag or bed shear stress is given by KAPDASLI and DYER (1986) as

$$\tau = 70\ D^{0.3} \qquad (6.18)$$

The equation is based on flume experiments which were found to relate reasonably with the little amount of field data and is limited to D < 0.9 mm. The initial size of the ripples produced by the authors was λ = 15-20 cm and η = 2 cm comparable to ripples observed in the fine sand facies after a storm and in coarser sediment during calm periods.

The friction velocity can be calculated by applying

$$u_* = \sqrt{\tau \rho} \qquad (6.19)$$

Total drag and related friction velocities were calculated for the same grain-sizes already applied for wave threshold velocities (Table 6.3).

D[cm]	τ	u*
0.06	30	5.4
0.03	24.4	4.9
0.018	21	4.5
0.013	18.8	4.2
0.006	15.1	3.8

Table 6.3: Threshold boundary shear stresses and friction velocities calculated from eq. 6.18 and 6.19.

Having calculated u_* = 2.3 cm/s for a rippled bed during peak flow in a storm it becomes clear that the threshold velocity is not exceeded and no bedload transport caused by currents alone occur.

6.4 Wave-current interaction

In overseas investigations, the relationship of waves and currents in causing bedload transport have been expressed in vector diagrams to evaluate their combined effect on magnitude and direction of sediment transport (VINCENT *et al.*, 1983, in NIEDORODA *et al.*, 1985; SNEDDON *et al.*, 1988).

As the boundary shear stresses were best comparable they were used in a diagram as applied on data measured on a plane bed on the Texas shelf (SNEDDON *et al.*, 1988).

For the inner shelf of Tauranga the vector method was applied for storm and fair weather conditions at Aanderaa-site 1 (h=28 m) over a rippled bed with a mean grain-size of 0.2 mm. To represent storm conditions the 15-18/7/88 storm was chosen. As waves change over a storm cycle from wind waves with low periods (7 s) to swell waves (14 s) two vector diagrams representing early and late storm conditions were produced.

Storm; example (1) and (2):
current: U_{100} = 35 cm/s
u_* = 2.3 cm/s from eq.6.14 (Table 6.2)
τ_c = 5.3 dyn/cm^2 from eq.6.19
direction 315°

waves: H = 3 m
T = 7 and 14 s
L = 75 (deep water wave) and 210 m from eq.6.8
u_{max} = 27 and 70 cm/s from eq.6.7
d_0 = 300 and 60 cm from eq.6.11
direction 270° obtained from ripple alignment

The used parameters representing fair weather conditions were estimated from the available wave and current data for Tauranga.

example (3):
current: U_{100} = 8 cm/s
u_* = 0.5 cm/s
τ = 0.25 dyn/cm^2
direction 180°

waves: H = 0.7 m
direction 190_o
T = 7 s
L = 75 m
u_{max} = 6 cm/s
d_0 = 14 cm

The current boundary shear stress was obtained by applying eq.6.19 using u_* from Table 6.2 for a rippled bed with z_0 = 0.2 cm. For waves the boundary shear stress is given by

$$\tau_w = 1/2\ f_w\ \rho\ u_0^2 \qquad (6.20)$$

where the wave friction factor f_w for a rippled bed was obtained from a nomogram given in LOSADA *et al.* (1987; Fig.6.10).

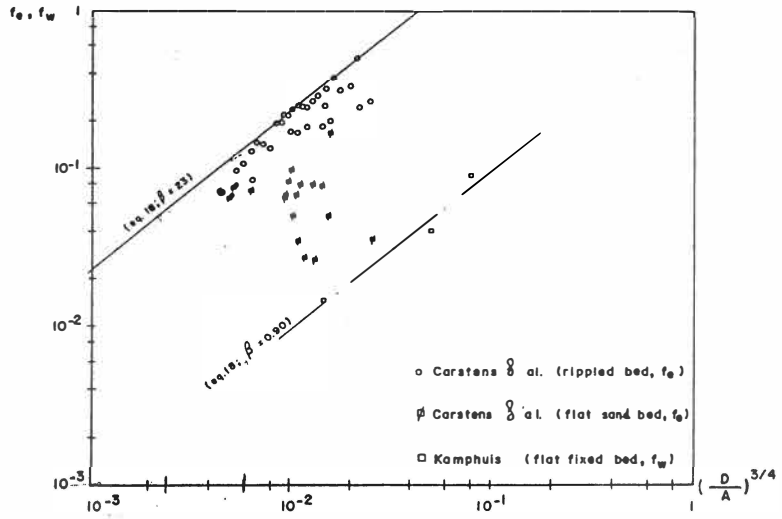

Fig.6.10: Friction factor vs grain-size/wave orbital diameter. f_e and f_w are typically nearly equal (COWELL and NIELSEN, 1984).

The wave friction factor f_w and the calculated boundary shear stress are given for the three examples:

(1) f_w = 0.01; τ_w = 25 dyn/cm^2

(2) f_w = 0.04; τ_w = 15 dyn/cm^2

(3) f_w = 0.1; τ_w = 2 dyn/cm^2

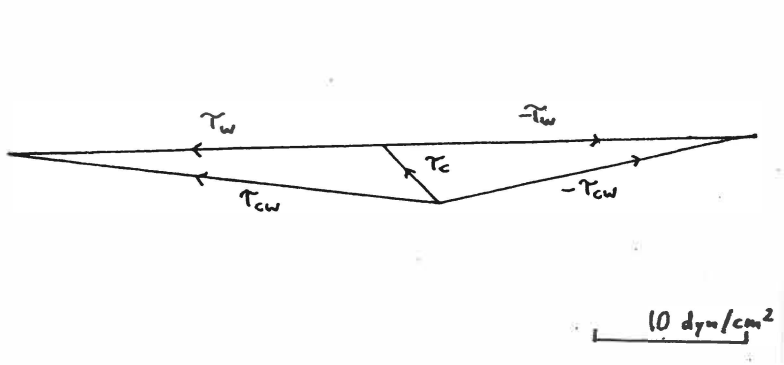

(1) τ_w = 25, τ_c = 5.3; τ_{cw} = 29 dyn/cm^2

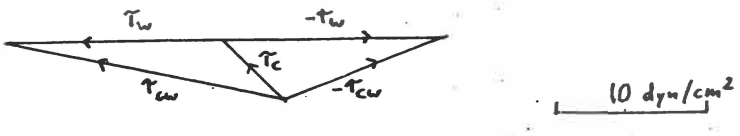

(2) τ_w = 15, τ_c = 5.3; τ_{cw} = 19 dyn/cm²

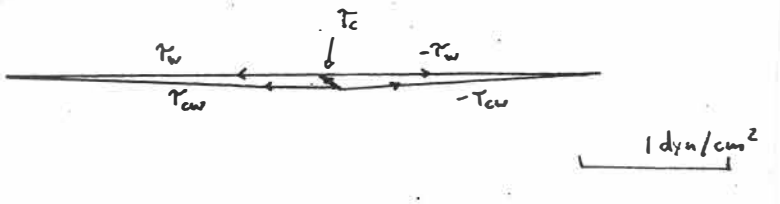

(3) τ_w = 2, τ_c = 0.25; τ_{cw} = 2.2 dyn/cm²

Fig.6.11a-c: Vector diagrams for examples 1-3 (a-c)

Fig.6.11a-c shows that the total boundary shear stresses are increased due to the combined action of wave and currents. Comparisons with Table 6.3 suggest that sediment movement during the storm occurs under high period waves at A1. Under short period waves (case 2) only the fine material is moved. The diagrams also indicate that, in contrast to the oscillatory stroke of linear waves, net bedload transport (case 1) occurs at the positive end of the vector triangle. The direction of the transport depends on the τ_c/τ_w angle and is, because of the higher magnitude, more in the direction of τ_c.

The vector diagrams do not consider that the direction of u_* may be different from U_{100} because of higher friction effects at the sea-floor.

It also neglects that U_{100} already measures the effect of waves superimposed on the unidirectional current. This effect can be ascertained applying GRANT and MADSEN's (1979) iterative procedure to calculate the "apparent" bed roughness and the friction velocity u_{*cw} of the mean current altered by the superimposition of waves. GRANT and MADSEN's (1979) method has been tested during the CODE experiment on the Californian shelf and has been found reasonably accurate in characterising the behavior of currents on the sea-

floor (CACCHIONE and DRAKE, 1982; DRAKE *et al.*, 1984; CACCHIONE *et al.*, 1987). The calculation of u_{*cw} for case 1 gave a mean current of 4.1 cm/s is obtained compared to u_* = 2.3 cm/s (Table 6.2); a similar increase in u_{*cw} was also noted by DRAKE *et al.* (1985) during their observations whereas DAVIS *et al.*(1988) conclude from theoretical investigations that u_{*cw} decreases with increasing wave orbital velocities. The u_{*cw} exceeds the threshold velocity for very fine sand given in Table 6.3. The complete procedure is described in Appendix 6.2.

Apart from the physical bed roughness and the "apparent" bed roughness, the roughness caused by near bed sediment stratification affects the mean flow in a non-linear manner.

6.4.2 Bedload/suspended-load transport

The exceeding of the threshold stresses under the combined action of waves and currents at a depth of 28 m during storm conditions with high wave orbital velocities is indicative that bedload transport is taking place. The transport contains a directional component contributed by the current (Fig.6.11). With an increase in wave orbital velocities due to shallower water depth further inshore, bedload transport with a net translation becomes more important.

Suspended-load transport also occurs during storm conditions but it is probably the more important transport mode during fair weather conditions when fine material stirred up by waves is transported by the superimposed current in a preferentially onshore direction.

6.5 Conclusions

1) Sediment motion is initiated by waves c. 50% of the time at dump-site C, and < 40% at dump-site D, for fine sand (2 ϕ). Storms associated with high sediment transport occur less than 5 % of the time.

2) Onshore sediment transport by Stokesian drift is not a significant process over the dump-sites, but is probably of more importance further inshore.

3) The bedforms reflect the direction and the magnitude of the last storm event following a concept developed by CLIFTON and DINGLER (1984). For the 15-18 July storm wind waves (T = 7 s) of H > 3 m and swell waves (T = 11-14 s) of H = 1-1.5 m were necessary to form the observed ripples at Aanderaa-site 2.

4) Current measurements indicate that currents are wind-driven on the inner shelf off Tauranga. The observed storm currents are oriented in the direction of the wind. Fair weather currents predominate in an onshore direction.

5) Threshold velocities for mean current flow are exceeded during peak flow in storms on a plane bed for very fine sand but not on a rippled sea-floor. The GRANT and MADSEN (1979) concept predicts an increase in the mean current velocity over a rippled bed by the superimposition of waves causing movement of very fine sand during storms. Total boundary shear stresses increase due to the action of currents. Currents also cause a directional component in bedload transport.

CHAPTER 7

SYNTHESIS AND CONCLUSIONS

7.1 Introduction

The results of the investigations presented in Chapters 4 to 6 are combined in this chapter to develop a spatial and temporal model for the dispersion of the dredge spoil, using the example of dump-mound C in the survey area. It is also attempted to evaluate the specific hydrodynamic processes responsible for the sediment facies distribution in the survey area. The environmental impact by former and future dumping is assessed and the prospects for beach nourishment are discussed. Conclusions and recommendations for future dumping and research are presented.

7.2 Definition of zones in the survey area

In the thesis, the terms "inner shelf zone" and "nearshore zone" were used when referring to a position in the survey area instead of applying the concept of shoreface and inner shelf zone outlined at the beginning of Chapter 3. In the west of the survey area neither a change in slope nor a seaward fining was noticed which describes the shoreface/inner shelf boundary. In the east the slope gradient decreases significantly at the 22 m water depth but the surficial sediment becomes coarser rather than finer.

Therefore, the "shoreface" concept cannot be applied for the west of the survey area. In the east of the survey area and further east along the coast the steep part of the shelf down to 20-22 m may be termed "shoreface".

7.3 A temporal and spatial model for dredge spoil dispersion (Fig.7.1)

During the dredging operations in 1977/78 a mixture of medium and coarse sand (dredged volume c. 2 million m^3) and water was collected in a dredge hopper and dumped over dump-site C building a mound of c. 9 m height on the sea-floor. The initially unconsolidated dredge spoil developed into a stable dump-mound that had a constant height during the interval from October 1985 to May 1988.

7.3.1 The settling of a dump-mound

A temporal model of the dump-mound settling is suggested based on the results of the bathymetry surveys and sediment analysis from Chapters 4 and 5. The settling of the dump-mound which is divided in three periods is then related to the dispersion of the dredge spoil and the responsible hydrodynamic processes.

I) Between July 1978 and January 1980 a reduction of c. 240,000 m^3 in dump-mound volume occurs (Table 4.3). Following the argument in Section 4.6.1, self-consolidation of a dump-mound, is, apart from erosion, an important process for volume reduction, in particular during the first three years after the dumping. As an unconsolidated mass of material is more accessible to erosion by waves and currents than a compacted surface, higher erosion rates may also occur during this period.

II) Volume reduction of the mound becomes significantly smaller between January 1980 and October 1985 (Table 4.3). Accumulation of material in the near vicinity of the dump-mound is much higher than in period I (Table 4.3; Fig.4.10). In addition to DEMARS *et al.*'s (1984) results, smaller reduction and higher accumulation rates in the grid suggest that compaction is of minor importance in period II and that erosion dominates.

III) From October 1985 onwards no significant volumetric reduction was found (Fig.4.8). After seven years the dump-mound appears to be stable. A sediment analysis of the dredge spoil at dump-site C shows that well sorted, positively skewed, medium to coarse sand with a low pumice content occurs. This and the existence of bedforms (λ = 0.3 - 1 m) suggest that a stable dump-mound surface has developed.

7.3.2 Dispersion of dredge spoil

Volume calculations and graphic display indicate that about two thirds of the eroded material are deposited in a semi-circle up to 300 m south of the dump-mound during period II (Table 4.3). A wedge shoreward of dump-mound C on the sub-bottom seismic record (Fig.5.17), also indicates the accumulation of material from the dredge spoil in the same zone.

The following two processes may be responsible for the accumulation of material near the dump-mound. At the shoreward side of the dump-mound, sediment transport is enhanced by the decrease of the threshold velocity in a downslope, onshore direction (KOBAYASHI, 1982). Thus material is transported over a short distance and deposited directly shoreward of the dump-mound. No sediment samples were collected from the accumulation zone but the side-scan sonograph shows megaripple which generally occur in coarse sand. The induced grain-size suggests that predominantly large grains were transported as bedload and/or in intermittent suspension (HANES, 1988) over a small distance of 300 m.

At this stage, no evidence can be presented that autosuspended gravity mass transport or turbidity currents of an unconsolidated part of the dredge spoil occur on the relatively steep slope of c. 1:50 of the mound and deposit directly south of it. Turbidity currents as a process in the shoreface zone have been suggested by WRIGHT (1987) and are also known to occur in lakes (SCHNEIDER, 1986, pers.comm.).

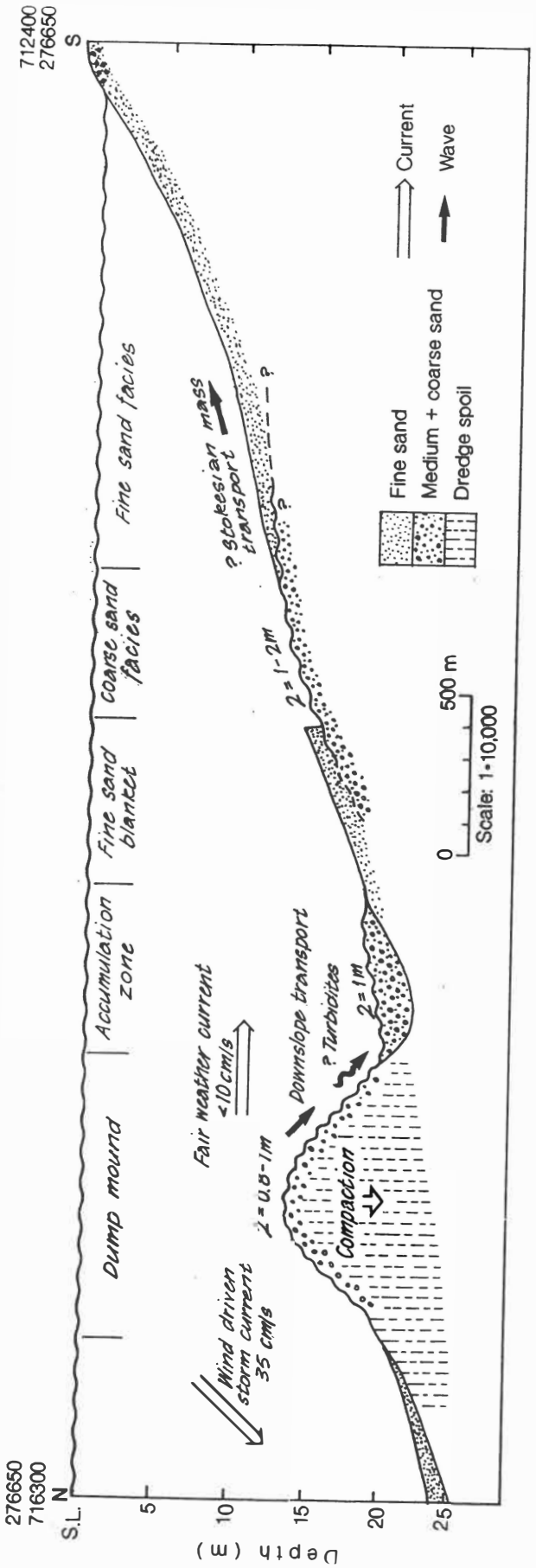

Fig.7.1: N-S oriented beach - offshore profile showing the sediment facies distribution + hydrodynamic processes responsible for the dispersion of the dredge spoil.

Whereas the majority of the coarser material is deposited near the dump-mound, fine sand and pumice spread over a larger area. Moderately sorted, negatively skewed, medium to coarse sand shoreward of the dredge spoil and accumulation zone suggest that fine sand and pumice from both zones are deposited in the coarse sand facies. The fine material is prone to undergo further transport and eventually be deposited in the fine sand facies.

The mixing of the fine sand and pumice from the dredge spoil with the natural fine sand facies does not allow tracing the dredge spoil over a large area. The fine sand blanket is thought to migrate over the coarse sand, predominantly in an onshore southerly direction (skewness data). Thus, parts of the dredge spoil are available for frequent exchange of material between beach, surfzone and nearshore zone.

HEALY (1989, pers.comm.) observed unusually high amounts of pumice at Mount Maunganui Beach subsequent to dumping operations in 1979. This is suggestive that at least some of the pumice is transported quickly to the beach.

The migrating of the fine sand blanket occurs due to the acting wave and current conditions. From the current measurements undertaken in this study it appears that weak currents in a southerly onshore direction dominate under fair weather conditions. As the threshold velocities under waves for fine sand are exceeded about 30-60% of the time depending on the water depth, suspended-load transport of fine material in a southerly direction under the combined effects of wave and currents may be an important process for onshore movement of sediment during fair weather conditions.

Strong alongshore flow was observed during an easterly storm at 28 m water depth. These short-term infrequent events induce high total boundary shear stresses causing bedload transport with a net component. Additional current measurements, in particular of the direction along a shore-normal profile, are necessary to assess the effect of storm flow for the sediment budget. The inferred net onshore movement of dredge spoil from bathymetry and sediment data indicates that frequently occurring weak sediment transport under fair weather conditions is important for the sediment budget on a

long-term scale. COWELL and NIELSEN (1984) suggest for the New South Wales inner shelf that sediment transport under fair weather conditions is of higher importance than during storms.

A process which could enhance the onshore movement of fine material shoreward of the dump-mound is Stokesian mass transport. However, this process may only be important in the nearshore zone in water depth below 7 m and assuming that no stronger adverse downwelling currents occur at the same time.

The occurrence of shells (Strutholaria papulosa), observed in water depths between 10 and 20 m in the survey area, at New Zealand east coast beaches after strong storms supports the onshore movement of material during a late phase of a storm event (HEALY, 1989; pers.comm.). The observation of shells and pumice at the beach suggests that the closure depth of beach-inner shelf sediment exchange during a storm can reach the dump-site indicating that sediment transport may also occur directly from the dump-mound to the beach. This would be in agreement with observations from the New South Wales inner shelf where BOYD (1982) gives a closure depth of 25 m for large storm events.

7.3 Origin of megaripple 'fingers'

The patchy distribution of coarse and fine sand on the inner shelf off Tauranga is interpreted as the local exposure of the coarse sand facies underneath the fine sand blanket. Wave-formed megaripples, which react in size and direction to storm events, occur in the coarse sand. The fine sand is either flat or rippled after storm events. In areas of high biological activity (Motuotau Island) the ripples are deformed to an irregular rippled bioturbated surface.

Fine and coarse sand react as separate units to the hydrodynamics, a process suggested by COOK and GORSLINE's (1972) observation that fine sand is likely to move as a whole unit under lower orbital velocities than the coarse sand. This process has not been observed for the survey area but the migrating of scour depressions has been observed elsewhere (e.g. HUNTER *et al.*, 1988).

Different hydrodynamic processes have been suggested for the generation of the megaripple patches or fingers observed on various shelves around the world but never finally proven by measurements in the field. The hypotheses by the different authors are applied and evaluated for the Tauranga inner shelf.

Rip currents (MORANG and McMASTERS, 1980; COOK, 1982) of sufficient power have not been observed on the northern Bay of Plenty coastline. They would also not explain the location of megaripple patches to at least 4 km offshore.

Standing waves (HUNTER *et al.*, 1988) have not measured either and are unlikely to cause the irregular distribution of the megaripple patches.

Wave refraction (BLACK and HEALY, 1988) causing a wave convergence zone with higher wave orbital velocities and higher erosion of fine sediment leads to the generation of a locally limited megaripple field. Future wave refraction studies may show if an irregular pattern of patches with highly variable sizes between 20 and 40 m water depth, can be explained by local wave energy convergence.

Downwelling currents transverse to the shore-normal oriented patches (SWIFT and FREELAND, 1978) and parallel to them (CACCHIONE *et al.*, 1984) have been used to explain their formation. Wind-driven currents with a peak flow of U_{100} = 0.35 m/s were measured during storms in this study. These currents are certainly capable to transport fine sand, initially stirred-up by waves, in suspension over large distances. After the storm, when current and wave orbital velocities are weak, the suspended fine sand deposits accidentally in an irregular pattern. Thus it is likely that the patches form under combined wave-current processes during storms.

7.4 Environmental consequences of dredge spoil dispersion

The highest environmental impact caused by the dumping of dredge spoil occurs at the dump-site where burial of benthic organisms firstly leads to the extinction of life at the dump-ground (KESTER *et al.*, 1983). Former dumping off Tauranga caused a zone of reduced biological diversity at the dump-sites and in their surroundings (Fig.7.2, HEALY *et al.*, 1988). The effects of dumping to the marine ecosystem in the case of Tauranga are described in detail in the environmental assessment report (HEALY *et al.*, 1988).

The environmental impact by the dispersal of the dredge spoil in the area around the dump-sites is harder to analyse. HEALY *et al.*'s (1988) zone of reduced diversity extends to the northwest; a direction for which no significant net sediment transport has been assessed in this study. The authors note that probably dumping short of the dump-sites is responsible for the extension of the zone. No reduced diversity was found in the main southerly direction of sediment onshore movement indicating that the environmental impact by the dispersion is not severe. The environmental effect of deposition of fine material in the coarse sand facies and the mixing with the natural fine sand facies is negligible. Especially in the latter case, the fine sand and pumice from the dredge spoil do not cause a change in the physical properties of the fine sand facies which determine the basic habitat of benthic organisms (KESTER *et al.*, 1983). By the adding of sediment from the dump-sites to the fine sand blanket, the fine sand is more likely to spread and cover more of the coarse sand or the shell grit zone after HEALY *et al.* (1988; Fig.7.2) around Motuotau Island which displays a very narrow range of diversity and abundance. If an aerial reduction of this zone which is distributed more irregularly around the island than shown in Fig.7.2 (additional sediment samples during this study) is a serious environmental impact, is debatable.

The burial of little emergent reefs around Motuotau Island which display an abundant and diverse marine life (HEALY *et al.*, 1988) would be a more serious environmental impact, in particular as Motuotau Island is proposed to become a Marine

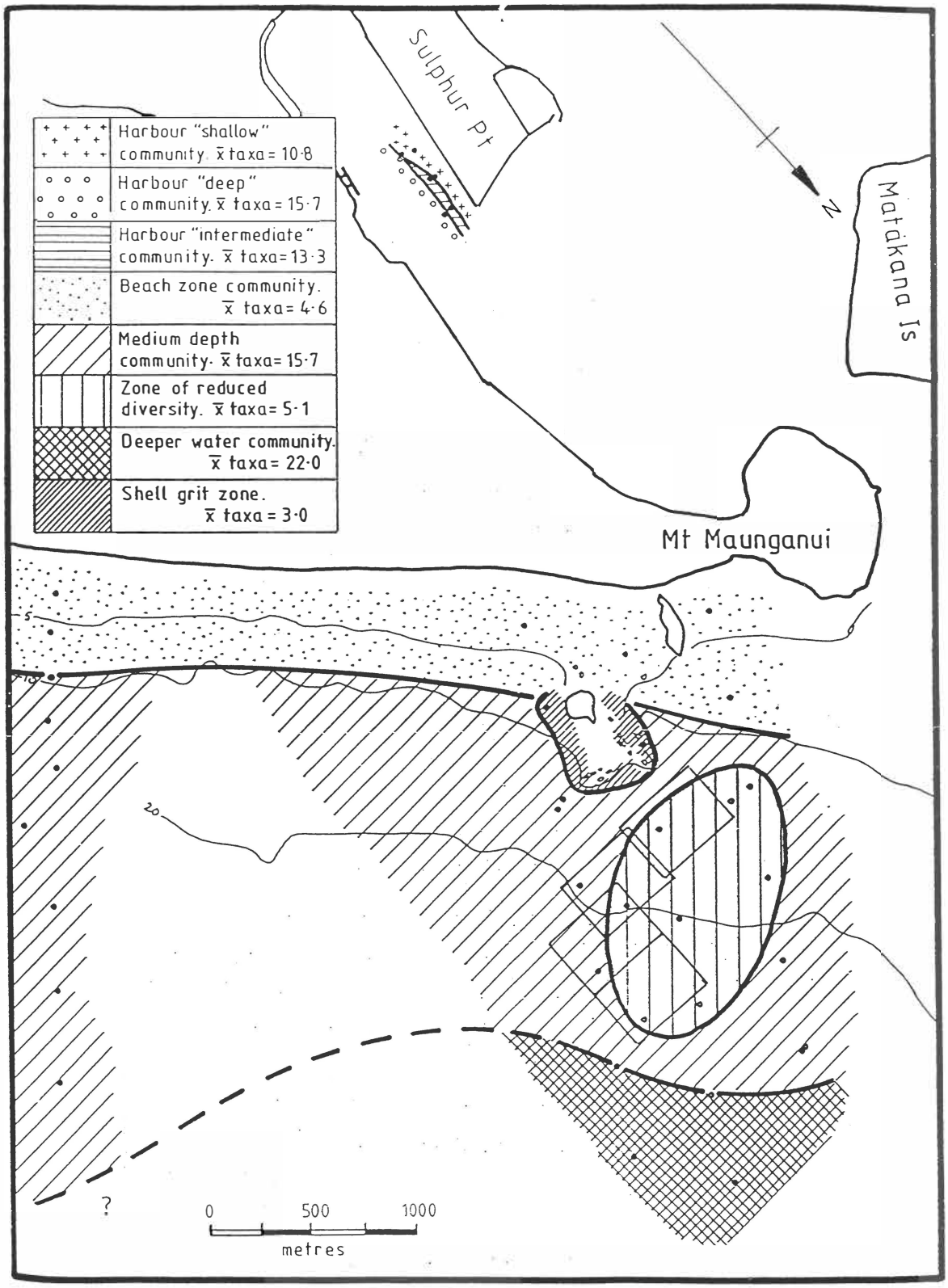

Fig.7.2: Map of the sediment bottom "communities" (from HEALY *et al.*, 1988)

Reserve. However, as most of the eroded dredge spoil is deposited near the dump-mound. and fine sand and pumice probably distributed over a large area, the danger of this happening is minor, in particular when dumping small volumes of dredge spoil at the more offshore dump-site D. Future dumping of large volumes of spoil at dump-site D would probably eventually lead to a net accumulation of material around submerged rocks around Motuotau Island which may reduce the abundance of marine life. It is not possible to quantify the amount of future accumulation and monitoring will be necessary to evaluate the environmental effects. It is then a political question how much accumulation can be accepted from a economical and ecological point of view.

It was found in Chapter 4 that a dump-mound appears to be stable after about 7 years thus reducing its dispersion effects to a limited period of time. However, the method of spreading material over a larger area, as applied during dumping in 1988, may lead to a different dispersion history. Wide-spread material has a larger surface where waves and currents will act on thus eroding more material. In addition, it will not compact as quickly as material disposed at a mound which may also enlarge the amount and period of dispersion.

Thus, from dispersion point of view, building up a mound from dredge spoil reduces the effects of dispersion and is a preferential solution to the spreading method. However, it has to be evaluated by wave refraction studies if dump-mounds cause wave focussing at the shoreline thus enhancing erosion of material from Mount Maunganui Beach.

7.5 Beach nourishment

At present the Mount Maunganui Beach is not eroding (Chapter 2). This is probably due to the weak littoral drift and parts of the dredge spoil which has been added to the material available for exchange between beach, surfzone and nearshore zone (upper shoreface). However, the fine sand and pumice of the dredge spoil which feed the fine sand blanket, and are eventually transported to the beach during fair weather conditions, are not compatible with

the natural medium sand of the beach. Therefore the fine sand and pumice do not remain constantly at the beach which is indicated by the textural parameters of the beach sand. Thus the current dumping of dredge spoil on the inner shelf is not the most effective means for beach nourishment.

Under the possible scenario of increasing rates of sea-level rise due to the greenhouse effect beach nourishment may become a very important method to conserve beaches (WEGGEL, 1986). The Mount Maunganui tombolo with its low altitude above sea-level and low dunes would suffer severely under a higher sea-level and increasing number of storms causing erosion predicted to occur with the greenhouse effect (DE FREITAS, 1987). The consequences for the town of Mount Maunganui as a large holiday resort and port with relatively high real estate values could be serious.

The dredging of large volumes of material from dredge-sites inside and outside the harbour in the future provides the opportunity to diminish the effects of a possible sea-level rise by dumping the dredge spoil in the nearshore zone and thus directly nourishing Mount Maunganui Beach. When monitoring the dispersion of material dumped in 2 - 4 m water depth in the nearshore zone outside a tidal inlet, North Carolina, U.S.A., SCHWARTZ and MUSIALOWSKI (1977) found that the dump-piles were modified to a disposal bar which migrated landward through the surfzone, in particular during periods with increased wave activity.

For Tauranga, medium and coarse sand from maintenance dredging in the Entrance and Cutter Channel are most compatible with the natural beach sand and therefore most effective for beach nourishment purposes. Fine sand from further inside the harbour is less useful as it will be preferentially winnowed out from the beach, transported offshore and incorporated in the fine sand facies.

7.6 Conclusions

In the conclusions, the aims of the study, listed in chapter 1, are addressed:

1. To what extent, at what rates and in which directions does the dredge spoil disperse?

The reduction of the dump-mound at dump-site C is documented by echo-sounding charts recorded between 1978 and 1988. An analysis of the echo-sounding data shows that the summit of the mound was reduced by c. 3 m equivalent to a volume reduction of c. 240,000 m^3. Apart from erosion, compaction is responsible for the reduction in dump-mound volume, in particular during and in the first two to three years after the dumping. About two thirds of the eroded material from the dump-mound is deposited in a semi-circle up to 300 m south of the dump-mound. The rest is distributed over a larger area and does not allow to be traced. From 1985 onwards the dump-mound is stable suggesting the development of a compacted lag surface on the dump-mound.

2. How does the dredge spoil change the natural sediment facies distribution on the inner shelf?

The natural sediment facies distribution in the area around the dump-sites consists of coarse sand patches with megaripples overlain by a mobile featureless to lightly rippled fine sand sheet. Further offshore at water depths between 25 and 30 m medium sand with ripples occurs.

The dumping of medium sand from dredge-sites inside and outside Tauranga Harbour on the inner shelf causes a zone of medium sand around the dump-sites. Sorting and skewness data and pumice contents indicate that fine material and pumice eroded from the dredge spoil deposit in the coarse sand facies shoreward of dump-site C. The deposition in the coarse sand is probably only temporary. Eventually, fine material from the dredge spoil mixes with the fine sand sheet which migrates as a whole over the coarse sand thus distributing the fine dredge spoil over a large area.

3. How do the hydrodynamic processes which act on the inner shelf relate to the dredge spoil dispersion and inner shelf sediment transport?

Wave and current data for the inner shelf off Tauranga are limited. Wave threshold velocities for fine sand over dump-site C are exceeded up to 50% of the time. The stirred up sediment would be available for transport by weak fair weather current, probably occurring in a southerly onshore direction most of the time.
Lower wave threshold velocities on the shoreward dump-mound slope may be responsible for the downward net transport of coarser material from the dump-mound and its deposition in a small zone south of the dump-mound. Wind-driven currents occur during storms. Under the combined action of waves and currents high total boundary shear stresses with a net component are capable to produce bedload transport. Transport of fine sand in suspension during a storm and its accidental deposition afterwards is a likely explanation for the exposure of the coarse-grained ripples underneath the fine sand blanket.

4. What effects are caused by the dumping with respect to the marine ecosystem and to beach nourishment?

Dumping of dredge spoil leads to a zone of reduced diversity over and west of former dump-sites (HEALY *et al.*, 1988). To date, the environmental impact to the proposed Marine Reserve around Motuotau Island appears to be minor. The coarse sand facies or shell grit zone around the island may be reduced by future dumping because of the nourishing of the fine sand sheet from fine material from the dredge spoil. The burial of reefs by the effects of dumping is not a reason for concern at the present stage.

Beach nourishment of coarse dredge spoil may occur directly from the dump-mound during late storm phases. The fine sand and pumice from the dredge spoil which deposit in the nearshore zone and take apart in the exchange between beach and nearshore zone are unlikely to remain constantly on the beach because of their hydraulic properties.

7.7. Recommendations

7.7.1 Recommendations for future research

i) Echo-sounding surveys are a good means to monitor the dispersion of dredge spoil. Surveys over larger areas around future dumping and a control-site not affected by the dumping should provide valuable information about sediment transport from dump-sites and over natural sea-floor, in particular directly after storms.

ii) Compaction tests of dredge spoil provide the opportunity to compare the ratio of compaction and erosion during the reduction process of the dump-mound. This will help to assess the dispersion rates, in particular in the first years after the dumping.

iii) Tracer experiments, for instance with titanomagnetite which can be then traced by a magnetometer, may show the dispersal pattern of material around dump-sites over a certain time period.

iv) Direct sediment transport measurements of bedload transport with sediment traps and suspended-load transport.

v) Shallow coring is necessary to determine the vertical structure of the fine and coarse sand facies.

vi) Repeated side-scan sonar survey will show how mobile the sediments, in particular the fine sand, are on the inner shelf.

vii) Long-term wave and current measurements are necessary to predict sediment movement on the basis of hydrodynamic data.

7.7.2 Recommendations for future dumping

The current dump-site D is appropriate for future dumping as long as volumes of dredge spoil do not exceed 2 - 3 million m^3 and dumping occurs on mounds which stabilize after a short period of time (c. 7 years). Before a new dump-mound is built up, wave refraction investigations should be undertaken to prove that wave focussing induced by the mound does not cause erosion at the beach. During future dumping, the environmental sensitive area around Motuotau Island should be monitored by echo-sounding to determine if an abnormal accumulation of sediment occurs. The effects of dredge spoil dispersion would be diminished when material was dumped in water depths beyond 30 m where lower wave orbital velocities entrain the sediment.

In order to nourish the beach, dumping in the nearshore zone is a more efficient method than the current dumping on the inner shelf.

APPENDIX

APPENDIX CHAPTER 4

Programs used for graphic display and volume calculations

A4.1 SAS programs were applied to graphic display of bathymetric changes.

G3GRID program: three-dimensional pictures of sea-floor bathymetry of dump-mound (Fig.4.7)

```
DATA TD78;
INFILE GRID FIRSTOBS = 2;
INPUT Y X Z78 Z80 Z83 Z86;
Z78 = -1*Z78;
Z80 = -1*Z80;
Z83 = -1*Z83;
Z86 = -1*Z86;

PROC G3GRID DATA=TD78 OUT=GRIDO;
GRID Y*X = Z78/SPLINE
           AXIS1 = 0 TO 600 BY 20

FILENAME SASQMS '[] SASQMS.DAT';
GOPTIONS DEVICE = QMS CHARACTERS NODASH NOFILL;

TITLE 'BATHYMETRY 1978';

PROC G3D DATA = GRIDO;


PLOT Y*X = Z78/ROTATE = 45
               TILT = 60
               SIDE
               ZTICKNUM = 7
               ZMIN = -22
               ZMAX = -10;
```

GCONTOUR program: bathymetry map (Fig.4.)

```
DATA TD78;
INFILE GRID FIRSTOBS = 2;
INPUT Y X Z78 Z80 Z83 Z86;
*END;

FILENAME SASQMS '[]SASQMS.DAT';
GOPTIONS DEVICE = QMS CHARACTERS NODASH NOFILL;

TITLE 'BATHYMETRY 1978';
```

```
PROC GCONTOUR DATA = TD78;
AXIS1 LENGTH = 15 CM;
AXIS2 LENGTH = 15 CM;

PLOT Y*X = Z78/LEVELS = 12 TO 20 BY 2
                LLEVELS = 2 8 3 4 1
                HAXIS = AXIS1
                VAXIS = AXIS2
                NOAXIS;
```

GCONTOUR program: bathymetry changes (Fig.4.)

```
DATA TD78;
INFILE GRID FIRSTOBS = 2;
INPUT Y X Z78 Z80 Z83 Z86;
Z7880 = Z78 - Z80;
Z7883 = Z78 - Z83;
Z7886 = Z78 - Z86;
Z8386 = Z83 - Z86;
Z8086 = Z80 - Z86;
Z8083 = Z80 - Z83;

FILENAME SASQMS '[]SASQMS.DAT';
GOPTIONS DEVICE = QMS CHARACTERS NODASH NOFILL;

TITLE 'CHANGES IN BATHYMETRY 1978-83';

PROC GCONTOUR DATA = TD78;

AXIS1 LENGTH = 15 CM;
AXIS2 LENGTH = 15 CM;


PLOT Y*X = Z8083/LEVELS=-1.5 TO 1.0 BY 0.5
                LLEVELS = 2 8 3 4 5 1
                HAXIS = AXIS1
                VAXIS = AXIS2
                NOAXIS;
PLOT Y*X = Z7886/LEVELS=-2.4 TO 1.6 BY 0.8
                LLEVELS = 2 8 3 4 5 1
                HAXIS = AXIS1
                VAXIS = AXIS2
                NOAXIS;
```

GPLOT program: transect plots (Fig.4.)

```
DATA TRSECT1;
INFILE TRSECT1 FIRSTOBS=2;
INPUT DIST BA78 BA80 BA81 BA83 BA85 BA86 BA87;

BA78 = -1*BA78;
BA80 = -1*BA80;
BA81 = -1*BA81;
BA83 = -1*BA83;
BA85 = -1*BA85;
BA86 = -1*BA86;
BA87 = -1*BA87;
```

```
FILENAME SASQMS '[]SASQMS.DAT';
GOPTIONS HPOS=80 VPOS=60 DEVICE=QMS CHARACTERS NODASH NOFILL;
TITLE1 'TRANSECT 2';
SYMBOL1 W=1 C=BLACK L=1 I=SM5 V=NONE;
SYMBOL2 W=1 C=BLACK L=2 I=SM5 V=NONE;
SYMBOL3 W=1 C=BLACK L=3 I=SM5 V=NONE;
SYMBOL4 W=1 C=BLACK L=4 I=SM5 V=NONE;
SYMBOL5 W=1 C=BLACK L=5 I=SM5 V=NONE;
SYMBOL6 W=1 C=BLACK L=6 I=SM5 V=NONE;
SYMBOL7 W=1 C=BLACK L=7 I=SM5 V=NONE;

DATA ANNO;

   LENGTH FUNCTION $ 8;
   RETAIN XSYS '2' YSYS '2';
   INPUT FUNCTION $  X  Y  LINE  STYLE  $  SIZE  POSITION  $ TEXT $
CHAR30.;
   CARDS;
LABEL 200 -21 . TRIPLEX 1.5 6 SURVEY 27-7-78
MOVE 0 -21 .        .    . . .
DRAW  150 -21 1        .    . 4 .
LABEL 200 -22 . TRIPLEX 1.5 6 SURVEY 7-1-80
MOVE 0 -22  .        .    . . .
DRAW 150 -22  2        .    . 4 .
LABEL 200 -23 . TRIPLEX 1.5 6 SURVEY 30-3-81
MOVE 0 -23  .        .    . . .
DRAW 150 -23  3        .    . 4 .
LABEL 200 -24 . TRIPLEX 1.5 6 SURVEY 23-12-83
MOVE  0 -24 .        .    . . .
DRAW  150 -24 4        .    . 4 .
LABEL 50 -11 . TRIPLEX 2.0 6 C
LABEL 1600 -23 . TRIPLEX 2.0 6 D
;
RUN;

PROC GPLOT DATA=TRSECT1;

AXIS1 VALUE=(F=TRIPLEX H=1)
      LABEL=(F=TRIPLEX H=2 'DISTANCE (M)')
      ORDER= 0 TO 1600 BY 200
      MINOR=(N=0);

AXIS2 LABEL=(F=TRIPLEX H=2 A=90 'WATERDEPTH (M)')
      ORDER = -26 TO -10 BY 1
      MINOR =(N=0);


   PLOT BA78 * DIST=1
        BA80 * DIST=2
        BA81 * DIST=3
        BA83 * DIST=4/OVERLAY
                   HAXIS = AXIS1
                   VAXIS=AXIS2
                   ANNOTATE=ANNO;
```

A4.2 A PASCAL program written with the help of Toni Fenton was used for the volume calculations (Table 4.3).

```
Program Volcalc (infile, outfile);

VAR
   infile, outfile: TEXT;
   b:Char;
   Bed1 : ARRAY [0..12,0..12] of Real;
   Z78, Z80 , Z83, Z86, Y, X, Z, Z7880,
   aggrade, degrade,Volchange, changes,totvol : Real;
   I,J                 :Integer;
Procedure INPUT_DATA;
   Begin
      OPEN (infile,'Grid.dat',History := old);
      RESET (infile);
      OPEN (outfile,'Changes.Dat', History := new);
      REWRITE (outfile);
      readln(infile,b);
      I:=0; J:=0;
While (J < 13)  DO
  Begin
   Readln (infile, Y, X, Z78,Z80,Z83,Z86);
   Z7880:=Z78-Z86;
   Bed1[I,J]:= Z7880;
   I:=I+1;
   If I=13 then
    begin
     I:=0; J:=J+1;
    end;
  END;
END;

Procedure Calculate;
   Begin
     For I:=0 to 11 DO
     For J:=0 to 11 DO
      Begin
       Changes:=  (Bed1[I,J]   +   Bed1[I+1,J]   +   Bed1[I,J+1]  +
Bed1[I+1,J+1])/4;
       volchange := changes * 2500;
       Totvol:=Totvol + VolChange;
       Writeln(outfile, VolChange:8:2);
       IF volchange >= 0 then Aggrade := Aggrade + volchange;
       IF volchange < 0 then Degrade := Degrade + volchange;

      End;
   End;

Begin
INPUT_DATA;
Calculate;
writeln(outfile, 'Total Aggradation', aggrade:12:2);
writeln(outfile, 'Total Degadation', degrade:12:2);
writeln(outfile, 'Total volume change', Totvol:12:2);
End.
```

APPENDIX CHAPTER 5

A5.1 Definition of textural parameter

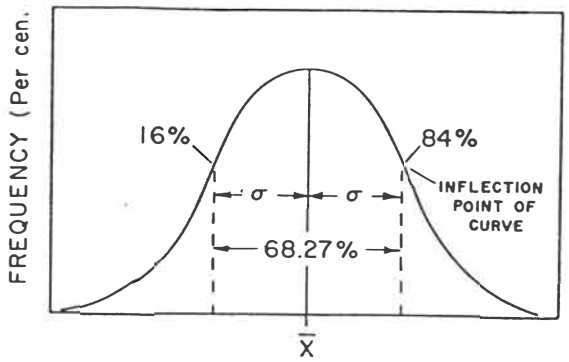

A normal frequency distribution curve. Text explains symbols.

Standard size classes of sediment

Limiting Particle Diameter (mm)	(φ units)	Size Class		
2048	-11	V. Large	Boulders	GRAVEL
1024	-10	Large		
512	- 9	Medium		
256	- 8	Small		
128	- 7	Large	Cobbles	
64	- 6	Small		
32	- 5	V. Coarse	Pebbles	
16	- 4	Coarse		
8	- 3	Medium		
4	- 2	Fine		
2	- 1	V. Fine		
1	0	V. Coarse	Sand	
1/2	+ 1 — 500 (Microns μ)	Coarse		
1/4	+ 2 — 250	Medium		
1/8	+ 3 — 125	Fine		
1/16	+ 4 — 62	V. Fine		
1/32	+ 5 — 31	V. Coarse	Silt	MUD
1/64	+ 6 — 16	Coarse		
1/128	+ 7 — 8	Medium		
1/256	+ 8 — 4	Fine		
1/512	+ 9 — 2	V. Fine		
			Clay	

Scale	
1m	
10^{-1}	
10^{-2}	
10^{-3}	
10^{-4}	
10^{-5}	

Sorting and skewness values for graphically obtained statistics expressed as verbal descriptive summaries (after Folk 1974).

Standard deviation (sorting)	*Verbal description*
0–0.35φ	very well sorted
0.35–0.50φ	well sorted
0.50–0.71φ	moderately well sorted
0.71–1.00φ	moderately sorted
1.00–2.00φ	poorly sorted
2.00–4.00φ	very poorly sorted
4.00+φ	extremely poorly sorted
Skewness	
+1.00–+0.30	strongly fine-skewed
+0.30–+0.10	fine-skewed
+0.10–−0.10	near-symmetrical
−0.10–−0.30	coarse-skewed
−0.30–−1.00	strongly coarse-skewed

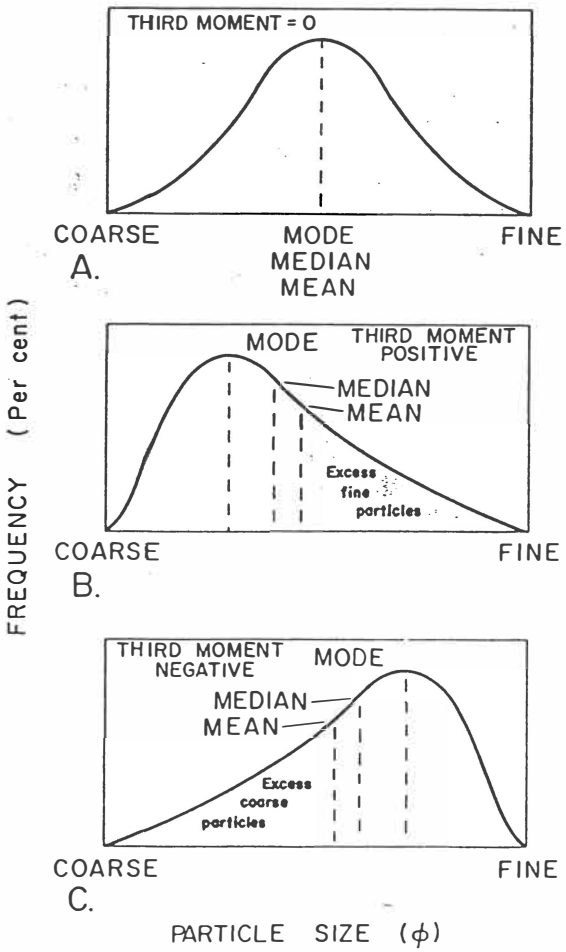

Frequency-distribution curves having various skewness. In B and C, the word "skewness" may be substituted for "third moment."

A5.2 List of textural data of analysed sediment samples

No.	M_z	sort.	skew.
Sediment sampling program (May 1988)			
Harbour sediments			
H1	68.5% fine sand; 31.5% mud		
H2	1.73	0.66	-0.14
H3	2.41	0.99	0.50
H4	1.56	0.57	0.07
H5	2.10	0.60	-0.16
H6	81% fine sand; 19% mud		
Offshore sediments			
O8	1.55	0.49	0.14
O9	1.72	0.42	0.24
O10	1.74	0.46	0.22
O11	0.54	0.61	0.34
O12	2.27	0.56	0.20
O13	2.37	0.66	0.07
O14	0.93	0.41	0.22
O15	2.28	0.54	0.08
O16	2.20	0.61	-0.28
O17	0.71	0.74	-0.20
O18	2.39	0.50	0.02
O19	2.20	1.14	-0.59
O20	1.99	0.55	0.09
O21	1.20	0.53	0.19
O22	2.37	0.60	-0.01
O23	-0.44	0.60	-0.02
O24	2.37	0.55	-0.07
O25	2.15	0.45	-0.06
O26	2.19	0.48	0.01
O27	-0.58	0.77	0.31
O28	-0.12	0.70	-0.17
O29	2.45	0.45	-0.03
O30	2.07	0.52	-0.06
O31	2.42	0.51	-0.02
O32	1.11	0.54	0.15
O33	1.54	0.59	0.08
O34	1.53	0.61	0.15
O35	2.41	0.61	0.0
O36	2.45	0.60	-0.03
O37	2.23	0.59	0.06
O38	1.60	0.47	0.30
O39	2.14	0.54	0.01
O40	1.91	0.52	0.17
O41	2.43	0.73	-0.19
O42	2.57	0.67	-0.04
O43	2.19	0.59	0.01
O44	0.85	0.51	0.24
O45	0.82	0.56	0.29
O46	0.46	0.83	0.25
O46b	2.32	0.59	-0.27
O47	2.23	0.63	-0.13
O48	2.18	0.70	-0.32
O49	0.87	0.63	0.21
O50	0.38	0.58	-0.07

O51	0.48	0.78	-0.18	
O52	1.52	0.69	0.0	
O53	1.09	0.52	0.30	
O54	2.17	0.72	0.03	
O55	1.58	0.55	0.23	
O56	1.32	0.53	0.24	
O57	1.57	1.23	-0.42	
O58	1.81	0.64	0.08	
O59	1.38	0.52	0.10	
O60	1.37	0.42	0.25	
O61	2.44	0.50	-0.03	
O62	0.07	0.68	-0.03	
O63	1.66	0.52	0.23	
O64	2.30	0.74	-0.24	
O65	0.40	0.61	0.16	
O66	0.72	0.66	0.13	
O67	2.12	0.55	-0.11	
O68	1.92	0.50	0.08	
O69	1.91	0.44	0.07	
O70	2.36	0.68	0.16	muddy
O71	2.35	0.58	-0.09	
O72	2.48	0.48	-0.01	
O73	2.25	0.62	-0.05	
O74	2.36	0.51	-0.06	
O75	0.20	0.72	-0.11	
O76	0.43	0.45	0.22	
O78	2.56	0.47	-0.10	
O78	2.50	0.47	0.0	2nd sample
O79	2.32	1.10	-0.40	
O80	2.03	0.41	0.17	
O81	1.92	0.48	0.03	
O82	1.15	0.76	-0.19	
O83	2.14	1.03	-0.32	
O84	1.43	0.42	0.21	
O85	1.77	0.45	0.19	
O86	1.31	0.50	0.18	
O87	1.26	0.58	0.37	
O88	2.56	0.47	0.09	
O89	2.17	0.44	0.14	
O90	0.66	0.73	-0.14	
O91	2.18	0.48	0.04	
O92	1.15	0.35	0.18	
O94	2.16	0.44	0.10	
O95	2.24	0.52	-0.09	
O96	1.80	0.62	0.22	
O96	1.46	0.73	-0.04	2nd sample
O97	1.72	0.58	0.10	
O98	2.24	0.59	-0.14	
O99	-1.04	0.85	0.16	
Aanderaa sites				
A1	2.28	0.72	-0.02	
A2	0.63	0.66	0.12	
A3	2.26	0.59	-0.15	

```
SCUBA survey
S1c -0.21  1.00    0.0   crest
S1t -0.43  1.22    0.21  trough
S2   1.83  0.63    0.06
S3   2.72  0.92   -0.30  muddy
S4   0.27  0.45    0.16
S5   1.71  0.68    0.04
S6   0.65  0.70    0.31
S7   1.43  0.64    0.27
S8   1.07  0.62    0.39


Beach samples
B1d  1.62  0.57    0.06  dune
B1be 1.40  0.85   -0.17  berm
B1bo 1.99  0.42   -0.22  bottom
B2be 1.94  0.41    0.04
B2bo 1.63  0.54    0.06
B3be 1.99  0.40   -0.08
B3bo 1.80  0.59    0.18
Bcbe 1.32  0.48    0.16  control-site
Bcbo 1.44  0.61    0.46
```

A5.2 SAS program for digitized map with numbers (Fig.5.20)
The coordinates of the samples are given in the program.

```
DATA A;
INFILE TAUMAP FIRSTOBS= 4 OBS=418;
INPUT AX AY;
DATA B;
INFILE TAUMAP FIRSTOBS= 420 OBS=560;
INPUT BX BY;
DATA C;
INFILE TAUMAP FIRSTOBS= 569 OBS=597;
INPUT CX CY;
DATA D;
INFILE TAUMAP FIRSTOBS= 608 OBS=634;
INPUT DX DY;
DATA E;
INFILE TAUMAP FIRSTOBS= 636 OBS=665;
INPUT EX EY;
DATA F;
INFILE TAUMAP FIRSTOBS= 766 OBS=786;
INPUT FX FY;
DATA H;
INFILE TAUMAP FIRSTOBS= 667 OBS=688;
INPUT HX HY;
DATA I;
INFILE TAUMAP FIRSTOBS= 690 OBS=705;
INPUT IX IY;
DATA J;
INFILE TAUMAP FIRSTOBS= 707 OBS=717;
INPUT JX JY;
DATA K;
INFILE TAUMAP FIRSTOBS= 719 OBS=728;
INPUT KX KY;
DATA L;
```

```
INFILE TAUMAP FIRSTOBS= 730 OBS=739;
INPUT LX LY;
DATA M;
INFILE TAUMAP FIRSTOBS= 741 OBS=749;
INPUT MX MY;
DATA N;
INFILE TAUMAP FIRSTOBS= 751 OBS=764;
INPUT NX NY;
DATA O;
INFILE TAUMAP FIRSTOBS= 915 OBS=986;
INPUT OX OY;
DATA P;
INFILE TAUMAP FIRSTOBS= 988 OBS=1020;
INPUT PX PY;
DATA Q;
INFILE TAUMAP FIRSTOBS= 1022 OBS=1049;
INPUT QX QY;
DATA R;
INFILE TAUMAP FIRSTOBS= 1051 OBS=1133;
INPUT RX RY;
DATA S;
INFILE TAUMAP FIRSTOBS= 1135 OBS=1205;
INPUT SX SY;
DATA T;
INFILE TAUMAP FIRSTOBS= 1207 OBS=1270;
INPUT TX TY;
DATA U;
INFILE TAUMAP FIRSTOBS= 599 OBS=606;
INPUT UX UY;
DATA MAP;
  MERGE A B C D E F H I J K L M N O P Q R S T U ;

FILENAME SASQMS '[]SASQMS.DAT';
GOPTIONS HPOS=120 VPOS=80 DEVICE=QMS CHARACTERS NODASH NOFILL;
TITLE1 'MEAN GRAIN-SIZES [PHI]';
SYMBOL1 W=1 C=BLACK I=JOIN L=1 V=NONE;
SYMBOL2 W=1 C=BLACK I=NONE L=1 V=+;

DATA ANNO;
    LENGTH FUNCTION $8;
    RETAIN XSYS '2' YSYS '2';
    INPUT FUNCTION $ X Y LINE STYLE $ SIZE TEXT $ CHAR30. ;
    CARDS;
      <Coordinates>            <Sample number>
LABEL 276615 715430 . TRIPLEX 1 8
LABEL 277042 716084 . TRIPLEX 1 9
LABEL 275648 715360 . TRIPLEX 1 10
LABEL 276362 716901 . TRIPLEX 1 11
LABEL 276090 716386 . TRIPLEX 1 12
LABEL 275799 715906 . TRIPLEX 1 13
LABEL 275495 715372 . TRIPLEX 1 14
LABEL 275198 714840 . TRIPLEX 1 15
LABEL 274912 714307 . TRIPLEX 1 16
LABEL 275825 714695 . TRIPLEX 1 17
LABEL 276470 714570 . TRIPLEX 1 18
LABEL 277690 716720 . TRIPLEX 1 19
LABEL 277050 716743 . TRIPLEX 1 20
LABEL 276368 716956 . TRIPLEX 1 21
LABEL 275514 714164 . TRIPLEX 1 25
LABEL 275892 713567 . TRIPLEX 1 26
```

```
LABEL 276147 714079 . TRIPLEX 1 27
LABEL 276534 714644 . TRIPLEX 1 28
LABEL 276114 715195 . TRIPLEX 1 32
LABEL 276423 715721 . TRIPLEX 1 33
LABEL 276709 716240 . TRIPLEX 1 34
LABEL 277378 716192 . TRIPLEX 1 35
LABEL 277314 717290 . TRIPLEX 1 36
LABEL 277050 715630 . TRIPLEX 1 37
LABEL 276762 715120 . TRIPLEX 1 38
LABEL 276267 716659 . TRIPLEX 1 42
LABEL 275924 716117 . TRIPLEX 1 43
LABEL 275638 715644 . TRIPLEX 1 44
LABEL 275351 715105 . TRIPLEX 1 45
LABEL 275061 714550 . TRIPLEX 1 46a
LABEL 275061 714600 . TRIPLEX 1 46b
LABEL 275400 714555 . TRIPLEX 1 47
LABEL 275549 714850 . TRIPLEX 1 48
LABEL 275705 715097 . TRIPLEX 1 49
LABEL 275831 715350 . TRIPLEX 1 50
LABEL 275975 715611 . TRIPLEX 1 51
LABEL 276118 715856 . TRIPLEX 1 52
LABEL 276284 716148 . TRIPLEX 1 53
LABEL 276445 716346 . TRIPLEX 1 54
LABEL 276555 716691 . TRIPLEX 1 55
LABEL 276849 717191 . TRIPLEX 1 56
LABEL 276848 716465 . TRIPLEX 1 57
LABEL 276555 715952 . TRIPLEX 1 58
LABEL 276255 715455 . TRIPLEX 1 59
LABEL 275949 714944 . TRIPLEX 1 60
LABEL 275660 714420 . TRIPLEX 1 61
LABEL 276233 714764 . TRIPLEX 1 62
LABEL 276283 714987 . TRIPLEX 1 63
LABEL 276401 715115 . TRIPLEX 1 64
LABEL 276470 715307 . TRIPLEX 1 65
LABEL 276664 715655 . TRIPLEX 1 66
LABEL 276781 715837 . TRIPLEX 1 67
LABEL 276879 716013 . TRIPLEX 1 68
LABEL 276969 716161 . TRIPLEX 1 69
LABEL 277099 716351 . TRIPLEX 1 70
LABEL 277290 716691 . TRIPLEX 1 71
LABEL 275986 713828 . TRIPLEX 1 72
LABEL 276672 714849 . TRIPLEX 1 73
LABEL 276305 714333 . TRIPLEX 1 74
LABEL 276972 714580 . TRIPLEX 1 75
LABEL 276645 714320 . TRIPLEX 1 76
LABEL 276496 713712 . TRIPLEX 1 78
LABEL 276185 713545 . TRIPLEX 1 79
LABEL 276949 715450 . TRIPLEX 1 80
LABEL 277229 715940 . TRIPLEX 1 81
LABEL 276940 714860 . TRIPLEX 1 82
LABEL 277128 715140 . TRIPLEX 1 83
LABEL 277279 715402 . TRIPLEX 1 84
LABEL 277405 715647 . TRIPLEX 1 85
LABEL 277553 715921 . TRIPLEX 1 86
LABEL 277848 716479 . TRIPLEX 1 87
LABEL 276793 713615 . TRIPLEX 1 88
LABEL 277339 714613 . TRIPLEX 1 90
LABEL 277672 715165 . TRIPLEX 1 91
LABEL 276575 713080 . TRIPLEX 1 94
LABEL 277976 715730 . TRIPLEX 1 92
```

```
LABEL 274640 714481 . TRIPLEX 1 95
LABEL 274925 715013 . TRIPLEX 1 96
LABEL 275228 715515 . TRIPLEX 1 97
LABEL 275537 716047 . TRIPLEX 1 98
LABEL 275950 716645 . TRIPLEX 1 99
LABEL 275000 714150 . TRIPLEX 1 B1
LABEL 275450 713500 . TRIPLEX 1 B2
LABEL 276000 712900 . TRIPLEX 1 B3
LABEL 277115 716400 . TRIPLEX 1 AA1
LABEL 276460 715362 . TRIPLEX 1 AA2
LABEL 276258 714553 . TRIPLEX 1 AA3
MOVE 277500 712600 . . . .
DRAW 277500 712550 1 . . .
DRAW 278000 712550 1 . . .
DRAW 278000 712600 1 . . .
LABEL 277750 712620 . TRIPLEX 1 500 m
;
RUN;

PROC GPLOT DATA = MAP;
    AXIS1 ORDER = 274400 TO 278400 BY 4000
          LENGTH = 12 CM
          LABEL = NONE
          MINOR = NONE
          OFFSET = (0)
          VALUE = (F=TRIPLEX H=1);
    AXIS2 ORDER = 712500 TO 717500 BY 5000
          LENGTH = 15 CM
          LABEL = NONE
          MINOR = NONE
          OFFSET = (0)
          VALUE = (F=TRIPLEX H=1);
    PLOT AY * AX=1
         BY * BX=1
         CY * CX=1
         DY * DX=1
         EY * EX=1
         FY * FX=1
         JY * JX=1
         KY * KX=1
         LY * LX=1
         MY * MX=1
         NY * NX=1
         UY * UX=1/OVERLAY
                  FRAME
                  VAXIS = AXIS2
                  HAXIS = AXIS1
                  ANNOTAT = ANNO;

Coordinates of SCUBA and ROV survey:

LABEL 276000 716800 . TRIPLEX 1 S1
LABEL 278000 715200 . TRIPLEX 1 S2
LABEL 277100 714500 . TRIPLEX 1 S3
LABEL 276600 714450 . TRIPLEX 1 S4
LABEL 275750 715750 . TRIPLEX 1 S5
LABEL 277600 715600 . TRIPLEX 1 S6
LABEL 276700 715450 . TRIPLEX 1 S7
LABEL 275800 715300 . TRIPLEX 1 S8
LABEL 276350 714653 . TRIPLEX 1 R1
```

```
LABEL 277100 714680 . TRIPLEX 1 R2
LABEL 276147 714079 . TRIPLEX 1 R3
LABEL 276000 713200 . TRIPLEX 1 R4
```

APPENDIX CHAPTER 6

A6.1 Current plots

```
 DATA CURRENT;
INFILE CU;
INPUT TIME CURR_DIR CURR_SPD;

DATA WIND;
INFILE WIND;
INPUT TIME WIND_DIR WIND_SPD;

DATA JOINT;
 MERGE CURRENT WIND;
  BY TIME;

FILENAME SASQMS '[]SASQMS.DAT';
GOPTIONS HPOS=80 VPOS=60 DEVICE=QMS CHARACTERS NODASH NOFILL;
TITLE1 'WIND AND CURRENT DIRECTION VS TIME';
SYMBOL1 W=1 C=BLACK L=1 I=SM5 V=NONE;
SYMBOL2 W=1 C=BLACK L=2 I=SM20 V=NONE;
SYMBOL3 W=1 C=BLACK I=JOIN V=NONE;


DATA ANNO;

LENGTH FUNCTION $8;
RETAIN FUNCTION XSYS '2' YSYS '2';
INPUT FUNCTION $ X Y LINE STYLE $ SIZE POSITION $ TEXT $ CHAR30.;
CARDS;

LABEL 1000 45 . TRIPLEX 1.5 6 Current direction
MOVE -100 44 . . . . .
DRAW 900 44 1 . . 4 .
LABEL 1000 22 . TRIPLEX 1.5 6 Wind direction
MOVE -100 21 . . . . .
DRAW 900 21 2 . . 4 .
;
RUN;

PROC GPLOT DATA=JOINT;

AXIS1 VALUE=(F=TRIPLEX H=1.5 '8' '9'  '10' '11' '12' '13' '14' '15'
'16' '17'
'18' '19' '20' '21' '22' '23' '24' '25')
      LABEL=(F=TRIPLEX H=2 'TIME (Day/July/1988)')
      ORDER= -765 TO 23715 BY 1440
      MINOR=(N=0);

AXIS2 LABEL=(F=TRIPLEX H=2 A=90 'DIRECTION')
      ORDER = 0 TO 360 BY 45;
```

```
PLOT CURR_DIR * TIME=1
     WIND_DIR * TIME=2/OVERLAY
                FRAME
                VAXIS = AXIS2
                HAXIS = AXIS1
                ANNOTATE = ANNO;
```

A6.2 Iterative procedure to calculate u_{*cw} after GRANT and MADSEN (1979).

Data input see example (1) Chapter 6.

The friction velocity u_{*cw} is given by

$$u_{*cw}^2 = 1/2\ f_{cw}\ V_2\ u_o^2$$

where f_{cw} is the wave-current friction factor for codirectional flow obtained from Fig.A6.1, V_2 expresses the angle between waves and currents (a=45° for this case) from Fig.A6.2. The u_a/u_o ratio has to be assumed at first instance; GM79 suggest a value < 0.25 for shelf conditions. Thus f_{cw} = 0.028, V_2 = 0.25 and u_{*cw} = 4.1 cm/s.

In order to check u_{*cw}, the "apparent" bed roughness k_{bc} which is the physical bed roughness plus the roughness produced by waves is obtained from Fig.A6.3 with 120 cm and put in

$$U = u_{*cw}/k \ln 30z/k_{bc}.$$

which gives for z = 100 cm, U = 33 cm/s which is reasonably close to U_{100} (35 cm/s).

A problem is the inaccuracy when z_0 as the physical bottom roughness changes during a storm due to the wave height. Thus the bedforms observed in the after storm survey may only represent a stage at the end of the storm; bedforms during the storm may well be bigger thus causing higher z_0 values.

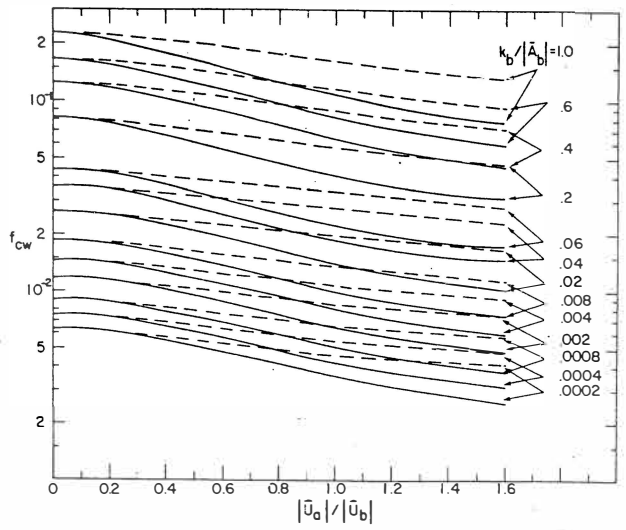

Fig.A6.1: Wave-current friction factor fo codirectional flow and transdirectional flow (angle < 60° solid lines; > 60° interpolate).

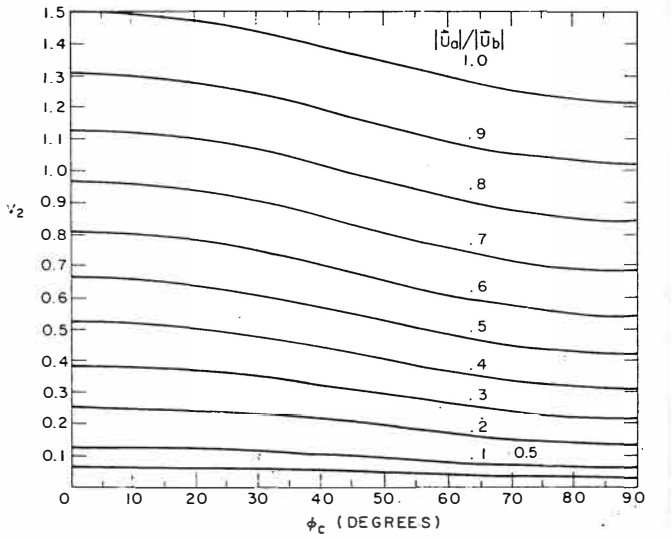

Fig.A6.2: Numerical solutions to V_2

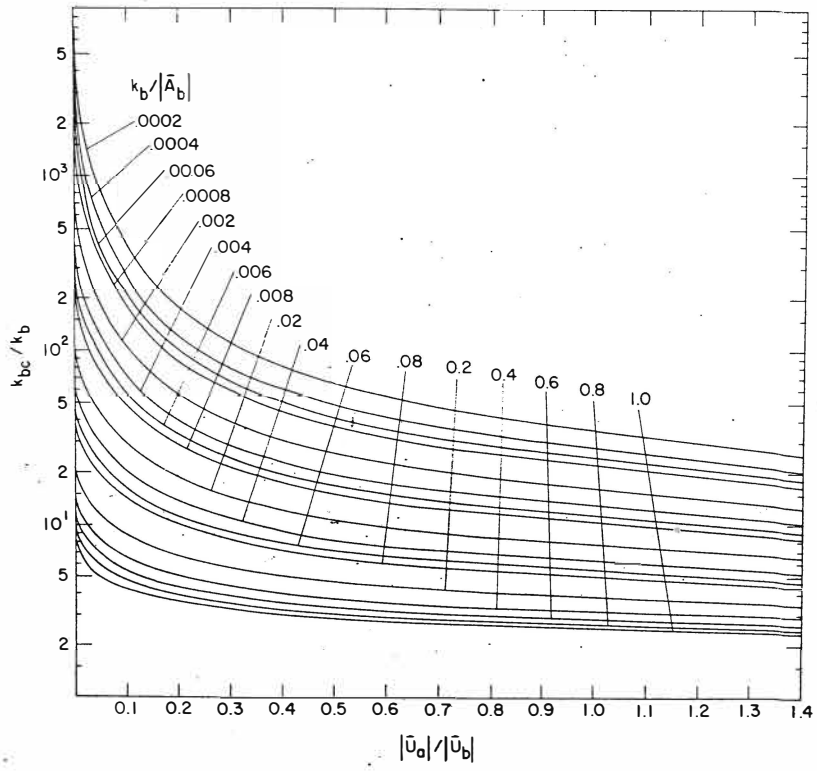

Fig.A6.3: Ratio of apparent bottom roughness k_{bc} to the physical bottom roughness k_b for codirectional flow.

LIST OF REFERENCES

BABA,J. and P.D.KOMAR, 1981. Measurements and analysis of settling velocities of natural quartz sand grains. *Journal of Sedimentary Petrology*, 51:631-640.

BARNETT,A.G., 1985. Tauranga Harbour Study; Part I: Overview; Part III: Hydrodynamics. Report to the Bay of Plenty Harbour Board.

BAY OF PLENTY HARBOUR BOARD SOUNDING CHARTS. Survey dates 27/7/78; 7/1/80; 30/3/81; 23/12/83; 30/10/85; 15/10/86; 21/9/87.

BLACK,K.P., 1984. Tauranga Harbour Study; Part IV: Sediment transport. Report for the Bay of Plenty Harbour Board; 159 p.

BLACK,K.P. and T.R.HEALY, 1981. Computer programs for wave refraction: wind wave generation, wave refraction diagrams and Fast Fourier analysis. *Occasional Report 6, Department of Earth Sciences, University of Waikato*; 76 p.

BLACK,K.P. and T.R.HEALY, 1982. Sediment transport investigations in a New Zealand tidal inlet. Proceedings of the 18th International Conference of Coastal Engineering: 2436-2457.

BLACK,K.P. and T.R.HEALY, 1983. Northland forestry port marsden points; side-scan sonar survey. Report to the Northland Harbour Board, 88p.

BLACK,K.P. and T.R.HEALY, 1988. Formation of Ripple Bands in a Wave-convergence Zone. *Journal of Sedimentary Petrology*, 58(2):195-207.

BOKUNIEWICZ, H.J. and R.B.GORDON, 1980. Deposition of dredged sediment at open water sites. Estuarine and Coastal Marine Science 10:289-303.

BOOTHROYD, J.C., 1978. Mesotidal inlets and estuaries. Chapter 6 in R.A.DAVIS (ed): Coastal sedimentary environments; Springer, New York:287-360.

BOYD,R., 1980. Sediment dispersal on the N.S.W. Continental Shelf. Proceedings of the 17th International Conference Coastal Engineering:1364-1381.

BRODIE,J.W., 1960. Coastal surface currents around New Zealand. *New Zealand Journal of Geology and Geophysics*, 3:235-252.

CACCHIONE,D.A. and D.E.DRAKE, 1982. Measurements of strom-generated bottom stresses on the continental shelf. *Journal of Geophysical Research*, 87:1952-1960.

CACCHIONE, D.A., D.E.DRAKE, W.D.GRANT and G.B.TATE, 1984. Rippled scour depressions on the inner continental shelf off central California. *Journal of Sedimentary Petrology*, 54:1280-1291.

CACCHIONE,D.A., W.D.GRANT, D.E.DRAKE and S.M.GLEN, 1987. Storm-dominated bottom boundary layer dynamics on the northern California continental shelf: measurements and predictions. *Journal of Geophysical Research*, 92:1817-1827.

CLIFTON,H.E., 1976. Wave-generated structures - a conceptual model. In R.A.DAVIS and ETHINGTON,R.L. (eds): Beach and nearshore processes. *Society of Economical Paleontologists and Mineralogists, Special Publication*, 24:126-148.

CLIFTON,H.E. and J.R.DINGLER, 1984. Wave-formed structures and paleoenvironmental reconstruction. *Marine Geology*, 60:165-198.

COFFEY,F.C. and P.NIELSEN, 1986. The influence of waves on current profiles. Proceedings of the 20th International Conference Coastal Engineering:82-96.

COLE,J.W., 1979. Structure, petrology and genesis of Cenozoic volcanism, Taupo Volcanic Zone, New Zealand. *New Zealand Journal of Geology and Geophysics*, 22:631-657.

COOK,D.O., 1982. Discussion: Nearshore bedform patterns along Rhode Island from side-scan sonar surveys. *Journal of Sedimentary Petrology*, 52:677-678.

COOK,D.O. and D.S.GORSLINE, 1972. Field observations of sand transport by shoaling waves. *Marine Geology*, 13:31-55.

COWELL,P.J and P.NIELSEN, 1984. Predictions of sand movement on the south Sydney inner-continental shelf, South-east Australia. University of Sydney, Coastal Studies Unit, Tech. Report 84/2.

DAHM,J. and T.R.HEALY, 1980. A Study of Dredge Spoil Dispersion off the Entrance to Tauranga Harbour. Report to the Bay of Plenty Harbour Board, 64 p.

DAHM,J., 1983. The Geomorphic Development, Bathymetric Stability and Sediment Dynamics of Tauranga Harbour. Unpub. M.Sc. Thesis, University of Waikato. 230 p.

DAVIES,A.G., R.L.SOULSBY and H.L.KING, 1988. A numerical model of the combined wave and curent bottom boundary layer. *Journal of Geophysical Research*, 93: 491-508.

DAVIES-COLLEY,R.J., 1976. Sediment Dynamics of Tauranga Harbour and the Tauranga Inlet. Unpubl. M.Sc. Thesis, University of Waikato. 148 p.

DAVIES-COLLEY,R.J. and T.R.HEALY, 1978. Sediment and hydrodynamics of the Tauranga entrance to Tauranga Harbour. *New Zealand Journal of Marine and Freshwater Research* , 12:225-236.

DE FREITAS,C.R., 1987. Perspectives of the impact of short-term climatic changes in New Zealand. *New Zealand Geographer*, 43(3):169-176.

DE LANGE,W.P., 1988. Wave climate and sediment transport within Tauranga Harbour, in the vicinity of Pilot Bay. Unpubl. Ph.D. thesis, University of Waikato.

DELL,P.M., T.R.HEALY and C.S.NELSON, 1985. A Preliminary Investigation of the Sediments of the Eastern Coromandel Inner Shelf and Implications for Across Shelf Transport. Proceedings of the Austrasian Conference on Coastal and Ocean Engineering 1:489-499.

DEMARS,K.R., R.P.LONG, S.STANTON and W.CHARLTON, 1984. Settlement and stability of ocean disposal mounds. Proceedings of the Conference on Dredging and Dredge Material Disposal:1040-1049.

DINGLER,J.R., 1979. The threshold of grain motion under oscillatory flow in a laboratory wave channel. *Journal of Sedimentary Petrology*, 49:287-294.

DRAKE,D.E., D.A.CACCHIONE and H.A.KARL, 1985. Bottom currentrs and sediment transport on San Pedro Shelf, California. *Journal of Sedimentary Petrology*, 55:15-28.

FIELD,M.E. and P.S.ROY, 1984. Offshore transport and sand body formation: evidence from a steep, high-energy shoreface, southeastern Australia. *Journal of Sedimentary Petrology*, 54:1292-1302.

GIBB,J.C., 1986. A New Zealand regional holocene eustatic sea-level curve and its application to determination of vertical tectonic movements. A contribution to IGCP-Project 200. *Royal Society of New Zealand Bull.*, 24:377-395.

GLEN,S.M. and W.D.GRANT, 1987. A suspended sediment stratification correction for combined wave and current flows. *Journal of Geophysical Research*, 92:8244-8264.

GORDON,A.D. and J.G.HOFFMAN, 1984. Sediment trasnport on the South-East Australian Continental Shelf. Proceedings of the 19th International Conference of Coastal Engineering:1952-1967.

GRACE,R., 1988. Ecological investigations of Acukland Harbour Board's alternative dredge spoil dump site off Browns Island, Waitemata Harbour. Report to the Auckland Harbour Board.

GRANT,W.D. and O.S.MADSEN, 1979. Combined wave and current interaction with a rough bottom. *Journal of Geophysical Research*, 84:1797-1808.

GRANT,W.D. and O.S.MADSEN, 1982. Moveable bed roughness in unsteady oscillatory flow. *Journal of Geophysical Research*, 87:469-482.

GRANT,W.D, A.J.WILLIAMS and S.M.GLENN, 1984. Bottom stress estimates and their prediction on the northern California continental shelf during CODE-1: The importance of wave-current interaction. *Journal of Physical Oceanography*, 14:506-527.

HAMMOND,T.M. and M.B.COLLINS, 1979. On the threshold of sand-sized sediment under the combined influence of unidirectional and oscillatory flow. *Sedimentology*, 26:

HAN,G.C. and D.A.MAYER, 1981. Current structure on the Long Island inner shelf. *Journal of Geophysical Research*, 86:4205-4214.

HANDS,E.B. and S.R.DeLOACH, 1984. An offshore mound construced of dredged material. Proceedings of the Conference on Dredging and Dredge Material Disposal:1030-1039.

HANES,D.M., 1988. Intermittent sediment suspension and its implications to sand tracer dispersal in wave-dominated environments. *Marine Geology*, 81:175-183.

HARMSWORTH,G., 1983. Quaternary stratigraphy of the Tauranga Basin. Unpubl. M.Sc. thesis, University of Waikato.

HARRAY, K.G., 1976. Beach erosion and sediments at Waihi Beach. Unpubl. M.Sc. thesis, University of Waikato; 94 p.

HARRIS,T.F.W., 1985. North Cape to East Cape. Aspects of Physical Oceanography. University of Auckland; 178 p.

HARRIS,T.F.W., T.S.HUGHES and E.M.VALENTINE,1983. Deepwater Waves off Hicks Bay and the North-East Coast, North Island. *Water and Soil Miscellaneous Publication*, 56; 83 p.

HEALY,T.R., 1985. Tauranga Harbour Study; Part II: Field data collection programme; Part IV: Morphological study. Report to the Bay of Plenty Harbour Board.

HEALY,T.R., K.G.HARRAY and B.RICHMOND, 1977: The Bay of Plenty Coastal Erosion Survey. *Occasional Report No.3, University of Waikato, Department of Earth Sciences*; 64 p.

HEALY,T.R. and R.M.KIRK, 1981. Coasts. Chapter 5 in SOONS,J. and M.J.SELBY (eds): Landforms of New Zealand. Longman-Paul:80-104.

HEALY,T.R., B.McCABE, R.GRACE and C.HARMS, 1988. Environmental assessment programme for Tauranga Harbour dredging and inner shelf spoil dumping. Report for the Bay of Plenty Harbour Board; 43 p.

HEALY,T.R., S.G.RYAN and C.HARMS, in press. Recent environmental issues concerning dredge spoil dumping. Proceedings of the Ecopolitics III Conference.

HOBBS,C.H. III, 1986. Side-scan sonar as a tool for mapping spatial variations in sediment type. *Geo-Marine Letters*, 5:241-245.

HUNTER,R.E., J.R.DINGLER, R.J.ANIMA and B.M.RICHMOND, 1988. Coarse-sediment bands on the inner shelf of the Southern Monterey Bay, California. *Marine Geology*, 80:81-98.

JOHNSON,B.H., M.J.TRAWLE and S.A.ADAMEC, 1988. Dredged material disposal modelling in Pudget Sound. *Journal of Waterway, Port, Coastal and Ocean Engineering*, 114(6):700-713.

KAPSDASLI,M.S. and K.R.DYER, 1986. Threshold conditions for sand movement on a rippled bed. *Geo-Marine Letters*, 6:161-164.

KEMP,P.H. and R.R.SIMONS, 1982. The interaction between waves and a turbulent current: Waves prograting with the current. *Journal of Fluid Mechanics*, 116:227-250.

KEMP,P.H. and R.R.SIMONS, 1983. The interaction between waves and a turbulent current: Waves prograting against the current. *Journal Fluid Mechanics*, 130:73-89.

KENNETT,J.S., 1982. Marine geology. Prentice-Hall, Inc., Eaglewood Cliffs, New Jersey; 813 p.

KESTER,D.R., B.H.KETCHUM, I.W.DUEDALL, and P.K.PARK, 1983. Wastes in the ocean, Vol.2: Dredged-material disposal in the ocean, John Wiley and Sons, New York; 299 p.

KETCHUM,B.H., D.R.KESTER and P.K.PARK, 1981. Ocean dumping of industrial wastes. Plenum, New York.

KOBAYASHI,N., 1982. Sediment transport on a gentle slope due to waves. *Journal of Waterway, Port, Coastal and Ocean Division, ASCE*, 108:254-271.

KOMAR,P.D., 1976. Beach processes and sedimentation. Prentice-Hall, Inc., Englewood Cliffs, New Jersey; 429 p.

KOMAR,P.D. and M.C.MILLER, 1973. The threshold of movement under oscillatory water waves. *Journal of Sedimentary Petrology*, 43:1101-1110.

KOMAR,P.D. and M.C.MILLER, 1975. The initation of oscillatroy ripple markes and the development of plane-bed at high shear stresses under waves. *Journal of Sedimentary Petrology*, 45:697-703.

LAVELLE,J.W., D.J.P.SWIFT, P.E.GADD, W.L.STUBBLEFIELD, F.N.CASE, H.R.BRASHEAR and K.W.HAFF, 1978. Fair weather and storm sand transport on the Long Island, New York, inner shelf. *Sedimentology*, 25:823-842.

LECKIE,D., 1988. Wave-formed, coarse-grained ripples and their relationship to hummocky cross-stratification. *Journal of Sedimentary Petrology*, 58:607-622.

LOSADA,M.A., J.M.DESIRE and J.MERINO, 1987. An energy approach of non-breaking wave-induced motion of bottom sediment particles. *Coastal Engineering*, 11:159-173.

MADSEN,O.S. and W.D.GRANT, 1976. Quantitative description of sediment transport by waves. Proceedings of the of 15th Coastal Engineering Conference:1093-1112.

McCABE,P., 1985. Mangawhia Harbour and the development of its dual inlet system. Unpubl. M.Sc. thesis, Department of Earth Sciences, University of Waikato; 203 p.

McLAREN,P., 1981. An interpretation of trends in grain-size measures. *Journal of Sedimentary Petrology*, 51:611-624.

McLAREN,P. and D.BOWLES, 1985. The effects of sediment transport on grain-size distributions. *Journal of Sedimentary Petrology*, 55:457-470.

MILLER,M.C and P.D.KOMAR, 1980a. Oscillation sand ripples generated by laboratory apparatus. *Journal of Sedimentary Petrology*, 50:173-182.

MILLER,M.C. and P.D.KOMAR, 1980b. A field investigation of the relationship between oscillatory ripple spacing and near-bottom water orbital motions. *Journal of Sedimentary Petrology*, 50:183-191.

MILLER,M.C., I.N.McCAVE and P.D.KOMAR, 1977. Threshold of sediment motion under unidirectional current. *Sedimentology*, 24:507-527.

MORANG,A. and R.L.McMASTER, 1980. Nearshore bedform patterns along Rhode Island from side-scan sonar surveys. *Journal of Sedimentary Petrology*, 50:831-840.

MORTON,R.W., 1983. Precision Bathymetric Study of dredged-Material Capping in Long Island Sound. in KESTER,D.R., B.H.KETCHUM, I.W.DUEDALL and P.K.PARK (eds): Wastes in the ocean, Vol.2; Dredged-Material Disposal in the ocean; John Wiley and Sons:99-122.

NIEDORODA,A.W., C.M.MA, P.A.MANGARELLA, R.H.CROSS, S.R.HUNTWELL and D.D.TREADWELL, 1982. Measured and computed coastal ocean bedload transport. Proceedings of the 18th Conf of Coastal Engineering: 1353-1368.

NIEDORODA,A.W., D.J.P.SWIFT and T.S.HOPKINS, 1985. The shoreface. In DAVIS,R.A. (ed), Coastal Sedimentary Environments, New York, Springer:533-624.

NIEDORODA,A.W., D.J.P.SWIFT, T.S.HOPKINS and C.H.MA, 1984. Shoreface morphodynamics on wave dominated coasts. *Marine Geology*, 60:331-354.

QUAYLE,A.M. The climate and weather of the Bay of Plenty Region. *New Zealand Meteorological Service Miscallenious Publication*, 115 (1) 2nd edition; 56 p.

RIGLER,J.K. and M.B.COLLINS, 1984. Initial grain motion under oscillatroy flow: A comparison of some threshold criteria. *Geo-Marine Letters*, 3:43-48.

RILEY,P.B., I.S.MONRO and J.C.SCHOFIELD, 1985. Late Holocene sedimentation in Omaha Bay, North Island, New Zealand. *New Zealand Journal of Geology and Geophysics*, 28:299-312.

SAS/GRAPH User's Guide, 1985. Version 5 Edition; 583 p.

SCHWARTZ,R.K. and F.R.MUSIALOWSKI, 1977. Nearshore disposal: onshore sediment transport. Coastal Sediments '77:85-101.

SHI,N.C. and L.H.LARSEN, 1984. Reverse sediment transport induced by amplitude modulated waves. *Marine Geology*, 54:181-200.

SNEDDON,J.W., D.NUMMEDAL and A.F.AMOS, 1988. Storm- and fair weather combined flow on the Central Texas Continental Shelf. *Journal of Sedimentary Petrology*, 58:580-595.

SWIFT,D.J.P., A.G.FIGUEIREDO, G.L.FREELAND and G.F.OERTEL, 1983. Hummocky cross stratification and megaripples: a geological double standard. *Journal of Sedimentary Petrology*, 53:1295-1317.

SWIFT,D.J.P. and G.L.FREELAND, 1978. Current lineations and sand waves on the inner shelf, Middle Atlantic Bight of North America. *Journal of Sedimentary Petrology*, 48:1257-1266.

SWIFT,D.J.P., G.L.FREELAND and R.A.YOUNG, 1979. Time and space distribution of megaripples and associated bedfroms, Middle Atlantic Bight, North American shelf. *Sedimentology*, 26:389-406.

SWIFT.D.J.P., D.J.STANLEY and J.R.CURRAY, 1971. Relict sediments on continental shelves: a reconsideration. *Journal of Geology*, 79:322-346.

TROWBRIDGE,J. and O.S MADSEN, 1984. Turbulent wave boundary layers, Second order thory and mass transport. *Journal of Geophysical Research*, 89:7999-8007.

TRUETT,C.L., 1988. Dredged material behavior during open-water disposal. *Journal of Coastal Research*, 4(3):389-397.

VINCENT,C.E., R.A.YOUNG and D.J.P.SWIFT, 1982. On the relationship between bedload and suspended sand transport on the inner shelf, Long Island, New York. *Journal of Geophysical Research*, 87:4163-4170.

WALKER,R.G., 1984. Shelf and shallow marine sand. In WALKER,R.G. (ed): Facies models. 2nd edition, Geoscience Canada Reprint Series 1:141-170.

WEGGEL,R.J., 1986. Economics of beach nourishment under a scenario of rising sea-level. *Journal of Waterway, Port, Coastal and Ocean Engineering*, 112(3):418-426.

WRIGHT, L.D., 1981. Nearshore tidal currents and sand transport in a macrotidal environment. *Geo-Marine Letters*, 1:173-179.

WRIGHT,L.D., 1987. Shelf-Surfzone Coupling: Cross-Shore Transport Mechanisms on the Shore Face. Coastal Sediments' 87:25-40.

WRIGHT,L.D., J.D.BOON, M.O.GREEN and J.H.LIST, 1986. Response to the mid shoreface of the Southern mid-Atlantic Bight to a "Northeaster". *Geo-Marine Letters*, 6:153-160.